Iceland Liechtenstein Norway grants

Working together for a green, competitive and inclusive Europe

EMERALD e-toolkit for teaching purposes, basic knowledge about realizing biomimetic mechatronic systems

Răzvan PĂCURAR, Filip GÓRSKI, Filippo SANFILIPPO, Diana BĂILĂ, Branislav RABARA, Martin Bjaadal ØKTER, Dan-Sorin COMȘA, Emilia SABĂU, Magdalena ŻUKOWSKA, Dominik RYBARCZYK, Natalia WIERZBICKA, Radosław WICHNIAREK, Wiesław KUCZKO, Roman REGULSKI

EUROPEAN NETWORK FOR 3D PRINTING OF BIOMIMETIC MECHATRONIC SYSTEMS PROJECT

2023

TECHNICAL UNIVERSITY OF CLUJ-NAPOCA ROMANIA

UiA University of Agder

bizzcom

Editura RISOPRINT

Toate drepturile rezervate autorilor & Editurii Risoprint

*Editura **RISOPRINT** este recunoscută de **C.N.C.S.***
***(Consiliul Național al Cercetării Științifice)**.*
www.risoprint.ro ***www.cncs-uefiscdi.ro***

ISBN 978-973-53-3158-0

EMERALD e-toolkit for teaching purposes,
basic knowledge about realizing biomimetic mechatronic systems

AUTHORS

Răzvan PĂCURAR, Filip GÓRSKI, Filippo SANFILIPPO, Diana BĂILĂ, Branislav RABARA, Martin Bjaadal ØKTER, Dan-Sorin COMȘA, Emilia SABĂU, Magdalena ŻUKOWSKA, Dominik RYBARCZYK, Natalia WIERZBICKA, Radosław WICHNIAREK, Wiesław KUCZKO, Roman REGULSKI

Director editură: GHEORGHE POP

Acknowledgement: The publishing of this e-toolkit has been financially supported by the project entitled "European network for 3D printing of biomimetic mechatronic systems", The Education, Scholarships, Apprenticeships and Youth Entrepreneurship Programme – SEE Grants 2014-2021. Project reference: 21-COP-0019.

CONTENT

This project has been funded with support from the Iceland Liechtenstein Norway Grants. This publication [communication] reflects the views only of the authors, and the Commission cannot be held responsible for any use which may be made of the information contained therein.

INTRODUCTION

The „European network for 3D printing of biomimetic mechatronic systems – 21-COP-0019 - EMERALD project, which is part of the Education, Scholarships, Apprenticeships, and Youth Entrepreneurship Programme (ESAYEP) under the EEA Grants 2014-2021, represents a collaborative effort between technical universities coming from Romania (Technical University of Cluj-Napoca and University Politehnica Bucharest), Norway (University of Agder), Poland (Poznan University of Technology), and one private company coming from Slovakia (Bizzcom). This project that is part of the "2021 Cooperation Projects in Higher Education Area," which was implemented in the period 2022-2023 has been focusing on providing educational tools concerning the development of biomimetic mechatronic systems for people with special needs (with amputated arms) by 3D printing technologies. The EMERALD consortium partners have tried to find adequate methods of integrating theoretical knowledge with practical application in the field of biomimetic mechatronic systems realized by 3D printing technologies for people with special needs (with amputated arms) in the end. This integration can be clearly seen in the EMERALD e-toolkit manual, a comprehensive guide that has been developed in order to bridge the gap between theoretical aspects shown in the e-book that comprise basic knowledge and theoretical information as basics for real practical applications, focused on the conceiving, manufacturing and testing of biomimetic mechatronic systems for people with special needs (with amputated arms), using 3D printing technologies.

The e-toolkit manual which is the result of the collaborative creation of the EMERALD consortium partners serves as a detailed laboratory guide that goes beyond theoretical information, providing step-by-step instructions on how to design, manufacture and test biomimetic mechatronic systems realized by different types of 3D printing methods. The content of the e-toolkit manual is comprehensive, covering every essential stages in the development of such systems, beginning with the pre-validation of Computer Aided Design (CAD) models through Computer Aided Engineering (CAE) analyses, continuing with the selection of suitable materials for 3D printing, integrating of sensors and transducers and ending with programming, assembling, as well as the use of Virtual Reality / Augmented Reality applications being applied for these systems.

A key goal of the e-toolkit manual is to encourage the practical application of theoretical concepts learned in the course modules provided in the e-book by engaging both professors and students to go one step forward in producing practical case studies of biomimetic mechatronic systems for people with amputated arms, guiding them through each developing stage with detailed instructions that are being offered on the e-toolkit manual. This hands-on approach not only enhances learning, but also stimulates creativity, prompting the design of new personalized biomimetic mechatronic solutions. These solutions incorporate innovative ideas in shape and material selection, customized to specific manufacturing settings and use of different 3D printing technologies for the producing of real practical biomimetic mechatronic systems to support real patients with amputated arms in the end.

Iceland Liechtenstein Norway grants

Working together for a green, competitive and inclusive Europe

EMERALD

The Education, Scholarships, Apprenticeships and Youth Entrepreneurship

EUROPEAN NETWORK FOR 3D PRINTING OF BIOMIMETIC MECHATRONIC SYSTEMS

E-toolkit – Computer Aided Design

Project Title	**European network for 3D printing of biomimetic mechatronic systems** **21-COP-0019**
Output	**O2 - EMERALD e-toolkit manual for digital learning in producing biomimetic mechatronic systems**
Module	**Computer Aided Design (CAD)** - **Design of selected biomimetic 3D printed mechatronic devices**
Authors	**Filip GÓRSKI, Natalia WIERZBICKA, Magdalena ŻUKOWSKA, Dominik RYBARCZYK**

This project has been funded with support from the Iceland Liechtenstein Norway Grants. This publication [communication] reflects the views only of the authors, and the Commission cannot be held responsible for any use which may be made of the information contained therein.

TECHNICAL UNIVERSITY OF CLUJ-NAPOCA ROMANIA

UiA University of Agder

bizzcom

This project has been funded with support from the Iceland Liechtenstein Norway Grants. This publication [communication] reflects the views only of the authors, and the Commission cannot be held responsible for any use which may be made of the information contained therein.

1 Introduction

This toolkit presents practical information on how to a CAD model of a biomechatronic hand prosthesis can be built and structured. An example of modular prosthesis will be considered, with its adjustment to needs and preferences of an adult patient and converting static mechanical device into a mechatronic prosthesis, equipped with sensors for monitoring the activities performed by prosthesis user.

LEGAL INFORMATION: all the basic (input) CAD models, know-how and other intellectual property presented in this toolkit, if not stated otherwise, belongs to Poznan University of Technology. It is not allowed to use the shared materials for commercial purposes, they can be used solely for educational properties in the scope of the EMERALD project, by authorized persons taking part in training performed with participation of instructors accepted by PUT team.

This project has been funded with support from the Iceland Liechtenstein Norway Grants. This publication [communication] reflects the views only of the authors, and the Commission cannot be held responsible for any use which may be made of the information contained therein.

2 Design of mechanical part of the prosthesis

2.1 Main assumptions

The prosthesis has been prepared for continuous and demanding cycling for an adult patient. The modular mechanical prosthesis was originally generated automatically for the child. Then, the necessary changes were made to adapt it to an adult. After testing and optimizing the bicycle, the adult mechanical prosthesis was transformed into a mechatronic one through sensorization.

The modular model of the prosthesis has been described in multiple previous work by the team of authors [1-2], or supervised by them (Master's thesis [3] and [4]). Most of the descriptions in this chapter come from these works, as well as previously undisclosed project reports.

2.2 Generative CAD model – principles of operation

In this work, a project of an intelligent model of the upper limb prosthesis was implemented, which is characterized by a modular structure. The device is an integrated whole composed of many components with unified terminals. The model is loaded with anthropometric and configuration data directly from an external Excel file, enabling both the generation of anatomically matched prosthesis components and the manipulation of its variants to create any combination of all parts. Therefore, the model allows for the quick and fully automated production of many configurations of individualized prostheses for the same or many different patients. The architecture of the modular model is shown in Figure 1.

The concept of the model was made as part of the project "Automation of design and rapid production of individualized orthopedic and prosthetic products based on data from anthropometric measurements", serving the development of the prototype AutoMedPrint system built at the Faculty of Mechanical Engineering of the Poznań University of Technology.

This project has been funded with support from the Iceland Liechtenstein Norway Grants. This publication [communication] reflects the views only of the authors, and the Commission cannot be held responsible for any use which may be made of the information contained therein.

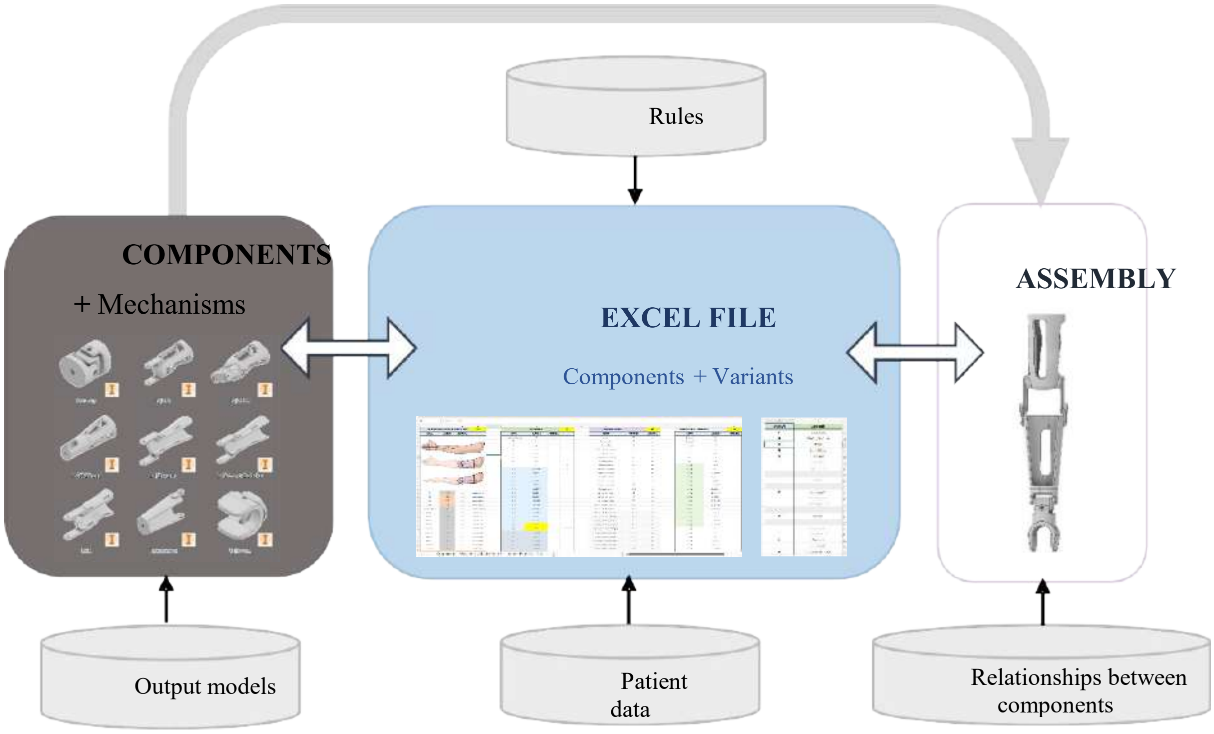

Figure 1 Architecture of the designed system [3]

The model consists of three types of main components - sockets, forearms and effectors. Types of individual elements of a given type are presented in Table 1. However, the modular prosthesis also includes sacroiliac joints (cardans) that function as a movable wrist joint, an assembly adapter and an elbow module that imitates flexion and extension in the frontal plane.

This project has been funded with support from the Iceland Liechtenstein Norway Grants. This publication [communication] reflects the views only of the authors, and the Commission cannot be held responsible for any use which may be made of the information contained therein.

Table 1 List of components of the modular model

Prosthetic sockets	Prosthetic forearms	Effectors
— CRS compression and relaxation socjet (4 variants) — Open socket (2 variants) — Semi-open socket (3 variants) — CRS socket for amputation within the forearm	— Forearm open — Open forearm with a tip dedicated to the adapter — Closed forearm with a tip dedicated to the adapter — Forearm completely closed with a tip dedicated to the adapter	— C-Handle — Fixed straight handle — Fixed angular handle — Straight handle with a spring — A mechanical hand
Connecting and auxiliary elements		
— Cross joints — 2 adapters	— External model of the elbow — A shaped piece that blocks the elbow joint	

All elements are designed from the beginning in a parametric angle, making the dimensions of the elements dependent on anthropometric measurements from scans of healthy upper limbs of patients.

2.3 Prosthesis model design

2.3.1 Prosthetic socket

The first stage of creating an autogenerating model of upper limb prostheses was modeling the structure of the prosthetic socket. The socket is generated on the basis of data from spatial scanning of the patient's residual limb. The algorithm developed by the team of the Rapid Manufacturing Laboratory of the Production Engineering Department of the Poznań University of Technology exports data from the STL mesh in the MeshLab program to a previously prepared template Excel file, which is connected to the autogenerating model.

In the MeshLab program, the STL grid of the patient's residual limb is located in the central part of the coordinate system so that the Z axis of the system is the imaginary axis of the arm.

This project has been funded with support from the Iceland Liechtenstein Norway Grants. This publication [communication] reflects the views only of the authors, and the Commission cannot be held responsible for any use which may be made of the information contained therein.

The scan of the stump must be oriented with its inner part in the direction of the X axis ("up") in order to correctly generate the loosening holes and tissue compression pads (Figure 2).

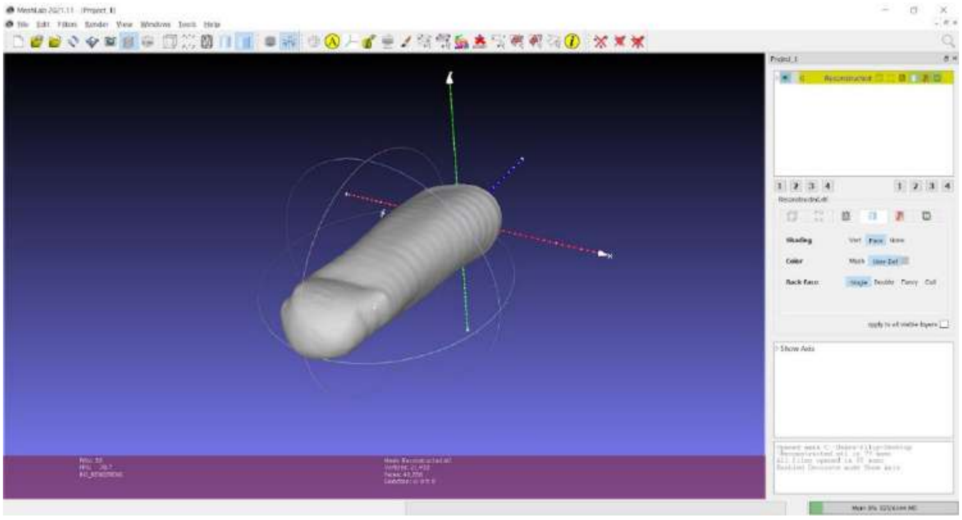

Figure 2 Correct orientation of the STL mesh in MeshLab

First, with the Offset from Plane command, six work planes (Figure 3) were created as offsets from the XY origin plane of the coordinate system (Figure 4). The value of the offsets of individual planes from the XY plane is defined by the user parameter P_n, where n∈〈1:6〉 is the number of the plane.

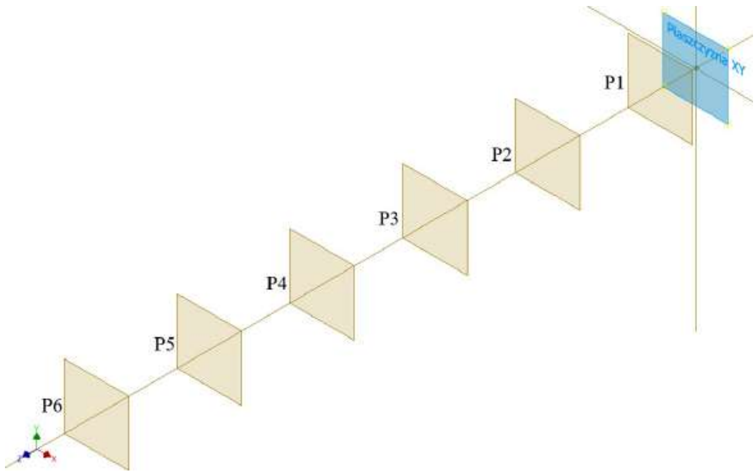

Figure 3 Construction planes defining cross-sections through the patient's vestigial limb

This project has been funded with support from the Iceland Liechtenstein Norway Grants. This publication [communication] reflects the views only of the authors, and the Commission cannot be held responsible for any use which may be made of the information contained therein.

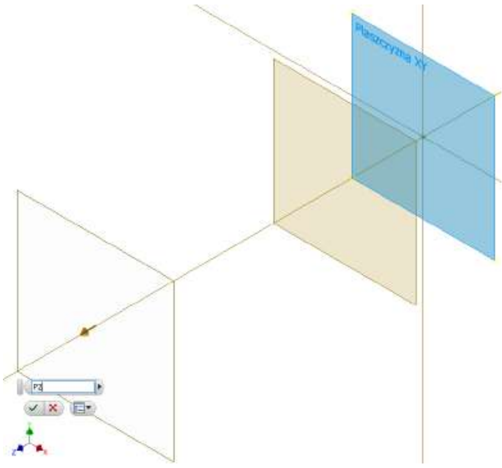

Figure 4 Generating a plane using the Offset from Plane function

The P1 plane marks the place of the first cross-section through the STL mesh of the patient's stump, and thus the edge of the prosthetic socket. The plane P6, on the other hand, marks the place of the last section through the distal part of the vestigial limb and defines the end of the socket. The positions of these two planes are determined in the special AutoMedPrint Limb Calibrator application provided by the team of the Virtual Design Laboratory of the Poznań University of Technology (Figure 5).

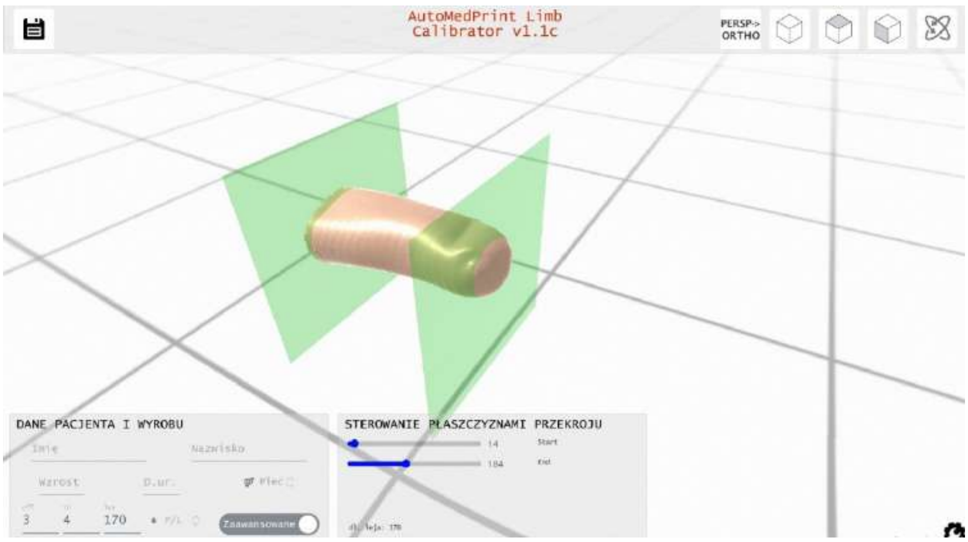

Figure 5 Determination of the extreme positions of the residual limb cross-sectional planes - the AutoMedPrint Limb Calibrator application

This project has been funded with support from the Iceland Liechtenstein Norway Grants. This publication [communication] reflects the views only of the authors, and the Commission cannot be held responsible for any use which may be made of the information contained therein.

The algorithm fills an Excel workbook with data, thanks to the implemented rules, the model is loaded with information necessary to generate the model (e.g. the value of the offset between the planes, or the position of the next planes. The user parameters created at this stage were combined with the model parameters (Figure 6) in the dialog box Inventor Parameters.

d0	Płaszczyzna konstrukcyjna1	mm	P1
d1	Płaszczyzna konstrukcyjna2	mm	P2
d2	Płaszczyzna konstrukcyjna3	mm	P3
d3	Płaszczyzna konstrukcyjna4	mm	P4
d4	Płaszczyzna konstrukcyjna5	mm	P5
d5	Płaszczyzna konstrukcyjna6	mm	P6

Figure 6 Model parameters related to construction planes

The next step in constructing the prosthetic socket was to create six sketches on previously generated planes. Each sketch is a spline curve built from eight points specified by x and y coordinates. Initially, splines were drawn based on random points. After combining the model parameters with the user parameters from Excel, using the Update Local function, the coordinates of the spline building points were updated. As a result of the update, the outline that a single spline forms is the outline of a cross-section through the vestigial limb (Figure 7).

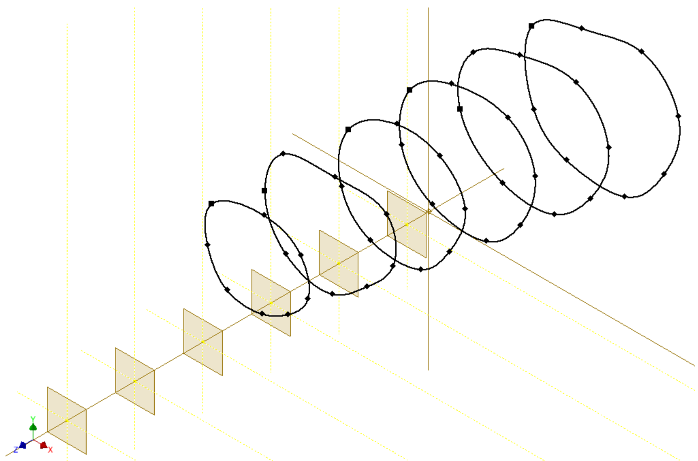

Figure 7 Six splines mapping the outline of cross-sections through the patient's vestigial limb

The data exported from one section in MeshLab are the x, y, z coordinates of the points forming the outline of the stump at the location of this section. The algorithm randomly selects

This project has been funded with support from the Iceland Liechtenstein Norway Grants. This publication [communication] reflects the views only of the authors, and the Commission cannot be held responsible for any use which may be made of the information contained therein.

eight points with a specified spacing between them and completes the cells in the Excel spreadsheet (Figure 8). The x coordinates are specified by the user parameter x_{i_j}, where i ∈ 〈1:8〉 is the spline point number and j ∈ 〈1:6〉 is the sketch number.

8	x1_1	-36,03267
9	y1_1	20,41032
10	x2_1	-10,21343
11	y2_1	32,27849
12	x3_1	20,57136
13	y3_1	37,30608
14	x4_1	39,542
15	y4_1	17,76262
16	x5_1	32,19633
17	y5_1	-11,46023
18	x6_1	11,69784
19	y6_1	-31,69644
20	x7_1	-18,21643
21	y7_1	-30,42693
22	x8_1	-34,93382
23	y8_1	-16,15504

Figure 8 The x, y coordinates of the spline building points, sketch #1

In the next step, using the Extrude from sketches function, six extrusions were created with a distance of each extrusion equal to 1 mm. Then, six work points were generated on the extruded faces using the Edge Loop Midpoint function (Figure 9).

Figure 9 Extrusions with work points

This project has been funded with support from the Iceland Liechtenstein Norway Grants. This publication [communication] reflects the views only of the authors, and the Commission cannot be held responsible for any use which may be made of the information contained therein.

Then another six sketches were created on the back faces of the extrusions. A single sketch consists of projected cutting edges and three offsets from the outline of the reference geometry (Figure 10). The first offset determines the wall thickness of the socket taking into account the offset of the prosthetic socket surface from the surface of the residual limb. The second offset defines the offset of the inner socket wall from the residual limb. The last offset determines the thickness of the compression pads, taking into account the offset of the socket surface from the stump surface.

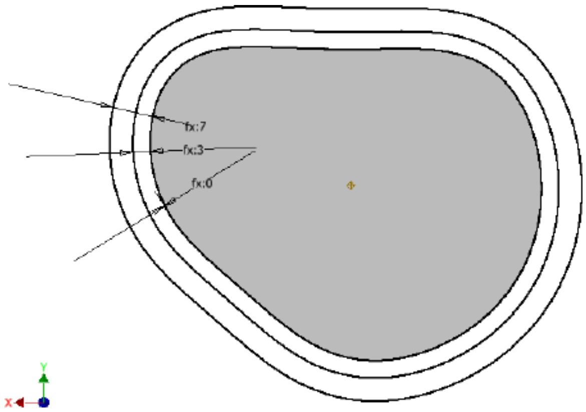

Figure 10 Three offsets from the section outline

After calculating the values of the offsets, applying them and using the loft function, a solid was obtained (Figure 11).

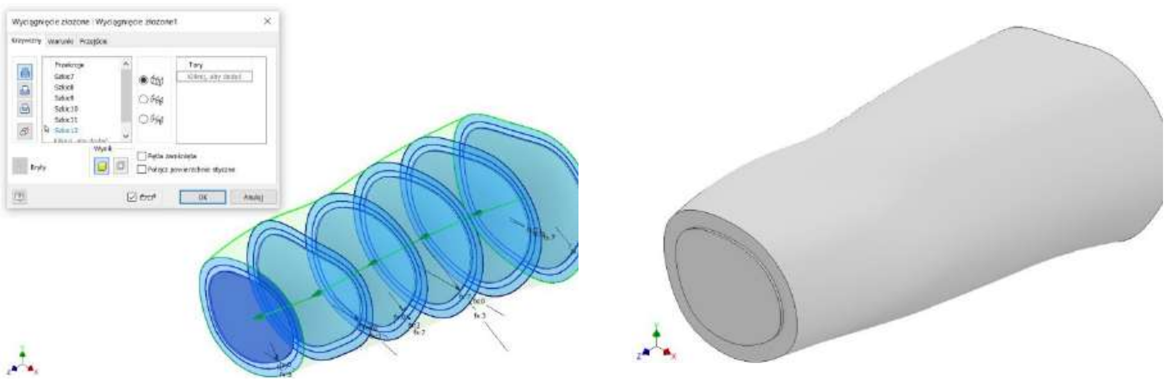

Figure 11 Execution of the Loft operation (A) and the resulting solid (B)

This project has been funded with support from the Iceland Liechtenstein Norway Grants. This publication [communication] reflects the views only of the authors, and the Commission cannot be held responsible for any use which may be made of the information contained therein.

Then, by performing the Loft operation again, this time in Cutout mode, the inner part of the solid was cut out (Figure 12).

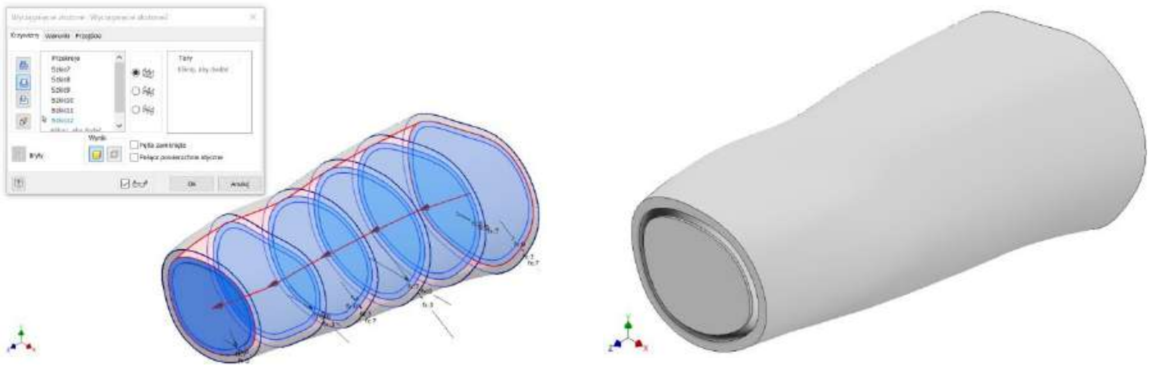

Figure 12 Execution of the Loft operation in Cutout mode (A) and the resulting solid (B)

At the last stage of generating the basic geometry of the prosthetic socket, its end was modeled. To do this, two Close Boundary operations were performed with a tangency condition assigned a parameter named boundary_close. As a result, two convex construction surfaces were generated, defined by the outer and inner edges of the geometry, respectively (Figure 13A). In addition, the Sculpture operation was performed, which resulted in generating a solid bounded by two surfaces of the envelope closure (Figure 13B).

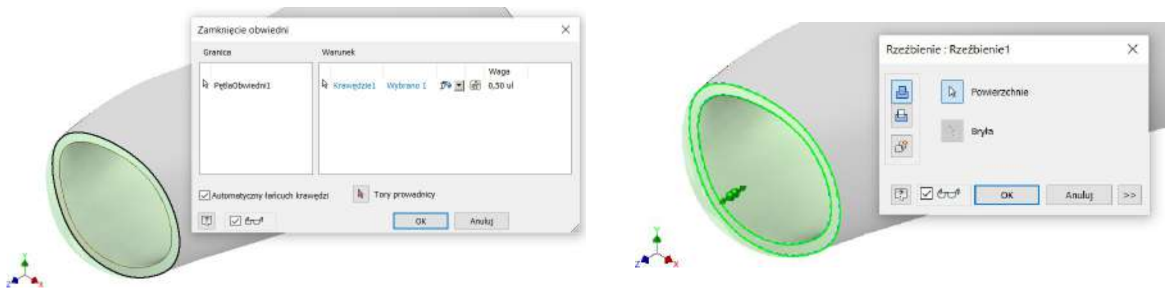

Figure 13 Perform a Close Boundary operation (A) and a Sculpture operation (B)

The next step was to model the geometry of the compression pads (the compression part of the socket) using the Loft operation in the New Solid mode, through previously created sketches. Then, a Loft operation was performed in Cutout mode based on the curves defining the thickness of the inserts (Figure 14A). The result was a second body with a wall thickness equal to that of the compression pads (Figure 14B).

This project has been funded with support from the Iceland Liechtenstein Norway Grants. This publication [communication] reflects the views only of the authors, and the Commission cannot be held responsible for any use which may be made of the information contained therein.

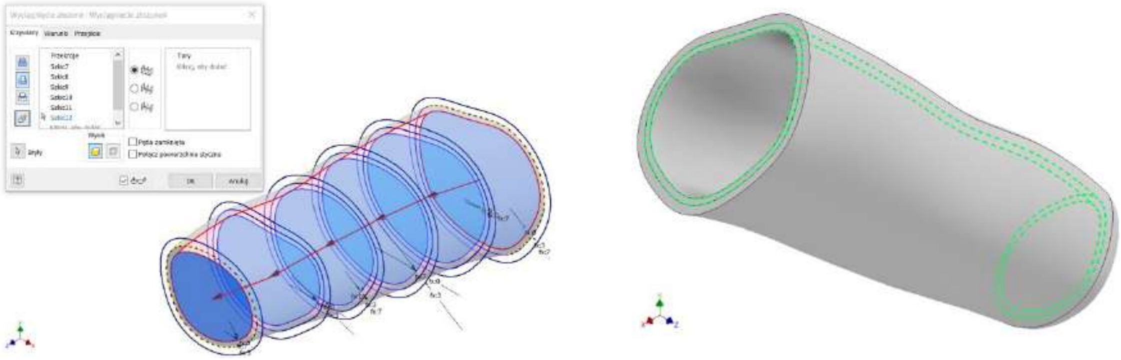

Figure 14 Execution of the Loft operation in Cutout mode (A) and the resulting solid (B)

In the next step, four holes were made to accommodate the tissue compressed by the inserts (relaxation part of the socket). For this purpose, two work planes were created using the Parallel to plane through point function, where Work Point 1 and the YZ and XZ planes were used as references in both cases. Four sketches were then created, with the reference points being two work points #1 and #6. Cuts were made in both solids using asymmetric Revolve operations in Cutout mode (Figure 15). Using the asymmetry mode gives you the ability to modify the size of the hole in two directions from the plane on which the sketch is located.

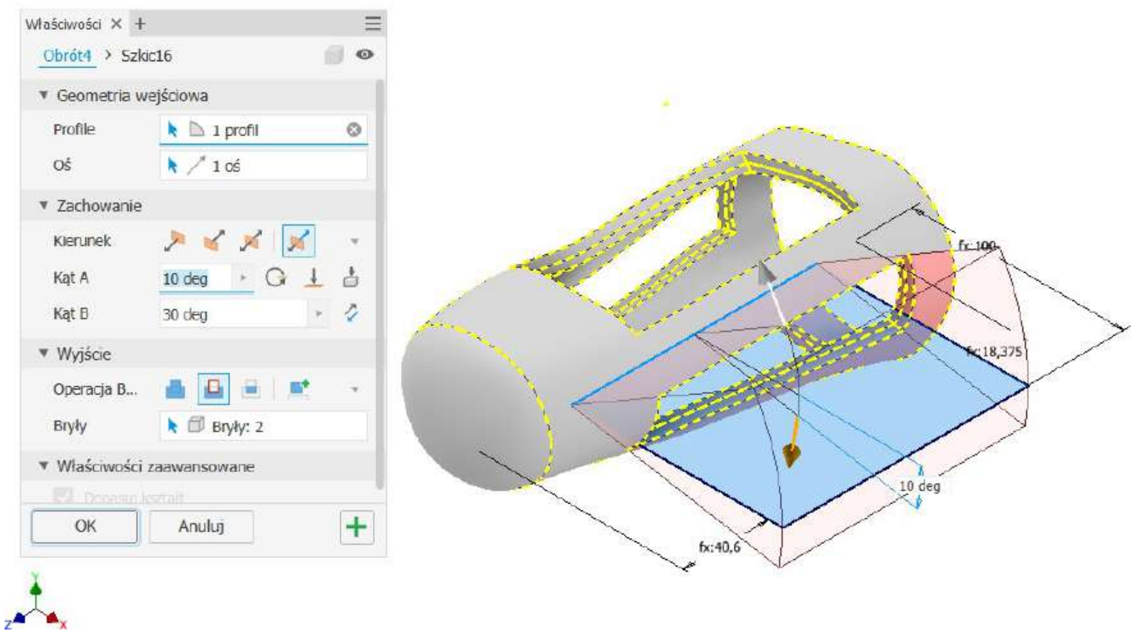

Figure 15 Making a hole using the Revolve operation

This project has been funded with support from the Iceland Liechtenstein Norway Grants. This publication [communication] reflects the views only of the authors, and the Commission cannot be held responsible for any use which may be made of the information contained therein.

The dimensions that define the sketches are assigned user parameters - they are calculated using rules implemented in the Excel spreadsheet.

Then, two Extrude operations were performed in Cut-out mode, trimming the compression pads to the length of the hole on the inside of the socket. In the next step, roundings of the geometry of the inserts and holes were created. Then, using the Create Combination function, the two solids were joined together and the rest of the fillets were made. As a result, the finished socket geometry was obtained (Figure 16).

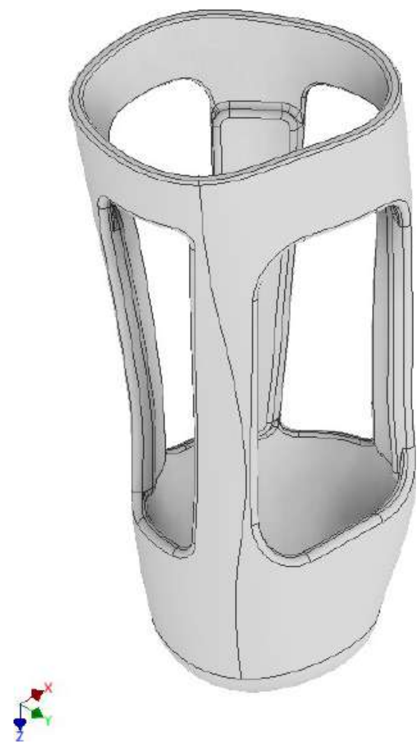

Figure 16 Modeled geometry of the prosthetic socket

The next step was to connect the CRS socket with the forearm. For this purpose, two solutions by making a version with universal mounting and the possibility of disabling the built-up bottom (Figure 17A) and with a version with recessed mounting (Figure 17B).

This project has been funded with support from the Iceland Liechtenstein Norway Grants. This publication [communication] reflects the views only of the authors, and the Commission cannot be held responsible for any use which may be made of the information contained therein.

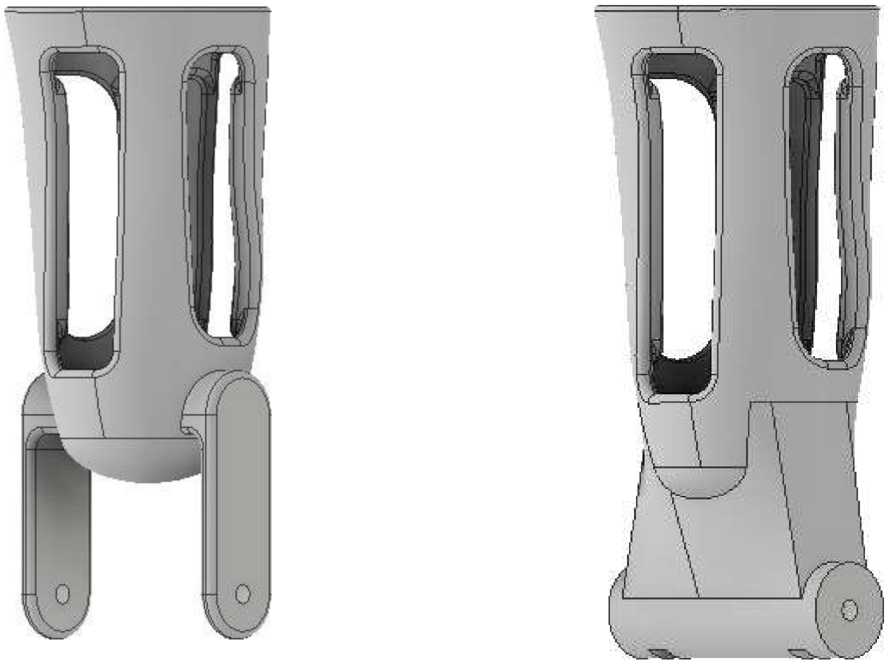

Figure 17 CRS sockets obtained as a result of analogous operations: A: with universal fastening; B: with flush mount

2.3.2 Forearm

The modular model of the prosthesis assumes the possibility of personalization and generating its modified variants. As part of this work, a model of the open forearm - dedicated to children and the closed forearm - for adults was presented. This is related to the load imposed by the user. The spatial form of the forearms is created by a complex extrusion, connecting two cross-sections - the first showing a rectangle with rounded corners and the second - its offset version, defined by the offset parameter. You can manipulate the parameter while keeping the width of the first sketch constant. Therefore, the parameter dimension_j was also introduced to the geometry of the forearms, matching it to the designed adapters. However, the offset parameter (Figure 18) was retained, enabling the automatic generation of a second cross-section proportional to the wrist, distanced by the length of the Forearm determined on the basis of the spatial scan (also the output parameter from the original supply sheet).

This project has been funded with support from the Iceland Liechtenstein Norway Grants. This publication [communication] reflects the views only of the authors, and the Commission cannot be held responsible for any use which may be made of the information contained therein.

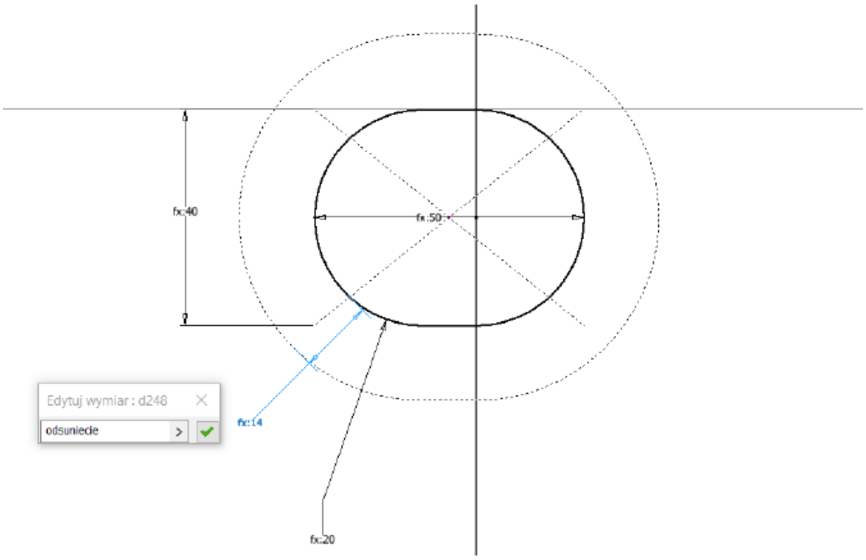

Figure 18 Base for forearm geometry

The introduction of a universal dimension then made it possible to associate other design features with it, such as e.g. joint spacing. Parameters describing other geometrical features, such as an indentation in the bottom wall, were also combined to proportionally change their size as the length of the component changes (Figure 20A). The dimension of additional extrusions used for assembly with a prosthetic socket was also increased, changing the radius of the element from 9 to 12 mm (Figure 20B) and the dimension of the diameter of the mounting hole was parameterized (, currently equal to 5.2 mm).

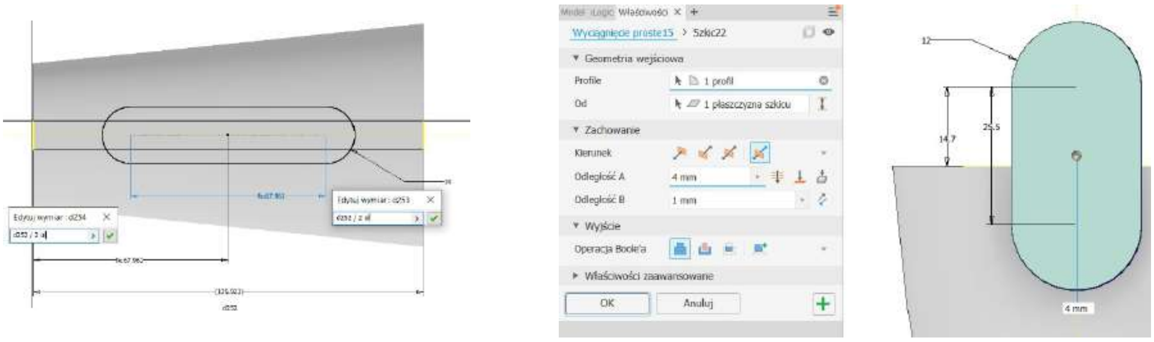

Figure 19 A: Relationship between the length of the Forearm and the dimensions of the notch in the bottom wall. B: Widening of the forearm assembly parts

This project has been funded with support from the Iceland Liechtenstein Norway Grants. This publication [communication] reflects the views only of the authors, and the Commission cannot be held responsible for any use which may be made of the information contained therein.

Then, three more variants of the Forearm were made, taking into account the assembly of adapters. They include a forearm in the classic open version with an appropriate tip, a forearm with a structure closed from the outside but empty inside (eliminating the operation of cutting in the upper and lower walls) and a completely built-up body.

The indentation in the tip dedicated to the assembly of the adapter was made at the initial stage of modeling the forearms, just before the use of the shell operation hollowing out the element from the inside. On the surface described by the base sketch, another one was added, on which the parameterized sketch of the external frame of the adapter was mapped. Then, it was moved away by 0.5 mm, designing the necessary clearance between the components, and a cutout was made in the solid at a distance of 22 mm, i.e. to the height of the adapter (Figure 21).

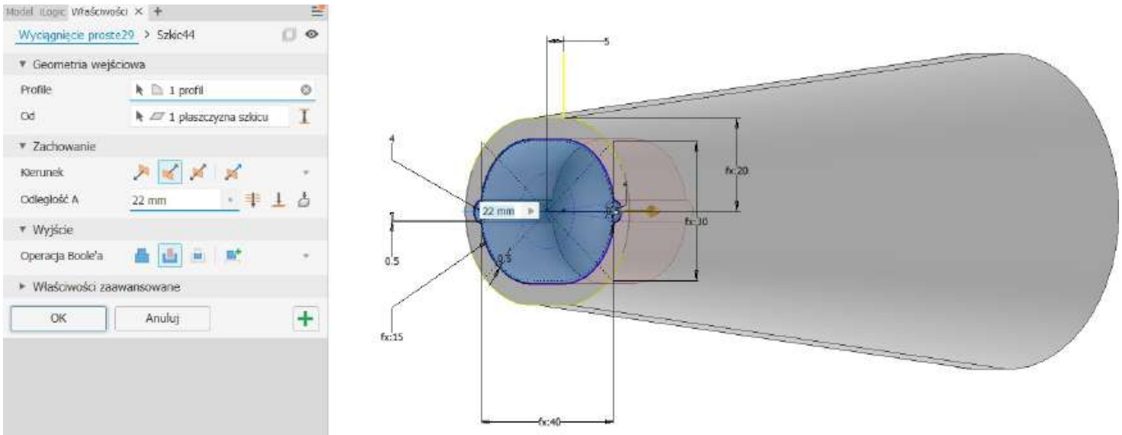

Figure 20 Designing geometry dedicated to the connection with the adapter - a cutout in the base solid

Further operations were performed at the end of modeling - a hole was designed for the convex part of the adapter, keeping 1 mm of clearance from the top and sides of the tab, a locking hole was made in the surface of the element and a widened indentation in the top

This project has been funded with support from the Iceland Liechtenstein Norway Grants. This publication [communication] reflects the views only of the authors, and the Commission cannot be held responsible for any use which may be made of the information contained therein.

wall, which provides additional space for the protruding part of the thermoplastic fiber fixing the smaller element inside the adapter.

These operations made it possible to obtain a matching tip to the adapter introduced at the start. Similar steps were then performed for the closed and fully closed forearm. The first of the built-up forearms has retained the form of a classic component. However, the operation of making cuts along the upper structure and in the lower part of the element was eliminated from its construction (Figure 22).

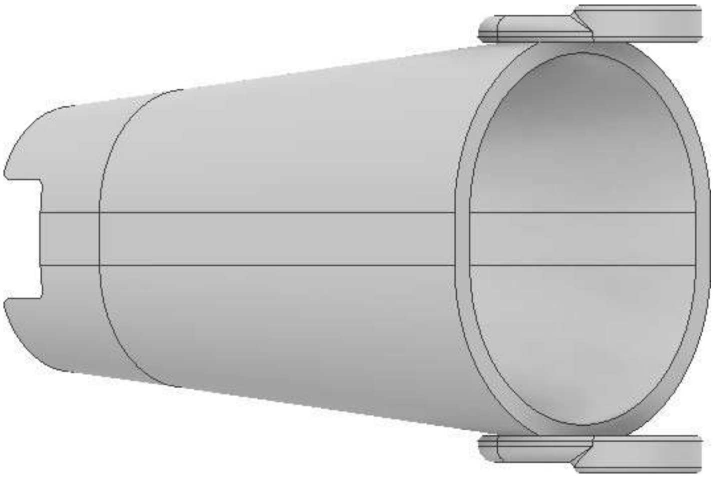

Figure 21 Closed forearm form

2.3.3 End effector

A C-handle was proposed as the effector, based on a simple horseshoe-shaped sketch (Figure 22).

This project has been funded with support from the Iceland Liechtenstein Norway Grants. This publication [communication] reflects the views only of the authors, and the Commission cannot be held responsible for any use which may be made of the information contained therein.

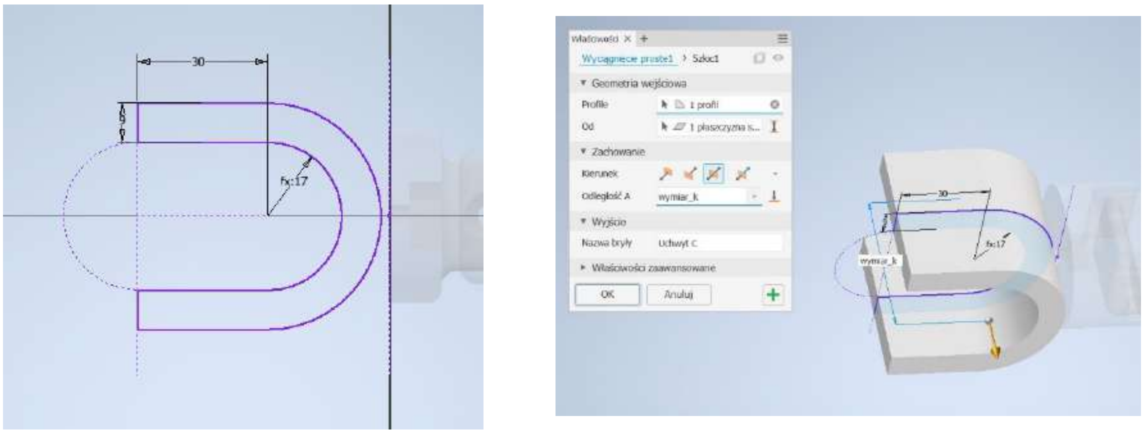

Figure 22 Start modeling the effector: A: sketch; B: straight pull out

An opening was then created to allow access to the mounting hardware of the adapter connecting the handle to the forearm (Figure 23).

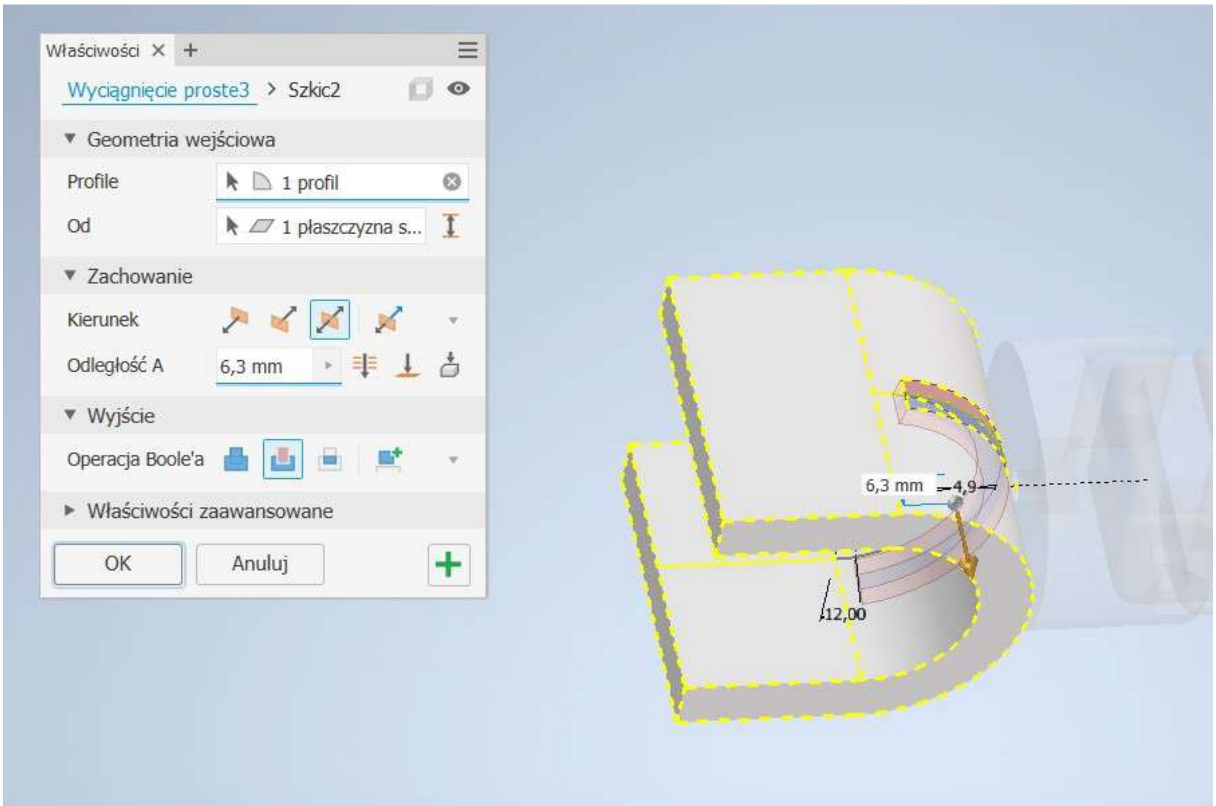

Figure 23 Opening for access to connecting elements

This project has been funded with support from the Iceland Liechtenstein Norway Grants. This publication [communication] reflects the views only of the authors, and the Commission cannot be held responsible for any use which may be made of the information contained therein.

The next stage of work was to tilt the walls and round all sharp edges (Figure 24).

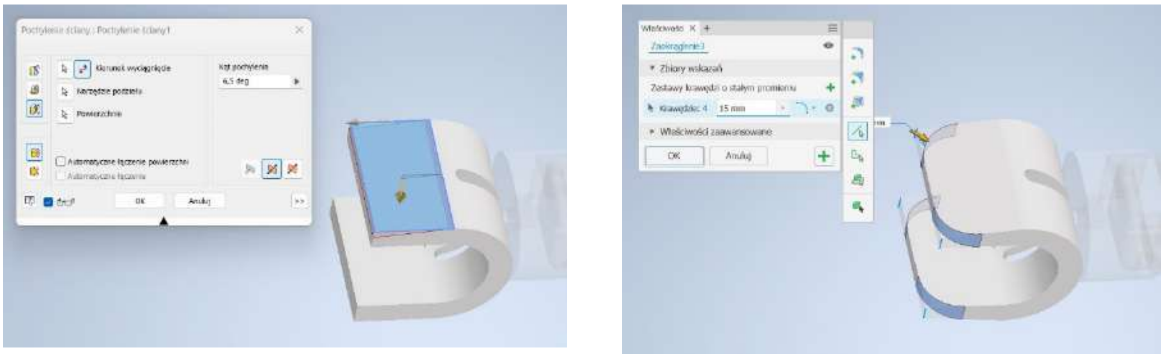

Figure 24 Successive stages of the formation of the effector: A: inclination of the walls, B: rounding of the walls

The last stage was to model the element connecting the handle with the forearm using the extrude function on a previously prepared sketch (Figure 25).

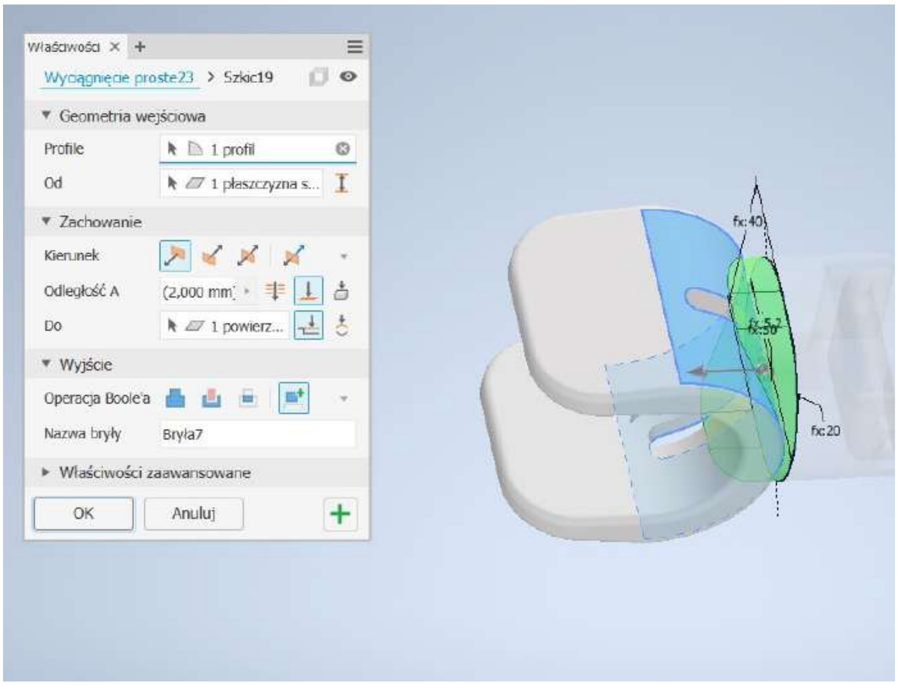

Figure 25 Connecting element to the wrist (extrude a previously prepared sketch)

This project has been funded with support from the Iceland Liechtenstein Norway Grants. This publication [communication] reflects the views only of the authors, and the Commission cannot be held responsible for any use which may be made of the information contained therein.

Depending on the application, various effectors have been prepared, which, thanks to parameterization, form a coherent whole with other components, enabling each time tailored construction variants.

2.4 Final version of bicycle prosthesis

The modular prosthesis was generated using an generative (intelligent) model prepared for pediatric cases (Figure 26). The resulting model had to be adapted to the requirements of an adult user.

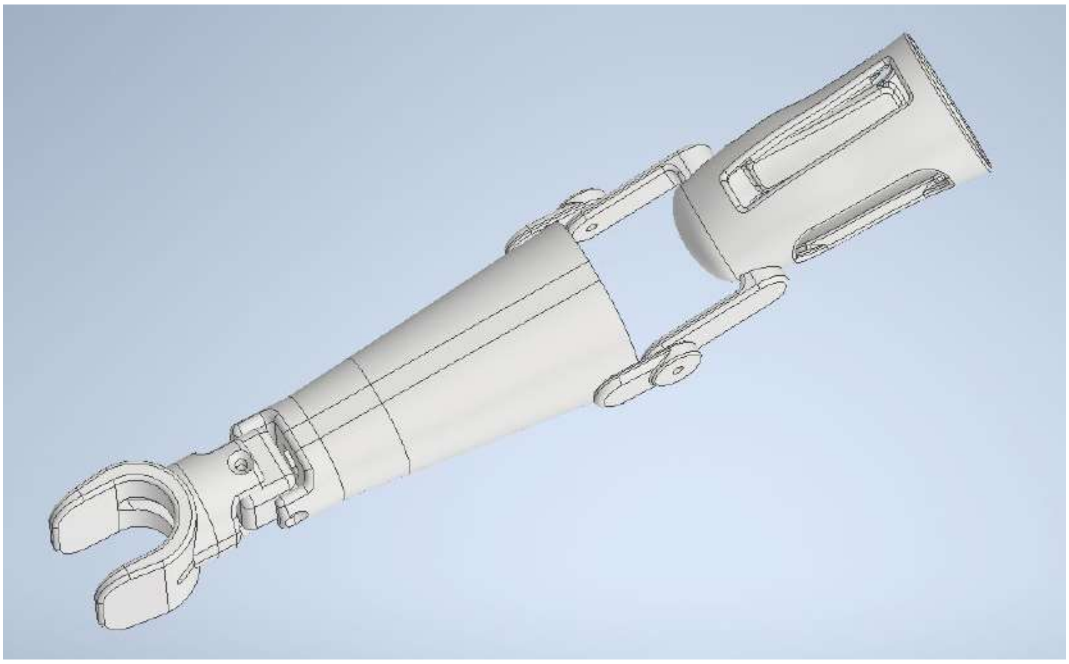

Figure 26 The effect of work of intelligent model - bicycle prosthesis for a child

First, the model was adjusted to the adult patient by 3D scanning and using functionalities of the intelligent model to re-create the geometry. Resulting prosthesis was 3D printed, assembled and tested by the patient (Figure 27).

This project has been funded with support from the Iceland Liechtenstein Norway Grants. This publication [communication] reflects the views only of the authors, and the Commission cannot be held responsible for any use which may be made of the information contained therein.

Figure 27 Prosthesis made for a selected adult patient – test with the bicycle

In the course of numerous tests and subsequent design iterations, the following modifications have been introduced:

- The CRS socket was modified as a result of removing the movable connection in the elbow joint. It was connected to the forearm rigidly due to too much load in the case of an adult - the proposed movable connection used in the case of children's prostheses was breaking.
- The mounting plane was moved away from the tip of the socket to a properly selected distance. A circular sketch was made on the plane with dimensions to match the forearm, and then a loft operation was performed between the assembly plane and the selected socket section to achieve a smooth transition between the solids. These operations were performed before soft tissue cuts in the socket structure, because the

This project has been funded with support from the Iceland Liechtenstein Norway Grants. This publication [communication] reflects the views only of the authors, and the Commission cannot be held responsible for any use which may be made of the information contained therein.

solid reached higher than the planned relaxation holes. Finally, mounting hardware was added to allow connection to the forearm (Figure 28).

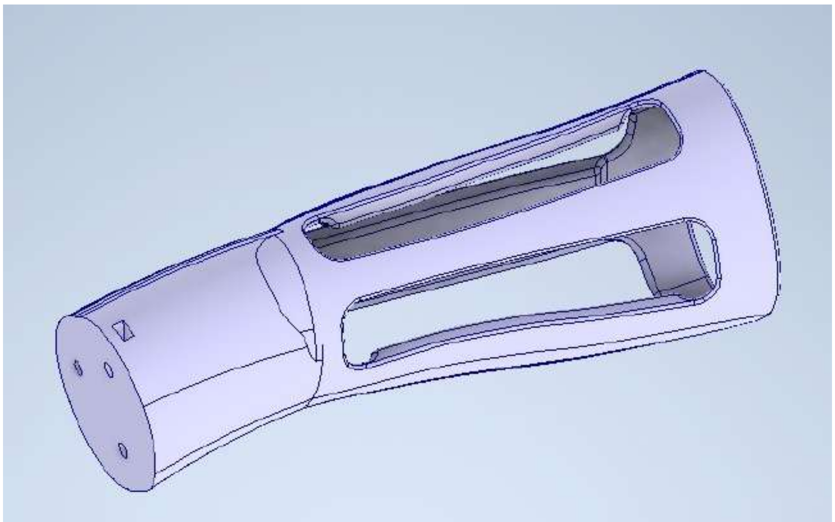

Figure 28 The final form of the CRS socket for an adult adapted to cycling

- Forearm - the model has been changed as a result of abandoning the movable joint in the elbow joint. In addition, its termination was modeled by using the function Close envelope with tangency condition. Finally, five mounting holes and two access holes were added (Figure 29).

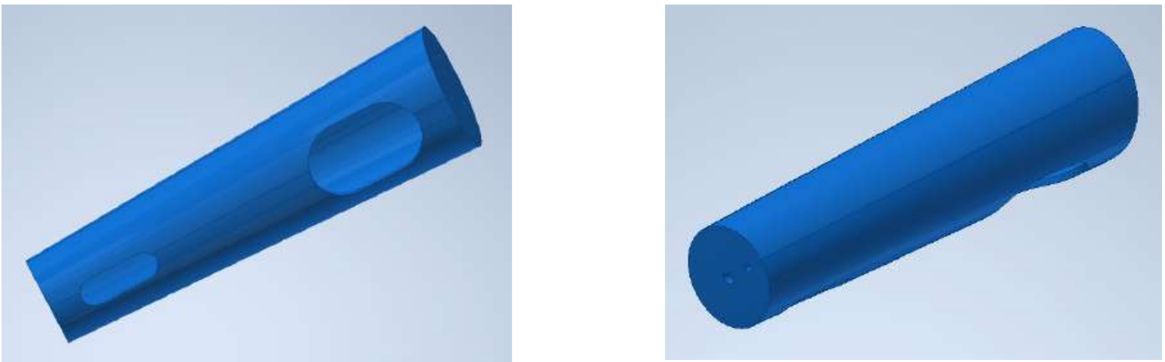

Figure 29 The final form of the forearm for an adult adapted to cycling

This project has been funded with support from the Iceland Liechtenstein Norway Grants. This publication [communication] reflects the views only of the authors, and the Commission cannot be held responsible for any use which may be made of the information contained therein.

- The C-handle has been modified by extending the jaws and narrowing the distance between them. These changes were introduced after listening to Mr. Maciej's comments - they increased the stability and comfort of cycling. In addition, the connection used in the wrist was abandoned - the lack of a joint resulted in an increase in stiffness with the simultaneous impossibility of rotation. This was possible after adjusting the angles for a given patient and his bike.

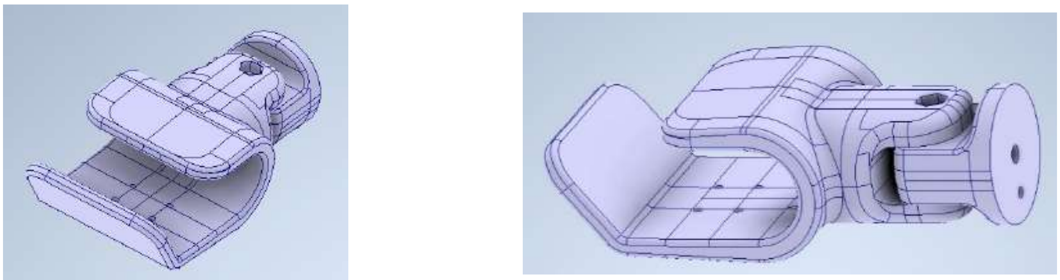

Figure 30 The final form of the C handle for an adult adapted to cycling

Figure 31 presents a complete model of the prosthesis prepared for an adult and adapted for cycling.

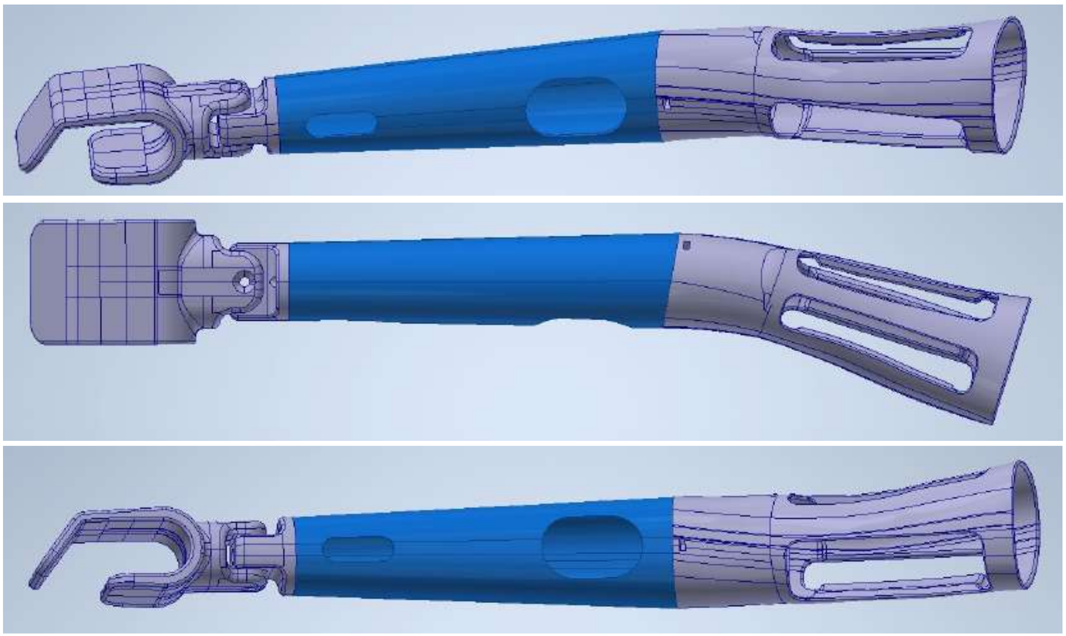

Figure 31 The final model of an adult bicycle prosthesis. View: A: Isometric; B: from above; B: from the side

This project has been funded with support from the Iceland Liechtenstein Norway Grants. This publication [communication] reflects the views only of the authors, and the Commission cannot be held responsible for any use which may be made of the information contained therein.

2.5 Design of electronic part of the biomechatronic prosthesis

2.5.1 Main concept of the mechatronic prosthesis

The aim of the work was to modify the hand prosthesis in order to create a biomechatronic device, used by human, with monitoring of activities performed in the prosthesis (mostly cycling or similar activities). Main aim was placing an electronic measuring system in the prosthesis, thanks to which it would be possible to determine its operating properties. The detailed purposes of the built electronic system were to:

- measurement of the orientation of the upper limb prosthesis in space,

- measurement of the force exerted in the wrist,

- saving data on the SD card.

The device consisted of the following components:

- microcontroller module (Arduino NANO),

- force sensor measuring amplifier module (HX711 with force sensor up to 200N),

- inertial sensor module (BOSCH BNO055),

- SD card module,

- power source (a USB connected powerbank).

The components were selected to fulfil their role in the simplest possible manner, ensuring robust operation, steady and stable communication, as well as maintaining as low price as possible (as the whole prosthesis is also a low-cost project). The schematic diagram of the designed device is shown in the Figure 32.

This project has been funded with support from the Iceland Liechtenstein Norway Grants. This publication [communication] reflects the views only of the authors, and the Commission cannot be held responsible for any use which may be made of the information contained therein.

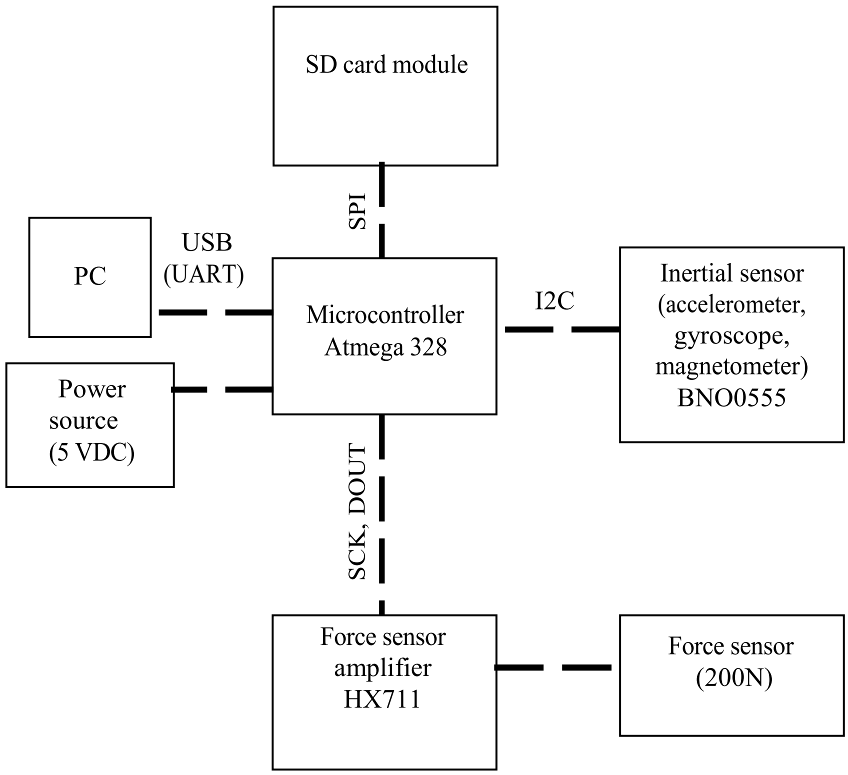

Figure 32 The schematic diagram of the electronic part of the prosthesis

2.5.2 Design modifications in biomechatronic prosthesis

The final mechanical version of the prosthesis was first manufactured and tested by the patient to confirm its usefulness. Then, another set of requirements were introduced – namely, to be able to fit the electronics of the prosthesis inside it, in a manner allowing steady riding on a bicycle or similar device, without risk of disconnecting or otherwise damaging the components, as well as not making them disturb the patient during the activities.

The following main changes have been introduced to the design:

- the forearm was modified to enable mounting of the microcontroller, inertial sensor and SD card module inside cavities of the forearm – insets were created with holes, for self-tapping purposes (Figure 33)

This project has been funded with support from the Iceland Liechtenstein Norway Grants. This publication [communication] reflects the views only of the authors, and the Commission cannot be held responsible for any use which may be made of the information contained therein.

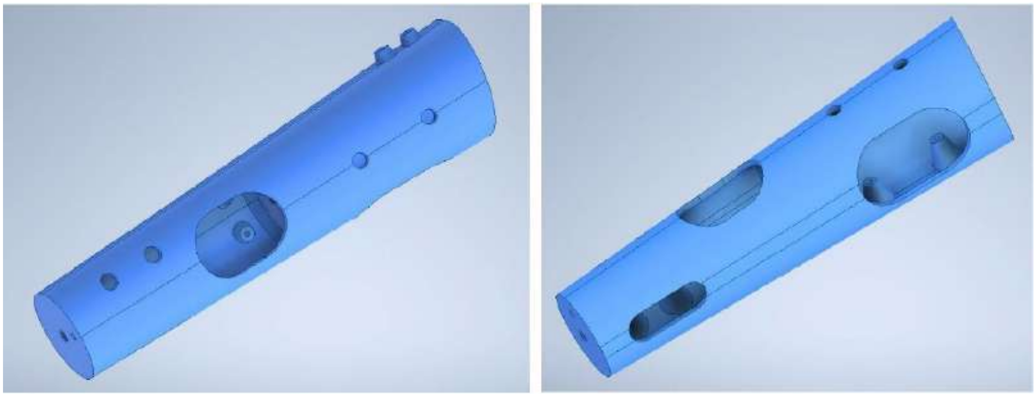

Figure 33 Modified forearm – visible mounting places for electronic components

- at the joint of forearm and CRS socket, insets were added for mounting of the force sensor (beam) – the place (elbow) was selected to easily detect the torques and forces during the bicycle ride
- a number of assembly holes and cable feedthroughs were added to enable unproblematic assembly of the electronic part inside the prosthesis.

Final version of the CAD model of the prosthesis is shown in Figure 34.

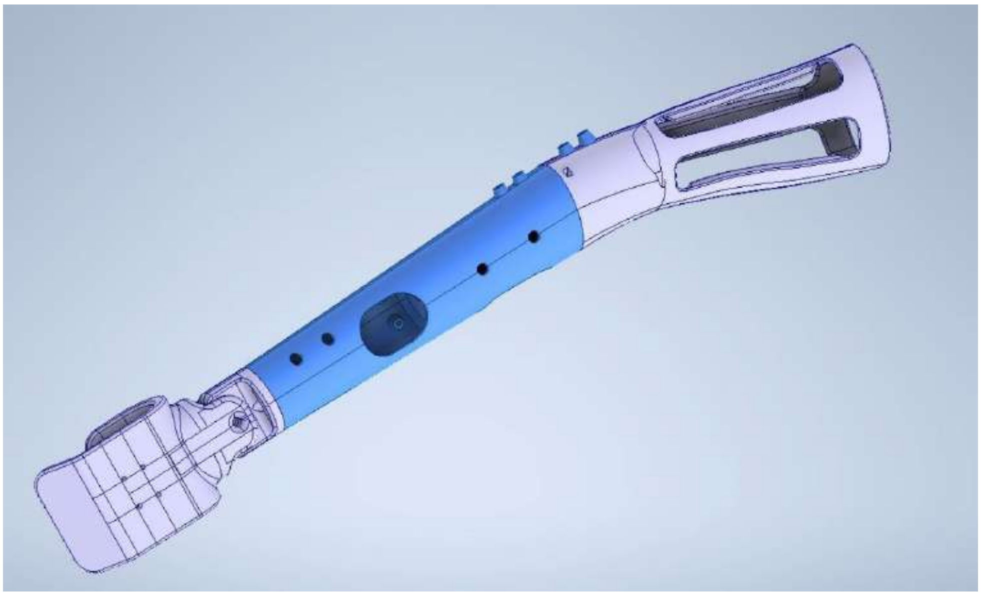

Figure 34 Final CAD model of the biomechatronic bicycle prosthesis

This project has been funded with support from the Iceland Liechtenstein Norway Grants. This publication [communication] reflects the views only of the authors, and the Commission cannot be held responsible for any use which may be made of the information contained therein.

3 Summary

In this toolkit, it was shown how a modular model of a low-cost 3D printed bicycle prosthesis can be designed and then converted into a simple biomechatronic device, equipped with sensors for biometrics of the bicycle ride activity. The toolkit is a part of the set of instructions, focused on the prosthesis model. The resulting model was 3D printed in further steps and then assembled, tested in laboratory conditions and then in real conditions, with the patient – this is described in other toolkits of the EMERALD project.

Literature

1. Górski, F., Wichniarek, R., Kuczko, W., Żukowska, M., Rybarczyk, J., & Lulkiewicz, M. (2022). Evaluation of a Prototype System of Automated Design and Rapid Manufacturing of Orthopaedic Supplies. In Advances in Manufacturing III: Volume 5-Biomedical Engineering: Research and Technology Innovations, Industry 4.0 (pp. 1-15). Cham: Springer International Publishing.
2. Górski, F., Wichniarek, R., Kuczko, W., & Żukowska, M. (2021). Study on properties of automatically designed 3d-printed customized prosthetic sockets. Materials, 14(18), 5240.
3. Komorowska O., 2022, Automation of design of modular upper limb prosthesis, Master's Thesis (supervision: Górski F.), Poznan University of Technology
4. Słupińska S., 2021, Automation of design of low-cost upper limb cosmetic prostheses, Master's Thesis (supervision: Górski F.), Poznan University of Technology

EMERALD

The Education, Scholarships, Apprenticeships and Youth Entrepreneurship

EUROPEAN NETWORK FOR 3D PRINTING OF BIOMIMETIC MECHATRONIC SYSTEMS

E-toolkit
Computer Aided Engineering

Project Title	**European network for 3D printing of biomimetic mechatronic systems 21-COP-0019**
Output	**O2 – E-toolkit for teaching purposes, basic knowledge about realizing biomimetic mechatronic systems**
Module	**Computer Aided Engineering (CAE)**
Authors	**Dan-Sorin COMȘA, Răzvan PĂCURAR**

This project has been funded with support from the Iceland Liechtenstein Norway Grants. This publication [communication] reflects the views only of the authors, and the Commission cannot be held responsible for any use which may be made of the information contained therein.

Contents

This project has been funded with support from the Iceland Liechtenstein Norway Grants. This publication [communication] reflects the views only of the authors, and the Commission cannot be held responsible for any use which may be made of the information contained therein.

1. Introduction

The objective of this application is to evaluate the strength characteristics of an upper-limb prosthesis (Fig. 1) by simulating a distal tensile test with the finite element analysis (FEA) module SolidWorks Simulation [WWW2022b] included in the SolidWorks CAD package [WWW2022a]. The principle of the test is shown in Figure 2. As one may notice, the prosthesis is subjected to a distal traction load after being firmly attached to a rigid support that fits inner surfaces of the upper arm. The traction load gradually increases from 0 (zero) to 750 N.

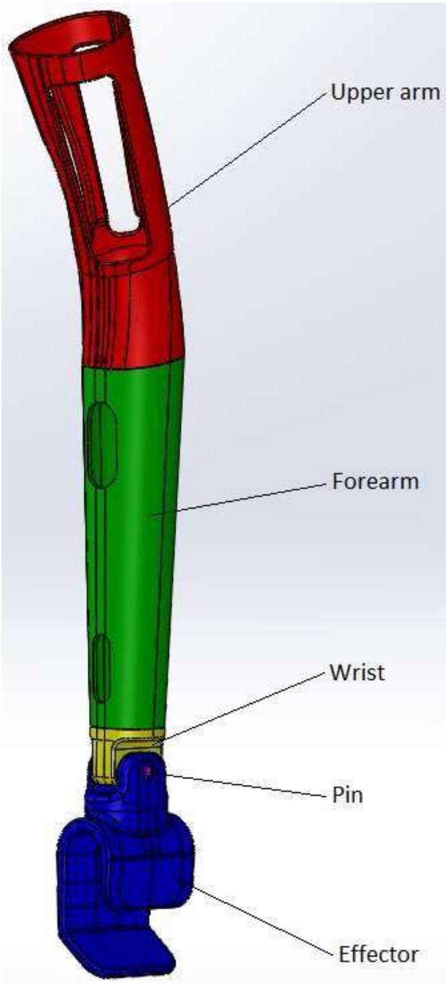

Figure sthesis

This project has been funded with support from the Iceland Liechenstein Norway Grants. This publication [communication] reflects the views only of the authors, and the Commission cannot be held responsible for any use which may be made of the information contained therein.

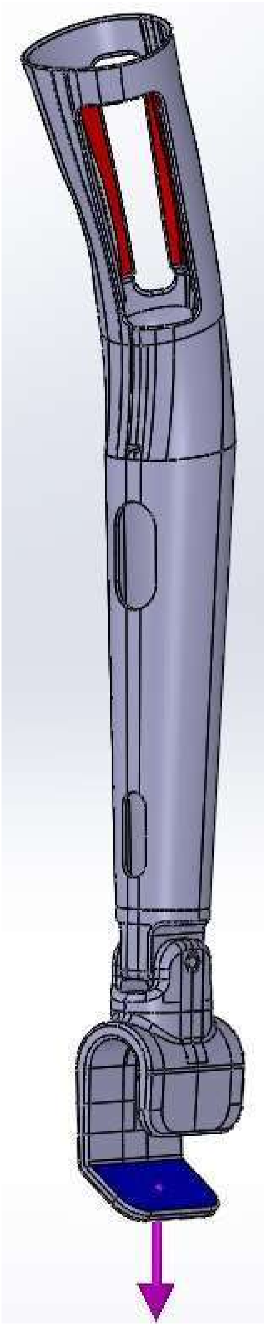

Figure 2: Principle of the distal tensile test simulated for evaluating the strength characteristics of the upper-limb prosthesis (red surfaces – regions where the upper arm is firmly attached to a rigid support; blue surface – support of the traction load)

This project has been funded with support from the Iceland Liechtenstein Norway Grants. This publication [communication] reflects the views only of the authors, and the Commission cannot be held responsible for any use which may be made of the information contained therein.

The following hypotheses are adopted when preparing the finite element model of the tensile test:

- The prosthesis components are made of PETG exhibiting an isotropic linear elastic behavior. Table 1 lists the physical and mechanical properties of this material that are relevant for the finite element model of the tensile test.
- The prosthesis components are bonded together along their contact surfaces.

Table 1: Physical and mechanical properties of PETG [Kan2020]

Mass density ρ [kg/m^3]	Elastic modulus E [MPa]	Poisson's ratio ν [-]	Yield strength Y [MPa]
1270	1660	0.419	30.3

The input files needed for preparing the finite element model of the tensile test are stored in the folder *Upper-limb prosthesis FEA*:

Upper arm.SLDPRT – 3D model of the upper arm (Fig. 1)
Forearm.SLDPRT – 3D model of the forearm (Fig. 1)
Wrist.SLDPRT – 3D model of the wrist (Fig. 1)
Effector.SLDPRT – 3D model of the effector (Fig. 1)
Pin.SLDPRT – 3D model of the pin (Fig. 1)
Upper-limb prosthesis.SLDASM – 3D model of the prosthesis (Fig. 1)
EMERALD CAE Materials.sldmat – custom library storing the physical and mechanical properties of PETG listed in Table 1.

The selection set *Selection-Set1(10) Upper arm - Fixed* (defined in the file *Upper-limb prosthesis.SLDASM*) collects the surfaces where the upper arm is firmly attached to the rigid support.

The displacement (deflection), force and stress quantities manipulated by the FEA model are expressed using the following measurement units: displacement (deflection) – millimeter [mm]; force – Newton [N]; stress – megapascal [MPa] (1 MPa = 1 N/mm^2).

The next sections of this documentation describe the preparation of the FEA model and the interpretation of the numerical results.

This project has been funded with support from the Iceland Liechenstein Norway Grants. This publication [communication] reflects the views only of the authors, and the Commission cannot be held responsible for any use which may be made of the information contained therein.

2. Preparation of the finite element model

The FEA model of the tensile test (Fig. 2) is developed by performing the following steps:

a) Open the *Upper-limb prosthesis.SLDASM* model in SolidWorks (Fig. 3).

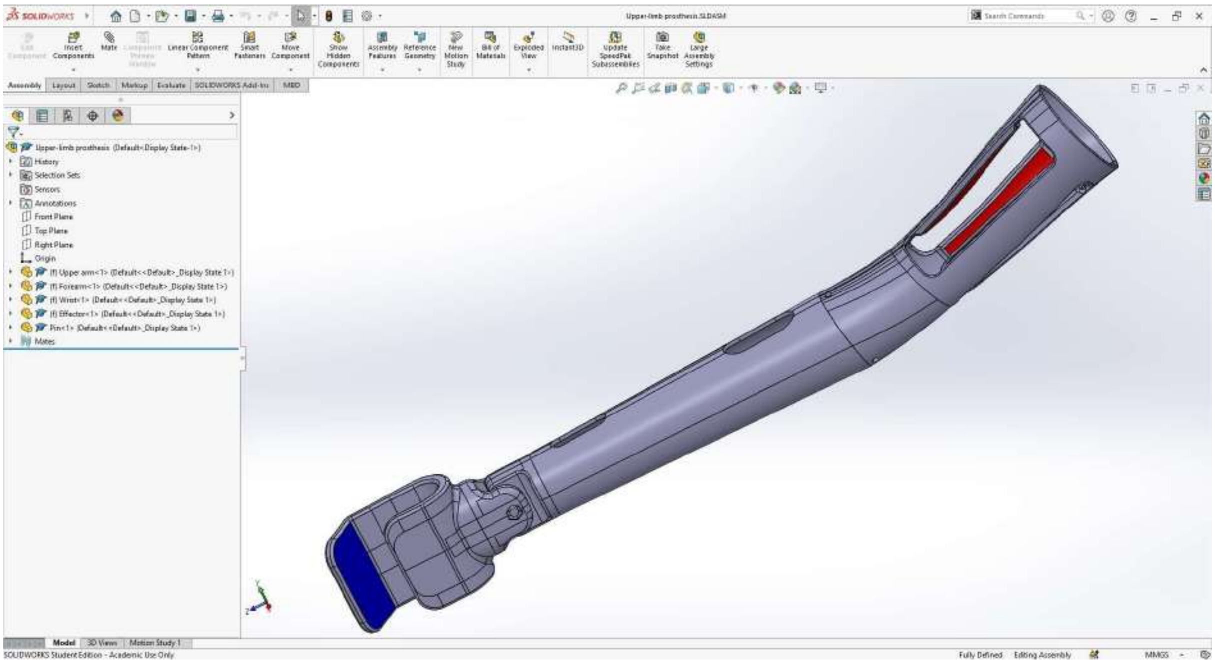

Figure 3: *Upper-limb prosthesis.SLDASM* model open in SolidWorks

b) Activate the SolidWorks Simulation module by accessing the “SOLIDWORKS Add-Ins” tab of the “Command Manager” toolbar (Fig. 4) and pressing the “SOLIDWORKS Simulation” button (Fig. 5). Consequently, the “Simulation” tab is included in the “Command Manager” toolbar (Fig. 6).

c) Change some working parameters of the SolidWorks Simulation module by accessing the “Simulation” menu and selecting the “Options…” command (Fig. 7). Consequently, the “System Options – General” window is displayed. In the “Default Options” panel, select the SI (MKS) unit system, then change the following measurement units: length/displacement [mm] and pressure/stress [N/mm^2] (Fig. 8).

This project has been funded with support from the Iceland Liechenstein Norway Grants. This publication [communication] reflects the views only of the authors, and the Commission cannot be held responsible for any use which may be made of the information contained therein.

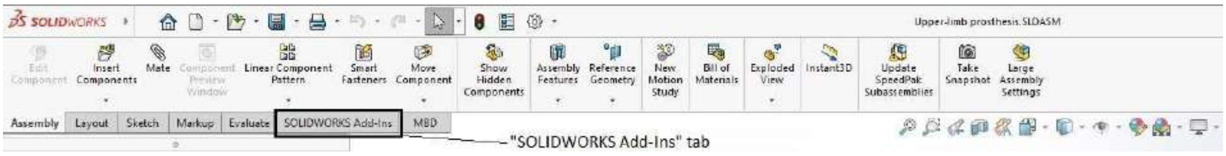

Figure 4: “SOLIDWORKS Add-Ins” tab in the “Command Manager” toolbar

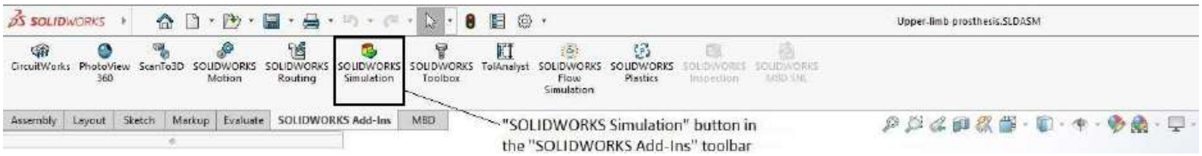

Figure 5: “SOLIDWORKS Simulation” button in the “SOLIDWORKS Add-Ins” toolbar

Figure 6: “Simulation” tab included in the “Command Manager” toolbar after the activation of the SolidWorks Simulation module

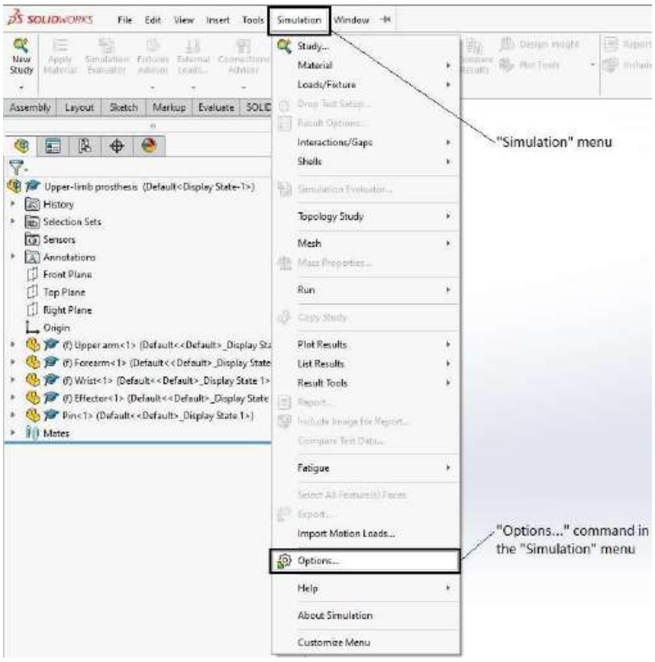

Figure 7: “Options…” command in the “Simulation” menu

This project has been funded with support from the Iceland Liechtenstein Norway Grants. This publication [communication] reflects the views only of the authors, and the Commission cannot be held responsible for any use which may be made of the information contained therein.

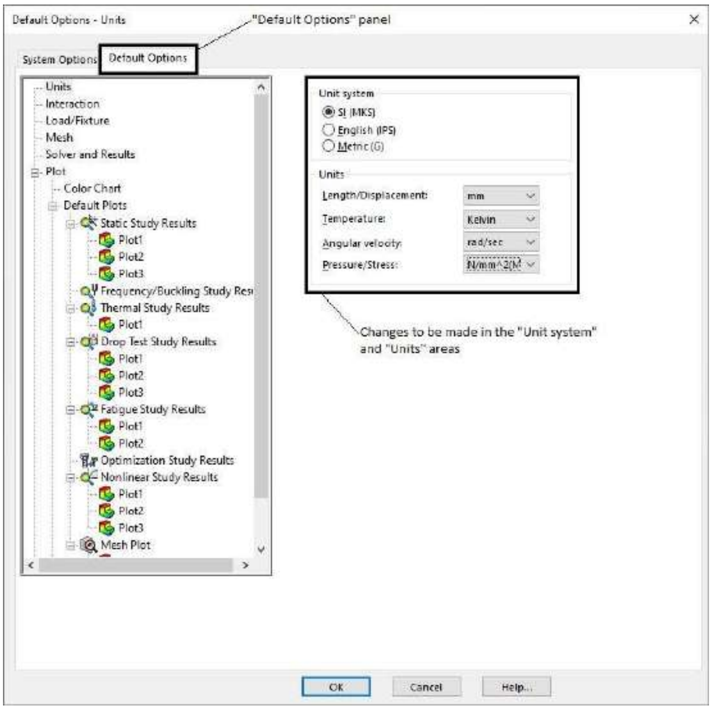

Figure 8: Changes to be made in the “Default Options” panel of the “System Options – General” window

d) Add the folder *Upper-limb prosthesis FEA* to the list of places where SolidWorks looks for material libraries by accessing the “Tools” menu and selecting the “Options…” command (Fig. 9). Consequently, the “System Options – General” window is displayed. In the “System Options” panel, select the “File Locations” entry (Fig. 10). Unroll the “Show folders for:” drop-down list and select the “Material Databases” item (Fig. 11). After pressing the “Add…” button (Fig. 12), the “Select Folder” window is displayed on the screen (Fig. 13). Look for the folder *Upper-limb prosthesis FEA*, select it and press the “Select Folder” button placed at the bottom of the “Select Folder” window (Fig. 13). Press the “OK” buttonplaced at the bottom of the “System Options – General” window (Fig. 14).
e) Enter the “Simulation” toolbar and press the “New Study” button (Fig. 15) to create a FEA model having the following characteristics (Fig. 16):
   - name of the FEA model: “Static 1”
   - type of the FEA model: “Static”.

   Press the “OK” button placed at the upper-left corner of the “Study” window (Fig. 16).

This project has been funded with support from the Iceland Liechenstein Norway Grants. This publication [communication] reflects the views only of the authors, and the Commission cannot be held responsible for any use which may be made of the information contained therein.

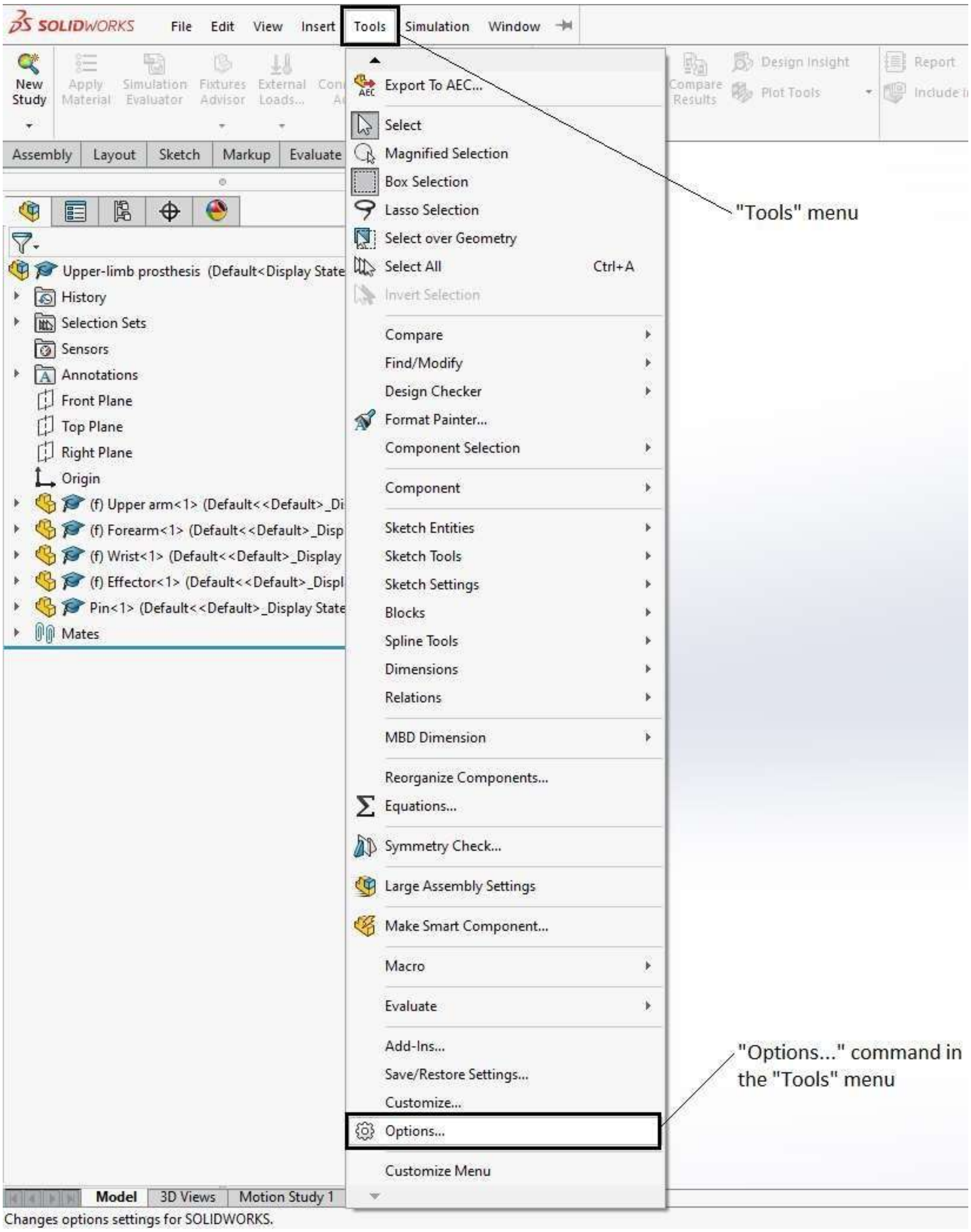

Figure 9: “Options...” command in the “Tools” menu

This project has been funded with support from the Iceland Liechenstein Norway Grants. This publication [communication] reflects the views only of the authors, and the Commission cannot be held responsible for any use which may be made of the information contained therein.

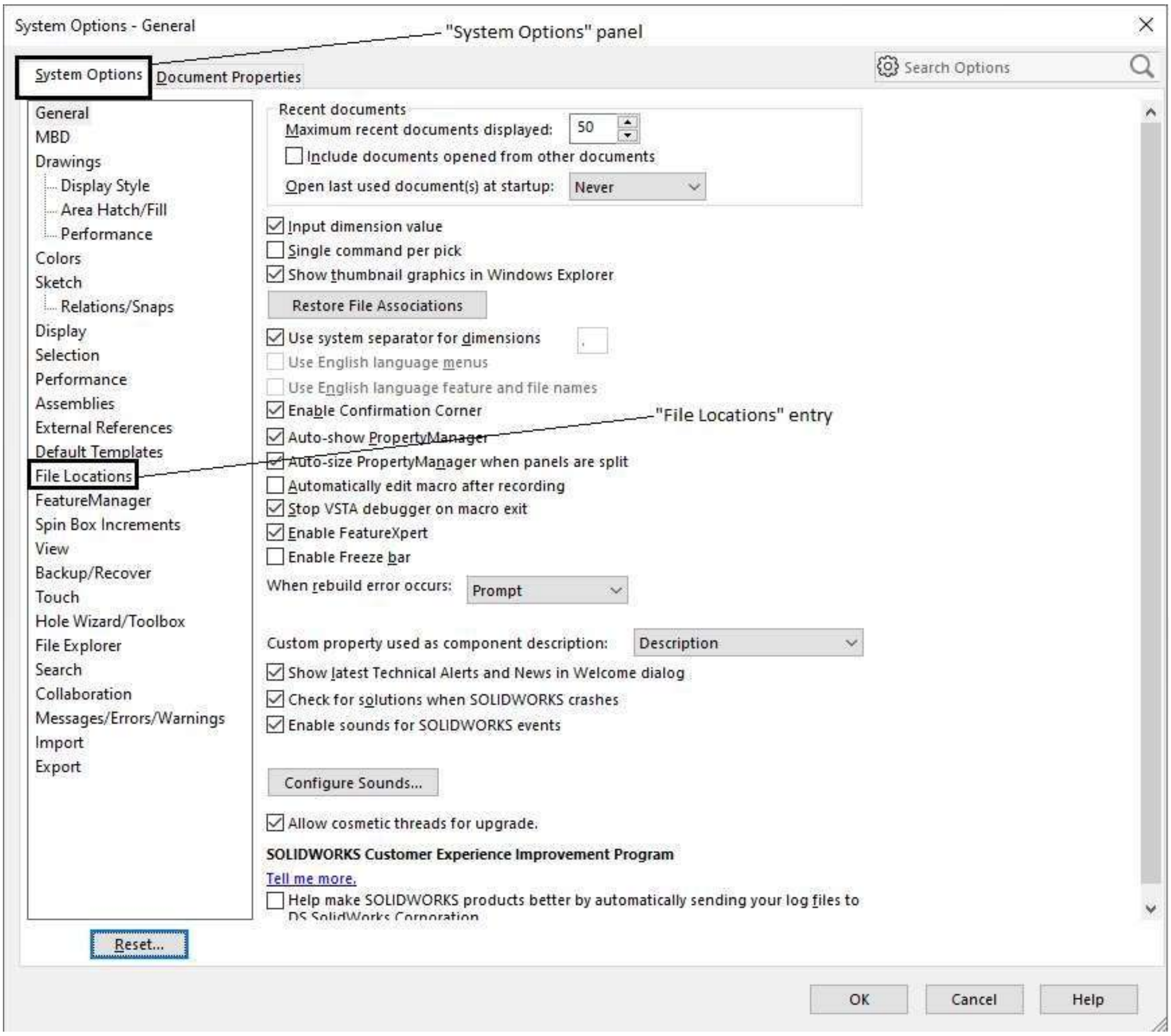

Figure 10: “File Locations” entry in the “System Options” panel of the “System Options – General” window

This project has been funded with support from the Iceland Liechenstein Norway Grants. This publication [communication] reflects the views only of the authors, and the Commission cannot be held responsible for any use which may be made of the information contained therein.

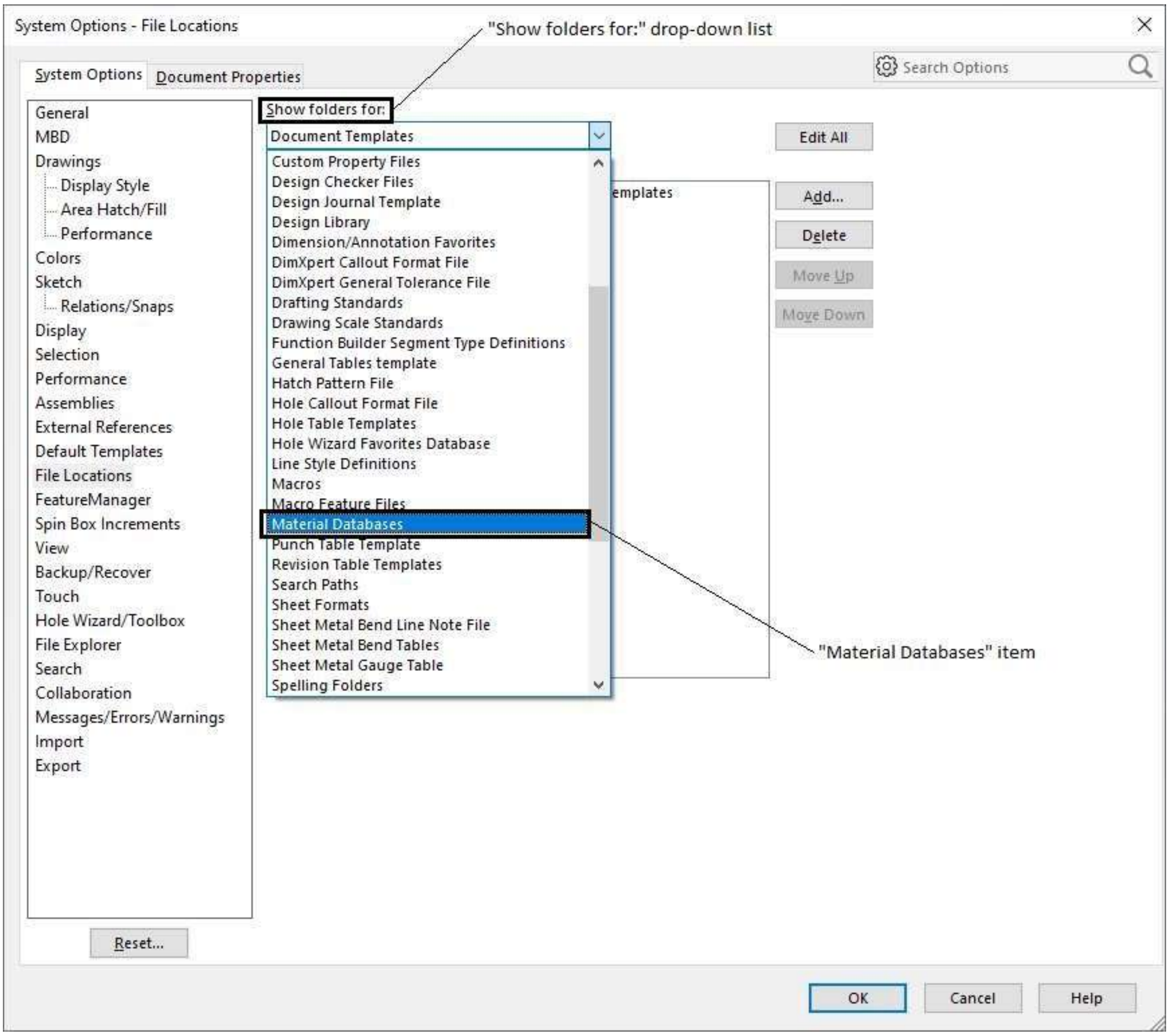

Figure 11: “Material Databases” item in the “Show folders for:” list

This project has been funded with support from the Iceland Liechtenstein Norway Grants. This publication [communication] reflects the views only of the authors, and the Commission cannot be held responsible for any use which may be made of the information contained therein.

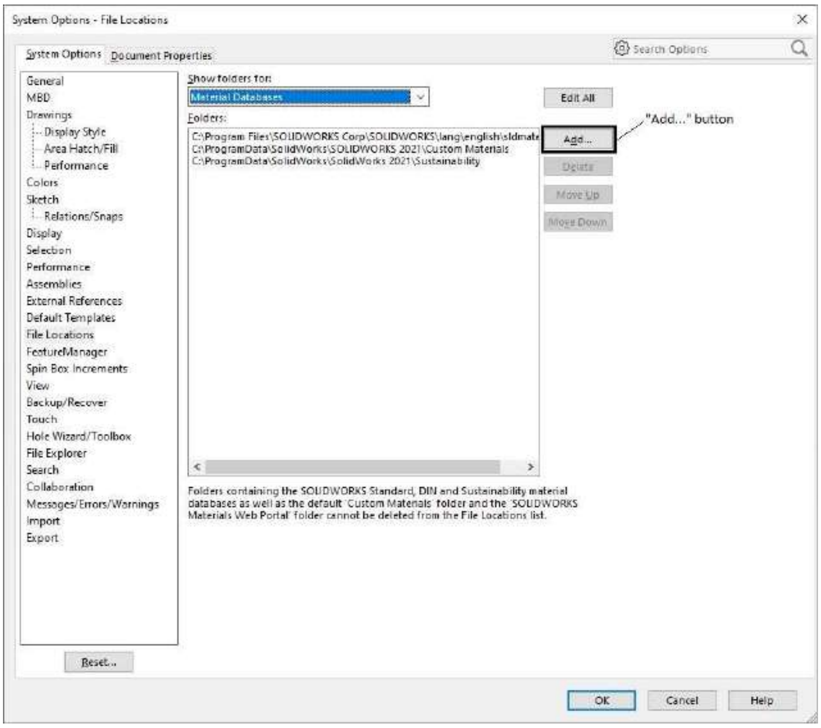

Figure 12: “Add…” button to be pressed for modifying the list of places where SolidWorks looks for material libraries

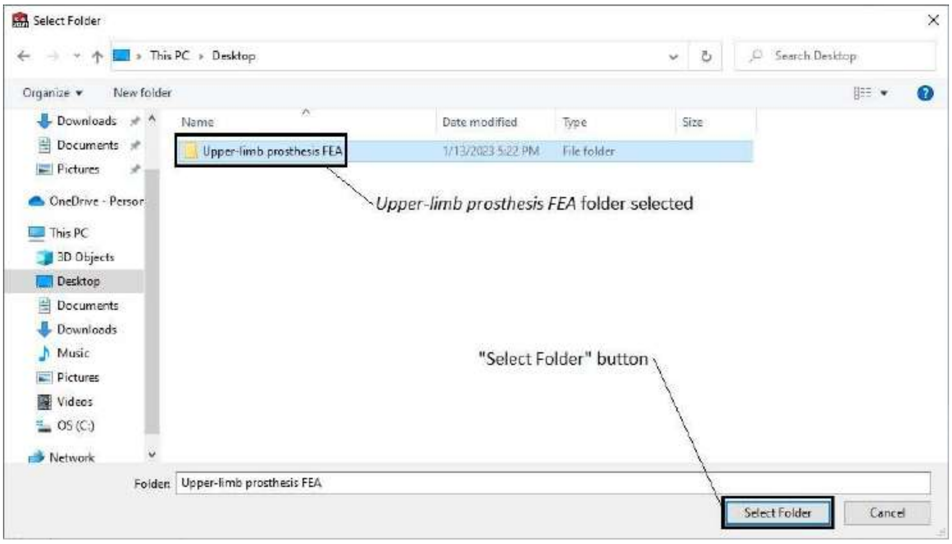

Figure 13: Selecting the folder *Upper-limb prosthesis FEA* for being added to the list of places where SolidWorks looks for material libraries

This project has been funded with support from the Iceland Liechtenstein Norway Grants. This publication [communication] reflects the views only of the authors, and the Commission cannot be held responsible for any use which may be made of the information contained therein.

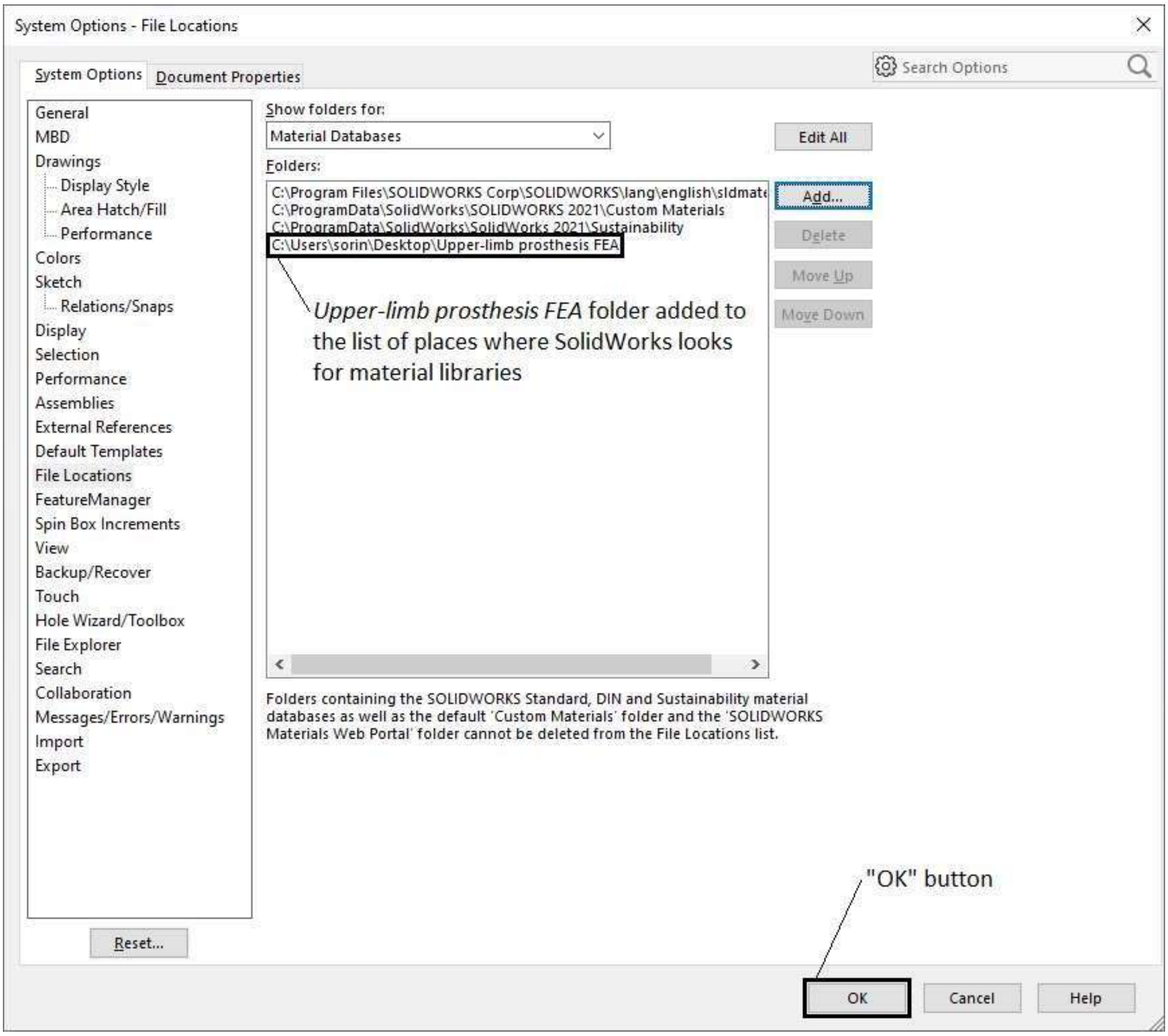

Figure 14: Folder *Upper-limb prosthesis FEA* included in the list of places where SolidWorks looks for material libraries

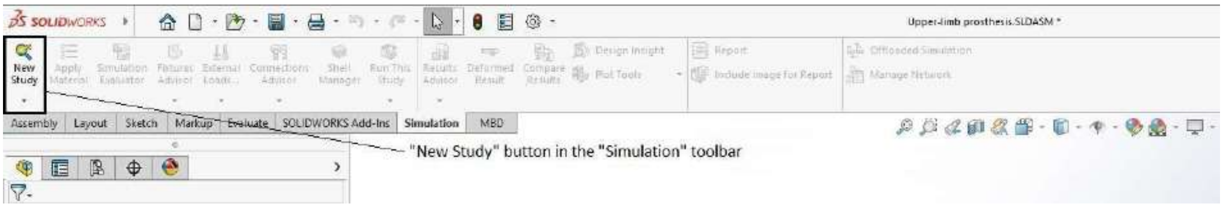

Figure 15: Creation of a new FEA model

This project has been funded with support from the Iceland Liechtenstein Norway Grants. This publication [communication] reflects the views only of the authors, and the Commission cannot be held responsible for any use which may be made of the information contained therein.

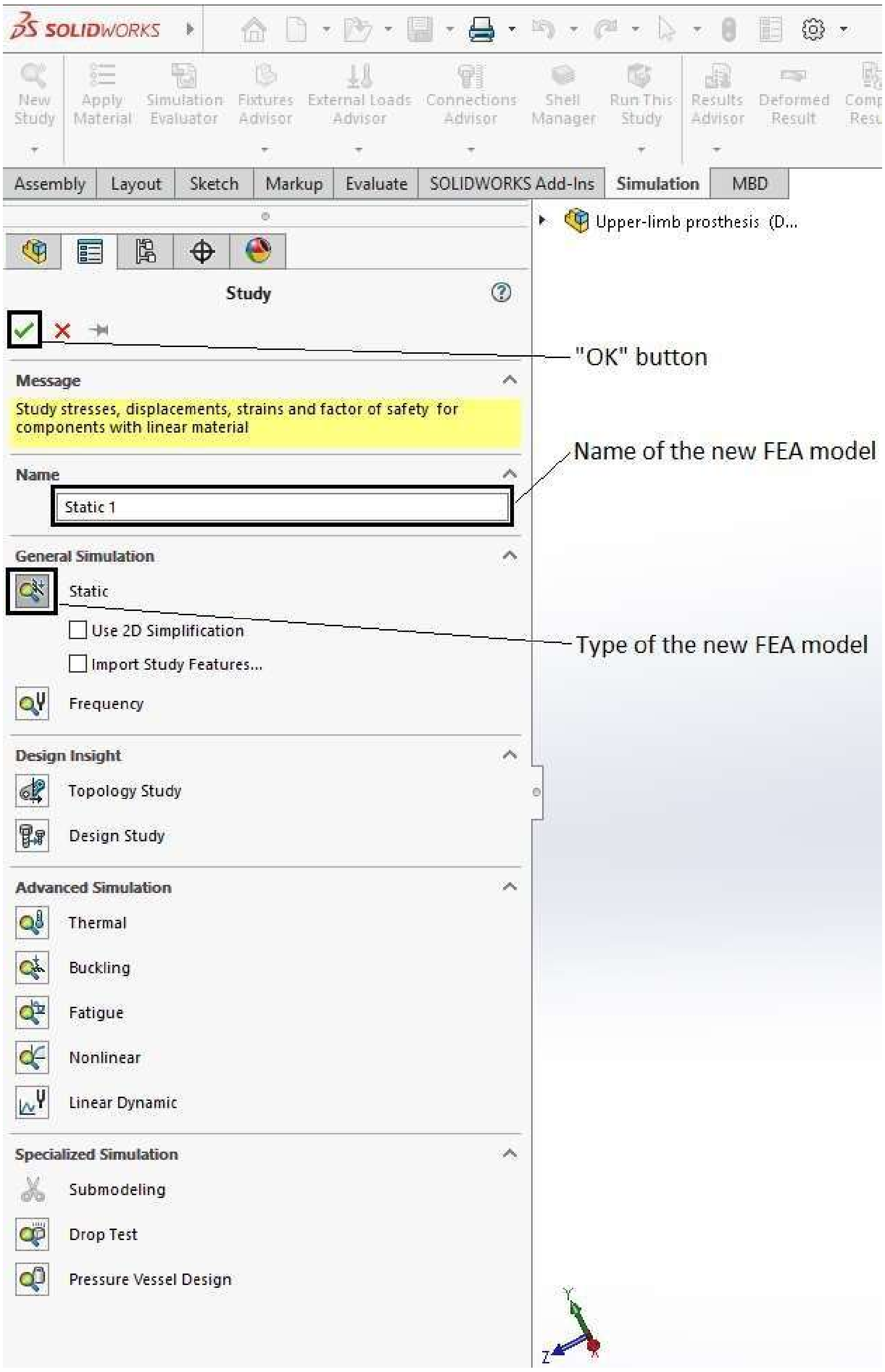

Figure 16: Defining the name and type of the new FEA model

This project has been funded with support from the Iceland Liechenstein Norway Grants. This publication [communication] reflects the views only of the authors, and the Commission cannot be held responsible for any use which may be made of the information contained therein.

f) Press the right button of the mouse on the “Parts” entry of the FEA tree and select the “Apply Material to All…” command from the drop-down menu to define the material properties of the prosthesis components (Fig. 17). Consequently, the “Material” window is displayed (Fig. 18). In that window, minimize the “SOLIDWORKS Materials” library, unroll the “EMERALD CAE Materials” library, unroll the “Plastics” category, select the “PETG” material, then press the buttons “Apply” and “Close” placed at the bottom of the “Material” window.

Note: The yield strength Y = 30.3 MPa (see the PETG material data listed in Table 1 and Figure 18) defines the upper limit of the von Mises equivalent stress that can be supported by the prosthesis components.

g) Do not change the option “Global Interaction (-Bonded-Meshed Independently-)” activated by default under the “Connections” and “Component Interactions” entries of the FEA tree (Fig. 19). This option is consistent with the hypotheses formulated in §1.

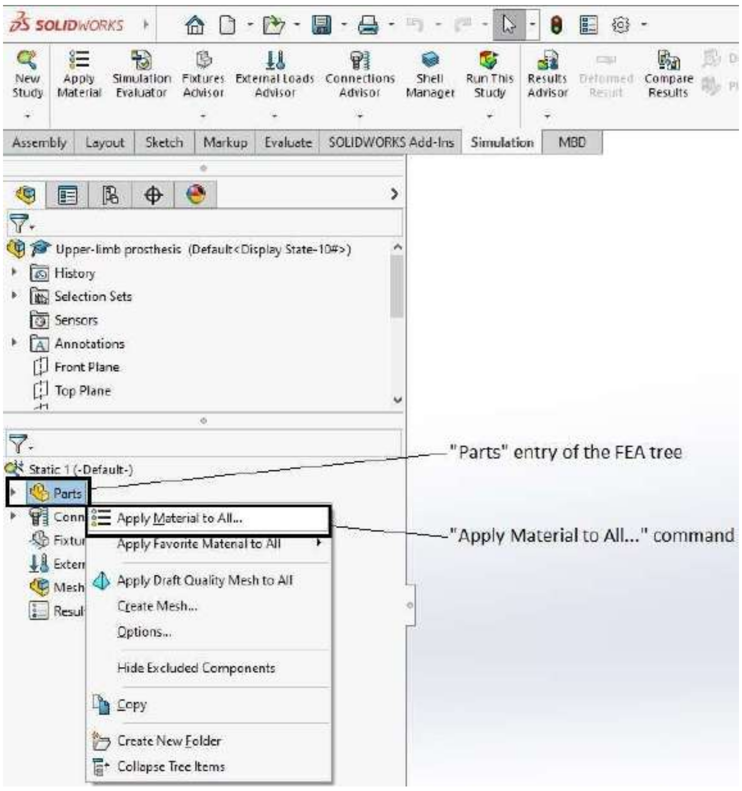

Figure 17: Defining the material properties of the prosthesis components

This project has been funded with support from the Iceland Liechenstein Norway Grants. This publication [communication] reflects the views only of the authors, and the Commission cannot be held responsible for any use which may be made of the information contained therein.

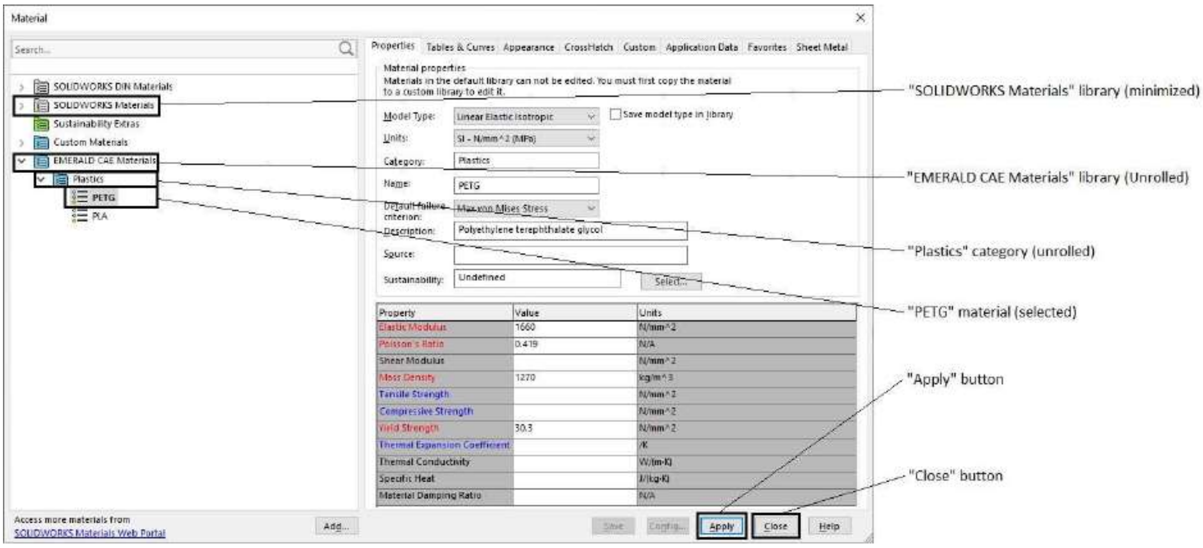

Figure 18: Associating the PETG material to the prosthesis components

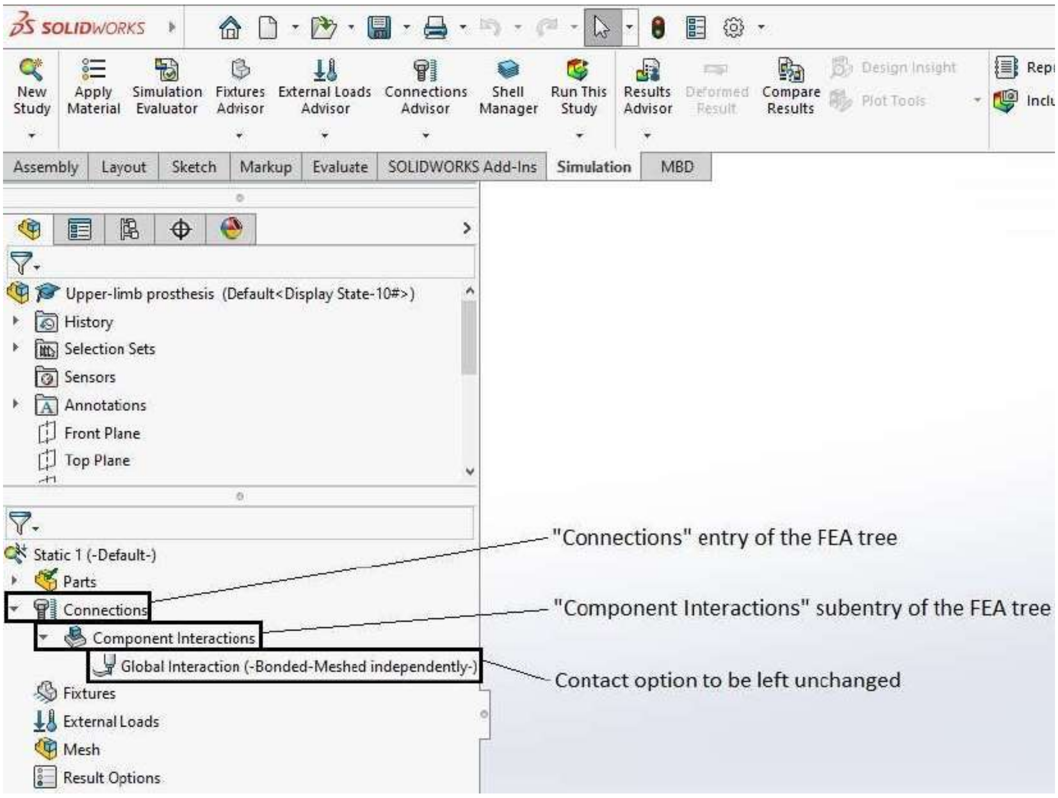

Figure 19: Contact option activated by default in the FEA tree (to be left unchanged)

This project has been funded with support from the Iceland Liechtenstein Norway Grants. This publication [communication] reflects the views only of the authors, and the Commission cannot be held responsible for any use which may be made of the information contained therein.

h) Press the right button of the mouse on the “Fixtures” entry of the FEA tree and select the “Fixed Geometry…” command in the drop-down menu (Fig. 20). Perform the following actions in the “Fixture” dialogue box to define a full locking boundary condition on some inner surfaces of the upper arm (Fig. 21):

- Press the left button of the mouse in the “Faces, Edges, Vertices for Fixture” selection box of the “Fixture” dialogue box
- Unroll the assembly tree placed at the upper-left corner of the SolidWorks graphics area
- Unroll the “Selection Sets” entry of the assembly tree
- Select “Selection-Set1(10) Upper arm - Fixed” in the assembly tree
- Press the “OK” button of the “Fixture” dialogue box.

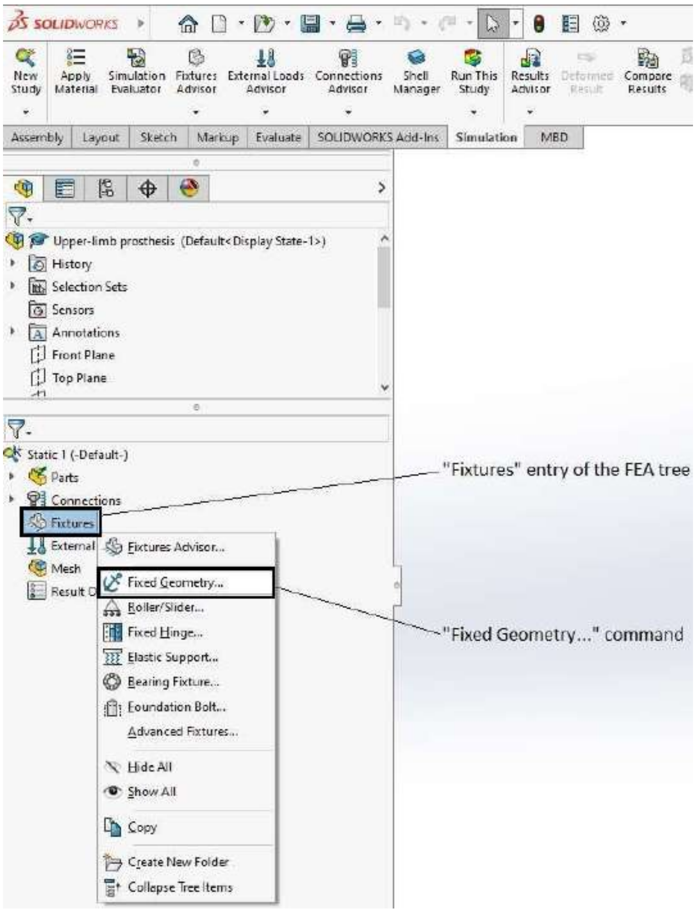

Figure 20: Defining full locking boundary conditions

This project has been funded with support from the Iceland Liechenstein Norway Grants. This publication [communication] reflects the views only of the authors, and the Commission cannot be held responsible for any use which may be made of the information contained therein.

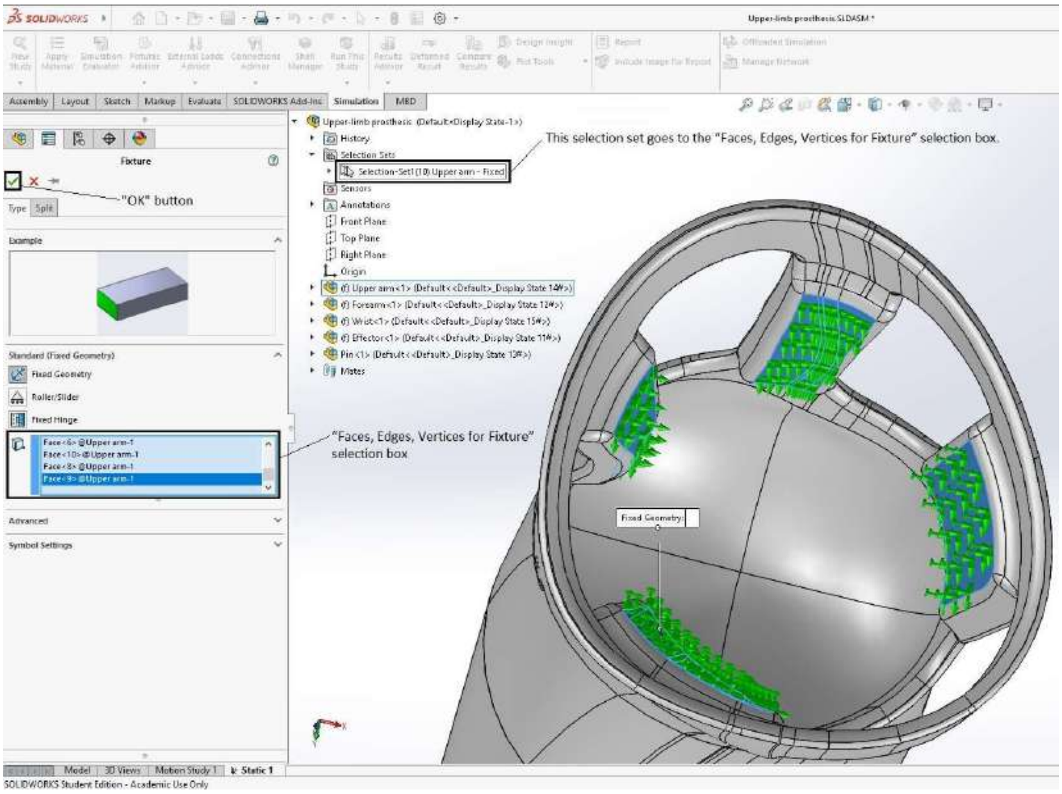

Figure 21: Full locking boundary conditions defined on some inner surfaces of the upper arm

i) Press the right button of the mouse on the "External Loads" entry of the FEA tree and select the "Force…" command in the drop-down menu (Fig. 22). Perform the following actions in the "Force/Torque" dialogue box to define the distal traction load that acts on the prosthesis (Fig. 23):
   - Activate the "Selected direction" radio button
   - Press the left button of the mouse in the "Faces, Edges, Vertices, Reference Points for Force" selection box
   - Select the blue surface of the prosthesis effector in the SolidWorks graphics area
   - Press the left button of the mouse in the "Face, Edge, Plane for Direction" selection box
   - Unroll the assembly tree placed at the upper-left corner of the SolidWorks graphics area

This project has been funded with support from the Iceland Liechenstein Norway Grants. This publication [communication] reflects the views only of the authors, and the Commission cannot be held responsible for any use which may be made of the information contained therein.

- Select “Front Plane” in the assembly tree
- Press the “Normal to Plane” button in the “Force” region of the “Force/Torque” dialogue box
- Do not change the force value specified by default (1 N) in the “Normal to Plane” input box
- Press the “OK” button of the “Force/Torque” dialogue box.

Note: The actual values of the traction force are defined in step (k) as load cases.

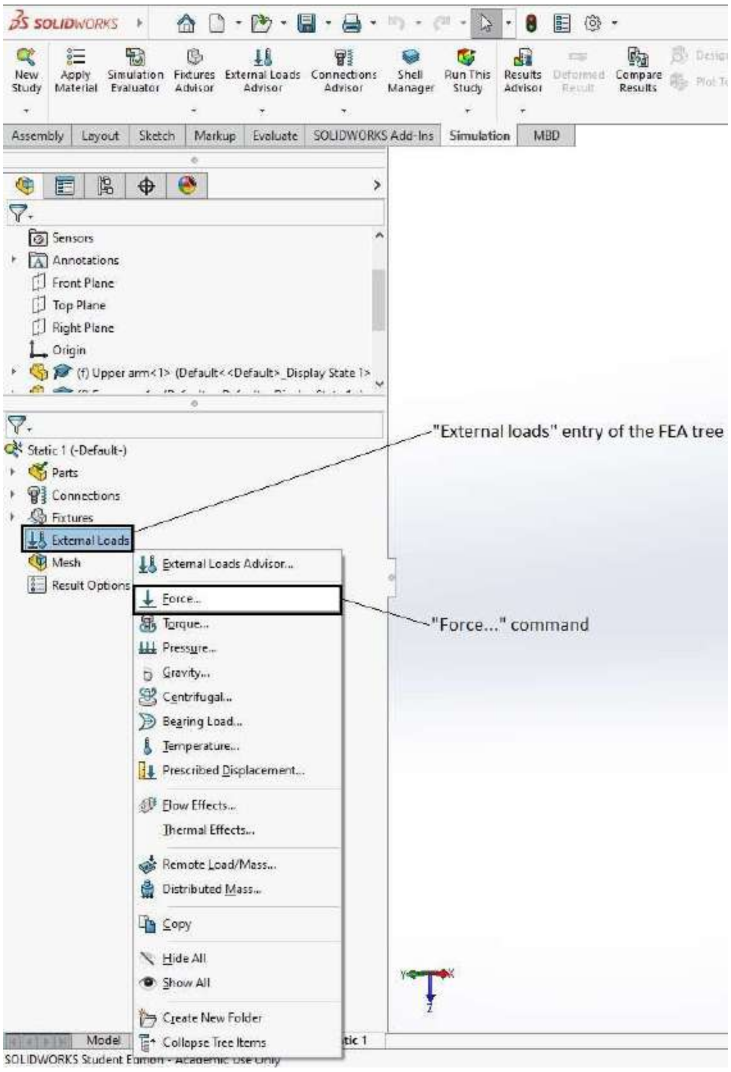

Figure 22: Defining a force-type boundary condition

This project has been funded with support from the Iceland Liechtenstein Norway Grants. This publication [communication] reflects the views only of the authors, and the Commission cannot be held responsible for any use which may be made of the information contained therein.

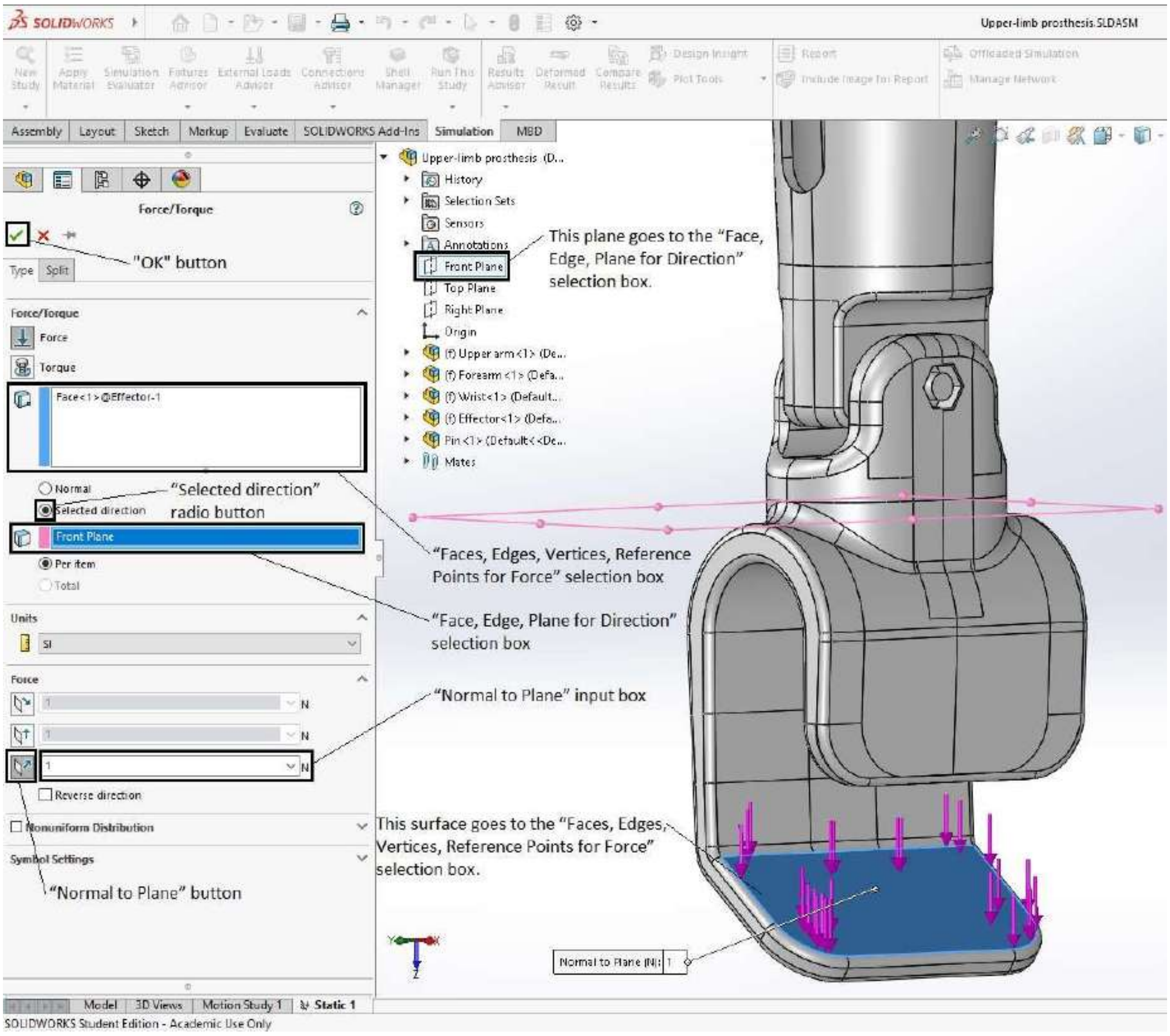

Figure 23: Defining the distal traction load that acts on the prosthesis

j) Press the right button of the mouse on the "Mesh" entry of the FEA tree and select the "Create Mesh…" command in the drop-down menu (Fig. 24). Perform the following actions in the "Mesh" dialogue box to generate the finite element mesh (Fig. 25):

- Move the "Mesh Factor" cursor to the "Fine" position
- Press the "OK" button of the "Mesh" dialogue box.

Note: The finite element mesh generated by SolidWorks Simulation is shown in Figure 26.

This project has been funded with support from the Iceland Liechtenstein Norway Grants. This publication [communication] reflects the views only of the authors, and the Commission cannot be held responsible for any use which may be made of the information contained therein.

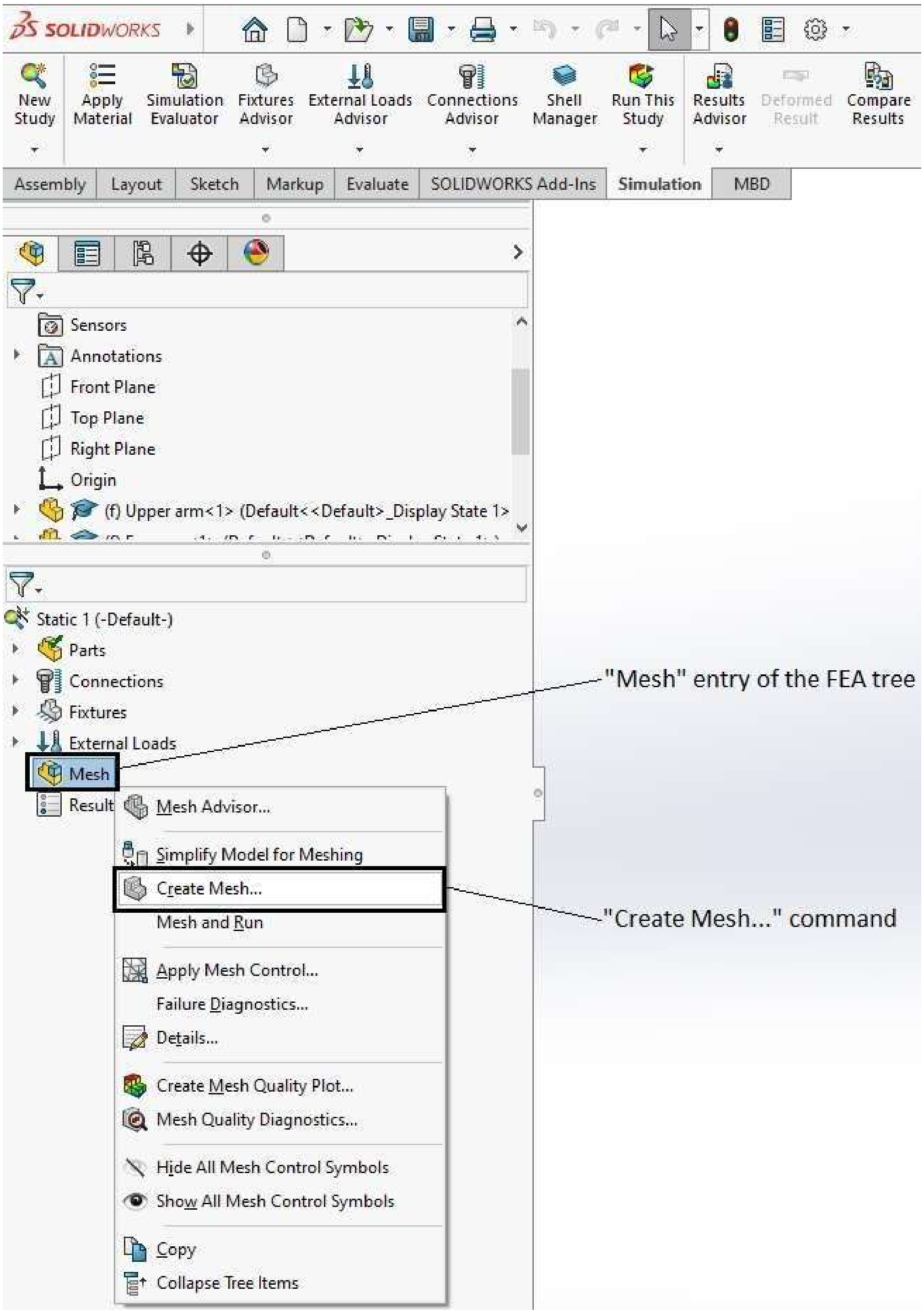

This project has been funded with support from the Iceland Liechtenstein Norway Grants. This publication [communication] reflects the views only of the authors, and the Commission cannot be held responsible for any use which may be made of the information contained therein.

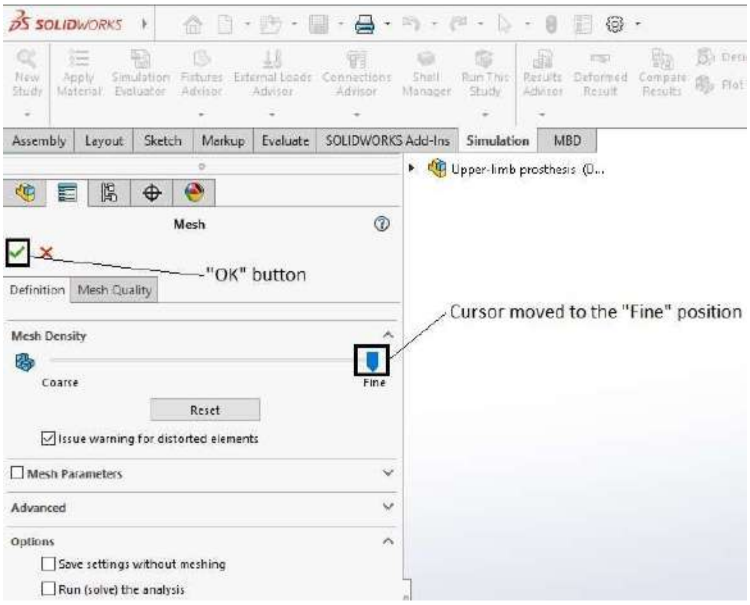

Figure 25: Defining the control parameters of the finite element mesh

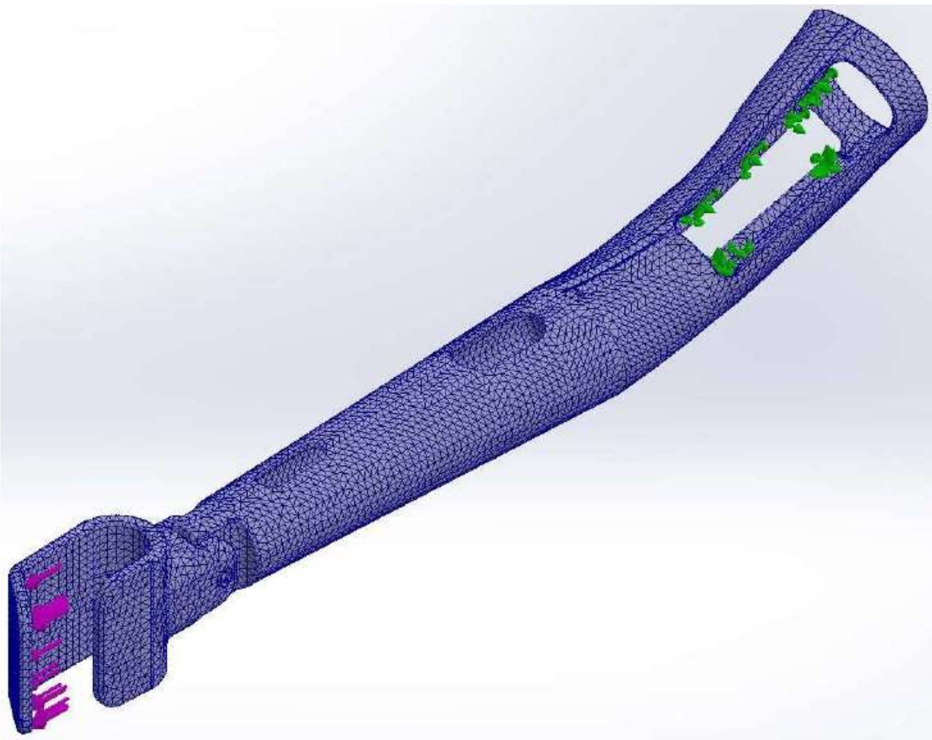

This project has been funded with support from the Iceland Liechtenstein Norway Grants. This publication [communication] reflects the views only of the authors, and the Commission cannot be held responsible for any use which may be made of the information contained therein.

k) Press the right button of the mouse on the root of the FEA tree and select the "Load Case Manager" command in the drop-down menu (Fig. 27). Consequently, the "Load Case View" tab is displayed at the bottom of the SolidWorks graphics area (Fig. 28). Perform the following actions in that tab to define the actual values of the traction load that acts on the prosthesis:
   - Press the left button of the mouse in the box labeled "+ Click here to add a primary load case" to define the first load case (Fig. 29)
   - Replace the "Suppress" status of the "Force-1" cell with 150 (Newton) i.e., the actual value of the pressure corresponding to "Load Case 1" (Fig. 29)
   - Press the left button of the mouse in the box labeled "+ Click here to add a primary load case" to define the second load case (Fig. 29)
   - Replace the "Suppress" status of the "Force-1" cell with 300 (Newton) i.e., the actual value of the pressure corresponding to "Load Case 2" (Fig. 30)
   - Proceed in the same manner to define "Load Case 3": 450 N, "Load Case 4": 600 N, and "Load Case 5": 750 N (Fig. 31)
   - Press the left button of the mouse in the box labeled "+ Click here to add a sensor to track a result" (Fig. 31)
   - Select the "+ Add Sensor…" command in the drop-down list displayed at the bottom of the "Load Case View" tab (Fig. 32)
   - Perform the following actions in the "Sensor" dialogue box to define a sensor for tracking the maximum value of the von Mises equivalent stress at the level of the entire FEA model (Fig. 33):
      - Select the option "Stress" from the "Results" drop-down list
      - Select the option "VON: von Mises Stress" from the "Component" drop-down list
      - Select the option "N/mm^2 (MPa)" from the "Units" drop-down list
      - Press the "OK" button placed at the upper-left corner of the "Sensor" dialogue
   - Come back to the "Load Case View" tab and press again the left button of the mouse in the box labeled "+ Click here to add a sensor to track a result" (Fig. 34)
   - Select the "+ Add Sensor…" command in the drop-down list displayed at the bottom of the "Load Case View" tab (Fig. 34)
   - Perform the following actions in the "Sensor" dialogue box to define a new sensor for tracking the maximum deflection at the level of the entire FEA model (Fig. 35):

This project has been funded with support from the Iceland Liechenstein Norway Grants. This publication [communication] reflects the views only of the authors, and the Commission cannot be held responsible for any use which may be made of the information contained therein.

- Select the option “Displacement” from the “Results” drop-down list
- Select the option “URES: Resultant Displacement” from the “Component” drop-down list
- Select the option “mm” from the “Units” drop-down list
- Press the “OK” button placed at the upper-left corner of the “Sensor” dialogue.

At this stage, the finite element model of the tensile test is prepared and transferred to the SolidWorks Simulation solver by pressing the “Run” button of the “Load Case View” tab (Fig. 36). The numerical results generated by the solver are interpreted in the next section.

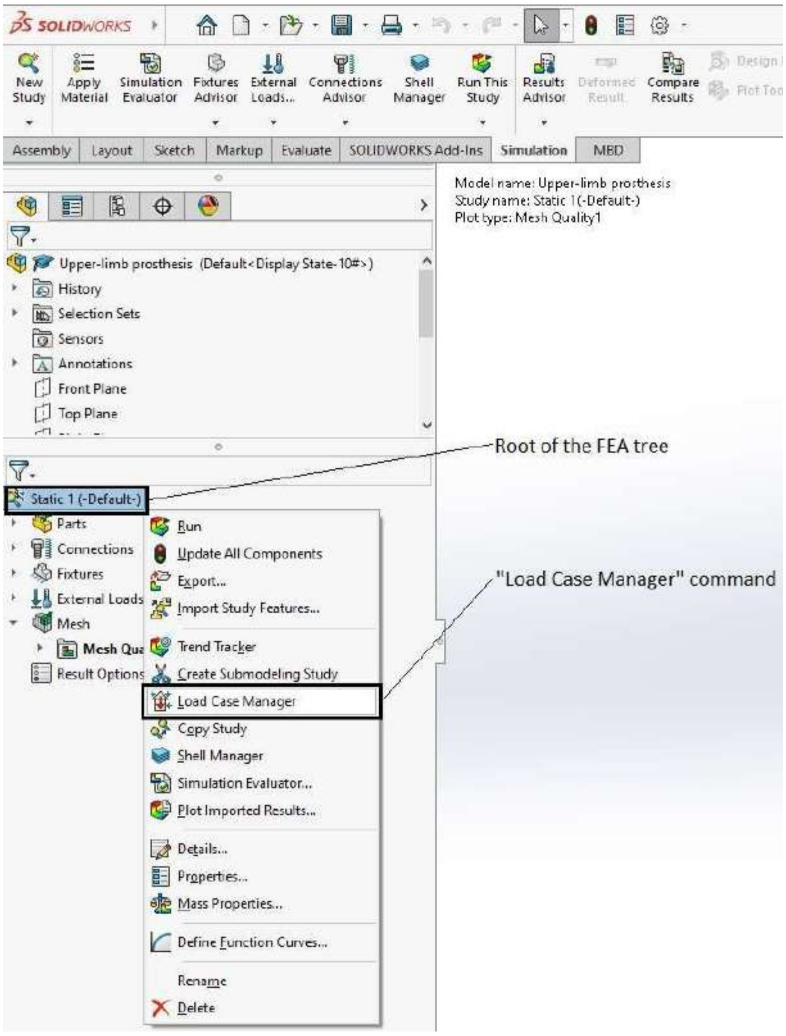

Figure 27: Accessing the Load Case Manager

This project has been funded with support from the Iceland Liechtenstein Norway Grants. This publication [communication] reflects the views only of the authors, and the Commission cannot be held responsible for any use which may be made of the information contained therein.

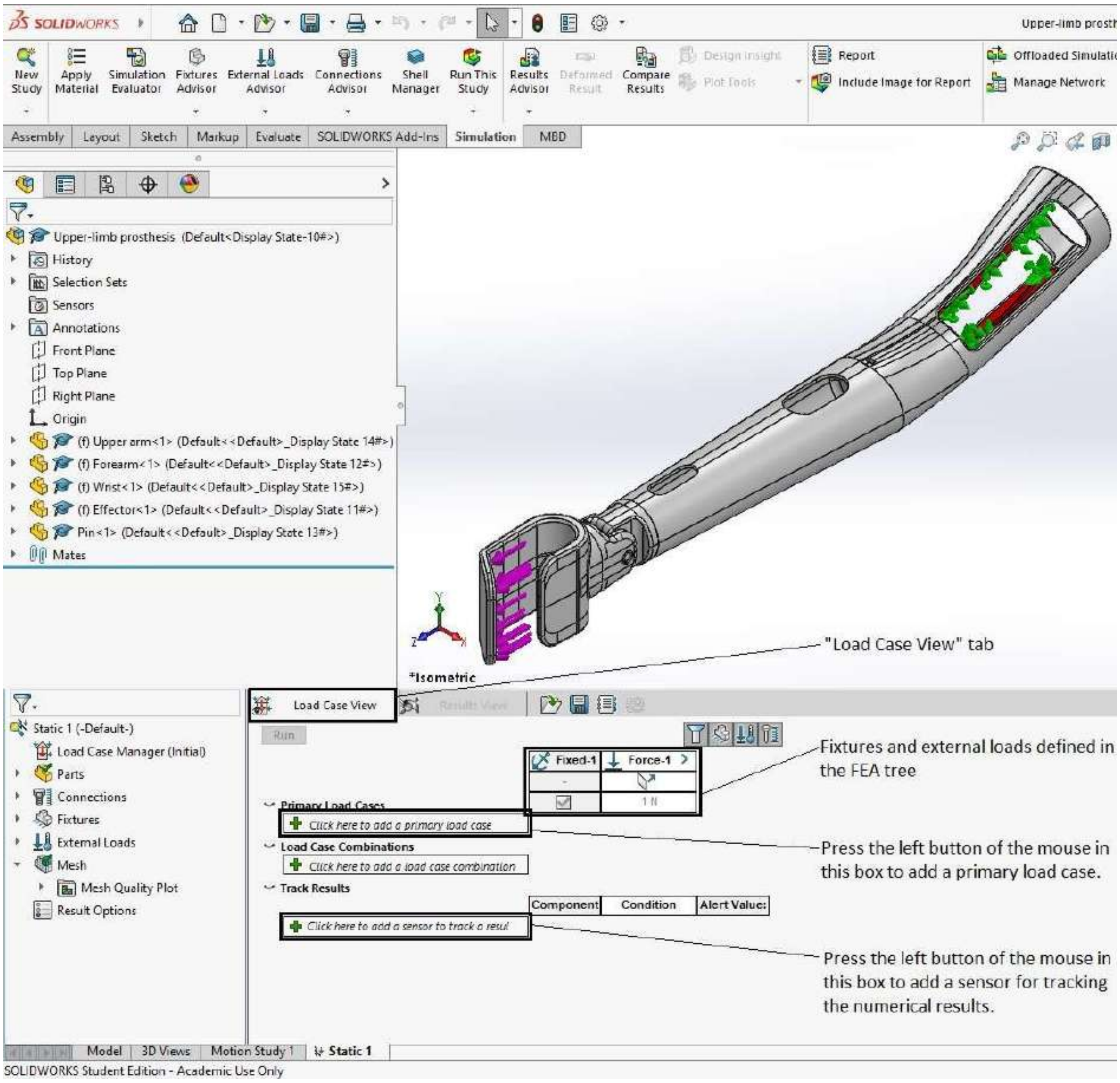

Figure 28: “Load Case View” tab displayed at the bottom of the SolidWorks graphics area

This project has been funded with support from the Iceland Liechenstein Norway Grants. This publication [communication] reflects the views only of the authors, and the Commission cannot be held responsible for any use which may be made of the information contained therein.

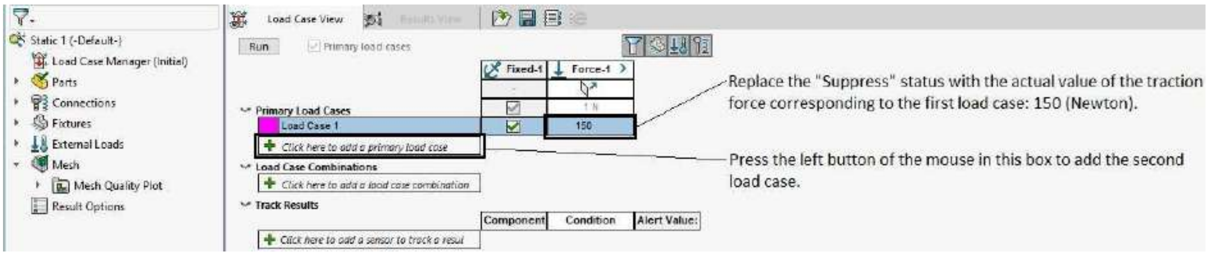

Figure 29: Defining the first load case (traction force of 150 N)

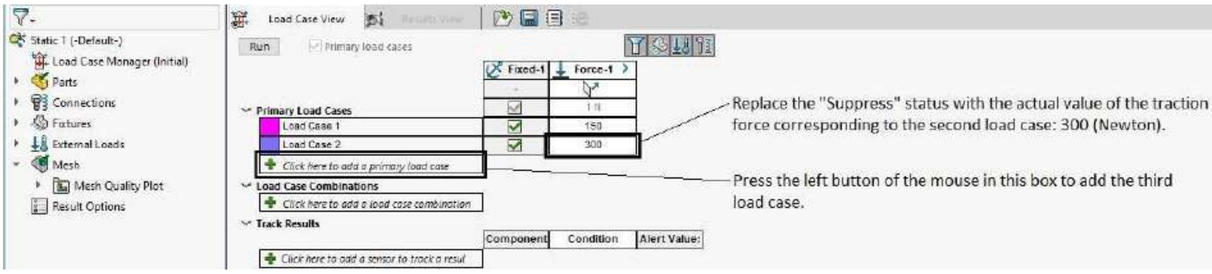

Figure 30: Defining the second load case (traction force of 300 N)

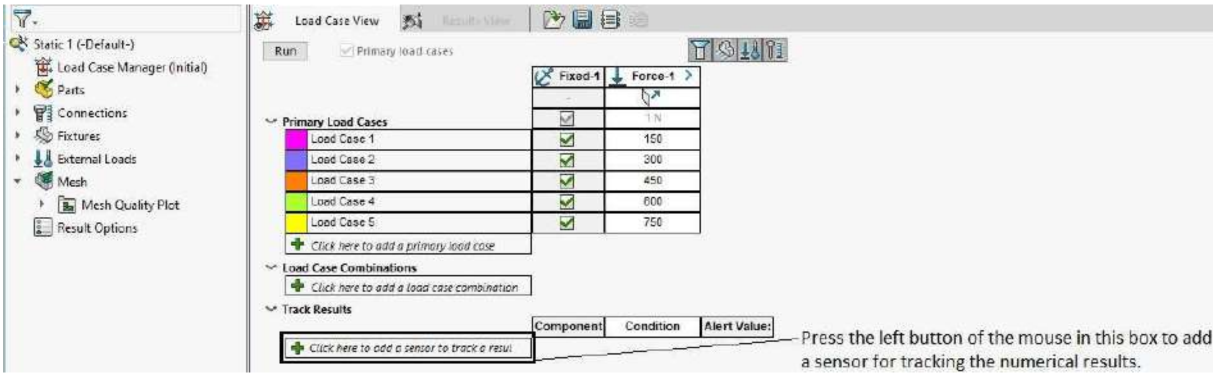

Figure 31: Actual values of the traction force defined as load cases

This project has been funded with support from the Iceland Liechenstein Norway Grants. This publication [communication] reflects the views only of the authors, and the Commission cannot be held responsible for any use which may be made of the information contained therein.

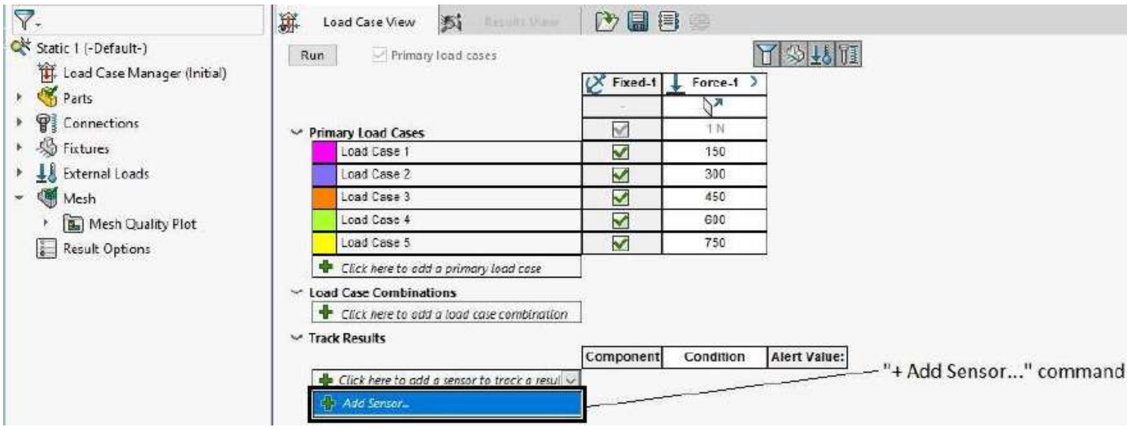

Figure 32: Initiating the definition of a sensor for tracking the numerical results

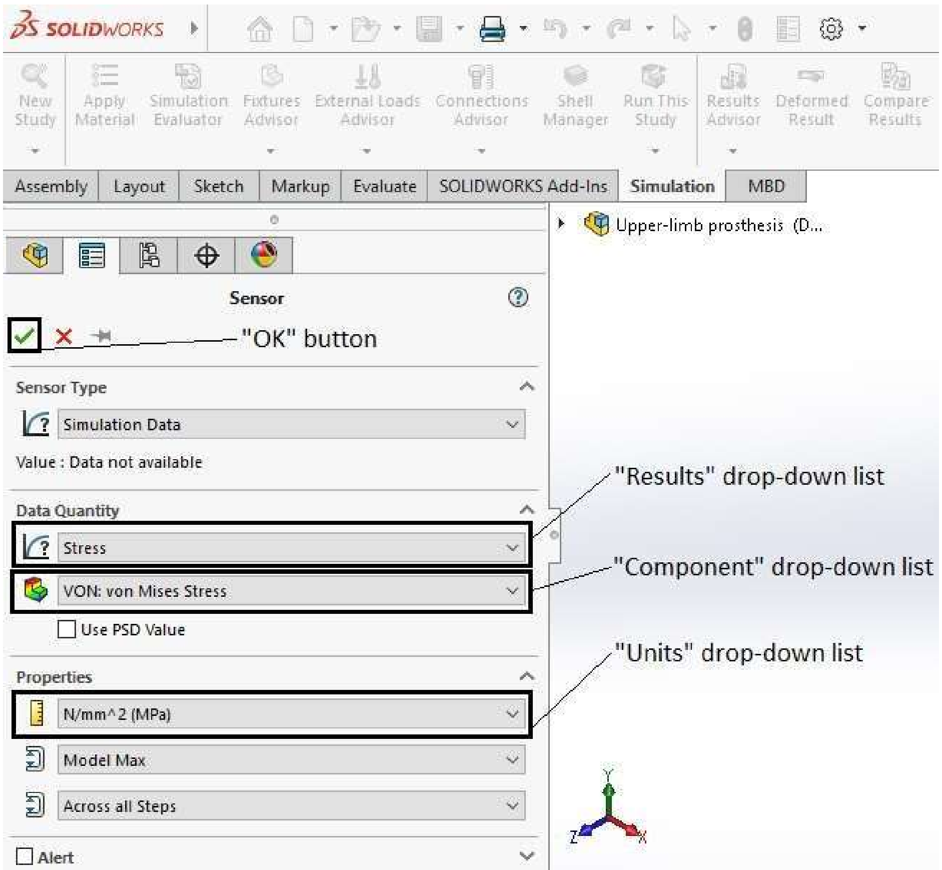

Figure 33: Definition of a sensor for tracking the maximum value of the von Mises equivalent stress at the level of the entire FEA model

This project has been funded with support from the Iceland Liechenstein Norway Grants. This publication [communication] reflects the views only of the authors, and the Commission cannot be held responsible for any use which may be made of the information contained therein.

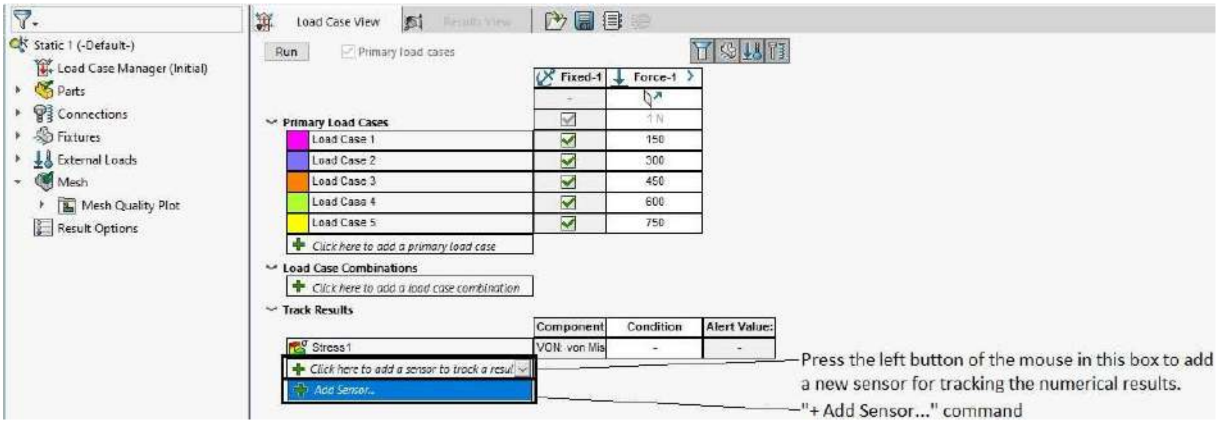

Figure 34: Initiating the definition of a new sensor for tracking the numerical results

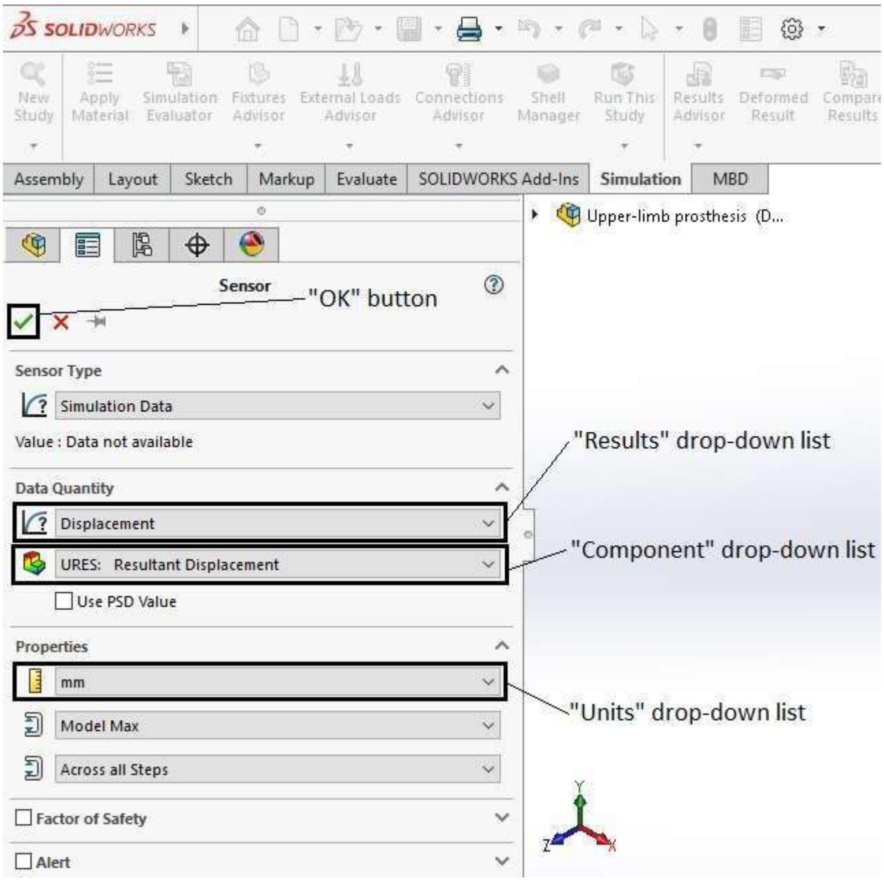

Figure 35: Definition of a sensor for tracking the maximum deflection at the level of the entire FEA model

This project has been funded with support from the Iceland Liechenstein Norway Grants. This publication [communication] reflects the views only of the authors, and the Commission cannot be held responsible for any use which may be made of the information contained therein.

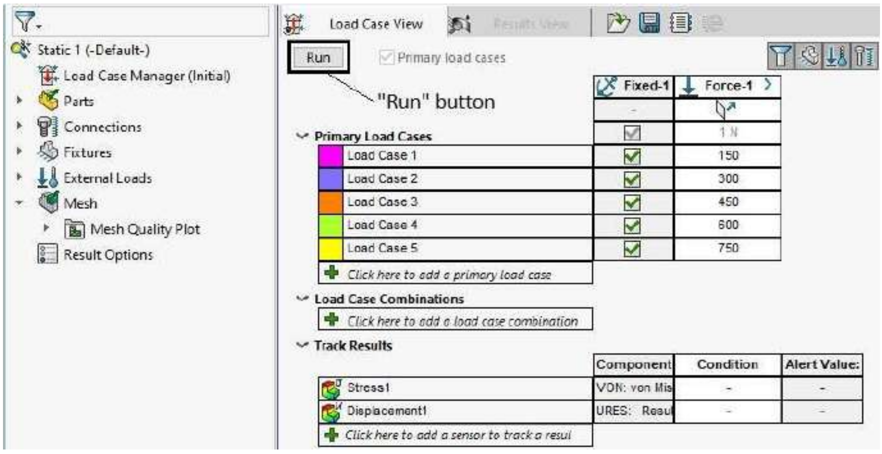

Figure 36: Transferring the finite element model to the SolidWorks Simulation solver

3. Interpretation of the numerical results

As soon as the solver finishes its job, the control is transferred to the "Results View" tab which is displayed at the bottom of the graphics area. At the same time, a color map showing the distribution of the von Mises equivalent stress at the level of the entire assembly appears on the screen (Fig. 37). This distribution corresponds to the first load case. The user can explore the other load cases by selecting them with the left button of the mouse in the first column of the "Primary Load Cases" table placed at the bottom of the "Results View" tab (see Figure 37, as well as the examples shown in Figures 38 and 39).

Perform the following actions to display the distribution of the deflection at the level of the entire assembly:

a) Press the right button of the mouse on the item "Displacement1 (-Res disp-)" under the "Load Case Results" entry of the FEA tree, and select the "Show" command in the drop-down menu to examine the distribution of the deflection (Fig. 40)
b) Examine the distribution of the deflection associated to different load cases by selecting them with the left button of the mouse in the first column of the "Primary Load Cases" table placed at the bottom of the "Results View" tab (see the examples shown in Figures 41 and 42).

This project has been funded with support from the Iceland Liechtenstein Norway Grants. This publication [communication] reflects the views only of the authors, and the Commission cannot be held responsible for any use which may be made of the information contained therein.

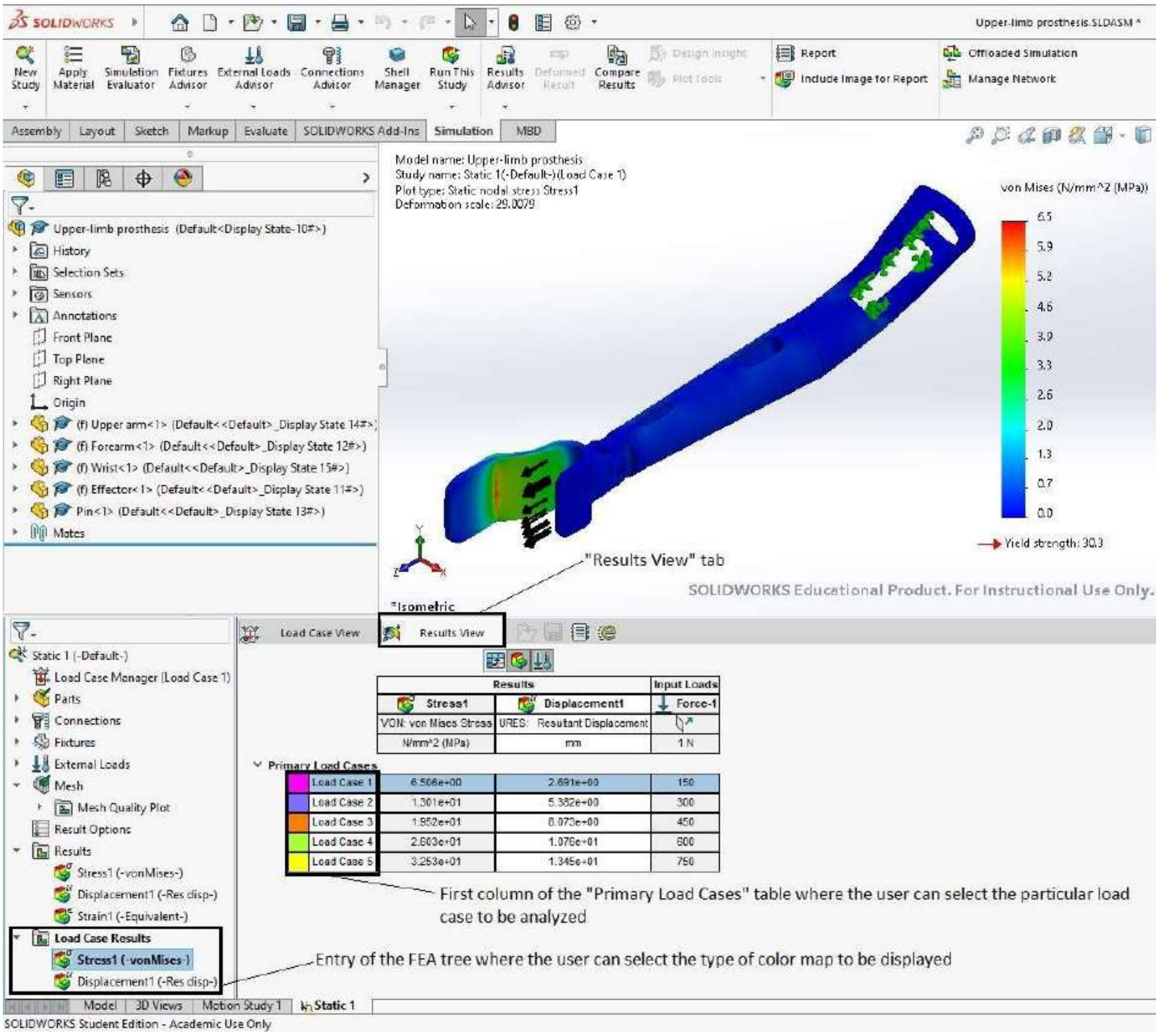

Figure 37: Analyzing the numerical results associated to different load cases with the help of the “Results View” tab and the “Load Case Results” entry of the FEA tree

This project has been funded with support from the Iceland Liechenstein Norway Grants. This publication [communication] reflects the views only of the authors, and the Commission cannot be held responsible for any use which may be made of the information contained therein.

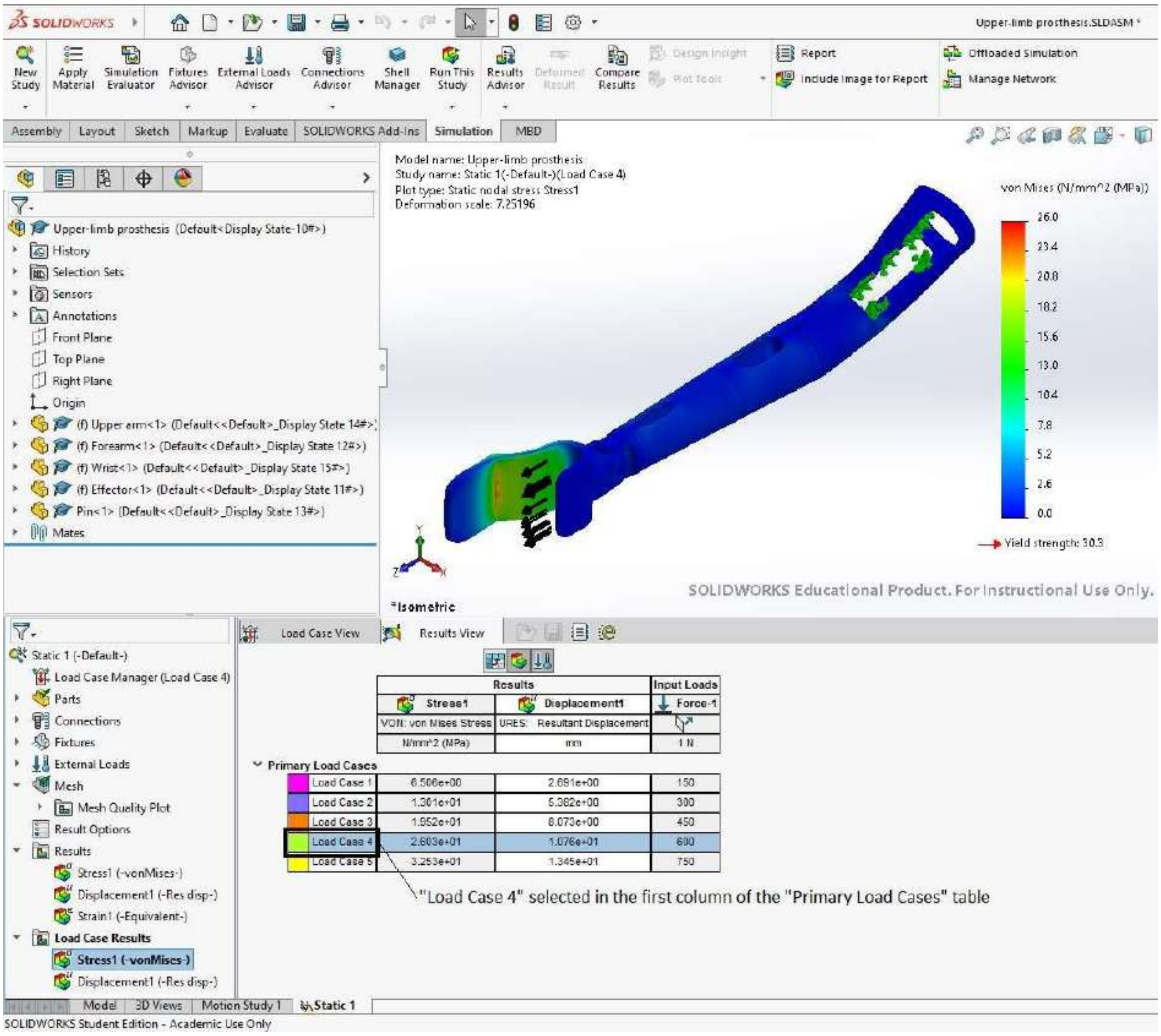

Figure 38: Color map showing the distribution of the von Mises equivalent stress at the level of the entire assembly (fourth load case: traction force of 600 N)

This project has been funded with support from the Iceland Liechenstein Norway Grants. This publication [communication] reflects the views only of the authors, and the Commission cannot be held responsible for any use which may be made of the information contained therein.

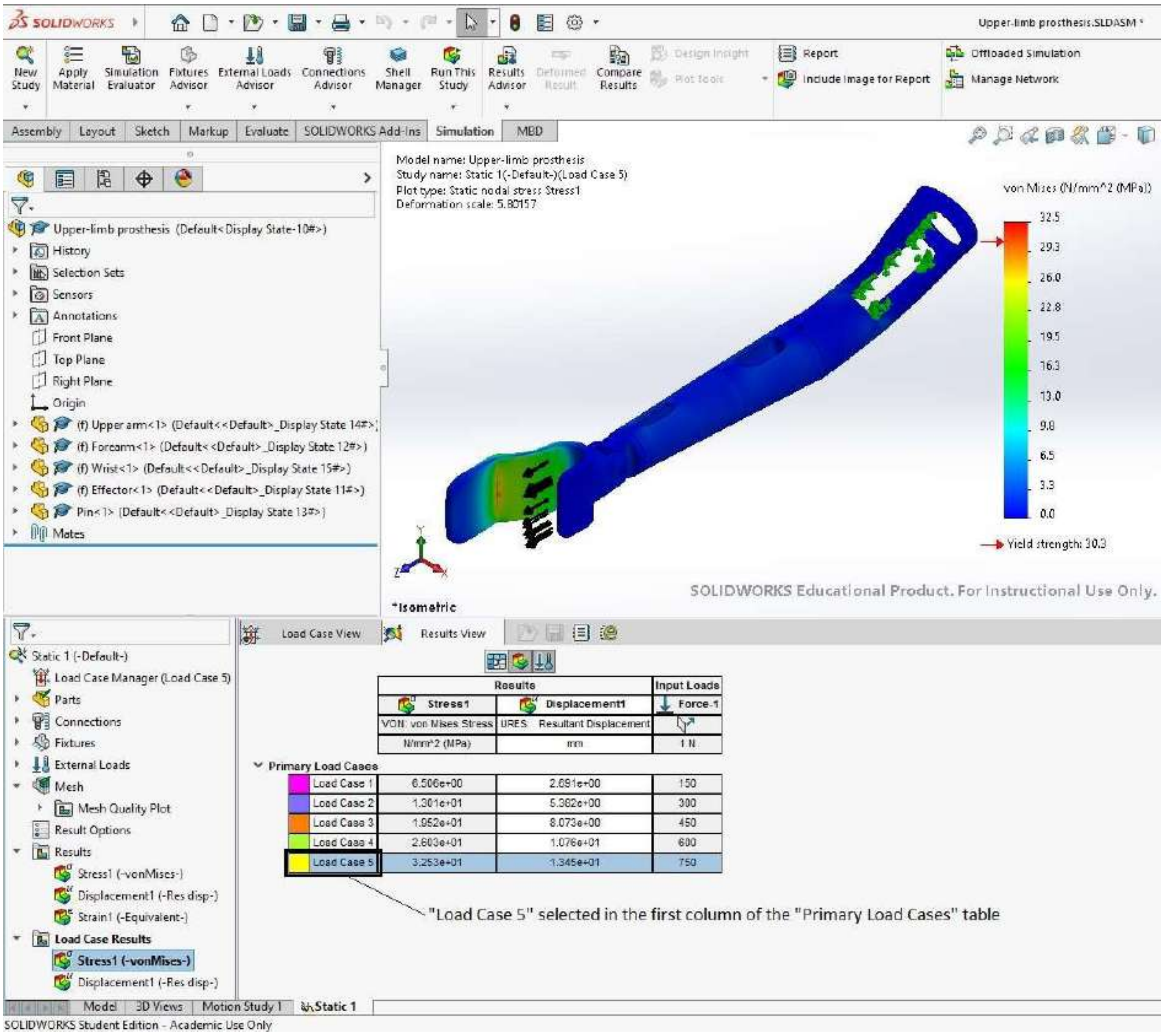

Figure 39: Color map showing the distribution of the von Mises equivalent stress at the level of the entire assembly (fifth load case: traction force of 750 N)

This project has been funded with support from the Iceland Liechenstein Norway Grants. This publication [communication] reflects the views only of the authors, and the Commission cannot be held responsible for any use which may be made of the information contained therein.

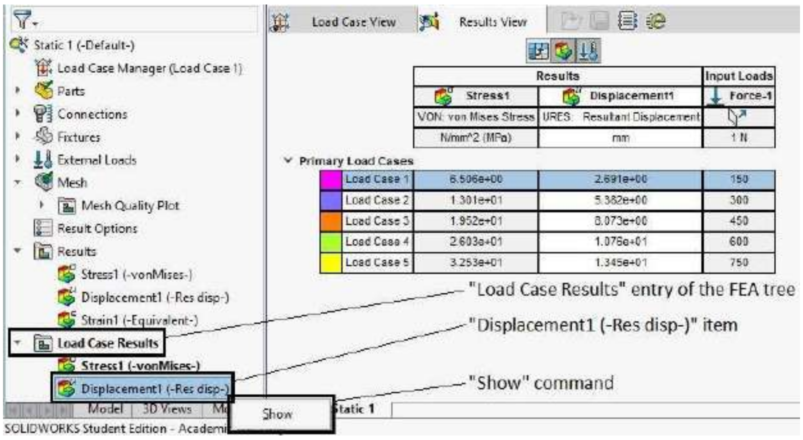

Figure 40: Selecting the distribution of the deflection to be examined

The maximum value of the von Mises equivalent stress $\sigma_{eq,max}$, the maximum deflection d_{max}, and the traction force F corresponding to different load cases are listed in the second, third and fourth column of the “Primary Load Cases” table placed at the bottom of the “Results View” tab (Fig. 43). Table 2 (see below) presents this data in a more readable format.

The plots in Figures 44 and 45 show the dependencies $\sigma_{eq,max}$ vs F and d_{max} vs F, respectively. Both diagrams allow noticing that the mechanical response of the prosthesis is linear. In fact, the dependencies $\sigma_{eq,max}$ vs F and d_{max} vs F are well approximated by the regressions

$$\sigma_{eq,max} = 4.337 \cdot 10^{-2} \cdot F, \quad (1)$$

and

$$d_{max} = 1.794 \cdot 10^{-2} \cdot F, \quad (2)$$

respectively (see the black lines in Figures 44 and 45).

It can be easily seen in Table 2 and Figure 44 that $\sigma_{eq,max}$ equals the yield strength of the PETG material Y = 30.3 MPa (as defined in the *EMERALD CAE Materials.sldmat* library – see Table 1 and Figure 18) for a traction force 600 N < F_{cr} < 750 N. This critical load results from Eq (1) as soon as the replacement $\sigma_{eq,max}$ = Y = 30.3 MPa is made:

$$F_{cr} = Y \cdot 100 / 4.337 = 30.3 \cdot 100 / 4.337 = 698.64 \text{ N}. \quad (3)$$

This project has been funded with support from the Iceland Liechtenstein Norway Grants. This publication [communication] reflects the views only of the authors, and the Commission cannot be held responsible for any use which may be made of the information contained therein.

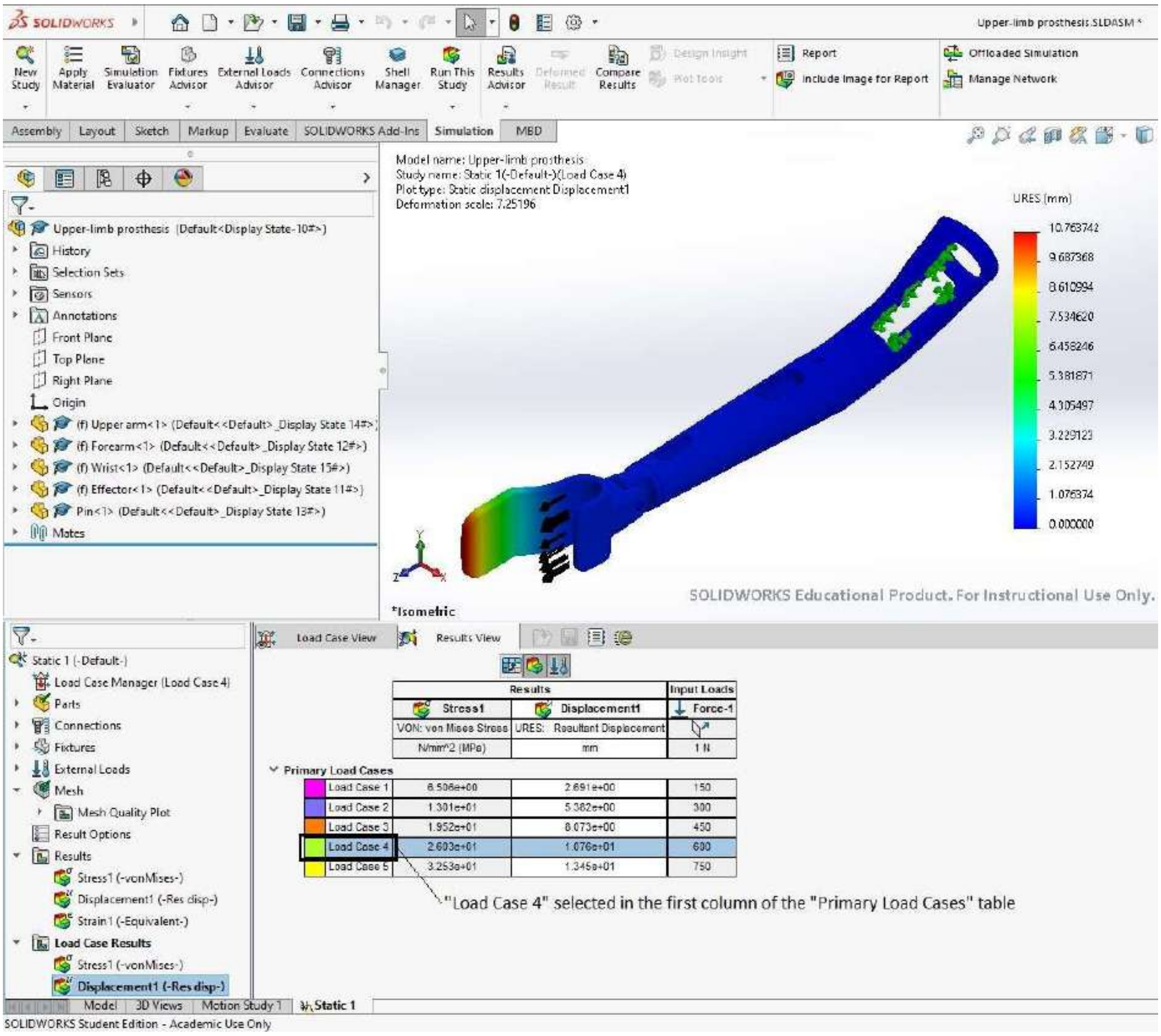

Figure 41: Color map showing the distribution of the deflection at the level of the entire assembly (fourth load case: traction force of 600 N)

This project has been funded with support from the Iceland Liechtenstein Norway Grants. This publication [communication] reflects the views only of the authors, and the Commission cannot be held responsible for any use which may be made of the information contained therein.

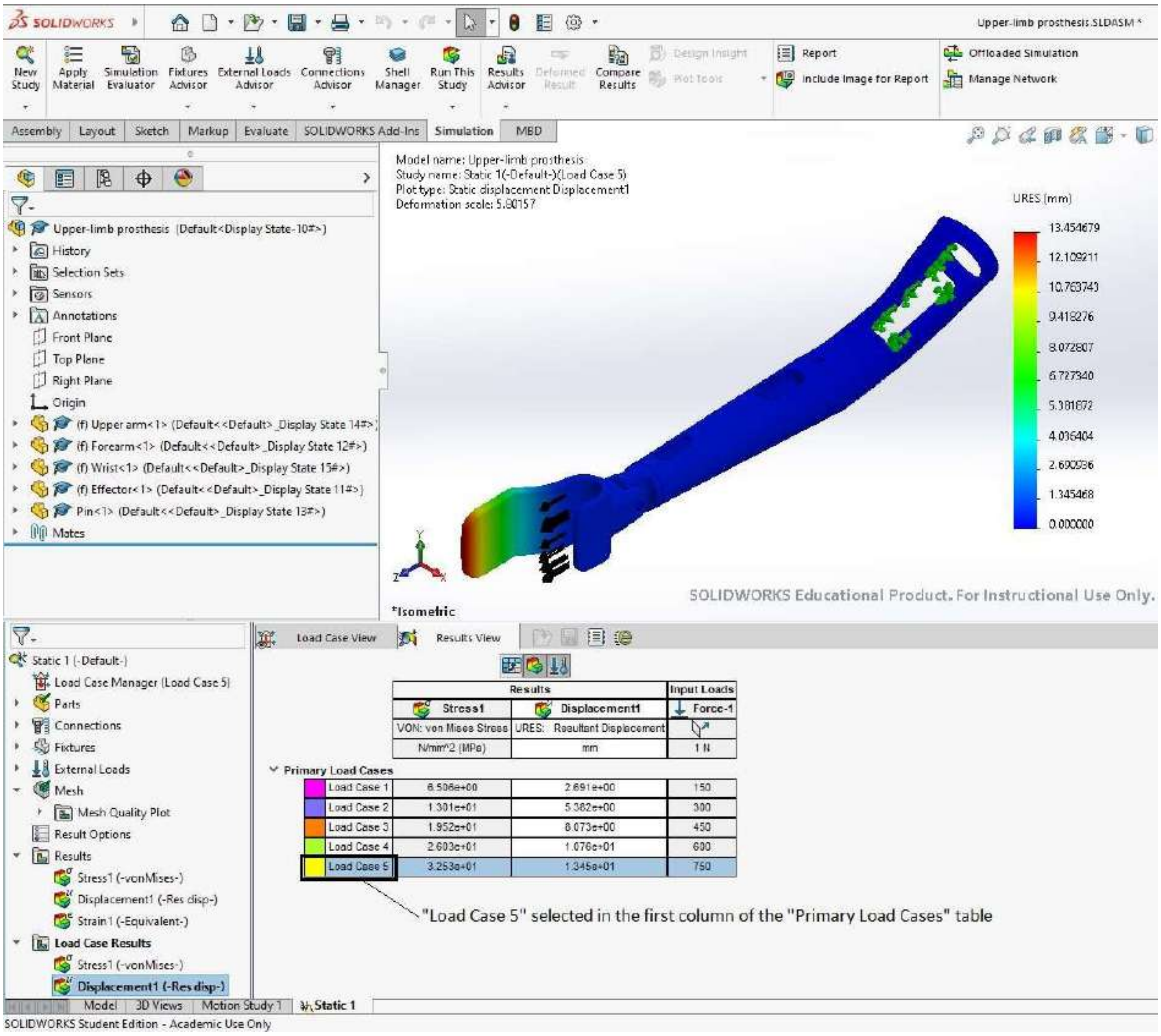

Figure 42: Color map showing the distribution of the deflection at the level of the entire assembly (fifth load case: traction force of 750 N)

This project has been funded with support from the Iceland Liechtenstein Norway Grants. This publication [communication] reflects the views only of the authors, and the Commission cannot be held responsible for any use which may be made of the information contained therein.

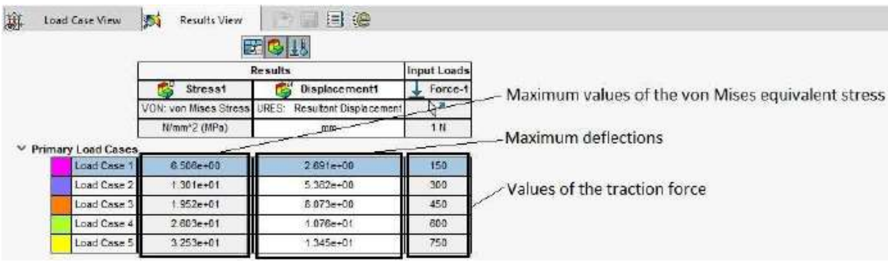

Figure 43: Maximum value of the von Mises equivalent stress, maximum deflection, and traction force corresponding to different load cases listed in the “Primary Load Cases” table

Table 2: Traction force, maximum value of the von Mises equivalent stress, and maximum deflection corresponding to different load cases (see also Figure 43)

Load case	Traction force F [N]	Maximum value of the von Mises equivalent stress $\sigma_{eq,max}$ [MPa]	Maximum deflection d_{max} [mm]
1	150	6.51	2.691
2	300	13.01	5.382
3	450	19.52	8.073
4	600	26.03	10.764
5	750	32.53	13.455

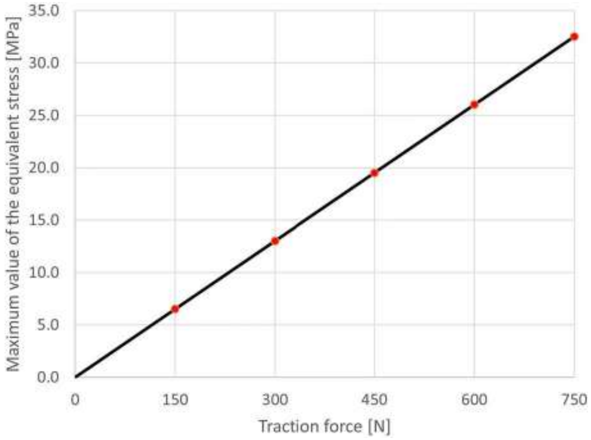

Figure 44: Dependence $\sigma_{eq,max}$ vs F: red dots – numerical results taken from Table 2; black line – linear regression defined by Eq (1)

This project has been funded with support from the Iceland Liechtenstein Norway Grants. This publication [communication] reflects the views only of the authors, and the Commission cannot be held responsible for any use which may be made of the information contained therein.

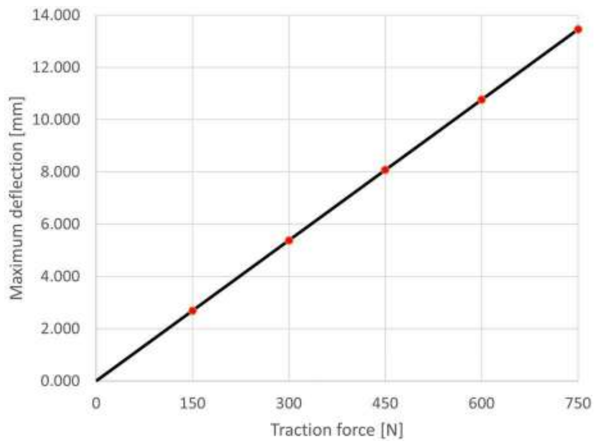

Figure 45: Dependence d_{max} vs F: red dots – numerical results taken from Table 2; black line – linear regression defined by Eq (2)

4. Suggestions for individual work

a) Evaluate the strength characteristics of the upper-limb prosthesis by simulating the distal tensile test under the hypothesis that all the components are made of PLA exhibiting an isotropic linear elastic behavior. Table 3 lists the physical and mechanical properties of this material that are relevant for the finite element model.

Table 3: Physical and mechanical properties of PLA [Far2016]

Mass density ρ [kg/m^3]	Elastic modulus E [MPa]	Poisson's ratio ν [-]	Yield strength Y [MPa]
1252	3500	0.36	59

Note: The properties listed in Table 3 are stored in the custom library *EMERALD CAE Materials.sldmat.*

b) Develop another design of the upper-limb prosthesis and evaluate its strength characteristics by simulating the distal tensile test.

This project has been funded with support from the Iceland Liechenstein Norway Grants. This publication [communication] reflects the views only of the authors, and the Commission cannot be held responsible for any use which may be made of the information contained therein.

References

[Far2016] Farah, S.; Anderson, D.G.; Langer, R. Physical and mechanical properties of PLA, and their functions in widespread applications — A comprehensive review. *Advanced Drug Delivery Reviews* **2016**, *107*, 367-392. [https://doi.org/10.1016/j.addr.2016.06.012]

[Kan2020] Kannan, S.; Ramamoorthy, M.; Sudhagar, E.; Gunji, B. Mechanical characterization and vibrational analysis of 3D printed PETG and PETG reinforced with short carbon fiber. In Proceedings of the International Conference on Physics and Chemistry of Materials in Novel Engineering Applications PCMNEA2020 (AIP Conference Proceedings 2270), Coimbatore, India, 6-7 February 2020; 030004. [https://doi.org/10.1063/5.0019362]

[WWW2022a] https://www.solidworks.com/

[WWW2022b] https://www.solidworks.com/product/solidworks-simulation

This project has been funded with support from the Iceland Liechenstein Norway Grants. This publication [communication] reflects the views only of the authors, and the Commission cannot be held responsible for any use which may be made of the information contained therein.

Iceland Liechtenstein Norway grants

Working together for a green, competitive and inclusive Europe

EMERALD

The Education, Scholarships, Apprenticeships and Youth Entrepreneurship

EUROPEAN NETWORK FOR 3D PRINTING OF BIOMIMETIC MECHATRONIC SYSTEMS

E-toolkit – 3D PRINTING

Project Title	**European network for 3D printing of biomimetic mechatronic systems** **21-COP-0019**
Output	**O2 - EMERALD e-toolkit manual for digital learning in producing biomimetic manufacturing method**
Module	**3D Printing**
Authors	**Diana BĂILĂ**

This project has been funded with support from the Iceland Liechtenstein Norway Grants. This publication [communication] reflects the views only of the authors, and the Commission cannot be held responsible for any use which may be made of the information contained therein.

Contents

This project has been funded with support from the Iceland Liechtenstein Norway Grants. This publication [communication] reflects the views only of the authors, and the Commission cannot be held responsible for any use which may be made of the information contained therein.

1 3D Printing toolkit for medical applications

Product 1: Personalized Orthosis – SLDPRT. file Poznan University of Technology Partner

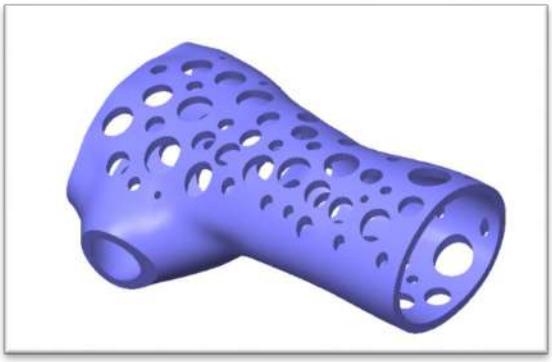

Fig.1. Personalised orthosis

1.1. CAD Modeling

CAD modeling is used by many designers to create elaborate computerized models of objects before they are physically produced. CAD stands for computer-aided design. Engineers, architects, and even artists utilize computers to assist in their design projects. Computers allow them to visualize their designs and confront problems before they have expended any of the resources necessary to put them into physical form. [1-88]
CAD modeling takes many different forms depending on the type of project. Some models are simple two-dimensional representations of various views of an object. Others are elaborate three-dimensional cross-sections that show every detail in great depth. Some CAD models are even animated, showing how all of the components of the model work together to complete its function.
Many different professions make use of computer-aided design. It is an important industrial art involved in automotive, aerospace, prosthetic, and artistic designs. The use of CAD modeling is massively widespread; anything from chairs to rockets can be designed with the aid of computer programs. Among other titles, CAD modelers are referred to as CAD monkeys, designers, and digital information engineers. A single CAD file, 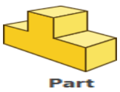

can be made, edited and continually tweaked until the object is ready for production.

This project has been funded with support from the Iceland Liechtenstein Norway Grants. This publication [communication] reflects the views only of the authors, and the Commission cannot be held responsible for any use which may be made of the information contained therein.

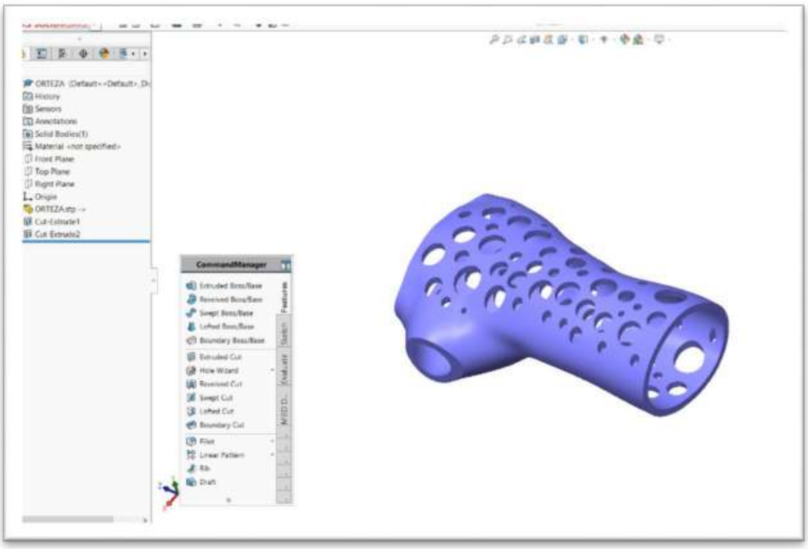

Fig.2. SolidWorks – SLDPRT. file

SolidWorks is a solid modeling computer-aided design (CAD) and computer-aided engineering (CAE) application published by Dassault Systèmes, as in figure 2. [1]

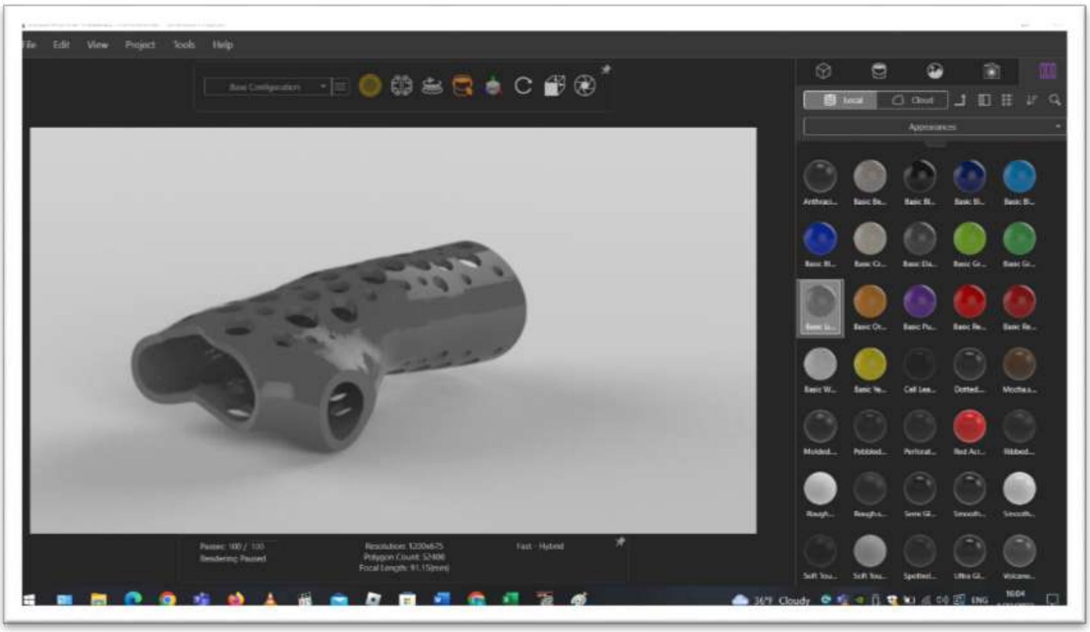

Fig.3. SolidWorks Visualize 2019 – orthosis with different texture mapping

This project has been funded with support from the Iceland Liechtenstein Norway Grants. This publication [communication] reflects the views only of the authors, and the Commission cannot be held responsible for any use which may be made of the information contained therein.

The CAD software permits to realize the three-dimensional models using different geometric entities such as, lines, rectangle, curves surfaces interconnected to a multitude of points in 3D space.

The 3D models can be realized by algorithms, using CAD software or by Reverse Engineering using a 3D scanner that collects information's concerning the dimensions and the 3D shape of the object. SolidWorks Visualize 2019 permits their surfaces to be further defined with texture mapping, as in figure 3 [1].

1.2. STL file

To design the personalised orthosis, it was starting a new work session in SolidWorks, on click "Part", because it's a single design component. After design the personalised orthosis, it will be saved with name "Personalised Orthosis", in SLDPRT format. For manufacture using 3D Printing technology, the solid part is converted in STL file, and it will be saved such as .stl and must to choose from properties menu the resolution (coarse, fine or custom) and it was choose fine quality for meshing the product, such in Figure 4. Total triangles are 52426 used for meshing.[1-88]

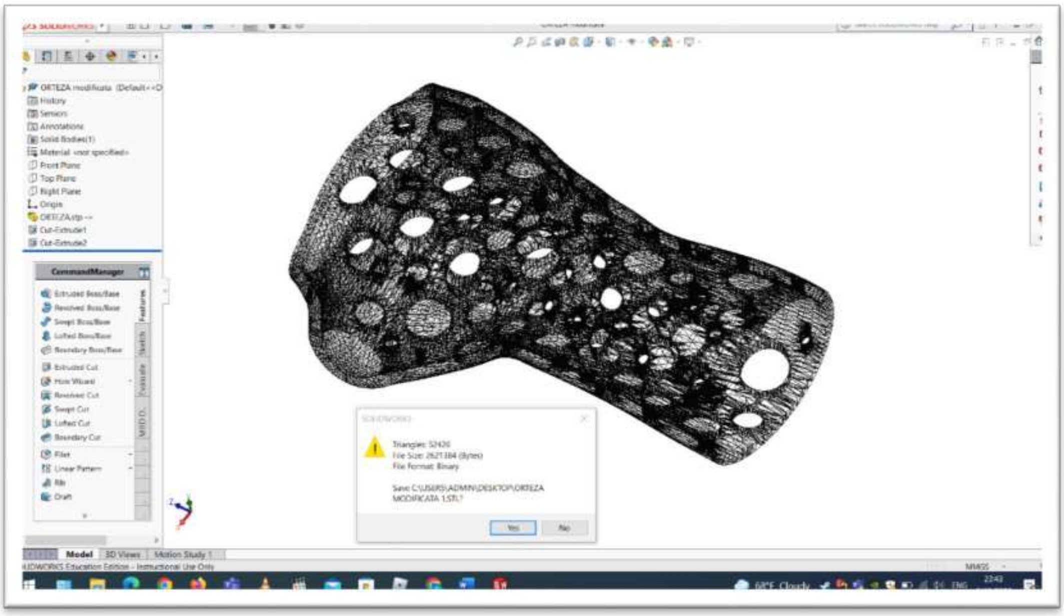

Fig.4.Orthosis meshing – STL. file

This project has been funded with support from the Iceland Liechtenstein Norway Grants. This publication [communication] reflects the views only of the authors, and the Commission cannot be held responsible for any use which may be made of the information contained therein.

1.3. 3D Printing software's

Additive Prototyping Technologies (AM) differ fundamentally from material removal processing technologies (cutting, EDM, laser processing) and redistribution processing technologies material (casting, injection, forging, stamping) by the fact that the parts are obtained by adding layer by layer material using a CAD file.

These technologies have emerged grace a result of the achievements and advances made in the field of fine mechanics, numerical control, laser technology, computers, software, and the new materials development.

The specificity of these additive manufacturing processes is their ability to make parts and complex three-dimensional objects, starting from a CAD file, without the need for it use of machine tools or certain tools. The basic element of prototype additive manufacturing technologies is "the section". [1-86]

The pieces are quantified in sections and made using a repetitive process of construction, section by section, reducing a three-dimensional problem to one flat. This dimensional reduction leads to a decrease in accuracy and quality surfaces due to the scale effect.

The steps required for the additive manufacturing of a part are as follows:

-designing the three-dimensional (3D) model of the part, using a design program computer aided (CAD);

-transferring the CAD model to the sectioning processor. The best-known method of sectioning is the approximation of the model with flat triangular elements.

- sectioning the 3D virtual model with parallel planes to the working plane of the rapid manufacturing machine of prototypes and generation of orders for control equipment of the machine.

-the construction of the part (material, supports required during the model, how will be added a new layer, marking the contours for each section, marking the area between the exterior and interior contour of a section.

- cleaning and finishing of the part (operations in which the supports used at construction and excess material are eliminated).[1-88]

Regarding solid CAD modelling, Additive Manufacturing systems are becoming an important and motivating factor for companies that produce solid modelling systems, such as: Solidworks, Unigraphics, I-DEAS, Catia, Inventor, Onshape, AutoCAD, Pro / Engineer, etc

This project has been funded with support from the Iceland Liechtenstein Norway Grants. This publication [communication] reflects the views only of the authors, and the Commission cannot be held responsible for any use which may be made of the information contained therein.

The best software used by FDM (Fused Deposition Modeling) printers are Ultimaker Cura, BCN 3D Cura, Voxelizer, Z-Suite, etc and for SLA (Stereolithography)/DLP (Digital Light Processing) printers are FormLabs, Photocentric, etc.

Using https://ultimaker.com/en/resources/manuals/software and downloaded free software https://ultimaker.com/en/products/ultimaker-cura-software, than it must to obtain the g-code file necessary to print the part. The first step consist in open Ultimaker Cura software and to introduce by drag the part, as stl.file, such in the Figure 5. The software permits to choose the 3D Printer that it is necessary to print, and in this case, it is used Ultimaker S5. For printing, it must to use a cable or a card memory or via wireless to connect the 3D printer to laptop to put in function the 3D Printer.[1-88]

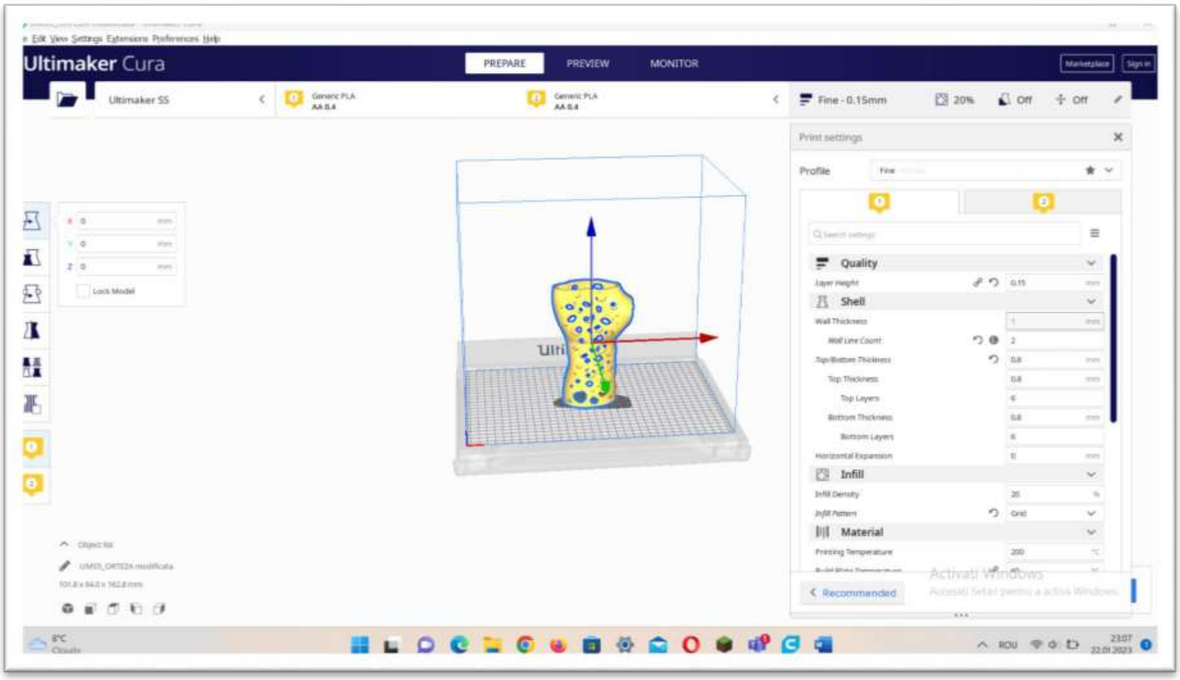

Fig.5. Open Ultimaker Cura software and introduce the STL. file of part

The software permit the move of the part on the work platform after the X,Y,Z axis , the change of the part scale after X,Y,Z axis, such as Figure 6. The rotation of the part after the X, Y, Z axis, the multiplication of the parts on the work platform and the mirror parts printing, it is permitted by the software.

This project has been funded with support from the Iceland Liechtenstein Norway Grants. This publication [communication] reflects the views only of the authors, and the Commission cannot be held responsible for any use which may be made of the information contained therein.

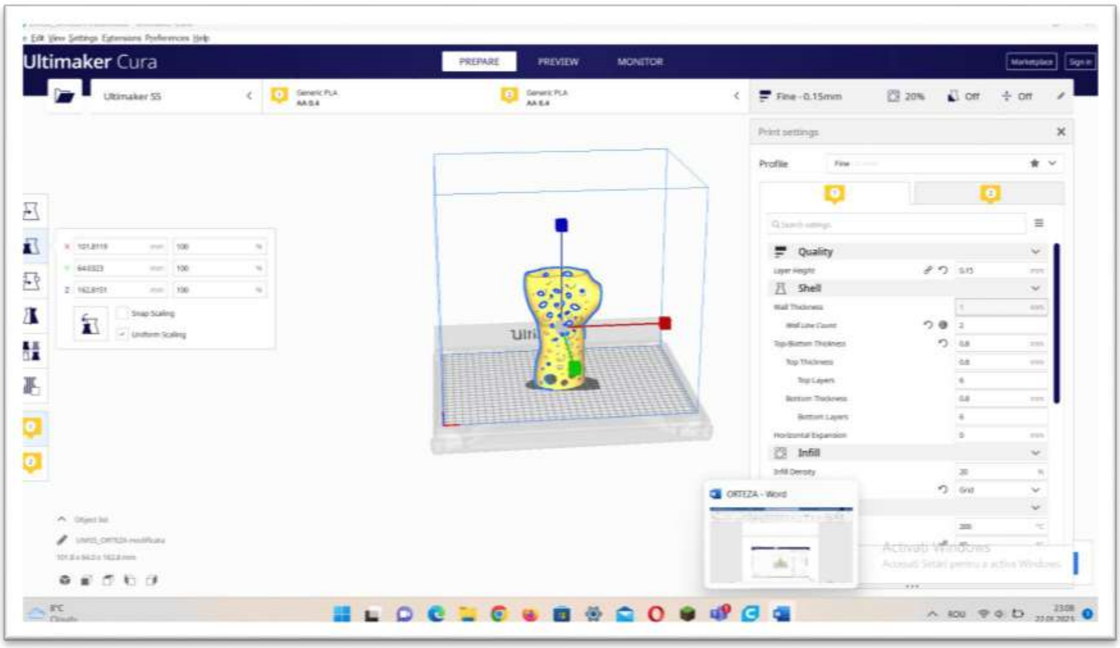

Fig.6. Change the part scale, after X, Y, Z axis

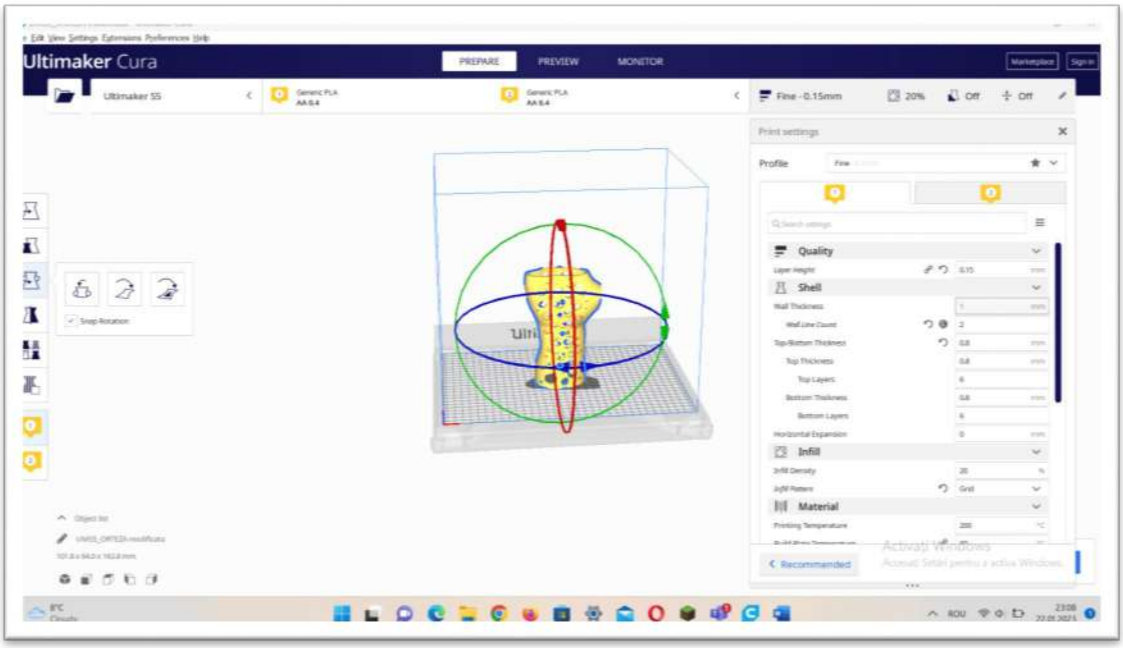

Fig.7. Rotation of the part after X, Y, Z axis

This project has been funded with support from the Iceland Liechtenstein Norway Grants. This publication [communication] reflects the views only of the authors, and the Commission cannot be held responsible for any use which may be made of the information contained therein.

The software permit to choose for printing different materials, as PLA, ABS, PET, etc. For the personalised orthosis, it was choosing ABS materials with the mechanical properties given in the Table 1.[1-88]

ABS and PLA are the most common FDM (Fused Deposition Modeling) printed materials and are typically similar in cost. ABS has superior mechanical properties but is harder to print compared to PLA. Material properties can be chosen using the free site https://www.totalmateria.com/page.aspx?ID=Home&LN=RO

Table 1. The mechanical properties of Acrylonitrile Butadiene Styrene (ABS)

Properties	Values	Units
Density	1.0-1.4	g/cm3
Poisson's Ratio	0.35	-
Shear Modulus G	1,03-1,07	GPa
Melting Temperature	200	ºC
Glass transition temperature	105	ºC
Thermal Conductivity	0,25	W/m-K
Extruded Temperature	200-230	ºC
Heat Deflection Temperature, 1,81 MPa	81	ºC
Young's modulus	1,79-3,2	GPa
Tensile Strength	29,8-43	MPa
Compressive Strength	76-78	MPa
Elongation at Break	10-50	%
Flexural modulus	2,1-7,6	GPa
Hardness Shore D	100	
Izod Impact Strength	58	kJ/m2
Yield Strength	28-120	MPa
Standard Tolerance	+/-0.05	mm
Biodegradable	-	-
Melt flow	12-23	g/10min
Rockwell Hardness	R102-R104	

Due to its lower printing temperature is easier to print with and therefore better suited for parts with fine details. ABS is best suited for applications where strength, ductility, machinability and thermal stability are required. ABS is more prone to warping. The mechanical properties of ABS are presented in Table 1.

This project has been funded with support from the Iceland Liechtenstein Norway Grants. This publication [communication] reflects the views only of the authors, and the Commission cannot be held responsible for any use which may be made of the information contained therein.

For 3D Printing process was used only an extruder, the extruder 1 (Fig.8), but in generally we can work with 2 extruders, one for supports and other for part manufacture, as in the Fig. 9. The software permit to custom the 3D Printing process of parts, as in Figure 10 (a and b) or to use the recommended parameters for part manufacturing as in Figure 11.[1-88]

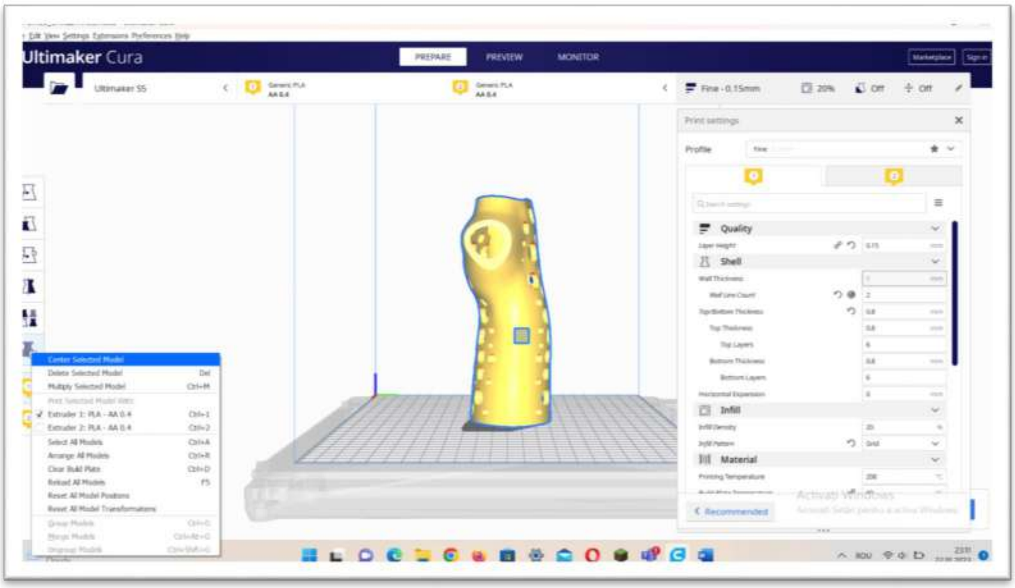

Fig 8. 3D Printing Extruder chosen

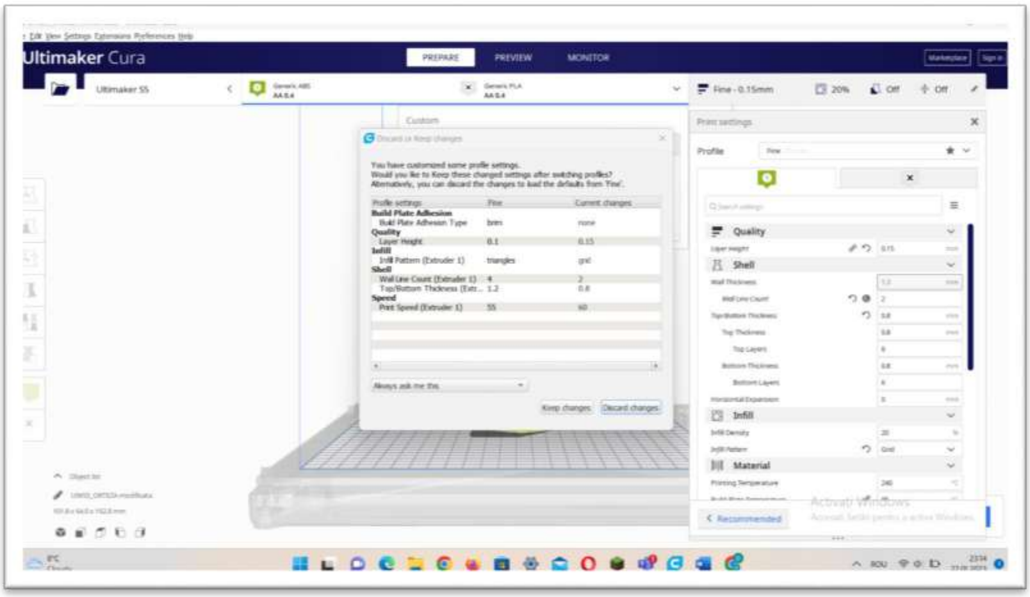

This project has been funded with support from the Iceland Liechtenstein Norway Grants. This publication [communication] reflects the views only of the authors, and the Commission cannot be held responsible for any use which may be made of the information contained therein.

Fig.9. Choosing the ABS filament for 3D Printing

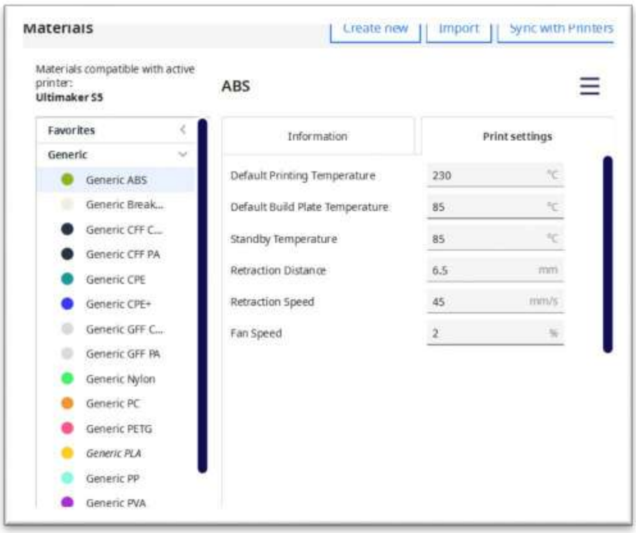

Fig.10a. Printing setting for ABS material

This project has been funded with support from the Iceland Liechtenstein Norway Grants. This publication [communication] reflects the views only of the authors, and the Commission cannot be held responsible for any use which may be made of the information contained therein.

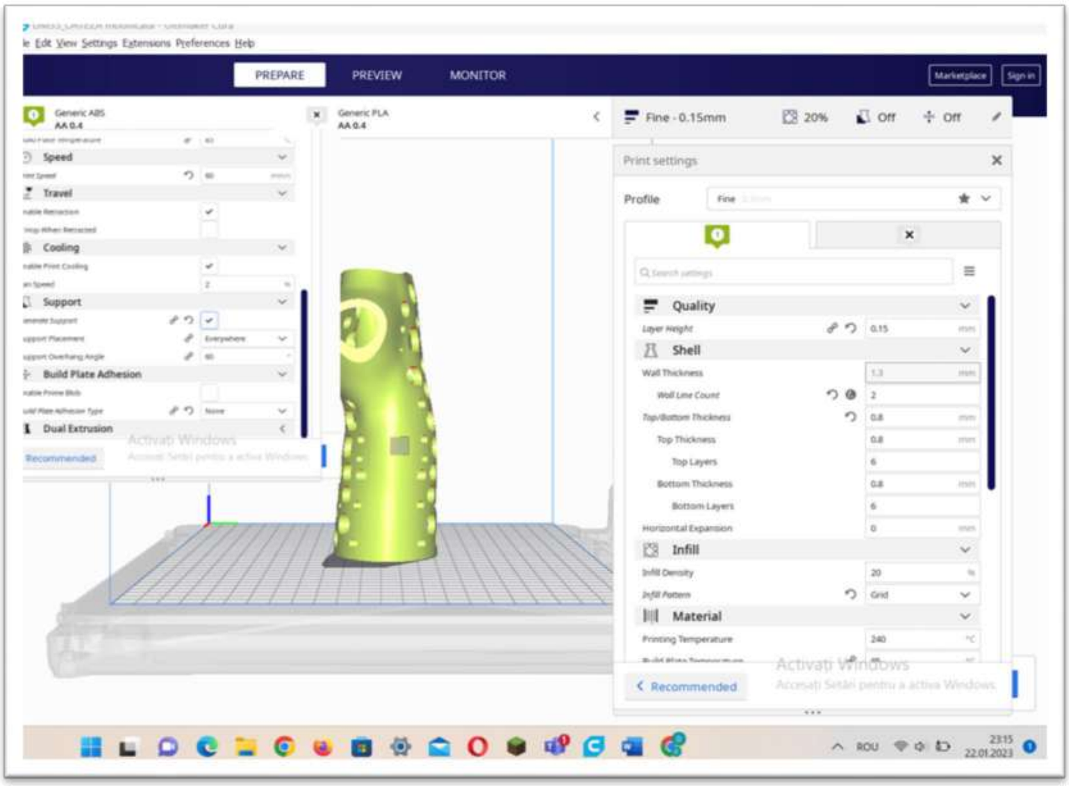

Fig.10b. Manufacturing parameters for custom 3D Printing without supports

This project has been funded with support from the Iceland Liechtenstein Norway Grants. This publication [communication] reflects the views only of the authors, and the Commission cannot be held responsible for any use which may be made of the information contained therein.

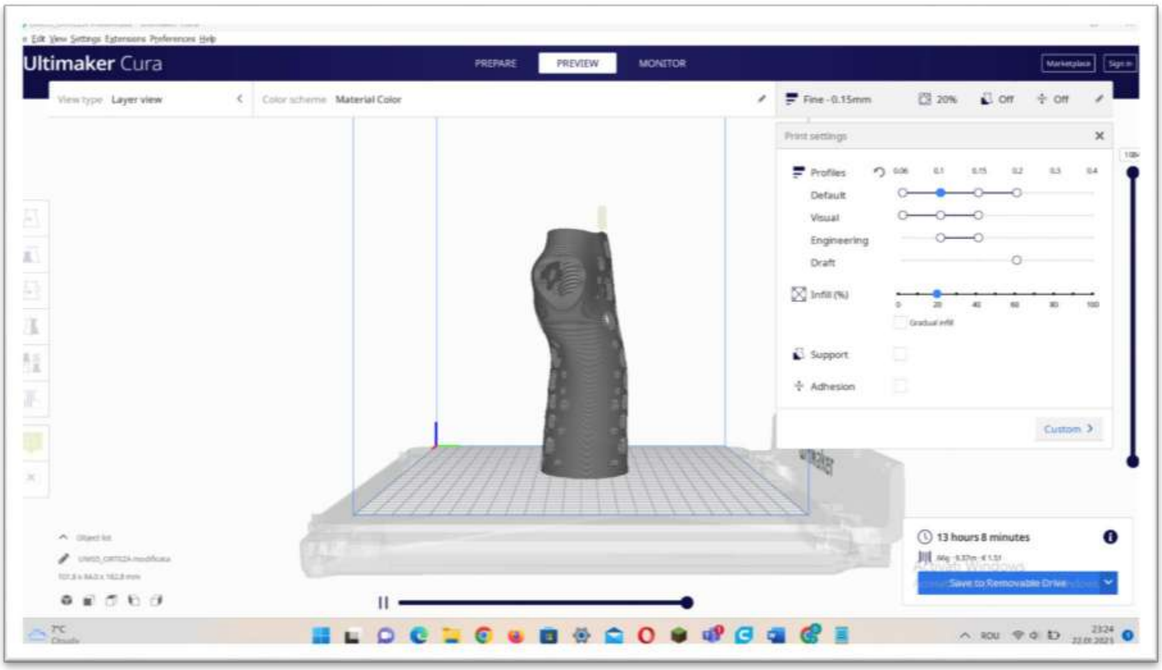

Fig.11. Recommended manufacturing parameters for the part by the software

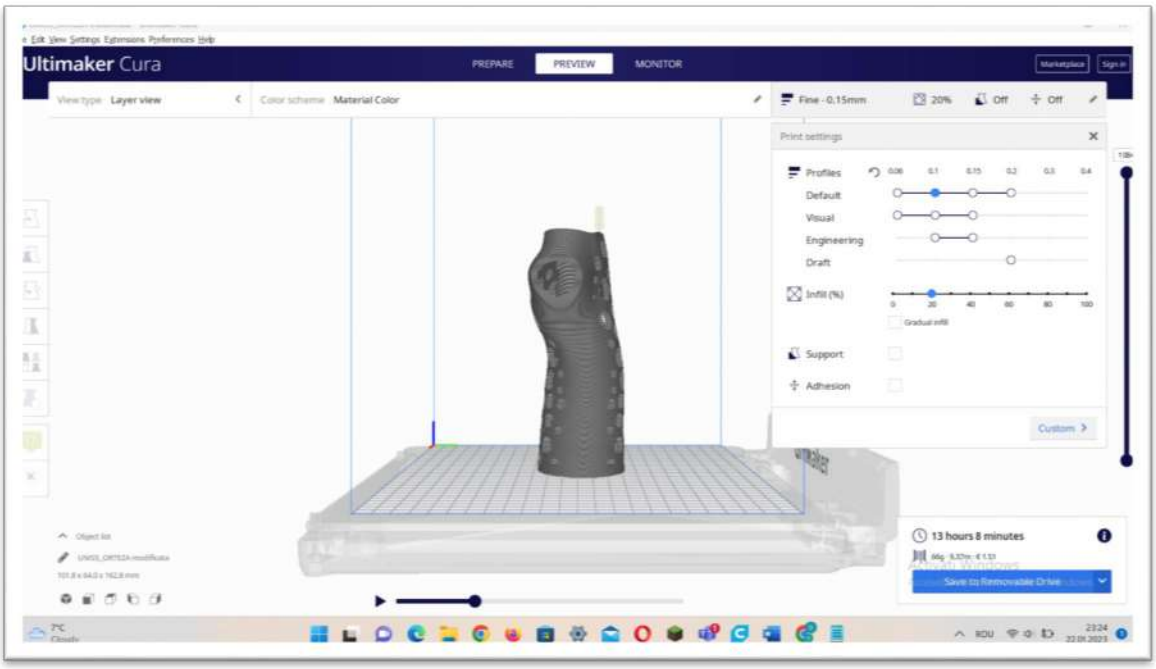

Fig.12. Preview the manufacturing 3D Printing process

This project has been funded with support from the Iceland Liechtenstein Norway Grants. This publication [communication] reflects the views only of the authors, and the Commission cannot be held responsible for any use which may be made of the information contained therein.

It must click the blue button slice to slicing the parts. The software gives information's concerning the time necessary for manufacturing (13 hours and 8 minutes), the cost of the part (1.51 euros if 1kg ABS filament cost of 25 euros) and the material consumption (66 g, filament length used 9.37 m). The software permit to used supports if it necessary to obtain parts with great accuracy or without supports if it must obtain part in a shorter time. The software permit to preview by a small video, the simulation concerning the 3D Printing process, as in the Figure 12.[1-88]

For saving the part file, the software Ultimaker Cura it necessary to click on Save Project, as in Figure 13, then it will obtain the Summary- Cura Project, as in the Figure 14, and it will save as 3mf. file 

, as in the Figure 15.

The software permit export file (Figure 16) with different extensions, and it was choose the extension file - g-code 

necessary to 3D Printing, as in Figure 17. In figure 18, it is presented how look the g-code for orthosis part. For time of printing is 13 hours and 8 minutes and the filament consumable is 66 g, length 9.37m, and the cost of part is 1.51 euro, if considered that the filament cost is 25 euro/kg.

This project has been funded with support from the Iceland Liechtenstein Norway Grants. This publication [communication] reflects the views only of the authors, and the Commission cannot be held responsible for any use which may be made of the information contained therein.

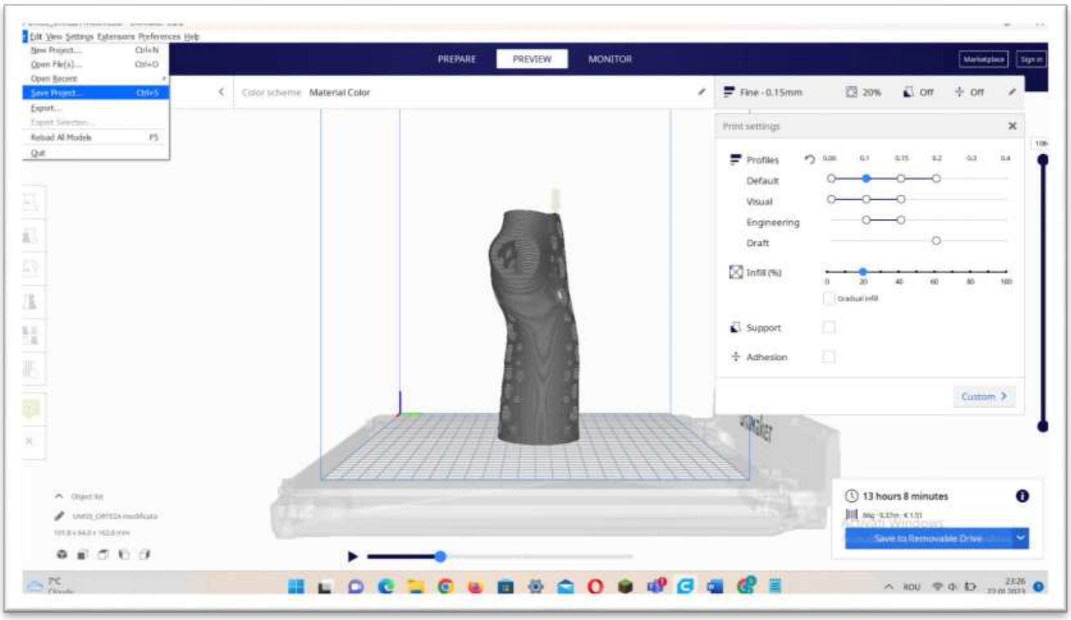

Fig.13. Save Project

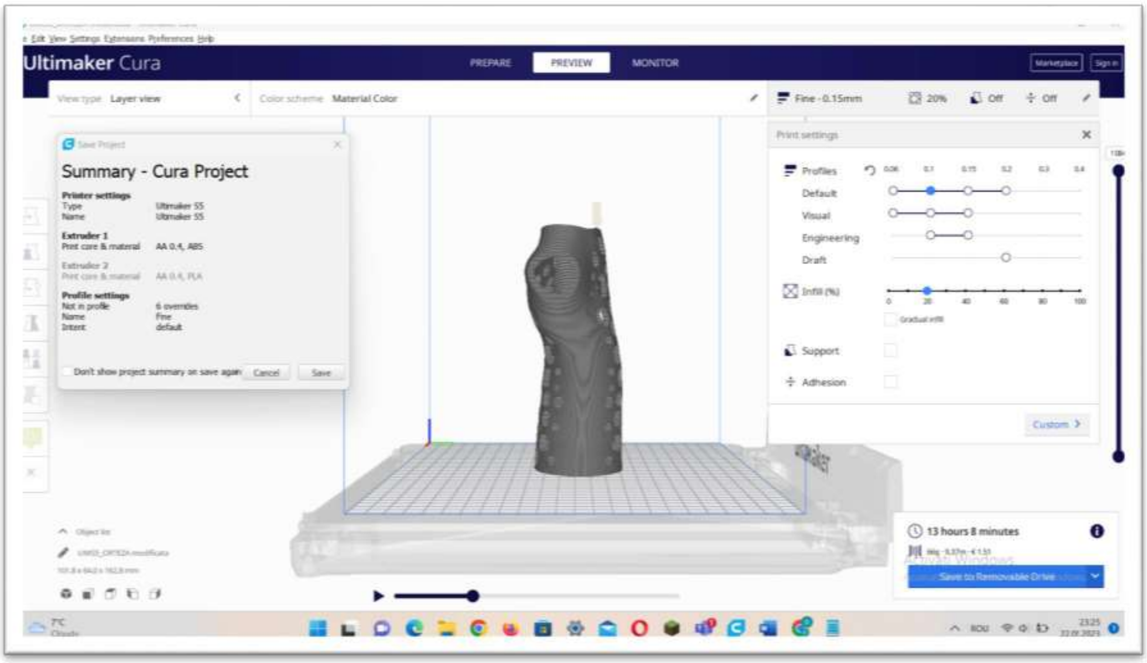

Fig.14. Summary- Cura Project

This project has been funded with support from the Iceland Liechtenstein Norway Grants. This publication [communication] reflects the views only of the authors, and the Commission cannot be held responsible for any use which may be made of the information contained therein.

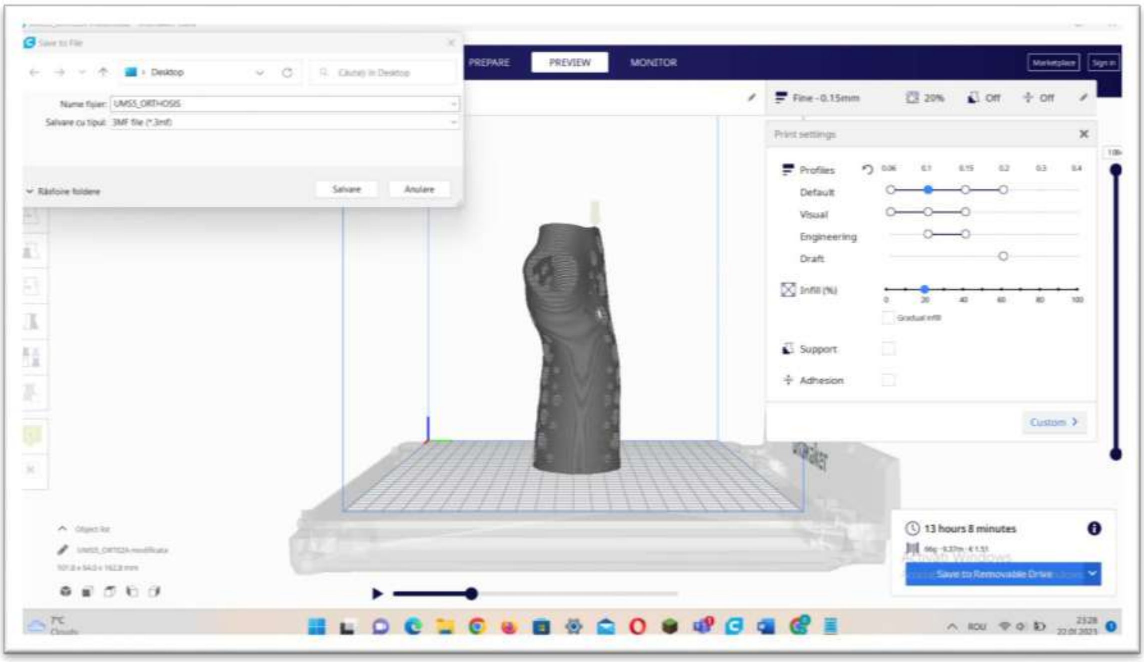

Fig.15. Save project as 3mf. file

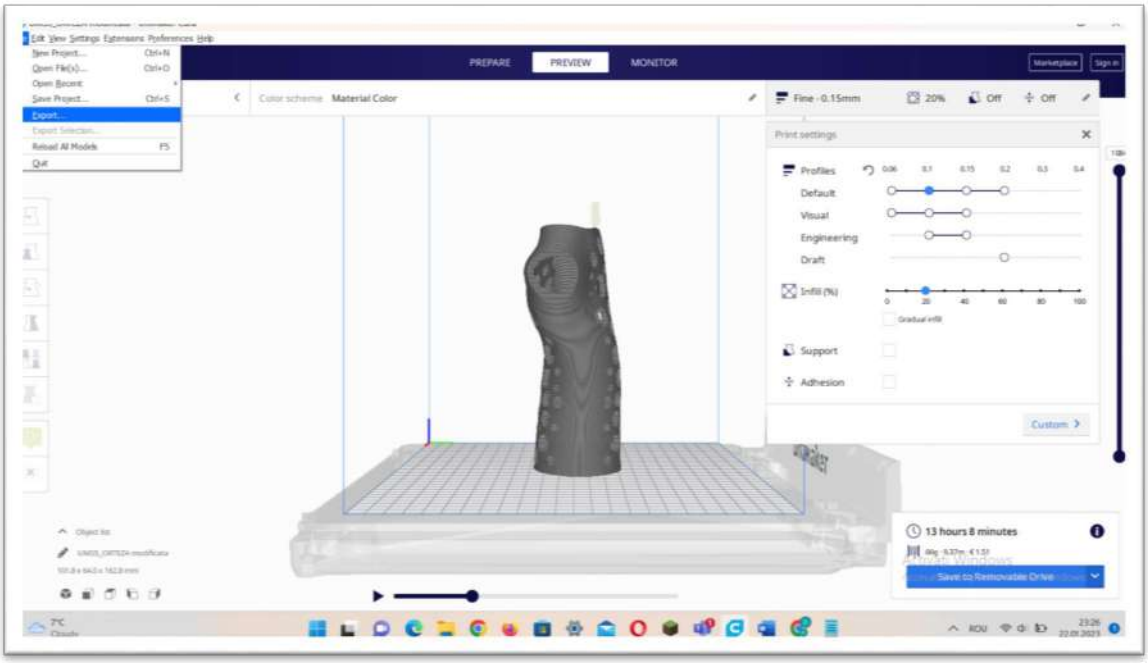

Fig.16. Export file

This project has been funded with support from the Iceland Liechtenstein Norway Grants. This publication [communication] reflects the views only of the authors, and the Commission cannot be held responsible for any use which may be made of the information contained therein.

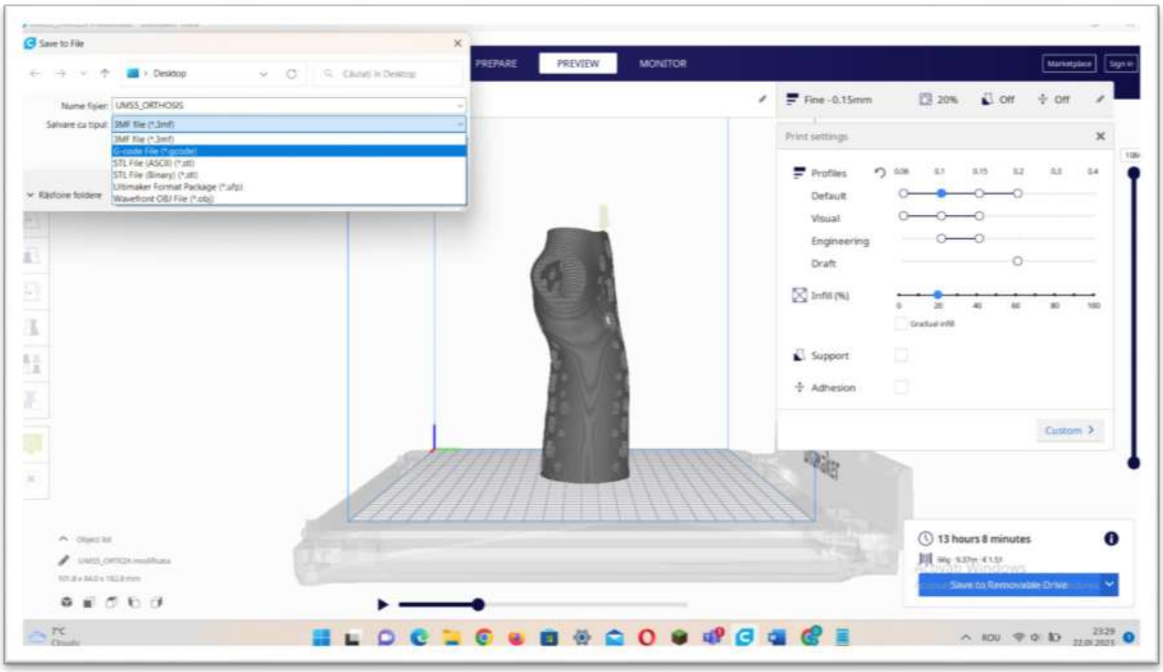

Fig.17. Different extension for file export

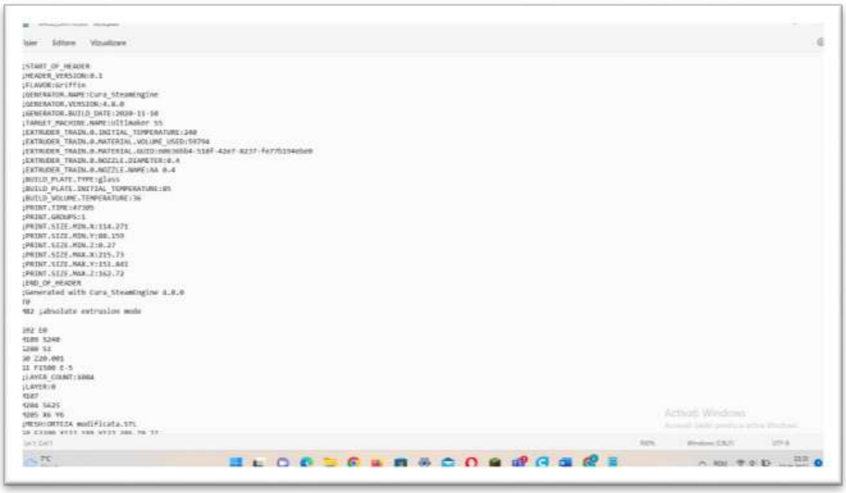

Fig.18. G-code file for personalized orthosis part

This project has been funded with support from the Iceland Liechtenstein Norway Grants. This publication [communication] reflects the views only of the authors, and the Commission cannot be held responsible for any use which may be made of the information contained therein.

Fig.19. Personalized Orthosis printed by FDM technology

Product 2: Robotic Arm – ASM, SLDASM. file Poznan University of Technology Partner

2.1. CAD Modeling

Many CAD files (13 elements) must be made, designed and saved as SLDPRT files and then will be assembled using Assembly to obtain the robotic arm, save as ASM, SLDASM file, as in the Fig.20. is ready for production.[1-88]

This project has been funded with support from the Iceland Liechtenstein Norway Grants. This publication [communication] reflects the views only of the authors, and the Commission cannot be held responsible for any use which may be made of the information contained therein.

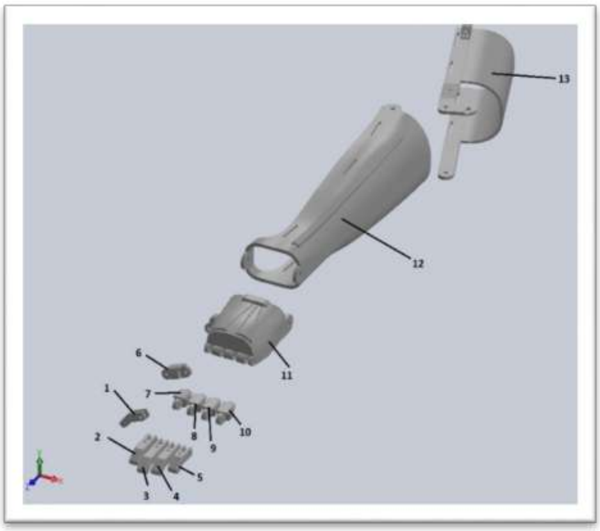

Fig.20. Exploded View – Robotic Arm

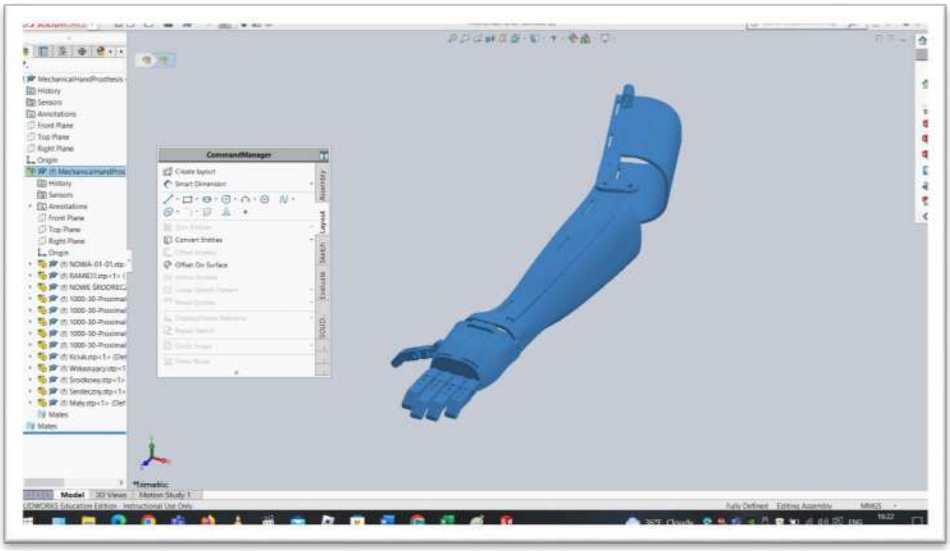

Fig.21. Robotic arm assembly – ASM, SLDASM. File

In the figure 21 is presented robotic arm assembly (all 13 elements), saved as ASM, SLDASM file. file to establish if the parts were well designed. In figure 22, it was used SolidWorks Visualize 2019, that permit to choose different texture mapping (in function of the material used, plastic, metallic, glass, etc.) for the robotic arm.[1-88]

This project has been funded with support from the Iceland Liechtenstein Norway Grants. This publication [communication] reflects the views only of the authors, and the Commission cannot be held responsible for any use which may be made of the information contained therein.

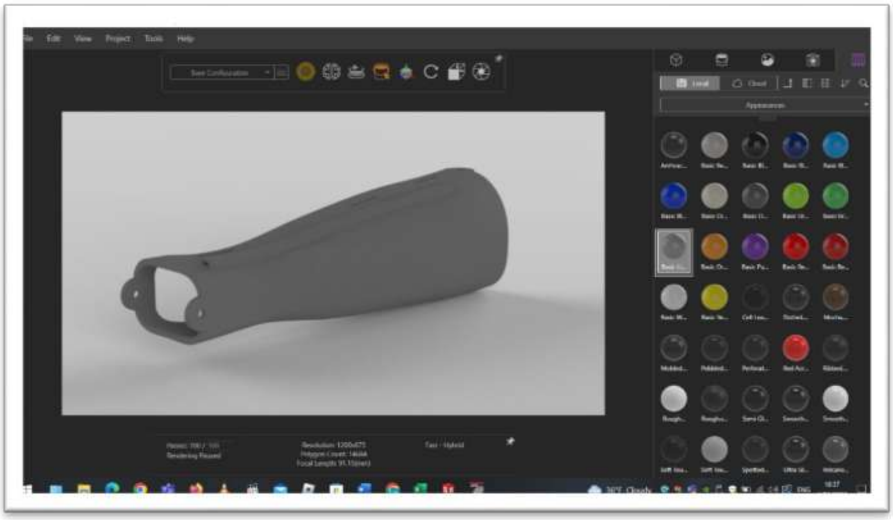

Fig.22. SolidWorks Visualize 2019 – robotic arm with different texture mapping

2.2. STL file

For manufacture using 3D Printing technology, the solid part is converted in STL file, and it will be saved such as .STL file and must choose from properties menu the resolution (coarse, fine or custom) and it was choose fine quality for meshing the product, such in Figure 23. Total triangles are 109616 used for meshing.[1-88]

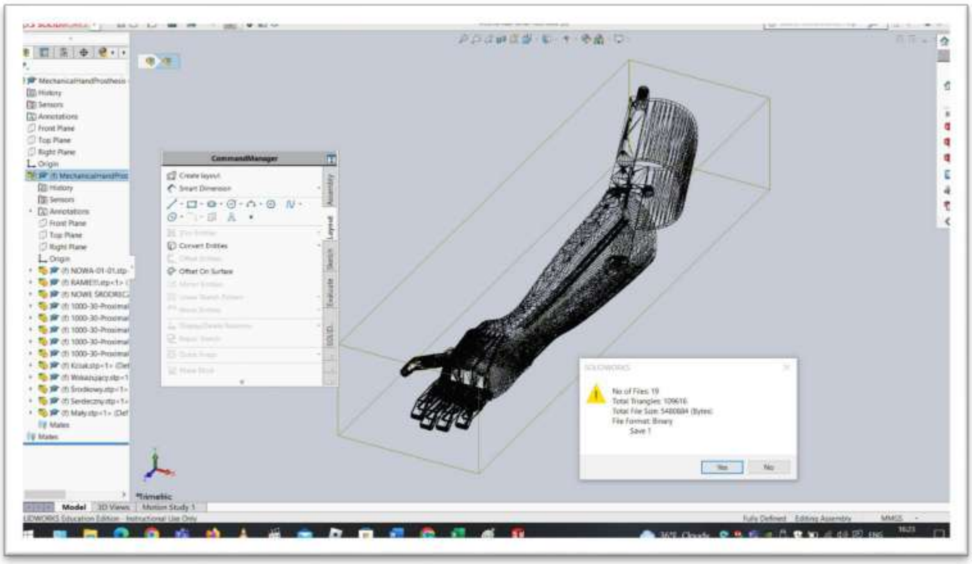

Fig.23.Robotic Arm – STL. file

This project has been funded with support from the Iceland Liechtenstein Norway Grants. This publication [communication] reflects the views only of the authors, and the Commission cannot be held responsible for any use which may be made of the information contained therein.

2.3. 3D Printing software's

The material chosen to be used for this product is PLA filament, having the mechanical properties presented in table 2. PLA is ideal for 3D prints where aesthetics is important.

Table 2. The mechanical properties of PLA (Polylactic Acid)

Properties	Values	Units
Density	1.25	g/cm3
Poisson's Ratio	0.36	-
Shear Modulus G	2.4	GPa
Melting Temperature	173	ºC
Glass transition temperature	60	ºC
Thermal Conductivity	0.13	W/m-K
Extruded Temperature	160-220	ºC
Heat Resistance	110	ºC
Young's modulus	3.5	GPa
Tensile Strength	61.5	MPa
Compressive Strength	93.8	MPa
Elongation at Break	6	%
Flexural strength	88.8	MPa
Hardness Shore D	85	A
Impact Strength	30.8	kJ/m2
Yield Strength	60	MPa
Standard Tolerance	+/-0.05	mm
Biodegradable	yes	-

This project has been funded with support from the Iceland Liechtenstein Norway Grants. This publication [communication] reflects the views only of the authors, and the Commission cannot be held responsible for any use which may be made of the information contained therein.

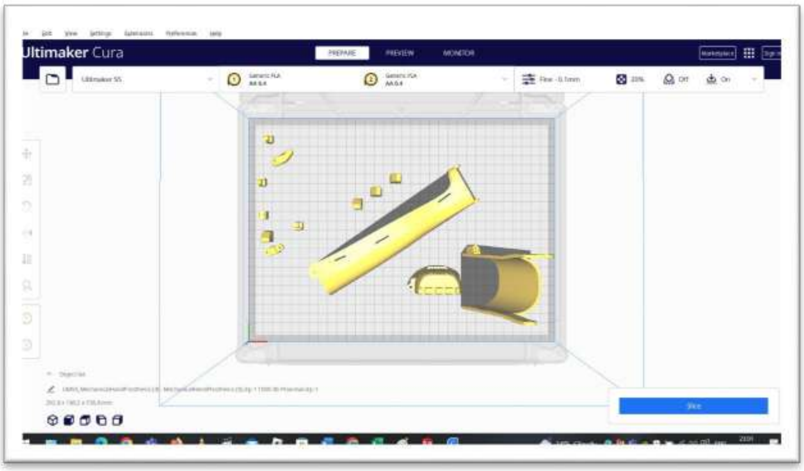

Fig.24. Drag the STL. files on the worktable of the 3D Printer using Ultimaker Cura

In the Figure 25 is shown the PLA filament choosing for 3D Printing and in the figure 26 are presented the printing setting for PLA filament used for FDM process.[1-88]

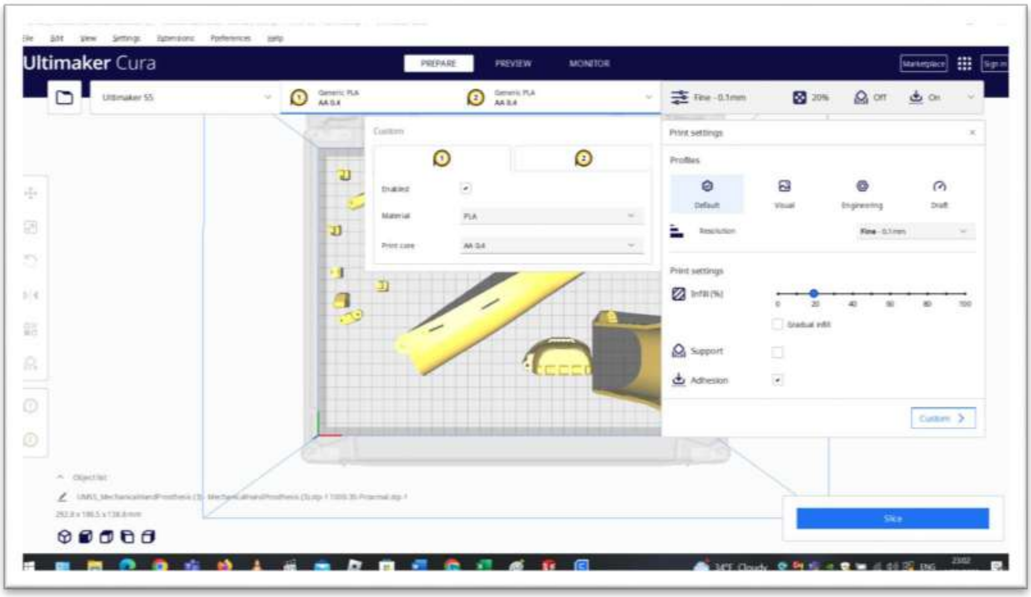

Fig.25. PLA filament choosing for 3D Printing

This project has been funded with support from the Iceland Liechtenstein Norway Grants. This publication [communication] reflects the views only of the authors, and the Commission cannot be held responsible for any use which may be made of the information contained therein.

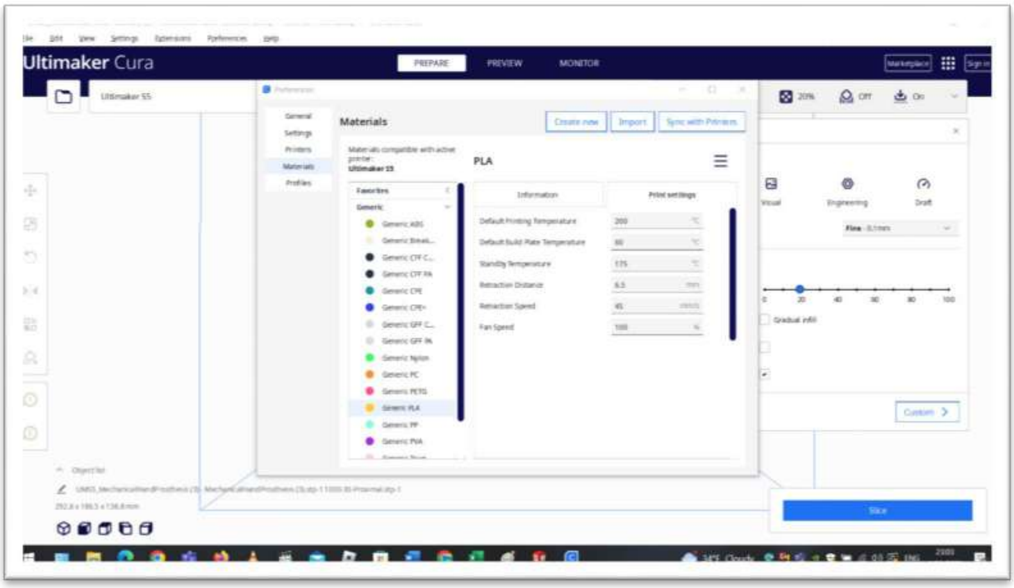

Fig.26. Printing setting for PLA material

In figure 24, all components of robotic arm saved as STL. files are drag on the worktable of the software, because are great dimensions and the Ultimaker S5 table does not permit, we can print simultaneous files at the scale 60%, as in the Figure 27 or we can print in multiples stages at the scale 100%. For 3D Printing, were used two extruders and was used the recommended manufacturing parameters given by software and were selected the supports. It must click the blue button slice to slicing the parts.[1-88]

This project has been funded with support from the Iceland Liechtenstein Norway Grants. This publication [communication] reflects the views only of the authors, and the Commission cannot be held responsible for any use which may be made of the information contained therein.

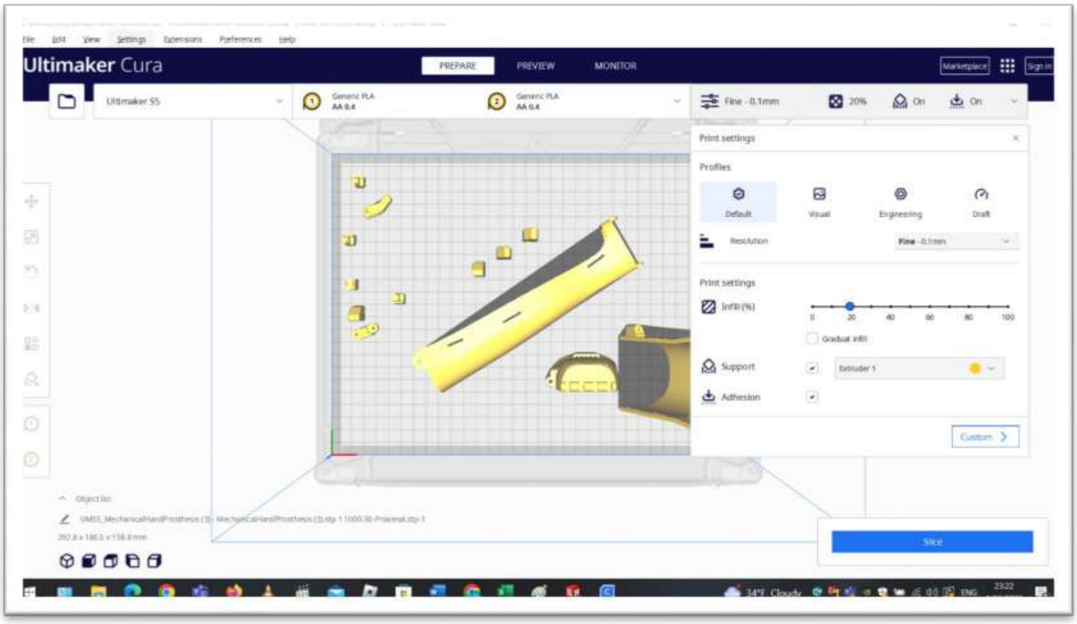

Fig.27. Prepare 3D Printing using two extruders and click slice

For the manufacturing of part exist two modes: recommended by software or custom, where it can personalise the 3D Printing process in function of the materials, the supports necessary, the speed, the temperature, the infill density of the support material. In figure 28, it is presented the recommended manufacturing parameters for robotic arm given by Cura software. In figure 29 is presented the preview of the manufacturing process, it is a small simulation.

The part can be saved as project 3mf. file 

as in Fig.30 and the summary report is shown in Fig.31. The file can be exported using different extensions: stl (ASCII and BINARY), g-code, obj, 3mf and ufp, such in figure 32. In figure 33 is presented the g-code file for Robotic Arm 

and in figure 34 is the printed robotic arm at scale 1:1. After the printing of the part, the supports are eliminated, and the surfaces are cleaned. The surfaces can be manufactured by different classical mechanical processes, such as drilling, milling, etc. The time for the printing process is 1 day 18 hours 39 minutes, the filament consumable is 157 g, filament length used is 19.82 m, the filament cost is 3.14 euros, if considered the PLA filament cost 25 euro/kg.

This project has been funded with support from the Iceland Liechtenstein Norway Grants. This publication [communication] reflects the views only of the authors, and the Commission cannot be held responsible for any use which may be made of the information contained therein.

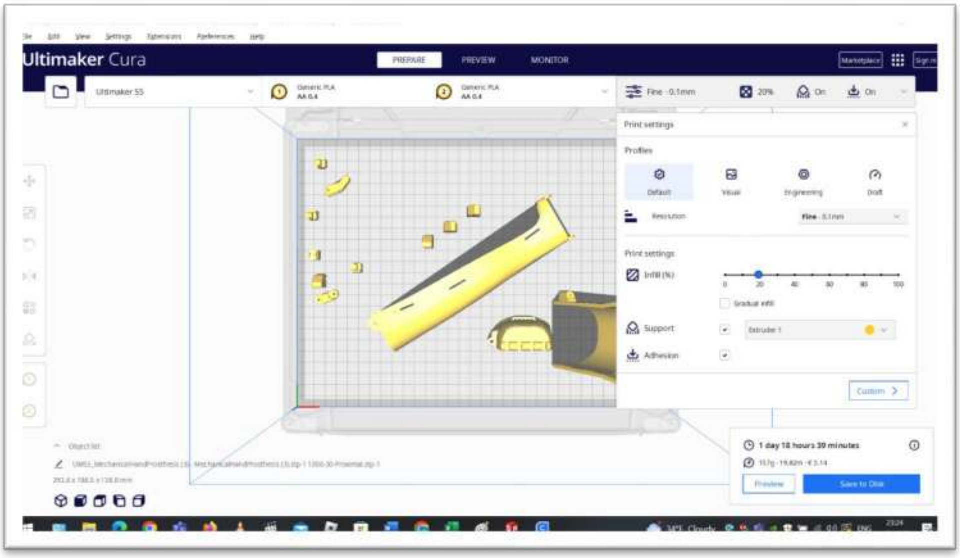

Fig.28. Recommended manufacturing parameters for the part by the software

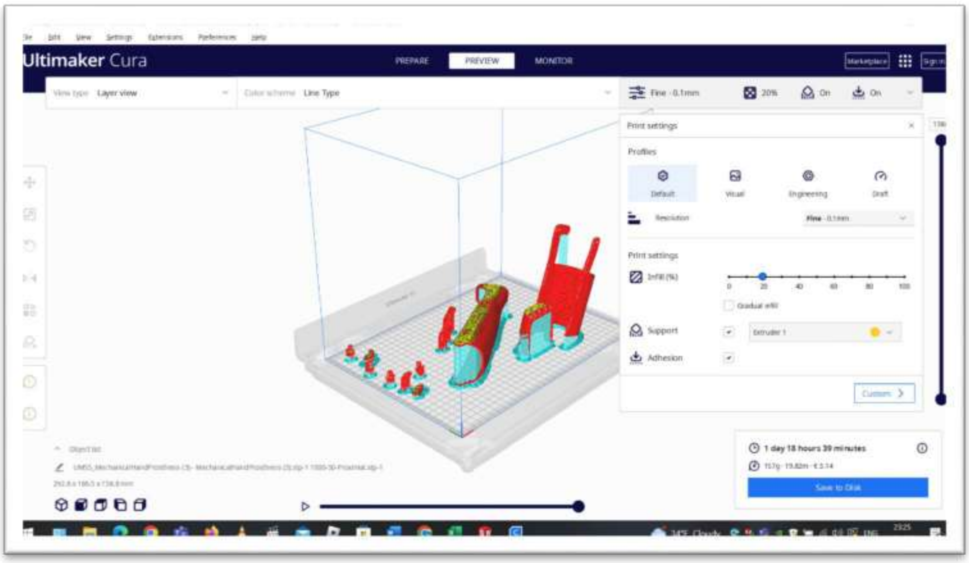

Fig.29. Preview the manufacturing 3D Printing process

This project has been funded with support from the Iceland Liechtenstein Norway Grants. This publication [communication] reflects the views only of the authors, and the Commission cannot be held responsible for any use which may be made of the information contained therein.

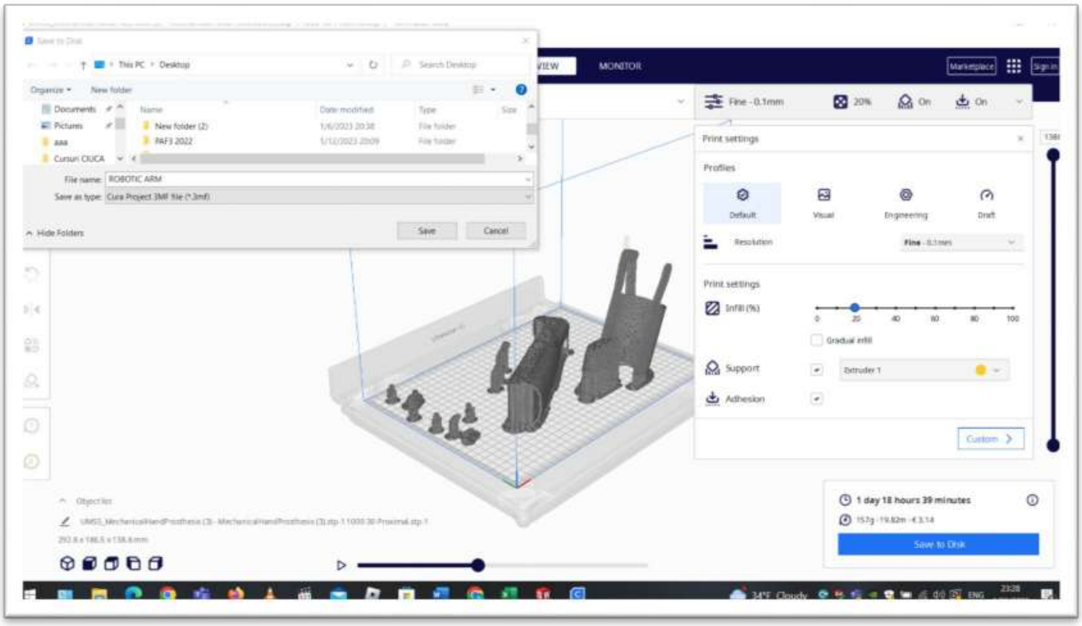

Fig.30. Save project as *3mf. file

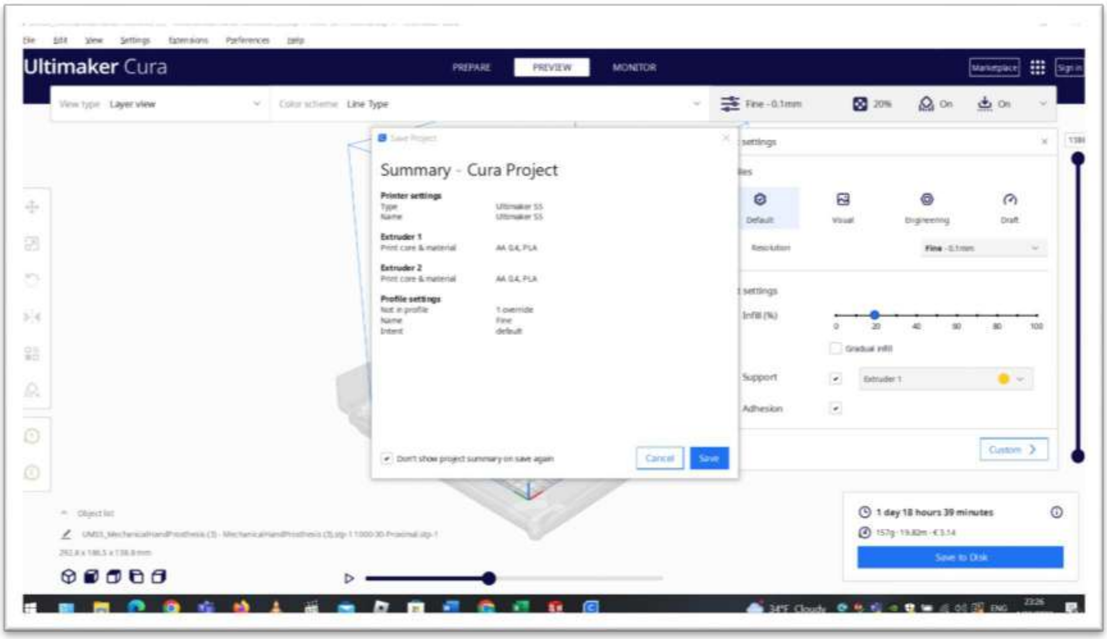

Fig.31. Summary- Cura Project

This project has been funded with support from the Iceland Liechtenstein Norway Grants. This publication [communication] reflects the views only of the authors, and the Commission cannot be held responsible for any use which may be made of the information contained therein.

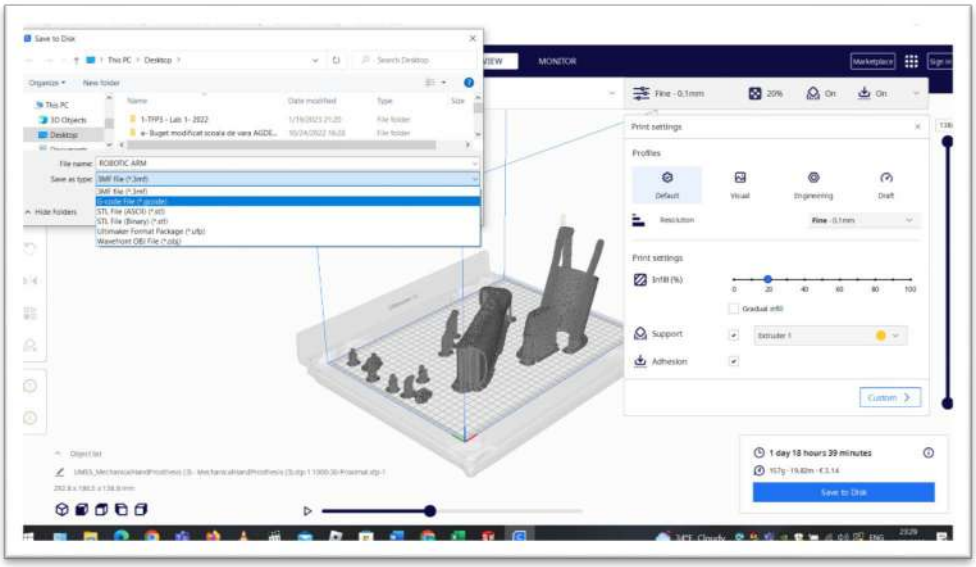

Fig.32. Different extensions for file export

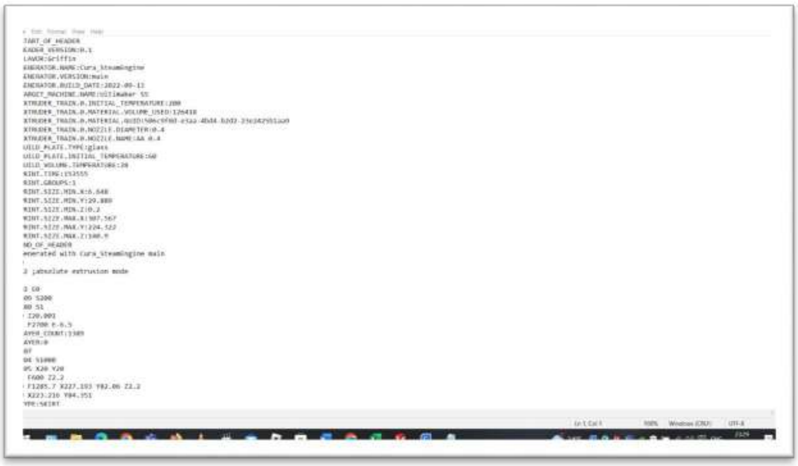

Fig.33. G-code file for Robotic Arm

Fig.34. Robotic Arm printed by FDM technology and assembled

This project has been funded with support from the Iceland Liechtenstein Norway Grants. This publication [communication] reflects the views only of the authors, and the Commission cannot be held responsible for any use which may be made of the information contained therein.

Product 3: 3D Fresh Printing of organ phantom for surgical applications – site https://www.embodi3d.com/

Physical organ models are the objects that replicate the patient-specific anatomy and have played important roles in modern medical diagnosis and disease treatment. 3D printing, as a powerful multi-function manufacturing technology, breaks the limitations of traditional methods and provides a great potential for manufacturing organ models.

Fresh 3D Printing (Freeform Reversible Embedding of Suspended Hydrogels) is an additive manufacturing technique for manufacturing different organ phantoms which can mimic the corresponding soft living tissue. [1-88]

The technology 3D Fresh Printing is similarly with the technologies SLA and DLP, only that used silicones or hydrogels, that permit to print different human organ models with the real consistency of the respective organs, that permit to help the students to University of Medicine to study their properties and to prepare the surgical operation stages planning, implantable epidermal devices, patient-specific pulse oximeters and in the tissue engineering applications. The printer must be modified, such as Tobeca 333, (Tobeca, France), that used the software Simplify 3D and as material a mono-component silicone by Elkem Silicones, France (AMSil 20101).

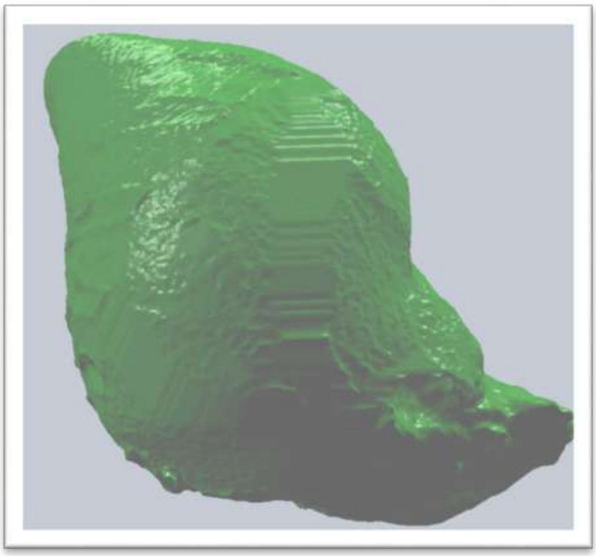

Fig.35. Liver model for printing

This project has been funded with support from the Iceland Liechtenstein Norway Grants. This publication [communication] reflects the views only of the authors, and the Commission cannot be held responsible for any use which may be made of the information contained therein.

The nature of FRESH printing offers the capability to 3D print object using layer-bylayer, non-planar or freeform approaches. The latter one produces geometries that are not possible to achieve in traditional 3D printing. Additionally, it solves one of the most tedious processes of 3D printing, which is to guarantee that the platform is completely flat, since the object can be manufactured in any location of the support bath. In general, the materials used is the thermo-reversible Pluronic F-127 based support bath supplied by Sigma Aldrich, USA. Fresh 3D printing is a particular type of DIW embedded 3D printing EMB3D technique. [1-88]

For the surgical operation stages planning, we can use the technology SLA and DLP, that are most simple to used and can permit the 3D Printing with a great accuracy the complex parts. In the SLA (Stereolithography) and DLP (Digital Light Processing) technologies are used photocurable vinyl- or epoxy- functional oligomers for photopolymerization. In table 3 are presented the mechanical properties of Bisphenol A Ethoxylate Diacrylate resin. Other resins used in SLA manufacturing are the polyurethane resins.

Table 3. The mechanical properties of Bisphenol A Ethoxylate Diacrylate

Bisphenol A Ethoxylate Diacrylate

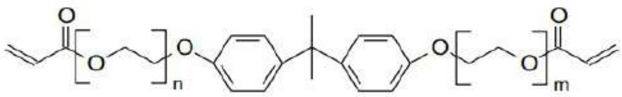

n + m ~ 4

INTRODUCTION

EBECRYL 150 is an ethoxylated bisphenol A diacrylate commonly used as reactive diluent in UV/EB cure applications. EBECRYL 150 can improve the cure response, hardness, and chemical resistance of UV/EB curable coatings and inks while maintaining good adhesion, and without imparting brittleness.

PERFORMANCE HIGHLIGHTS

EBECRYL 150 is characterized by:

- High reactivity
- Moderate viscosity
- High refractive index

UV/EB curable formulated products containing EBECRYL 150 are characterized by:

- Hardness
- Chemical resistance
- Good adhesion
- Improved wetting

The actual properties of UV/EB cured products also depend on the selection of other formulation components such as oligomers, additives and photoinitiators.

SPECIFICATIONS(1)	VALUE
Acid value, mg KOH/g, max.	5
Appearance	Clear liquid
Color, Gardner scale, max.	2
Viscosity, 25°C, cP/mPa·s	1150-1650
TYPICAL PHYSICAL PROPERTIES	
Density, g/ml at 25°C	1.14
Flash point, Setaflash, °C	>100
Functionality, theoretical	2
Refractive index (n_D at 20°C)	1.5294
Vapor pressure, mm Hg at 20°C	<0.01
TYPICAL CURED PROPERTIES(2)	
Tensile strength, psi (MPa)	6300 (43)
Elongation at break, %	9
Young's modulus, psi (MPa)	180000 (1241)
Glass transition temperature, °C(3)	41

This project has been funded with support from the Iceland Liechtenstein Norway Grants. This publication [communication] reflects the views only of the authors, and the Commission cannot be held responsible for any use which may be made of the information contained therein.

3.1. CAD Modeling

For 3D Printing of physical organ models, the medical images are first acquired through computer tomograph CT, magnetic resonance imaging MRI. Through the above procedures, the original image data, usually in DICOM (Digital Imaging and Communications in Medicine) format, will be obtained and then can be processed.

Image processing is a process of transforming DICOM images into 3D digital models. It is also a broad concept, including image segmentation, computer aided design (CAD) and format conversion.

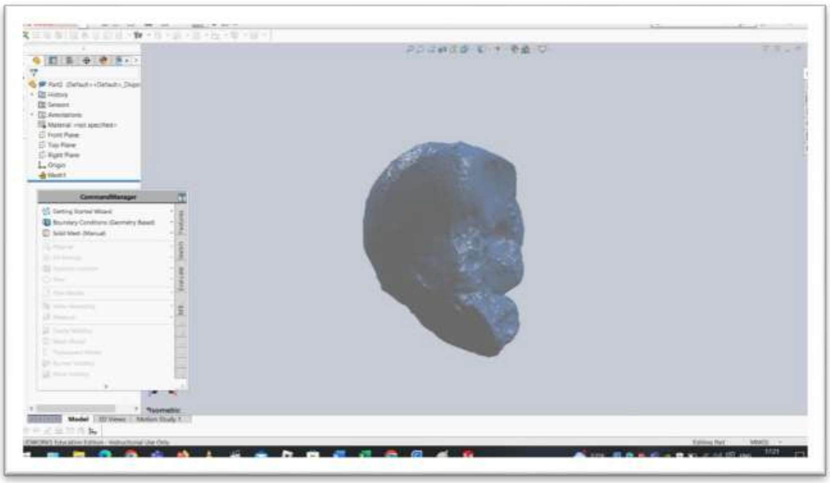

Fig.36. STL. file – liver phantom

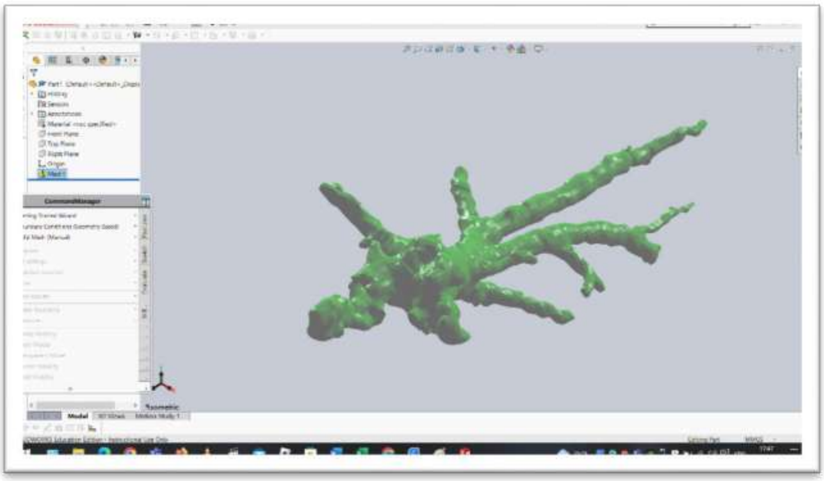

Fig.37. STL. file – blood vessel

This project has been funded with support from the Iceland Liechtenstein Norway Grants. This publication [communication] reflects the views only of the authors, and the Commission cannot be held responsible for any use which may be made of the information contained therein.

3.2. STL file

The file formats that 3D printers can accept are limited to several special 3D dataset files, mainly the Standard Tessellation Language (STL) format and some newer formats called Additive Manufacturing File Format (AMF) or 3D Manufacturing Format (3MF). The model data must be converted into files in these formats before it can be 3D printed.
There are several software can meet the demands of image processing, ranging from interactive medical image processing software like Mimics (Materialise), D2P (3D Systems), and CAD model processing software like Magics (Materialise), Geomagic Studio (3D Systems) and SolidWorks (Dassault Systems). In many cases, using multiple software together can integrate different functions.
For 3D Printing of the liver are 6 components, they are 6 different STL. Files (liver and blood vessels), that must be assembled and saved as ASM, SLDASM. file and printed 3D. We obtain the STL. files, such in the figures 36 and 37.

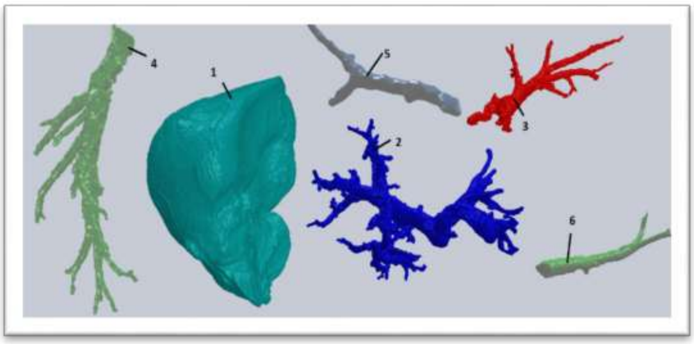

Fig.38. Exploded View – Liver phantom

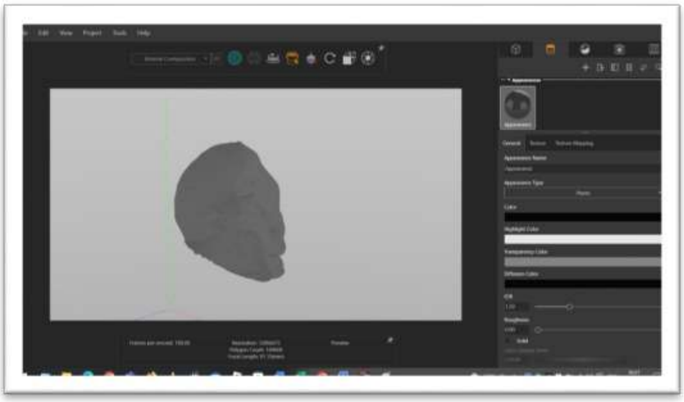

Fig.39. SolidWorks Visualize 2019 – Liver phantom with different texture mapping

This project has been funded with support from the Iceland Liechtenstein Norway Grants. This publication [communication] reflects the views only of the authors, and the Commission cannot be held responsible for any use which may be made of the information contained therein.

In Figure 38, it is presented the explode view of the components of liver phantom. In the Figure 39, it presented different texture mapping chosen, using SolidWorks Visualize 2019.

3.3. 3D Printing software's

For printing it used a SLA printer, FormLabs Form 2 and the free software PreForm and the resin chosen was Flexible and the layer thickness was 0.05 mm, such in Fig. 40.

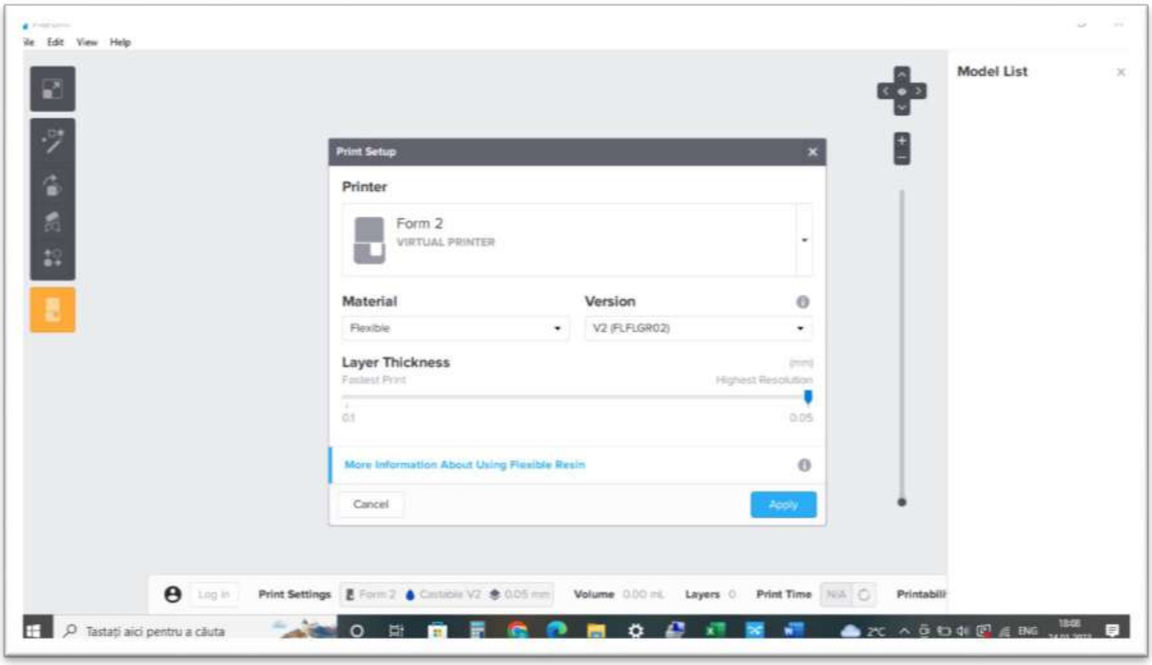

Fig. 40. Software PreForm, 3D printer, photopolymerisable resin and layer thickness chosen

In figure 41, it can click orientation to move the part on the worktable, in figure 42, it can chosen the supports necessary to sustain the part during the 3D Printing process. The layout chosen is presented in figure 43 and to print 3D it must to click on the orange button – Start a print, as in figure 44.

This project has been funded with support from the Iceland Liechtenstein Norway Grants. This publication [communication] reflects the views only of the authors, and the Commission cannot be held responsible for any use which may be made of the information contained therein.

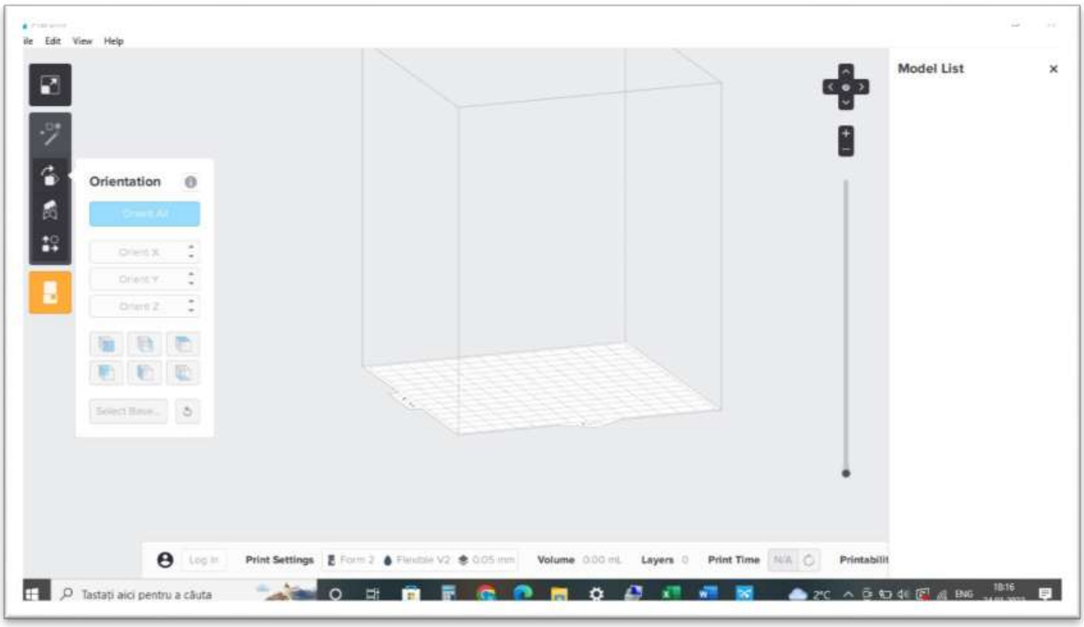

Fig.41. Orientation X,Y,Z on the worktable of the part

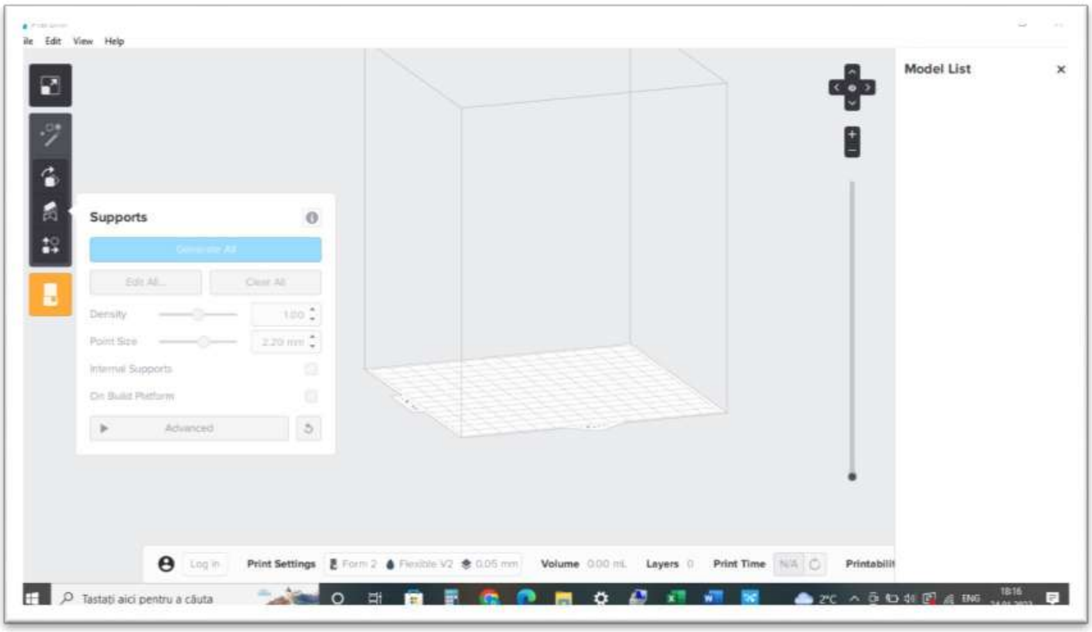

Fig.42. Supports chosen to sustain the part during the 3D Printing process

This project has been funded with support from the Iceland Liechtenstein Norway Grants. This publication [communication] reflects the views only of the authors, and the Commission cannot be held responsible for any use which may be made of the information contained therein.

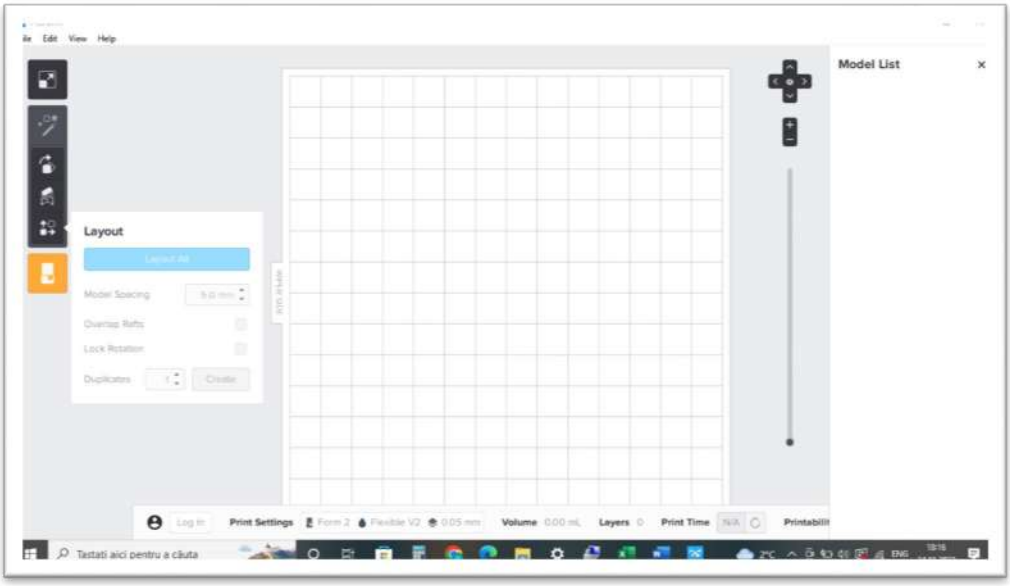

Fig.43. The layout chosen

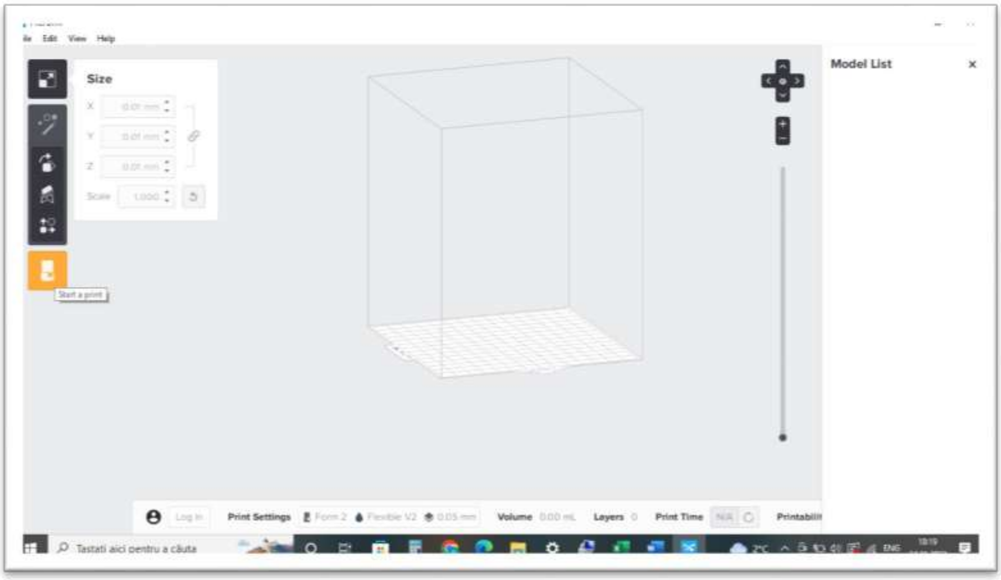

Fig.44. The orange button – Start a print

This project has been funded with support from the Iceland Liechtenstein Norway Grants. This publication [communication] reflects the views only of the authors, and the Commission cannot be held responsible for any use which may be made of the information contained therein.

In figure 45, it was dragging the liver phantom STL. file into the worktable of the 3D Printer, but the part has very great dimensions in comparison with the worktable space, it becomes red coloured.

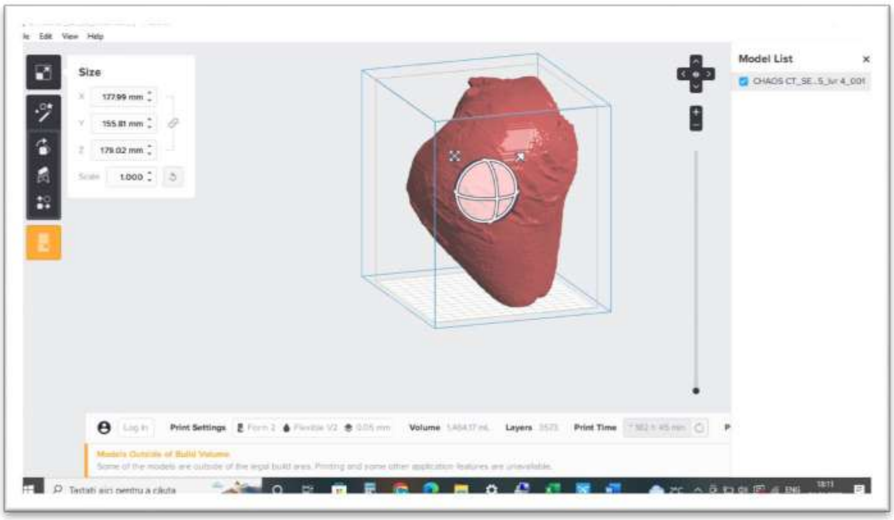

Fig.45. Drag the liver phantom STL. file on the worktable

In this case, it was changed the scale at 1:2 and was calculating orientation and generating the supports as in figure 46. [1-88]

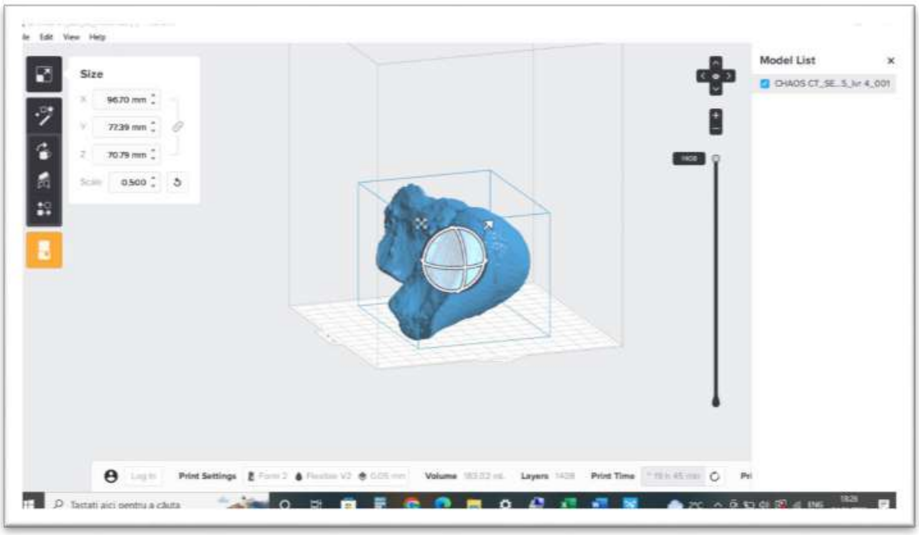

Fig.46. Change the scale at 1:2 and was calculating orientation and generating the supports

This project has been funded with support from the Iceland Liechtenstein Norway Grants. This publication [communication] reflects the views only of the authors, and the Commission cannot be held responsible for any use which may be made of the information contained therein.

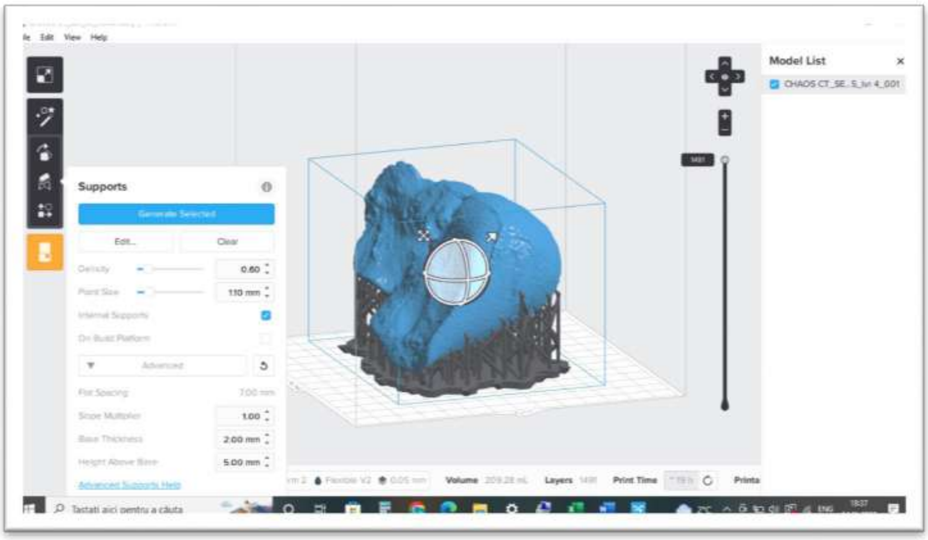

Fig.47. Calculating orientation and generating supports

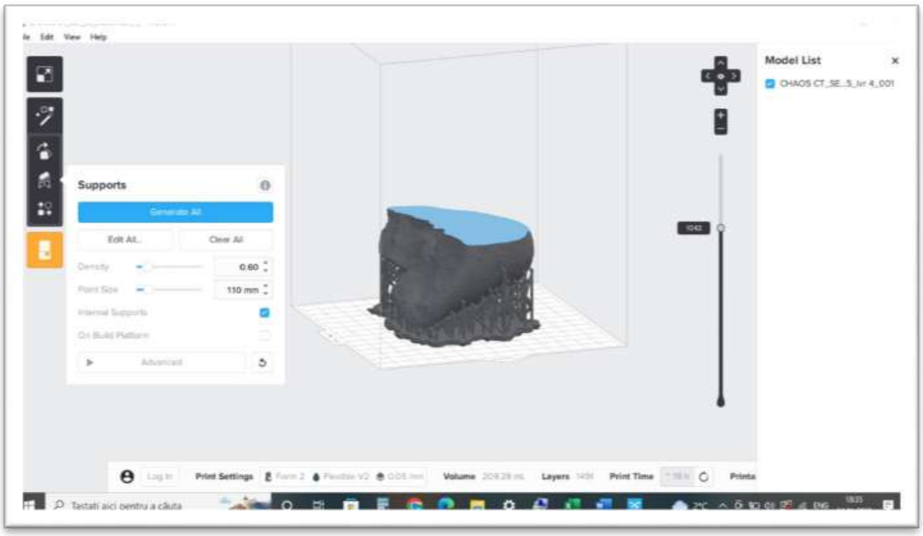

Fig.48. Surface printed at the layer 1042

For Orientation and Supports, it must click on the respective buttons and the program realized them automatically or we can realize them manually, such in figure 47. The program permit to see the slicing of the part, each layer, specify the number of the layer and the surface

This project has been funded with support from the Iceland Liechtenstein Norway Grants. This publication [communication] reflects the views only of the authors, and the Commission cannot be held responsible for any use which may be made of the information contained therein.

coloured with blue, that is printed at the layer 1042, such in figure 48. The program shows the resin volume used 209.28 mL, nb of layers 1491 and print time approximative 19 hours.

In figure 49, the printing setting of the part liver are saved such as LIVER.FORM 

, using the software PreForm. For 3D printing of the part, it must click on the orange button to print, such in figure 50, after connecting the printer on-line, or with a cable to the laptop.

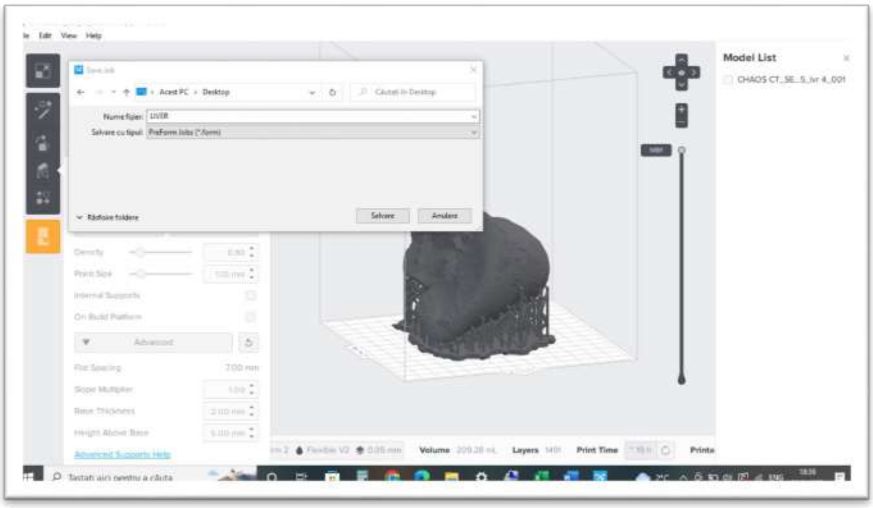

Fig.49. Save the file as Liver with the extension .FORM

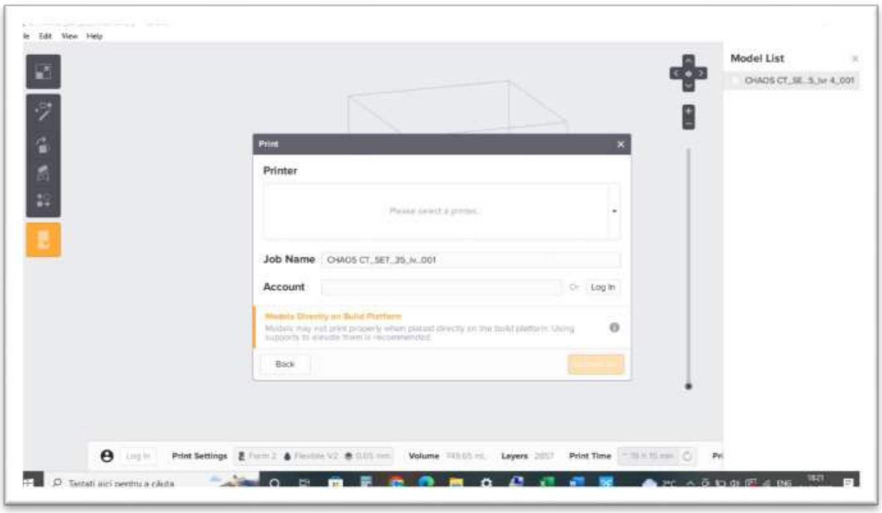

Fig.50. Click on the orange button to print

This project has been funded with support from the Iceland Liechtenstein Norway Grants. This publication [communication] reflects the views only of the authors, and the Commission cannot be held responsible for any use which may be made of the information contained therein.

In figure 51, it was dragging the blood vessel STL. file into the worktable of the 3D Printer and it was changed the scale at 1:2 and was calculating orientation and generating the supports as in figure 52.

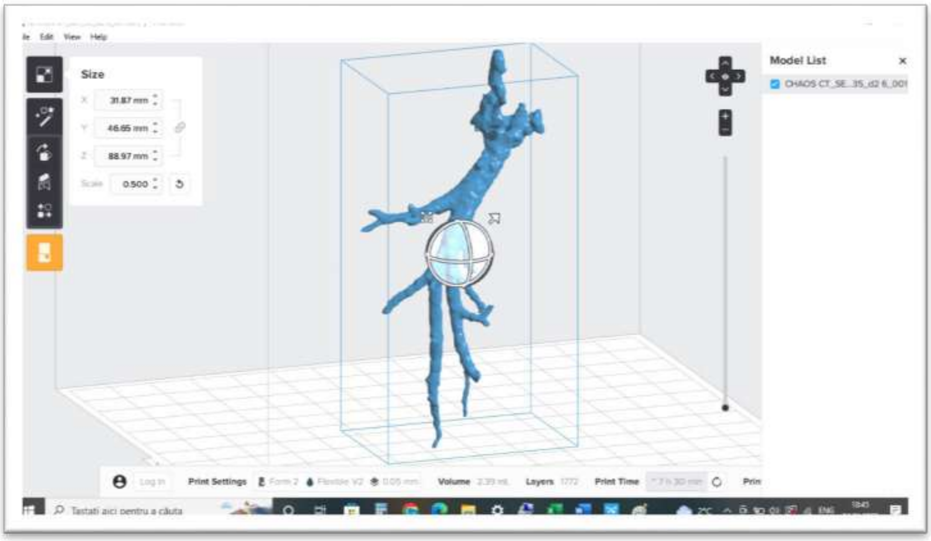

Fig.51. Drag the blood vessel STL. file on the worktable platform

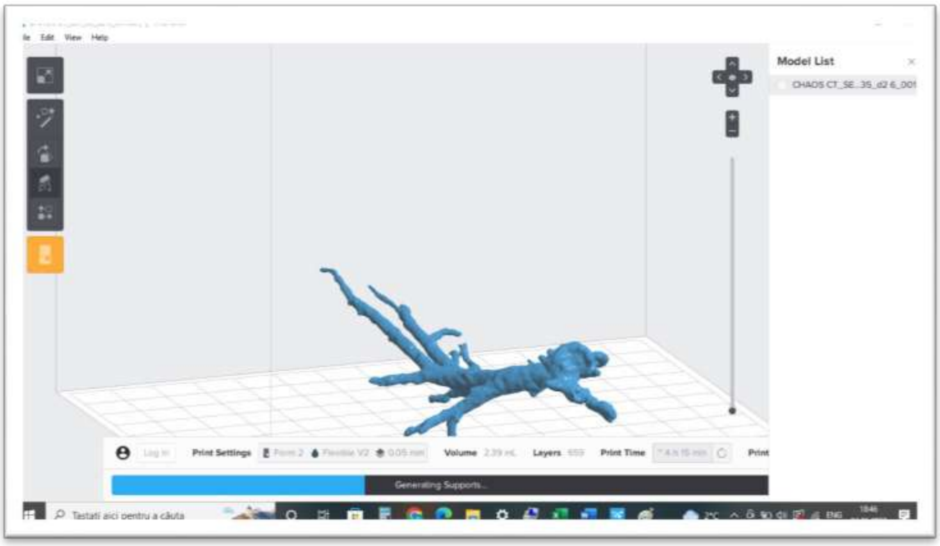

Fig.52. Calculating orientation and generating supports

First, are realized the supports, such in Figure 53 and then the part such in Figure 54.

This project has been funded with support from the Iceland Liechtenstein Norway Grants. This publication [communication] reflects the views only of the authors, and the Commission cannot be held responsible for any use which may be made of the information contained therein.

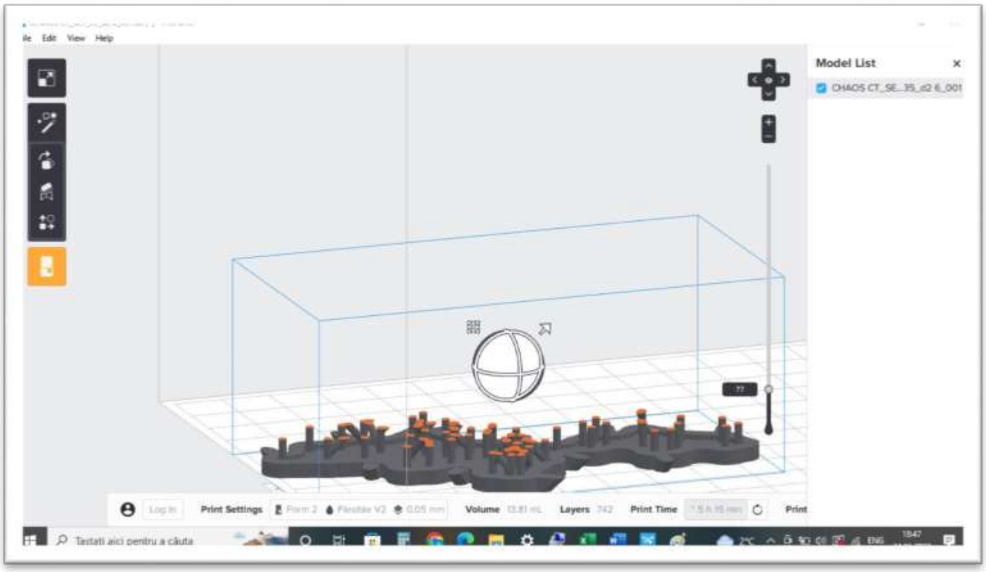

Fig.53. Supports generating

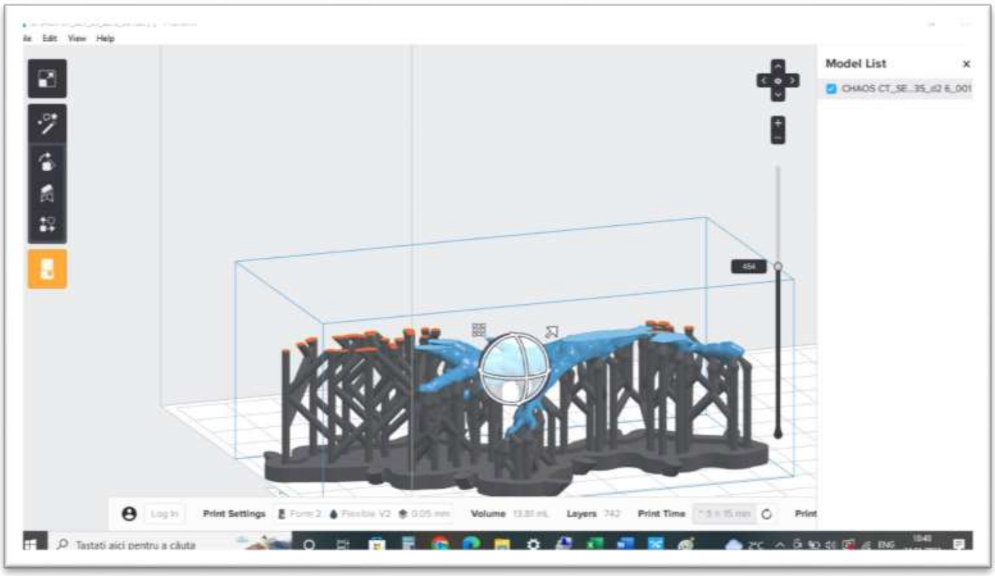

Fig.54. Part generating

In figure 55 was saved the file as Blood Vessel .FORM file  and in figure 56 was click on the Print command of the part and the 3D Printer will manufacture the part. Specifically of the SLA technology is that the parts are manufactured upside down.

This project has been funded with support from the Iceland Liechtenstein Norway Grants. This publication [communication] reflects the views only of the authors, and the Commission cannot be held responsible for any use which may be made of the information contained therein.

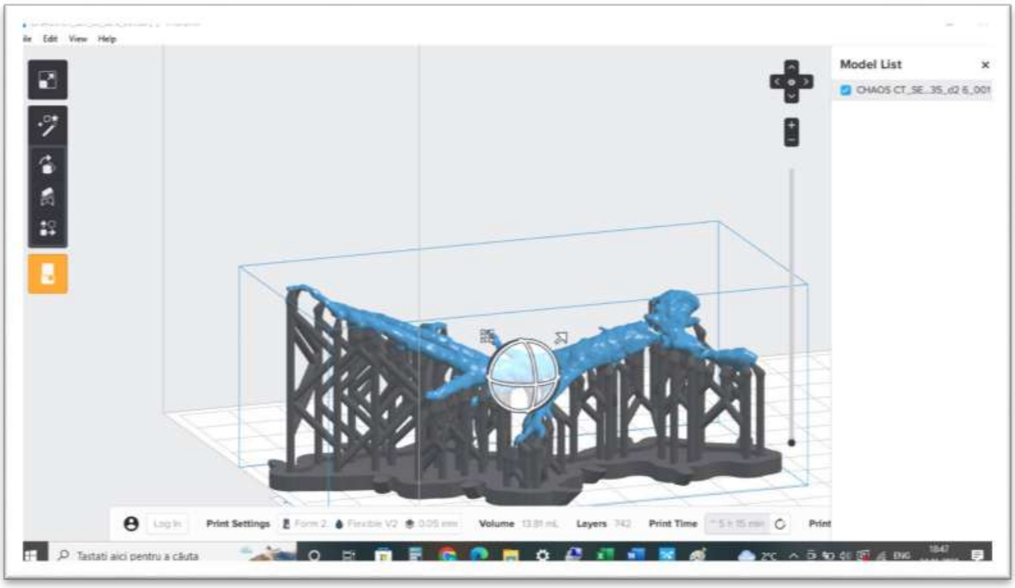

Fig.55. Save the file as Blood Vessel .FORM file

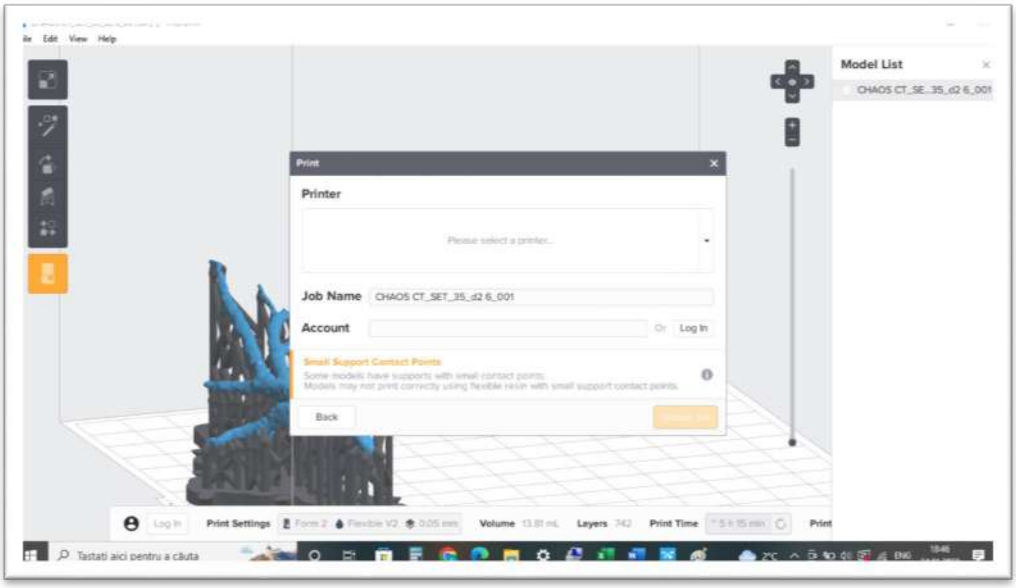

Fig.56. Print command of the part to 3D Printer

In the figure 57 is presented the liver phantom printed 3D using the SLA technology. After printing the parts, are eliminated the supports and the parts are cleaned in isopropyl alcohol

This project has been funded with support from the Iceland Liechtenstein Norway Grants. This publication [communication] reflects the views only of the authors, and the Commission cannot be held responsible for any use which may be made of the information contained therein.

and then are introduced in UV furnace to grow the mechanical properties during 30 minutes at the temperature of 210ºC.

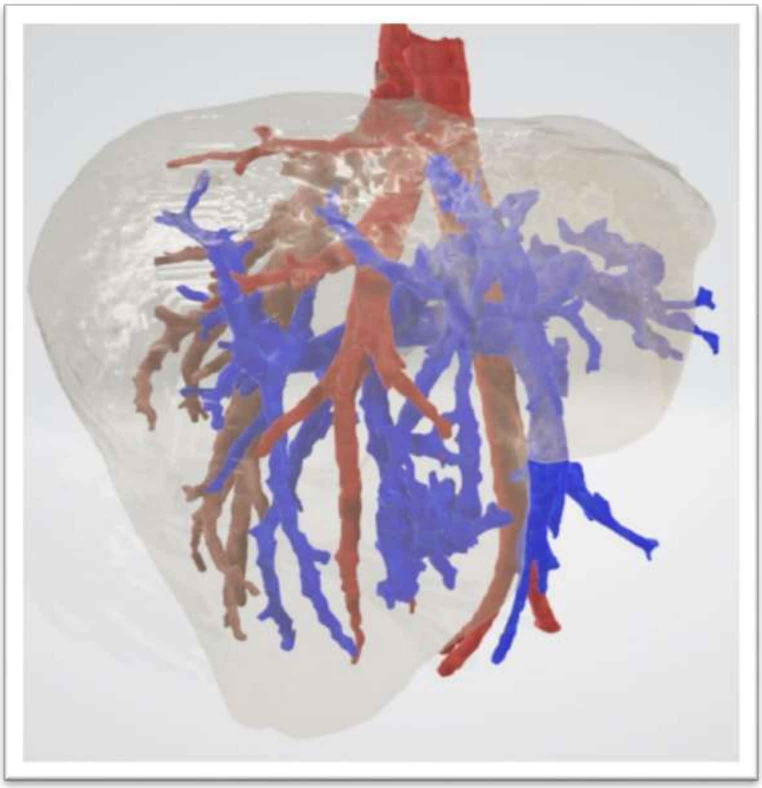

Fig.57. Liver phantom with blood vessels

4. Conclusions

In the future, further research on both multi-material and multi-colour prototypes could be performed, focusing on additive manufacturing technologies based on different silicones and plastic materials with different colours, necessary for different medical prothesis and devices. The use of different silicones would be interesting in order to manufacture more complex phantoms, in which not only the desired organ is 3D printed, but also the surrounding anatomical structures. For example, the tumour or blood vessels by changing the component ratios. [1-88]

The implications of the present research would be interesting for the manufacture of phantoms to be used in research and industry: medical imaging, preoperative surgical planning in hospitals, etc.

This project has been funded with support from the Iceland Liechtenstein Norway Grants. This publication [communication] reflects the views only of the authors, and the Commission cannot be held responsible for any use which may be made of the information contained therein.

5. References

1. Ratner Buddy D., Hoffman Allan S., Schoen Frederick J., Lemons Jack E.- Biomaterials Science, An introduction to materials in medicine –Academic Press, 2013;
2. https://en.wikipedia.org/wiki/3D_printing
3. https://3dscentral.3dsystems.com/?option=com_content&view=category&id=312& itemid=734
4. Butscher A., Bohner M., Roth C., Ernstberger A., Heuberger R., Doebelin N., Von Rohr P.R., Muller R., Printability of calcium phosphate powders for three-dimensional printing of tissue engineering scaffolds, Acta Biomaterialia, Vol.8, Iss.1, 2012, pp.373-385
5. http://www.bibus.hu/fileadmin/editors/countries/bihun/product_data/zcorp/documents/zcorp_series_zprinter_310_plus_manual_en.pdf
6. http://sldtech.com/wp-content/uploads/2008/10/consumables_catalog_.pdf
7. https://en.wikipedia.org/wiki/3D_bioprinting
8. Murphy S.V., Atala A., 3D bioprinting of tissues and organs, Nature Biotechnology, 32, 2014, pp.773-785
9. http://www.star-prototype.com/blog/top-7-methods-for-making-3d-rapid-prototypes/
10. https://en.wikipedia.org/wiki/Fused_deposition_modeling
11. http://www.erpro.fr/ABS-deposition?lang=fr
12. https://en.wikipedia.org/wiki/Stereolithography
13. http://intech-ind.com/sla-machines-in-rapid-prototyping/
14. MacDonald D. – Applying Stereolithography to produce usable prototypes and tooling, Proceedings of the 2nd European Conference on Rapid Prototyping and Manufacturing, Nottingham (UK), 1993, pp113- 118, ISBN 0951975919;
15. Earle J. – Graphics for engineers, 5th edition, Pretince-Hall, 1999, ISBN 0130160075;
16. Hague R., Dickens P.M. – Finite element analysis calculated stresses in investment casting shells using stereolithography models as patterns, Proceedings of 5th European Conference on Rapid Prototyping and Manufacturing, Helsinki (Finland) 14th – 16th june 1996, pp31-46, ISBN 0951975951;
17. http://envisiontec.com/3d-printers/ultra-3sp-family/
18. https://en.wikipedia.org/wiki/Digital_Light_Processing
19. The Best Industrial Metal and Plastic 3D Printers I 3D Systems
20. Berce P. & others - Tehnologii de fabricație prin adăugare de material și aplicațiile lor – Romanian Academy Edition, Bucharest 2014;
21. Electron-beam additive manufacturing - Wikipedia

This project has been funded with support from the Iceland Liechtenstein Norway Grants. This publication [communication] reflects the views only of the authors, and the Commission cannot be held responsible for any use which may be made of the information contained therein.

22. https://www.eos.info/precious-m-080
23. http://gpiprototype.com/files/dmlm/EOSINT%20M%20270%20Brochure.pdf
24. https://books.google.ro/books?id=QW8KBwAAQBAJ&pg=PA107&lpg=PA107&dq=EOSINT
25. https://www.3dsystems.com/3d-printers/prox-dmp-320
26. https://www.3dsystems.com/3d-printers/prox-dmp-300
27. https://www.3dsystems.com/3d-printers/prox-dmp-200
28. https://www.3dsystems.com/3d-printers/prox-dmp-100
29. https://www.concept-laser.de/en/products/machines.html
30. https://www.concept-laser.de/en/products/machines/m-line-factory.html
31. https://www.conceptlaser.de/fileadmin/Blaue_Broschueren/1708_X_LINE_2000R_EN_update
32. http://brochure.copiercatalog.com/3d-systems/brochure_phenix_systems_gb_2012.pdf
33. https://slm-solutions.com/products/machines/selective-laser-melting-machine-slm-500
34. https://slm-solutions.com/products/machines/selective-laser-melting-machine-slm-280-20
35. https://slm-solutions.com/products/machines/selective-laser-melting-machine-slm-125
36. http://www.arcam.com/wp-content/uploads/arcamebm-corp.pdf
37. https://www.autodesk.com/redshift/electron-beam-melting/
38. https://additiveindustries.com/uploads/media/588b3d45c16db/brochure-metalfab1.pdf
39. https://www.optomec.com/wp-content/uploads/2014/04/LENS_450_Datasheet-WEB.pdf
40. https://www.optomec.com/wp-content/uploads/2014/04/LENS_MR-7_WEB.pdf
41. https://www.optomec.com/wp-content/uploads/2014/04/LENS_850-R_Web_0716.pdf
42. http://iopscience.iop.org/article/10.1088/0022-3727/48/3/035303
43. http://docplayer.fr/52020123-Etude-du-controle-de-procede-de-projection-laser-pour-la-fabrication
44. https://www.3ders.org/articles/20151125-toshiba-to-unveil-metal-3d-printer-that-is-10-times
45. Ż. A. Mierzejewska, Process Optimization Variables for Direct Metal Laser Sintering, DOI: 10.1515/adms-2015-0021
46. http://www.industrial-lasers.com/articles/2016/02/web-exclusive-cladding-and-additive-manufacturing
47. Downloads/attar_e_simulation_of_selective_electron_beam_melting_proces.pdf
48. https://me-mechanicalengineering.com/electron-beam-machining-ebm/
49. https://www.rdmo.com/boiler-making-12/laser-13/laser-phenix-systems-pm100-dental-7529

This project has been funded with support from the Iceland Liechtenstein Norway Grants. This publication [communication] reflects the views only of the authors, and the Commission cannot be held responsible for any use which may be made of the information contained therein.

50. https://www.rtejournal.de/ausgabe2/103
51. http://lycees.ac-rouen.fr/maupassant/Melec/co/Communication/FTTH/web/res/image_14.png
52. https://www.laserstoday.com/2016/12/additive-manufacturing-using-laser-hot-wire-powder
53. http://www.myshared.ru/slide/1324038/
54. http://deuns.chez.com/sciences/cristallo/cristallo44.html
55. http://shopmetaltech.com/fabricating-technology/fabricating/nd-yag-or-fiber-laser-for-micro
56. https://en.wikipedia.org/wiki/Transverse_mode
57. https://extrudehone.com/enhanced-finishing-solution-metal-3d-printing
58. http://www.scielo.br/scielo.php?script=sci_arttext&pid=S1516-14392007000200019 [156] https://www.eos.info/additive_manufacturing/for_technology_interested
59. T. Hardenne. Application du laser cladding au rechargement et à la fabrication de pièces. Technical report, Université de Liège, 2011.
60. http://www.mdpi.com/2073-4352/3/4/517/htm
61. http://www.sciencedirect.com/science/article/pii/S0141635916300721#bib0225
62. http://www.mdpi.com/2075-4701/6/11/286/htm
63. http://www.nae.fr/wp-content/uploads/2015/07/FabAdditiveMetallique_TechnoOpportunites-NAE.pdf
64. http://www.scielo.br/scielo.php?script=sci_arttext&pid=S1516-14392015000700024
65. http://www.sciencedirect.com/science/article/pii/S0264127516313296
66. https://www.youtube.com/watch?v=KbXJb4wcxnw
67. http://www.mdpi.com/1996-1944/9/12/975#
68. http://www.mdpi.com/1996-1944/10/9/1055
69. https://www.intechopen.com/books/superalloys/comparison-of-additive-technologies-for-gradient
70. http://www.sciencedirect.com/science/article/pii/S0030399214000632
71. https://www.slideshare.net/carstenengel/selective-laser-melting-versus-electron-beam-melting
72. http://www.insidemetaladditivemanufacturing.com/blog/visual-guide-to-the-most-common-defects
73. http://slideplayer.com/slide/4731730/
74. http://www.sciencedirect.com/science/article/pii/S1359645417308170

This project has been funded with support from the Iceland Liechtenstein Norway Grants. This publication [communication] reflects the views only of the authors, and the Commission cannot be held responsible for any use which may be made of the information contained therein.

75. https://www.researchgate.net/publication/277020783_Surface_texture_measurement_for_additive
76. http://www.sciencedirect.com/science/article/pii/S135964541630088X
77. https://www.assemblymag.com/articles/93176-additive-manufacturing-takes-off-in-aerospace-industry
78. http://www.romanoff-west.com/laser-metal-mould-making-machine.html
79. https://alopexoninnovation.com/category/systems-engineering/
80. http://beta.metal-am.com/introduction_to_metal-additive_manufacturing/Design_advantages
81. https://www.researchgate.net/publication/294109314
82. https://www.sciencedirect.com/science/article/pii/S0264127519305751#fig0005
83. https://www.sciencedirect.com/science/article/pii/S0264127518300303?casa_token=NqqBRt_j0u4AAAAA:ypnAxH32t1hY5JaawJelewifiQYZUg0PskVYkAnWymwxaWc2RhSCkOn8R0uvV6etCNX2eY1RQd6G#f0020
84. Compressive failure modes and energy absorption in additively manufactured double gyroid lattices - ScienceDirect
85. https://www.metal-am.com/articles/material-selection-for-the-3d-printing-of-injection-moulding-tooling/
86. ISO/ASTM 52900:2021(en), Additive manufacturing
87. Ultimaker Cura: Ultimaker Cura: Powerful, easy-to-use 3D printing software
88. PreForm software

This project has been funded with support from the Iceland Liechtenstein Norway Grants. This publication [communication] reflects the views only of the authors, and the Commission cannot be held responsible for any use which may be made of the information contained therein.

Iceland Liechtenstein Norway grants

Working together for a green, competitive and inclusive Europe

EMERALD

The Education, Scholarships, Apprenticeships and Youth Entrepreneurship

EUROPEAN NETWORK FOR 3D PRINTING OF BIOMIMETIC MECHATRONIC SYSTEMS

E-toolkit –

NEW MATERIALS USED FOR THE DEVELOPED BIOMIMETIC MECHATRONIC SYSTEMS

Project Title	**European network for 3D printing of biomimetic mechatronic systems** **21-COP-0019**
Output	**O2 - EMERALD e-toolkit manual for digital learning in producing biomimetic manufacturing method**
Module	**New materials used for the developed biomimetic mechatronic systems** - **Database used for the smart (intelligent) materials properties**
Authors	**Diana BĂILĂ**

This project has been funded with support from the Iceland Liechtenstein Norway Grants. This publication [communication] reflects the views only of the authors, and the Commission cannot be held responsible for any use which may be made of the information contained therein.

Contents

This project has been funded with support from the Iceland Liechtenstein Norway Grants. This publication [communication] reflects the views only of the authors, and the Commission cannot be held responsible for any use which may be made of the information contained therein.

Total Materia used for determination of the materials properties

1 Total Materia database – Quick search for alloys

Total Materia is the world's most comprehensive materials database, having more than 20,000,000 property records for over 450,000 metallic and non-metallic materials presented in 26 languages. This database is world class quality, service and support, being trusted in over 160 countries, the smallest companies to global industry leaders all receive our complete specialist technical support. Total Materia is proprietary algorithms for the identification of unknown materials, using composition data from analytical sources, find matching materials, property data and equivalents in just seconds. This database is the largest single collection of advanced property data on the planet, having more than 150,000 materials with stress strain, fatigue data and much more for the design community, being a free page. This database permits lightning fast access for finding and comparing equivalent materials, existing international cross-references for 450,000 materials from 74 standards providing over 15,000,000 material connections.

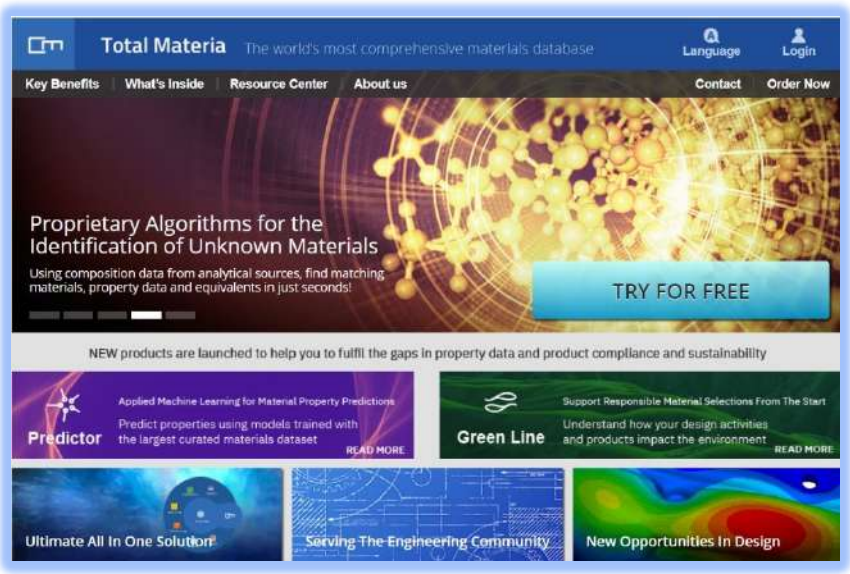

Fig.1. Total Materia database

This project has been funded with support from the Iceland Liechtenstein Norway Grants. This publication [communication] reflects the views only of the authors, and the Commission cannot be held responsible for any use which may be made of the information contained therein.

Total Materia database help solve diverse engineering challenges from the simplest to the complex, being used in: medicine industry, aerospace industry, energy industry, automotive industry, machinery industry, engineering industry, diversified.

By example, for the alloy Ti6Al4 V, we want to know the chemical composition and the mechanical properties, and we click on Advanced Search, as in the Figure 2.

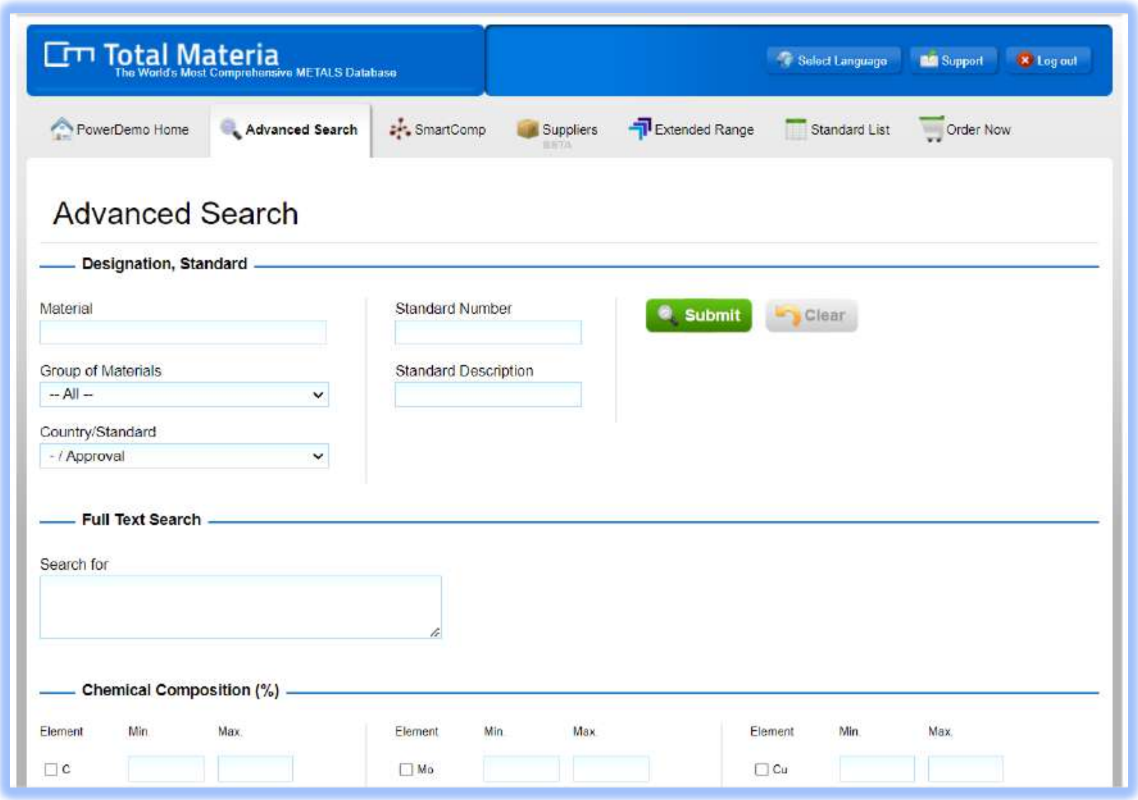

Fig.2. Advanced Search

In the figure 3, it is presented the choice of the standard in function of the country and group of materials.

It was choosing the alloy Ti6Al4V, making part of Titanium materials and was choose European Union standard, as in Figure 3. It must specify the material type, as example Bulk Materials, in Figure 4.

This project has been funded with support from the Iceland Liechtenstein Norway Grants. This publication [communication] reflects the views only of the authors, and the Commission cannot be held responsible for any use which may be made of the information contained therein.

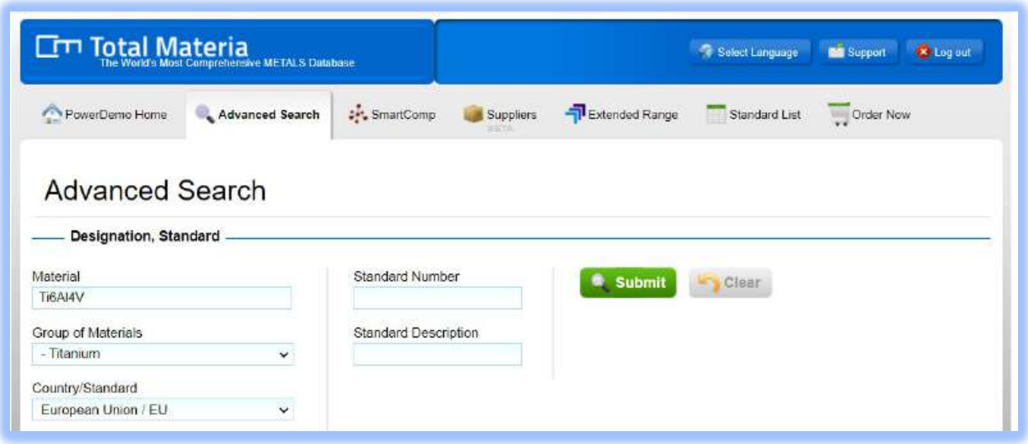

Fig.3. European Union standard choice

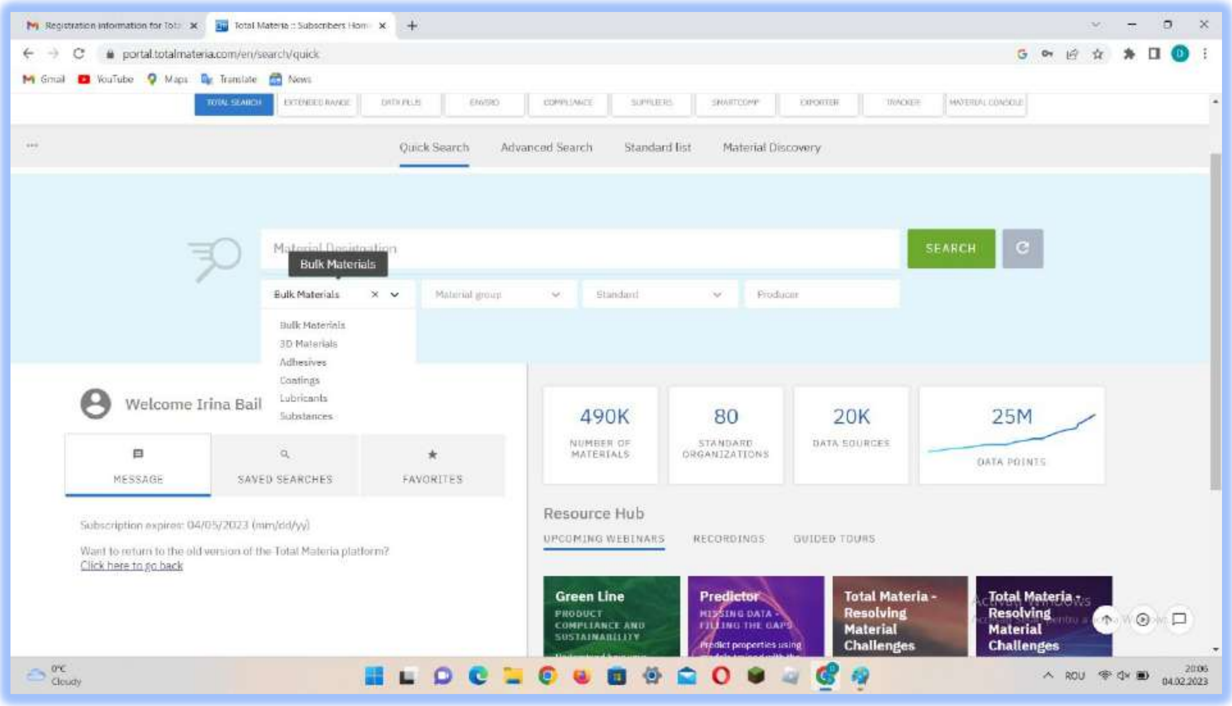

Fig.4. Material type

In figure 5, it is specifying the material group and in this case, nonferrous alloys and European standard choice, as in figure 6.

This project has been funded with support from the Iceland Liechtenstein Norway Grants. This publication [communication] reflects the views only of the authors, and the Commission cannot be held responsible for any use which may be made of the information contained therein.

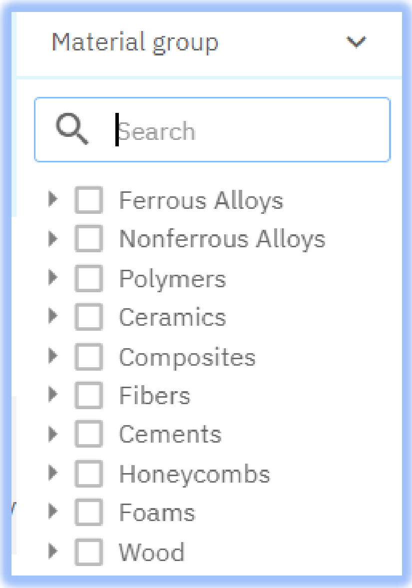

Fig.5. Material group

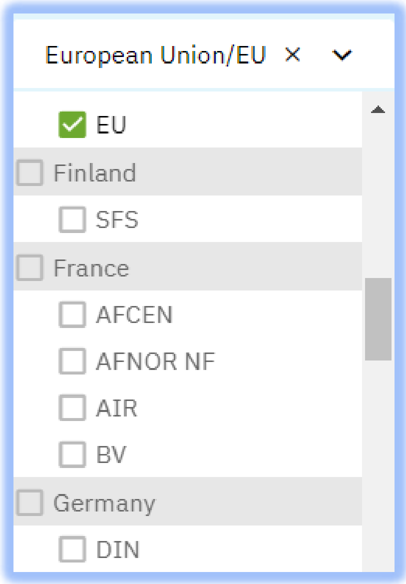

Fig.6. European standard choice

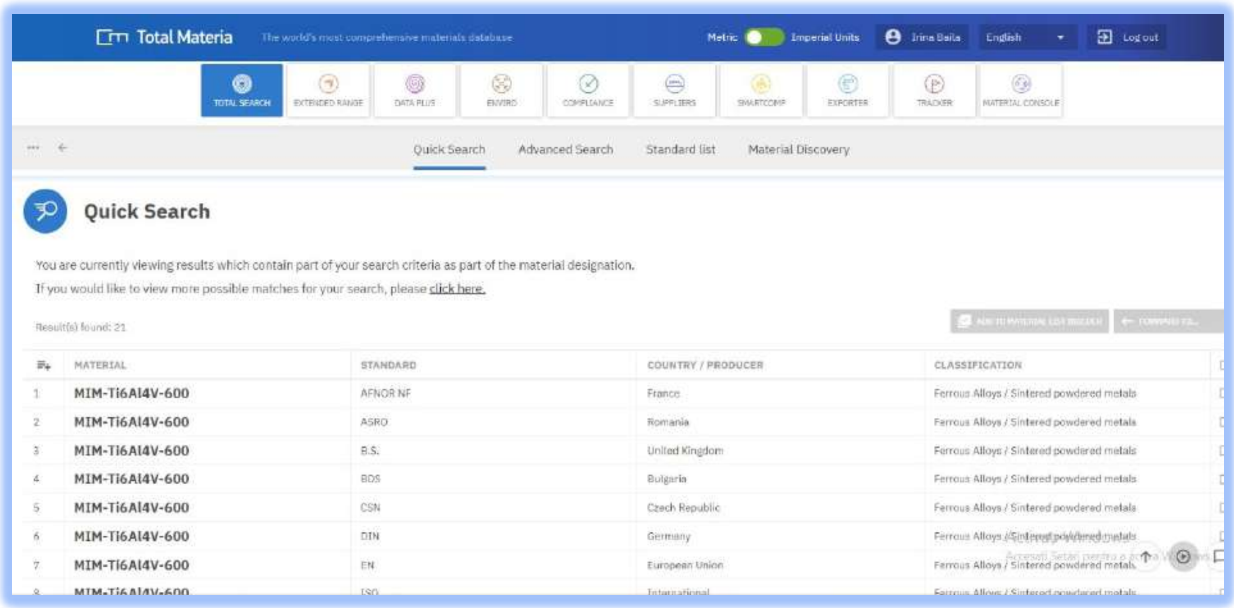

Fig.7. Different Ti6Al4V producers

When we give a quick search, as in figure 7, are presented different Ti6Al4V producers from different countries and using different standards.

This project has been funded with support from the Iceland Liechtenstein Norway Grants. This publication [communication] reflects the views only of the authors, and the Commission cannot be held responsible for any use which may be made of the information contained therein.

Fig.8. Ti6Al4V standard Fr AFNOR NF-Mechanical properties

The results it is the mechanical properties of the alloy Ti6Al4V, conforming of FR AFNOR NF standard, as in figure 8 and figure 9.

Fig.9. Mechanical properties Ti6Al4V at the temperature between 0-30ºC

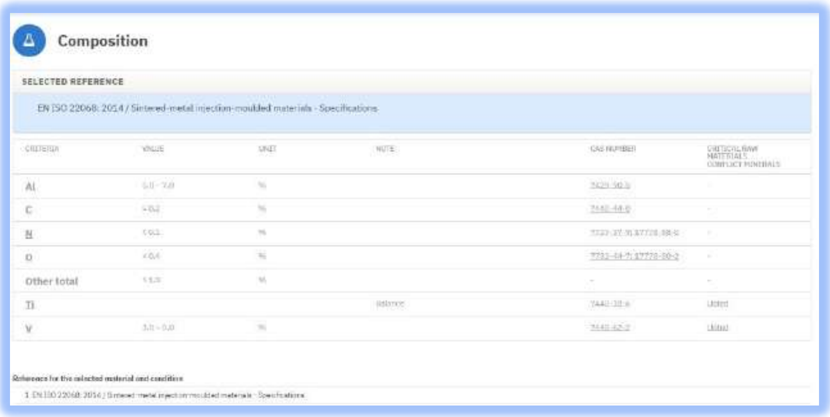

Fig.10. Chemical composition of Ti6Al4V

This project has been funded with support from the Iceland Liechtenstein Norway Grants. This publication [communication] reflects the views only of the authors, and the Commission cannot be held responsible for any use which may be made of the information contained therein.

In figure 9, the database gives us all information about the mechanical properties of the alloy Ti6Al4V in function of the temperature used in the process where it is used this material.
In figure 10, the database shows us the chemical composition of the alloy Ti6Al4V.

2. Total Materia database – Advanced Research for alloys

In the case of Advanced Research, by example for the Ti6Al4V, producer Vday Additive Manufacturing Technology Co., it is given the classification of different Ti alloys producers, as in figure 11.

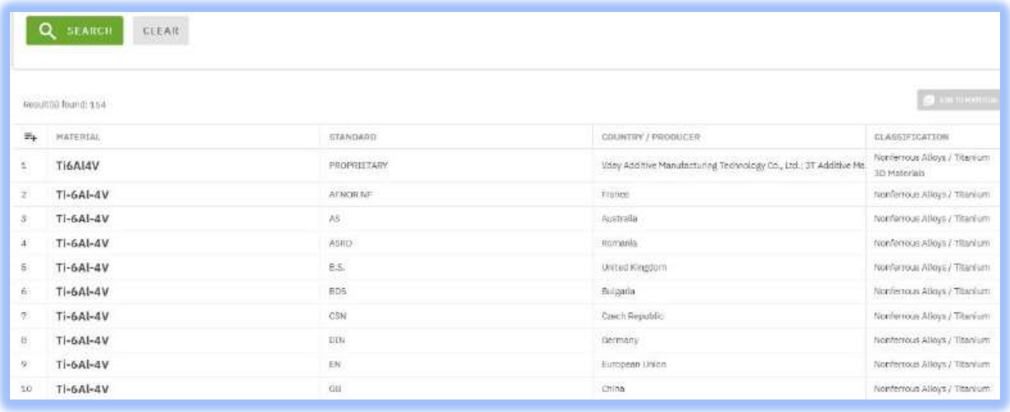

	MATERIAL	STANDARD	COUNTRY / PRODUCER	CLASSIFICATION
1	Ti6Al4V	PROPRIETARY	Vday Additive Manufacturing Technology Co., Ltd.; 3T Additive Ma	Nonferrous Alloys / Titanium 3D Materials
2	Ti-6Al-4V	AFNOR NF	France	Nonferrous Alloys / Titanium
3	Ti-6Al-4V	AS	Australia	Nonferrous Alloys / Titanium
4	Ti-6Al-4V	ASRO	Romania	Nonferrous Alloys / Titanium
5	Ti-6Al-4V	B.S.	United Kingdom	Nonferrous Alloys / Titanium
6	Ti-6Al-4V	BDS	Bulgaria	Nonferrous Alloys / Titanium
7	Ti-6Al-4V	CSN	Czech Republic	Nonferrous Alloys / Titanium
8	Ti-6Al-4V	DIN	Germany	Nonferrous Alloys / Titanium
9	Ti-6Al-4V	EN	European Union	Nonferrous Alloys / Titanium
10	Ti-6Al-4V	GB	China	Nonferrous Alloys / Titanium

Fig.11. Ti6Al4V alloy used in Additive Manufacturing

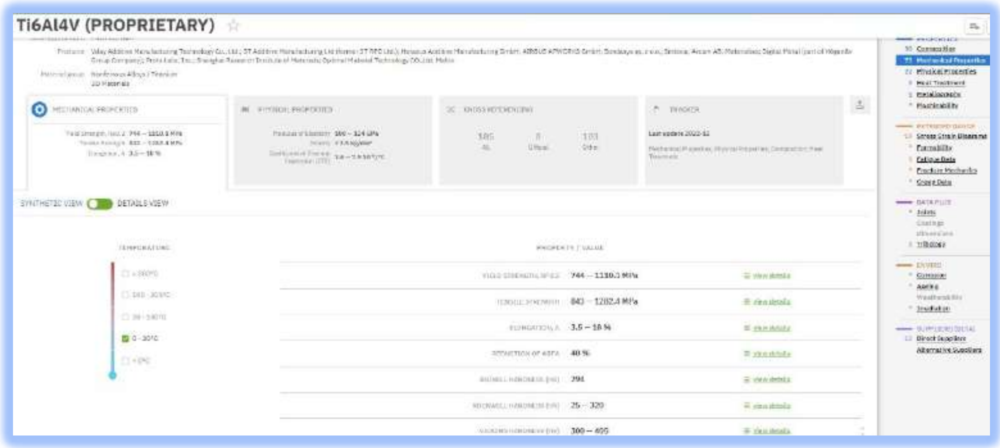

Fig.12. Mechanical properties of Ti6Al4V used in Additive Manufacturing

This project has been funded with support from the Iceland Liechtenstein Norway Grants. This publication [communication] reflects the views only of the authors, and the Commission cannot be held responsible for any use which may be made of the information contained therein.

In the figure 12, are presented the mechanical properties of Ti6Al4V used in Additive Manufacturing, for different temperature domains. The chemical composition of Ti6Al4V used in Additive Manufacturing is given in the figure 13. In the figure 14, the physical properties of Ti6Al4V used in Additive Manufacturing, for different temperature domains.

Ti6Al4V (PROPRIETARY)

REFERENCES

- 3T Additive Manufacturing Ltd, Product Data Sheets / Available at: www.3t-am.com, visited 2019
- Arcam AB, Product Data Sheets / Available at: www.arcam.com, visited 2016
- Digital Metal, Product Data Sheets / Available at: www.digitalmetal.tech, visited 2021
- Heraeus Additive Manufacturing GmbH, Product Data Sheets / Available at: www.heraeus.com, visited 2020
- Meltio, Product Data Sheets / Available at: https://meltio3d.com/, visited 2022
- Shanghai Research Institute of Material, Product Data Sheet / Available at: www.srim.com.cn, visited 2022

SELECTED REFERENCE

3T Additive Manufacturing Ltd, Product Data Sheets / Available at: www.3t-am.com, visited 2019

CRITERIA	VALUE	UNIT	NOTE	CAS NUMBER	CRITICAL RAW MATERIALS CONFLICT MINERALS
Al	5.50 – 6.75	%		7429-90-5	-
C	≤ 0.08	%		7440-44-0	-
Fe	≤ 0.3	%		7439-89-6	-
H	≤ 0.015	%		1333-74-0	-
N	≤ 0.05	%		7727-37-9; 17778-88-0	-
O	≤ 0.2	%		7782-44-7; 17778-80-2	-
Ti			Balance	7440-32-6	Listed
V	3.50 – 4.50	%		7440-62-2	Listed

Fig.13. Chemical composition of Ti6Al4V used in Additive Manufacturing

TEMPERATURE

- ☐ > 300°C
- ☐ 100 - 300°C
- ☐ 30 - 100°C
- ☑ 0 - 30°C
- ☐ < 0°C

PROPERTY	VALUE
MODULUS OF ELASTICITY	100 – 124 GPa
DENSITY	≥ 2.5 kg/dm³
COEFFICIENT OF THERMAL EXPANSION (CTE)	7.6 – 7.9 10^{-6}/°C
MELTING TEMPERATURE	1600 – 1750 °C

Fig.14. Physical properties of Ti6Al4V used in Additive Manufacturing

This project has been funded with support from the Iceland Liechtenstein Norway Grants. This publication [communication] reflects the views only of the authors, and the Commission cannot be held responsible for any use which may be made of the information contained therein.

Heat Treatment

Reference	Descriptions
Arcam AB, Product Data Sheets / Available at: www.arcam.com, visited 2015	Hot Isostatic Pressing (HIP) at 920°C for 120 minutes, 100 MPa.
3T Additive Manufacturing Ltd, Product Data Sheets / Available at: www.3t-am.com, visited 2019	Stress relieved at 800°C for 2 hours in a vacuum furnace with specimens on build plate.
Meltio, Product Data Sheets / Available at: https://meltio3d.com/, visited 2022	Stress Relief - Heat up to 730°C in 2 h - Hold at 730°C during 2 h - Cool down to Ambient T^a in 1 h 50 min

All references for the selected material

1 3T Additive Manufacturing Ltd, Product Data Sheets / Available at: www.3t-am.com, visited 2019
2 Arcam AB, Product Data Sheets / Available at: www.arcam.com, visited 2015
3 Meltio, Product Data Sheets / Available at: https://meltio3d.com/, visited 2022

Fig.15. Heat treatment used for the alloy Ti6Al4V used in Additive Manufacturing

The database gives us details concerning the heat treatment used for the alloy Ti6Al4V used in Additive Manufacturing, as in the figure 15.

As powdered; Spherical Shape and a few satellites; SEM image

GENERAL INFORMATION

As powdered	
Microstructure	Spherical Shape and a few satellites
Comment	SEM image

100x

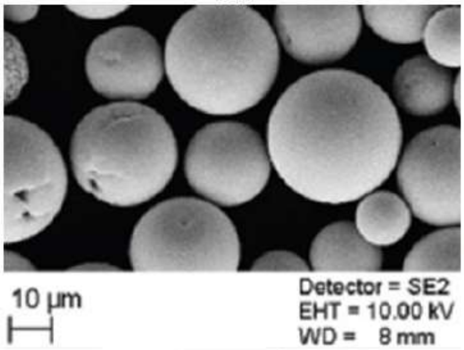

Microstructure

1/2

100x

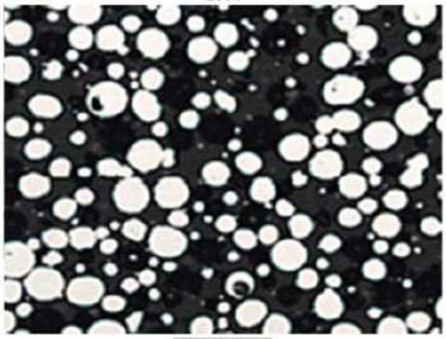

Microstructure

2/2

Fig.16. Metallography details for Ti6Al4V powders used in Additive Manufacturing

This project has been funded with support from the Iceland Liechtenstein Norway Grants. This publication [communication] reflects the views only of the authors, and the Commission cannot be held responsible for any use which may be made of the information contained herein.

Total Materia gives us details concerning the metallography of the alloy Ti6Al4V used in Additive Manufacturing, as in the figure 16 and the tribology is given in figure 18. In figure 17 are presented the similar materials with the same composition existing on the market.

The material does not have direct properties.
Similar materials that have these properties are listed in the table below.
Click on the material to view properties.

Result(s) found: 156

#	MATERIAL	STANDARD	COUNTRY / PRODUCER	EQUIVALENCE CATEGORY
1	S Ti 6408J (TiAl6V4AJ)	JIS	Japan	Composition 100%
2	TA6V	AFNOR NF	France	Composition 100%
3	Ti 6Al-4V Grade 5	PROPRIETARY	Allegheny Technologies Incorporated; Ulbrich Stainless Steel	Composition 100%
4	Ti-6Al-4V	ONORM	Austria	Composition 100%
5	Ti-6Al-4V	NBN	Belgium	Composition 100%
6	Ti-6Al-4V	NBR	Brazil	Composition 100%
7	Ti-6Al-4V	BDS	Bulgaria	Composition 100%
8	Ti-6Al-4V	CSN	Czech Republic	Composition 100%
9	Ti-6Al-4V	EN	European Union	Composition 100%
10	Ti-6Al-4V	SFS	Finland	Composition 100%

Fig.17. Similar Materials with the same composition existing on the market

Tribology

CONDITIONS (3)

- Tested Material - Heat treatment: As Built
- Tested Material - General comment: Standard Grade
- Tested Material - General comment: Performance Grade

SELECTED CONDITION

Tested Material **Heat treatment:** As Built

Tested Material

PROPERTY	T(°C)	VALUE	UNIT	NOTE
Surface Roughness		10	µm	Ra
		80	µm	Rz

Reference for the selected material and condition

1 Airbus Apworks GmbH, Product Data Sheets / Available at: www.apworks.de, visited 2018

All references for the selected material

1 Airbus Apworks GmbH, Product Data Sheets / Available at: www.apworks.de, visited 2018
2 Materialise, Product Data Sheets / Available at: www.materialise.com, visited Oct-2019

Fig.18. Tribology properties of Ti6Al4V used in Additive Manufacturing

This project has been funded with support from the Iceland Liechtenstein Norway Grants. This publication [communication] reflects the views only of the authors, and the Commission cannot be held responsible for any use which may be made of the information contained therein.

For welding and brazing are given different variants similar alloy of Ti, as in figure 19. In the figure 20, it is presented the stress strain diagram for Ti6Al4V used in Electron Beam Melting (EBM). The fatigue data is given in the figure 21, by ARCAM company.

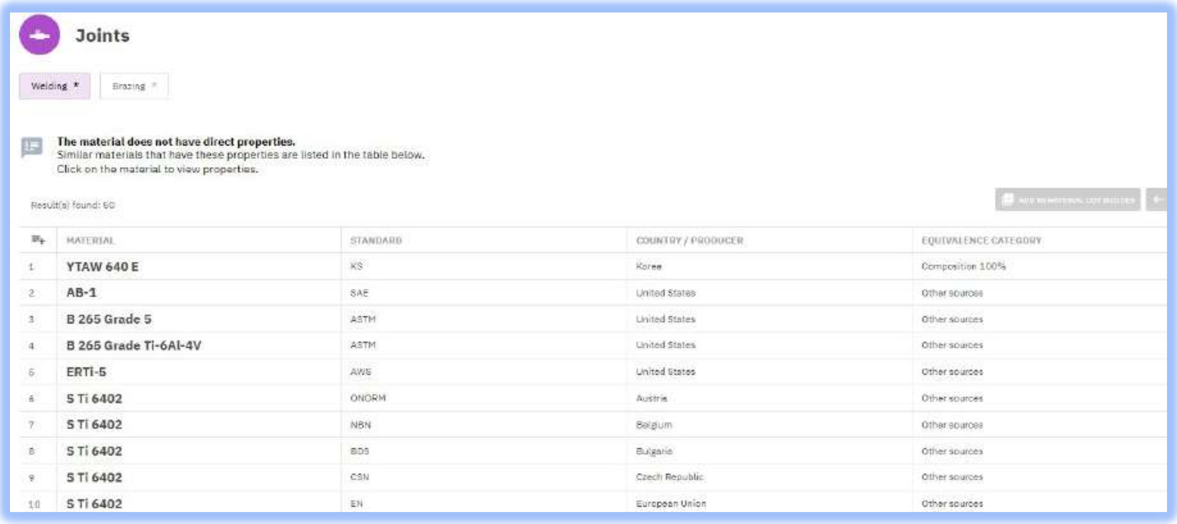
Joints
Welding * Brazing

The material does not have direct properties.
Similar materials that have these properties are listed in the table below.
Click on the material to view properties.

Result(s) found: 60

	MATERIAL	STANDARD	COUNTRY / PRODUCER	EQUIVALENCE CATEGORY
1	YTAW 640 E	KS	Korea	Composition 100%
2	AB-1	SAE	United States	Other sources
3	B 265 Grade 5	ASTM	United States	Other sources
4	B 265 Grade Ti-6Al-4V	ASTM	United States	Other sources
5	ERTi-5	AWS	United States	Other sources
6	S Ti 6402	ONORM	Austria	Other sources
7	S Ti 6402	NBN	Belgium	Other sources
8	S Ti 6402	BDS	Bulgaria	Other sources
9	S Ti 6402	CSN	Czech Republic	Other sources
10	S Ti 6402	EN	European Union	Other sources

Fig.19. Different variants similar alloy of Ti, used in welding and in brazing

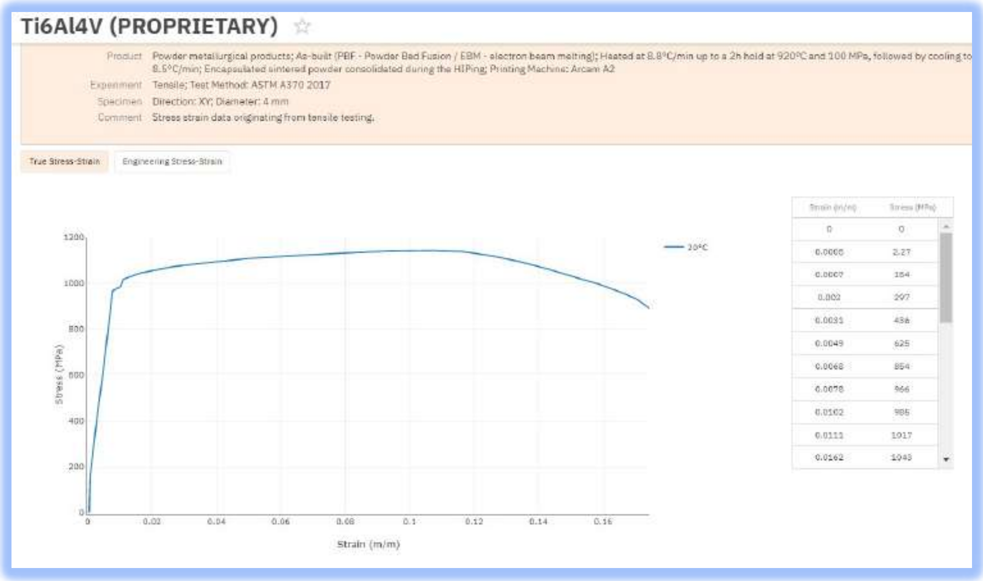

Fig.20. Stress strain diagram for Ti6Al4V used in Electron Beam Melting (EBM)

This project has been funded with support from the Iceland Liechtenstein Norway Grants. This publication [communication] reflects the views only of the authors, and the Commission cannot be held responsible for any use which may be made of the information contained therein.

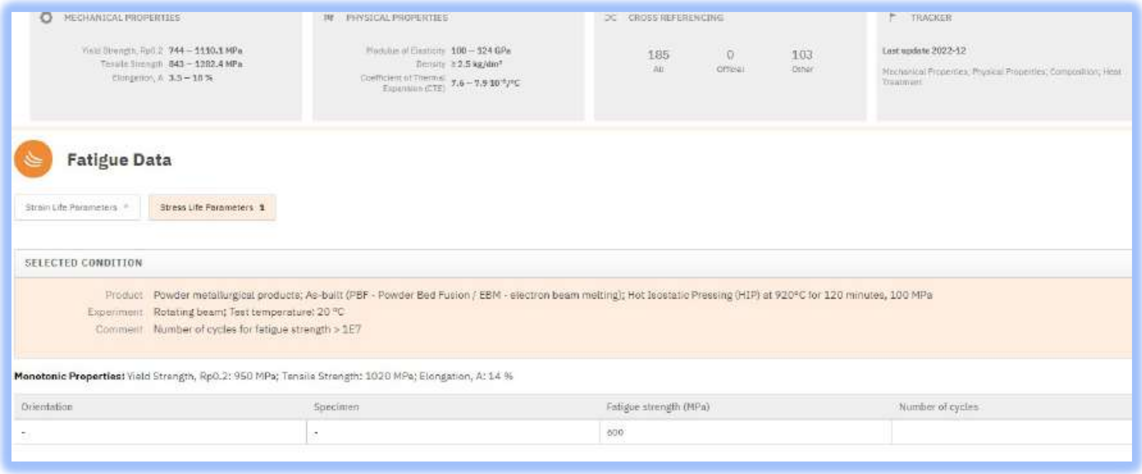

Fig.21. Fatigue data given for Ti6Al4V used in Electron Beam Melting (EBM)

Fig.22. Equivalents finder

The database permits us to find equivalents finder in function of the Brinell hardness [HB], Rockwell hardness [HR], Yield strength Rp0,2 [MPa], elongation A [%], tensile strength [MPa], reduction of area [%], Vickers hardness [HV], modulus of elasticity [GPa], density [kg/dm^3], melting temperature [°C], coefficient of thermal expansion (CTE) (10^{-6}/°C) or chemical composition, as in figure 22.

Total Materia give us the material description for the alloy Ti6Al4V used in Electron Beam Melting (EBM), specifying the applications domain, in the case of powder, is given the particles size distribution, additive laser manufacturing systems type that used this powder, the biocompatibility, as in figure 23.

This project has been funded with support from the Iceland Liechtenstein Norway Grants. This publication [communication] reflects the views only of the authors, and the Commission cannot be held responsible for any use which may be made of the information contained therein.

Material Description

Source	**Meltio**
Comment	3D printing (Additive manufacturing) - Direct Energy Deposition (DED) Machine: Meltio M450 Titanium alloy with high strength, low density, high fracture toughness, excellent corrosion resistance and superior biocompatibility
Application	Tools and prototypes, aerospace, marine, chemical
Source	**Optimal Material Technology CO.,Ltd**
Comment	3D printing (Additive manufacturing) - Selective Laser Melting (SLM) Machine: Concept Laser M2, EOS M 280. It has high purity, low oxygen content and good fluidity. Particle size distribution: 15-53 μm. Hall flow rate: 36 s/50g
Source	**Shanghai Research Institute of Materials**
Comment	3D printing (Additive manufacturing) - Selective Laser Melting (SLM), Electron Beam Melting (EBM) Particle size range: 15-45 μm. Particle size distribution d_{50}: ≤ 30 μm. Liquidity Flowability: ≤ 40s.
Source	**Proto Labs, Inc.**
Comment	3D printing (Additive manufacturing) - Direct Metal Laser Sintering (DMLS) Mechanical properties of Ti6Al4V are comparable to wrought titanium for tensile strength, elongation, and hardness.
Application	It is used in a variety of medical applications which require high strength.
Source	**Digital Metal (part of Höganäs Group Company)**
Comment	3D printing (Additive manufacturing) - Binder Jetting Machine: DM P2500
Source	**Materialise**
Comment	3D printing (Additive manufacturing) - Direct Metal Laser Sintering (DMLS) Titanium alloy that combines excellent mechanical properties with very low specific weight and corrosion resistance. Available like Standard Grade and Performance Grade.
Application	Aeronautics, functional prototypes, solid end-use parts, medical devices and spare parts
Source	**Arcam AB**
Comment	3D printing (Additive manufacturing) Titanium alloy with the high strength, good machinability, low weight ratio and outstanding corrosion resistance.
Application	Typically used for: direct manufacturing of parts and prototypes for racing and aerospace industry, biomechanical applications, such as implants and prosthesis, marine applications, chemical industry, gas turbines.
Source	**Sintavia**
Comment	3D printing (Additive manufacturing) - Direct Metal Laser Sintering (DMLS) Corrosion resistance, strength, temperature resistance and weight reduction.
Source	**Sondasys sp. z o.o.**
Comment	3D printing (Additive manufacturing) - Selective Laser Melting (SLM) Titanium alloy powder.
Source	**AIRBUS APWORKS GmbH**
Comment	3D printing (Additive manufacturing) - Laser Powder Bed Additive Layer Manufacturing (ALM) Light weight titanium alloy powder. Excellent mechanical properties and corrosion resistance. Smallest wall thickness (mm): 1.0
Application	Aerospace, motor racing, and also for the production of biomedical implants.
Source	**Heraeus Additive Manufacturing GmbH**
Comment	3D printing (Additive manufacturing) - Laser Powder Bed Fusion (PBF-LB) High strength titanium alloy with low weight, good biocompatibility and high corrosion resistance. Particle Size Distribution (μm): 15-45 and 15-53
Application	Medical, aerospace and automotive
Source	**3T Additive Manufacturing Ltd (former 3T RPD Ltd.)**
Comment	3D printing (Additive manufacturing) - Direct Metal Laser Sintering (DMLS) Machine: EOSINT M290, EOSINT M280, EOSINT M400, EOSINT M400-4 Titanium alloy powder. Corrosion resistance, lightweight, biocompatible, weldable.
Application	Prototyping, engineering, biomedical implants, small series production
Source	**Vday Additive Manufacturing Technology Co., Ltd.**
Comment	3D printing (Additive manufacturing) - Selective Laser Melting (SLM), Electron Beam Melting (EBM) Titanium alloy powder. High strength to weight ratio, good mechanical properties, excellent corrosion resistance, good biocompatibility
Application	Medical implants, automotive, aerospace, mold, energy and power, electronics

Fig.23. Material Description - for Ti6Al4V used in Electron Beam Melting (EBM)

In the figure 24, it is presented how can discovery the material type, choosing the domain for Brinell Hardness [HB], for the temperature 0-30ºC on X axis, meaning from 500 to 800, and the compression modulus [GPa], for the temperature 0-30ºC, from 100-124, and are given 2 group types, ferrous alloys and nonferrous alloy. In figure 25, the database permits us to see the material properties if it is known the standard ASTM, the standard number.

This project has been funded with support from the Iceland Liechtenstein Norway Grants. This publication [communication] reflects the views only of the authors, and the Commission cannot be held responsible for any use which may be made of the information contained therein.

Fig.24. Material discovery

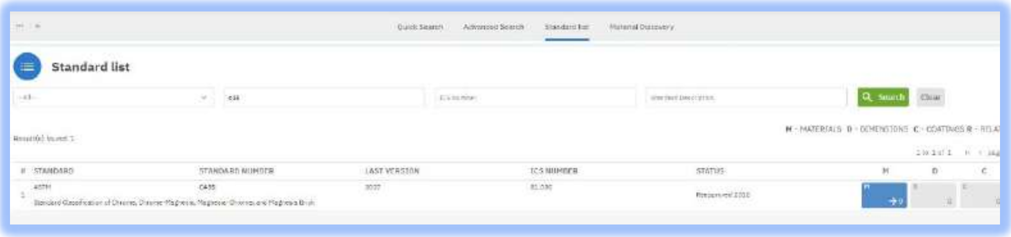

Fig.25. Standard list

3. Total Materia database – Search algorithms used for identification the unknown metallic materials

For the chemical composition Co 54,31 %, Cr 23,08 %, Mo 11,12 %, W 7,85 %, Si 3,35 % and Mn, Fe < 0,1, using the algorithms of the Total Materia database, it will identify the material with this chemical composition, as in the figures 26 and 27.

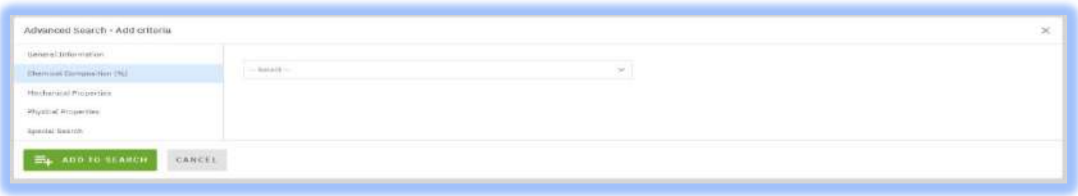

Fig.26. Algorithms used for identification the unknown materials

This project has been funded with support from the Iceland Liechtenstein Norway Grants. This publication [communication] reflects the views only of the authors, and the Commission cannot be held responsible for any use which may be made of the information contained therein.

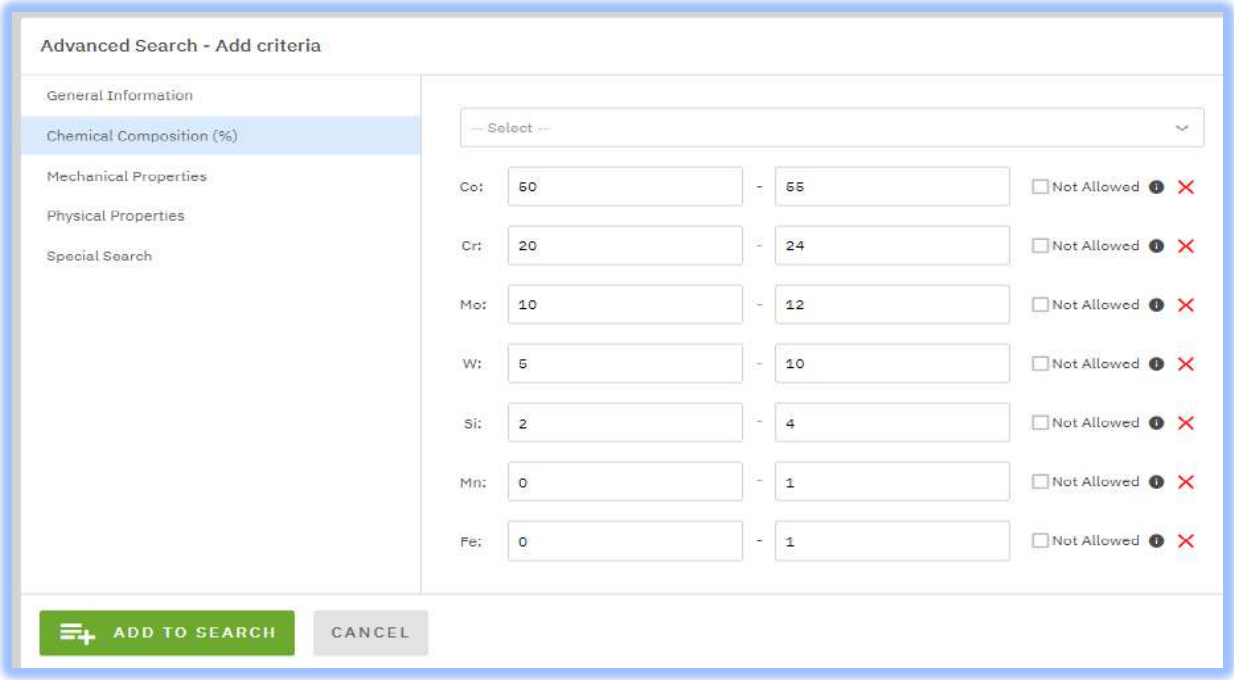

Fig.27. Chemical composition selection

When we want to change the chemical composition, it must click on clear.

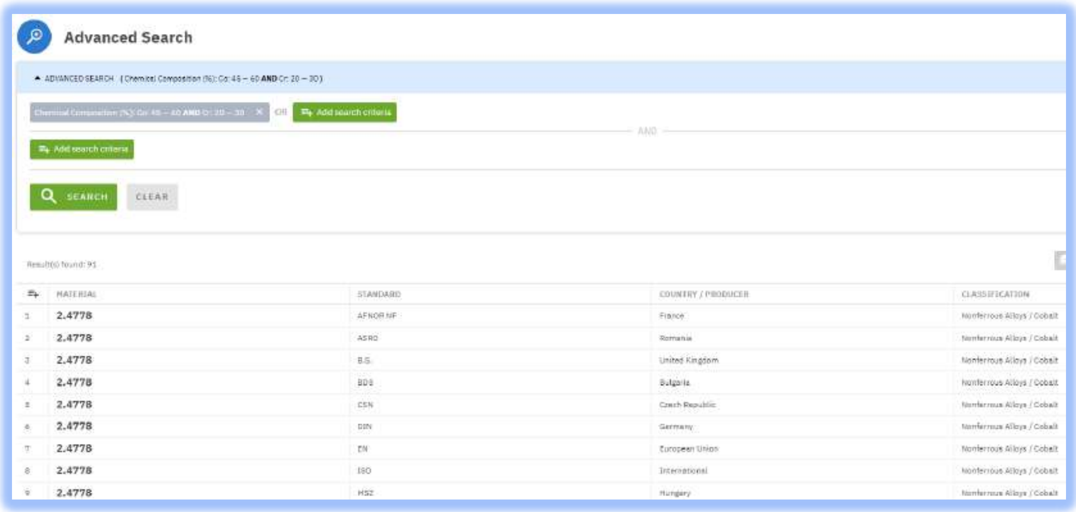

Fig.28. Co-Cr alloy results that have the respective chemical composition

In the figure 28 are presented the Co-Cr alloy results that have the respective chemical composition.

This project has been funded with support from the Iceland Liechtenstein Norway Grants. This publication [communication] reflects the views only of the authors, and the Commission cannot be held responsible for any use which may be made of the information contained therein.

The first is the material 2.4778, standard AFNOR NF, France and if we give click, can know the mechanical properties, the chemical composition, and its applications. In the figure 29 is presented the determination of the material: CoCr28 and their properties. The material description is presented in the figure 30.

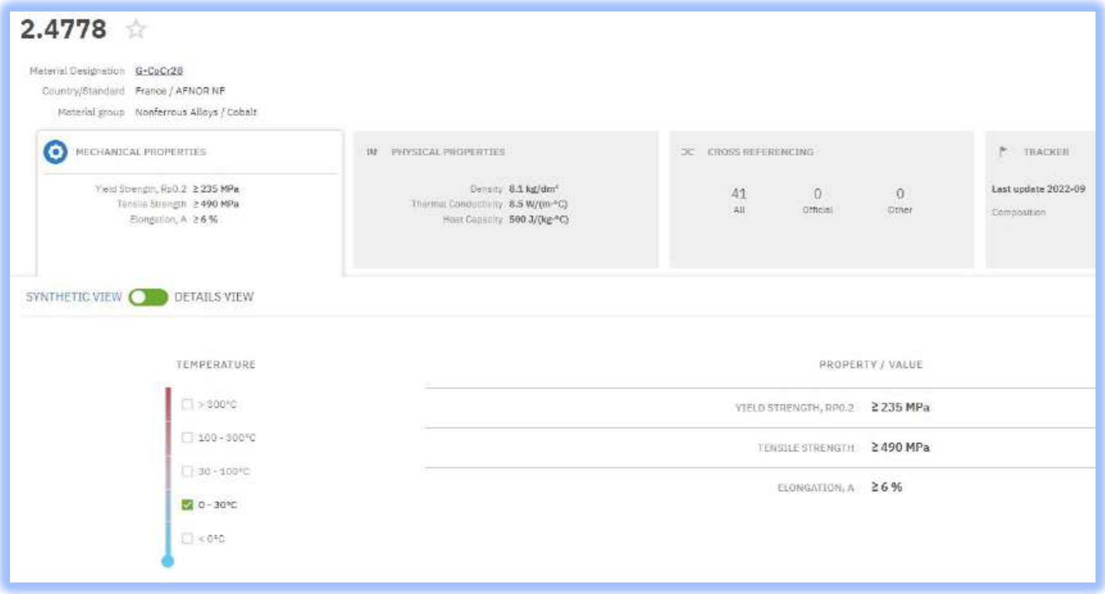

Fig.29. Determination of the material: CoCr28 and their properties

Fig.30. Material description of CoCr28

This project has been funded with support from the Iceland Liechtenstein Norway Grants. This publication [communication] reflects the views only of the authors, and the Commission cannot be held responsible for any use which may be made of the information contained therein.

4. *Total Materia database – polymers, ceramics and composite materials*

Total Materia database is used too for the polymers (Fig.31), ceramics and composite materials.

The database given 125 results of PLA types, as in the figure 32.

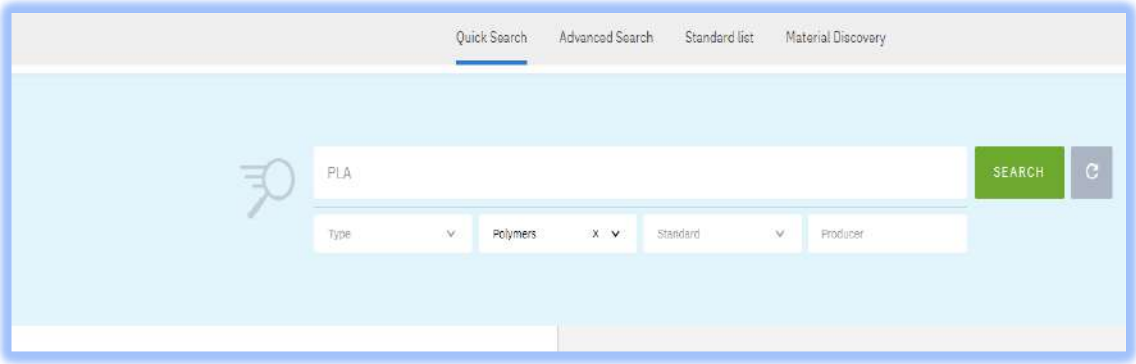

Fig.31. Total Materia database for the polymers

Result(s) found: 125

ADD TO MATERIAL LIST BUILDER

	MATERIAL	STANDARD	COUNTRY / PRODUCER	CLASSIFICATION
1	PLA	GENERIC		Polymers / Plastics, thermoplasts / Biopolymers (CA, CAB, PLA...) / PLA 3D Materials
2	PLA++	PROPRIETARY	Breathe-3DP	Polymers / Plastics, thermoplasts / Biopolymers (CA, CAB, PLA...) / PLA 3D Materials
3	PLA Crystal Clear	PROPRIETARY	Fillamentum	Polymers / Plastics, thermoplasts / Biopolymers (CA, CAB, PLA...) / PLA 3D Materials
4	PLA Extrafill	PROPRIETARY	Fillamentum	Polymers / Plastics, thermoplasts / Biopolymers (CA, CAB, PLA...) / PLA 3D Materials
5	PLA Filament	PROPRIETARY	Filament PM	Polymers / Plastics, thermoplasts / Biopolymers (CA, CAB, PLA...) / PLA 3D Materials
6	PLA Plus ProSpeed	PROPRIETARY	Rosa 3D	Polymers / Plastics, thermoplasts / Biopolymers (CA, CAB, PLA...) / PLA 3D Materials
7	PLA Premium Filament	PROPRIETARY	Airwolf 3D	Polymers / Plastics, thermoplasts / Biopolymers (CA, CAB, PLA...) / PLA 3D Materials
8	PLA Prografen color	PROPRIETARY	Advanced Graphene Products	Polymers / Plastics, thermoplasts / Biopolymers (CA, CAB, PLA...) / PLA 3D Materials

Fig.32. 125 results of PLA types existing on the database

In figure 33, are presented the mechanical properties of PLA crystal clear.

Database give us the manufacturing processes of PLA crystal clear, such as 3D Printing and temperature used in the manufacturing processes, as in figure 34.

This project has been funded with support from the Iceland Liechtenstein Norway Grants. This publication [communication] reflects the views only of the authors, and the Commission cannot be held responsible for any use which may be made of the information contained therein.

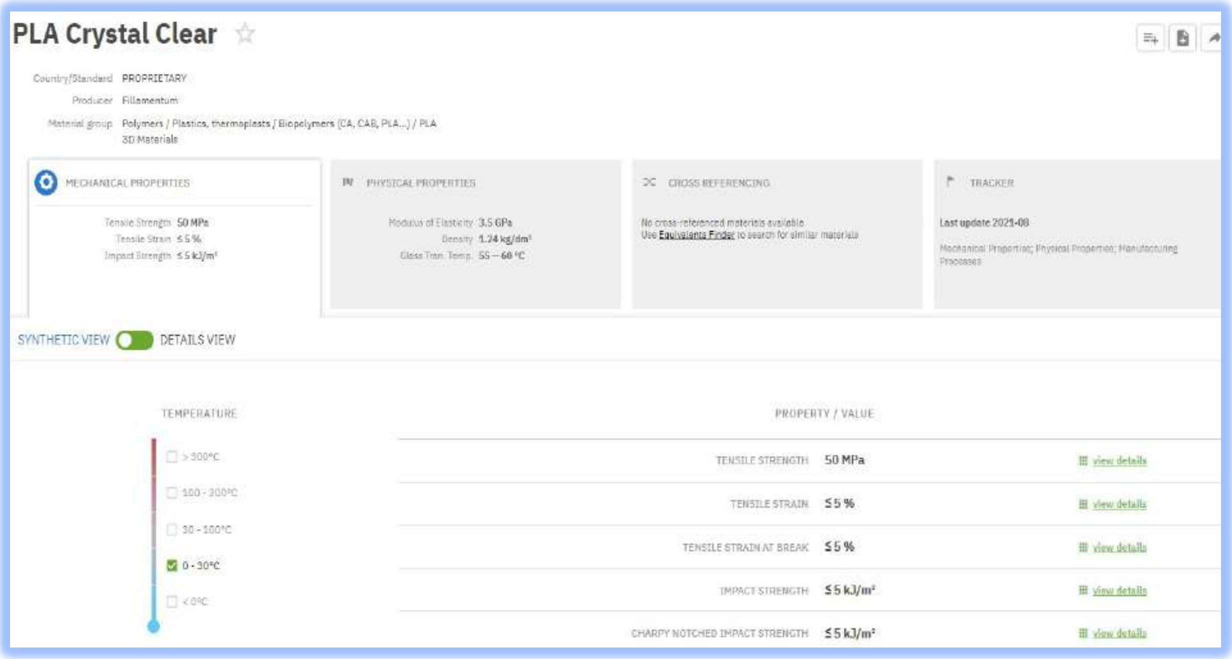

Fig.33. Mechanical properties of PLA crystal clear

Manufacturing Processes

PROPERTY	VALUE	UNIT
3D printing machine settings **Reference:** Fillamentum, Product Data Sheets / Available at: www.fillamentum.com, visited 2021		
Heated Bed Temperature	50 – 60	°C
Printing Temperature	210 – 230	°C

Reference for the selected material and condition

1 Fillamentum, Product Data Sheets / Available at: www.fillamentum.com, visited 2021

Fig.34. Manufacturing processes of PLA crystal clear

In the figure 35 is realized the material description for PLA materials, being specify that it is used in Fused Deposition Modeling (FDM) process.

This project has been funded with support from the Iceland Liechtenstein Norway Grants. This publication [communication] reflects the views only of the authors, and the Commission cannot be held responsible for any use which may be made of the information contained therein.

Fig.35. Material description for PLA filament

For ceramics, by example Hap, we obtain the results as in the figure 36.

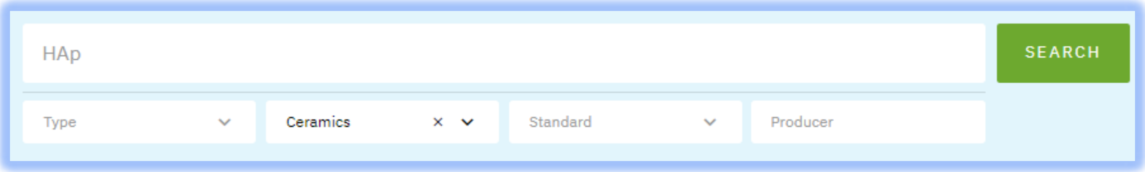

Fig.36. Ceramic search

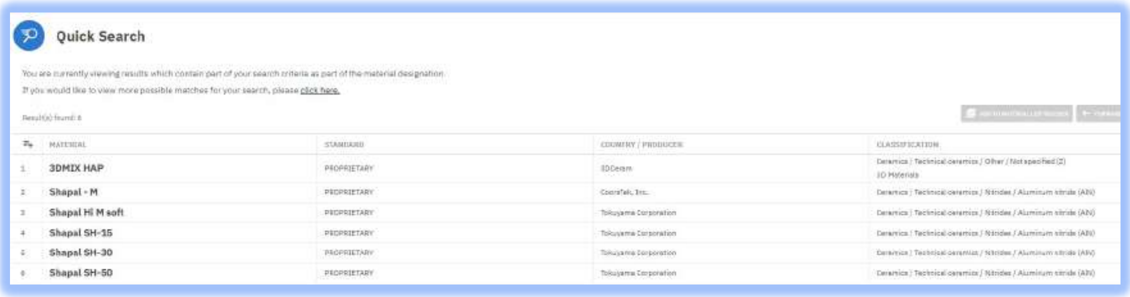

Fig.37. HAp variants existing on the database

In the figure 37, are given the Hap variants existing on the database, their producers, country and standards. In the figure 38 are given the mechanical properties of Hap.

This project has been funded with support from the Iceland Liechtenstein Norway Grants. This publication [communication] reflects the views only of the authors, and the Commission cannot be held responsible for any use which may be made of the information contained therein.

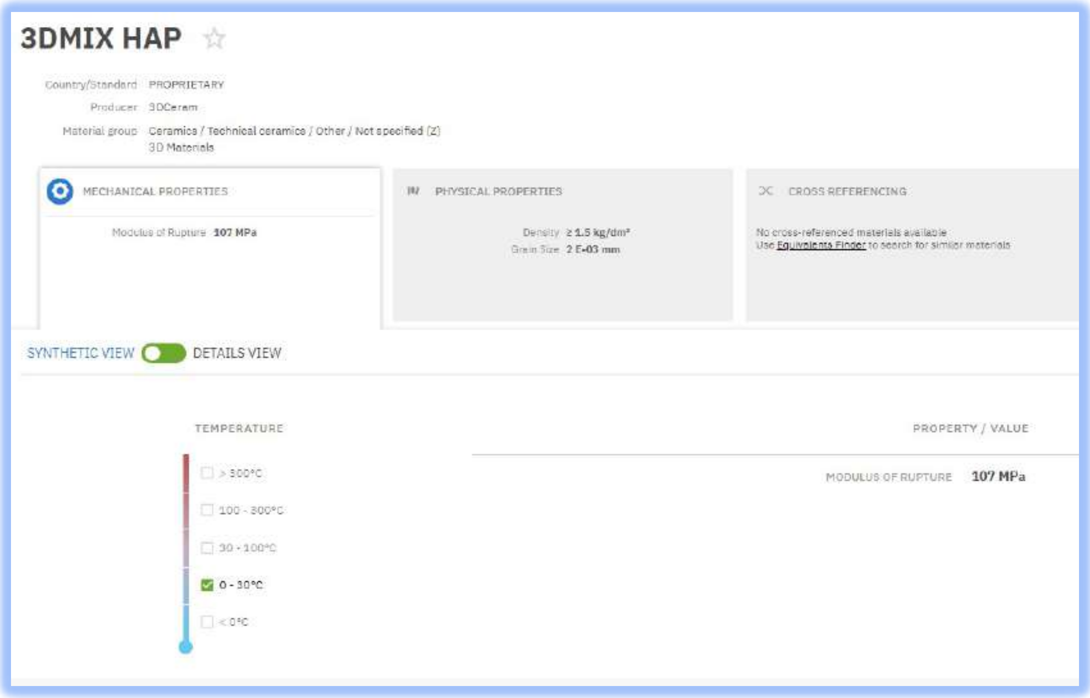

Fig.38. Mechanical properties of HAp

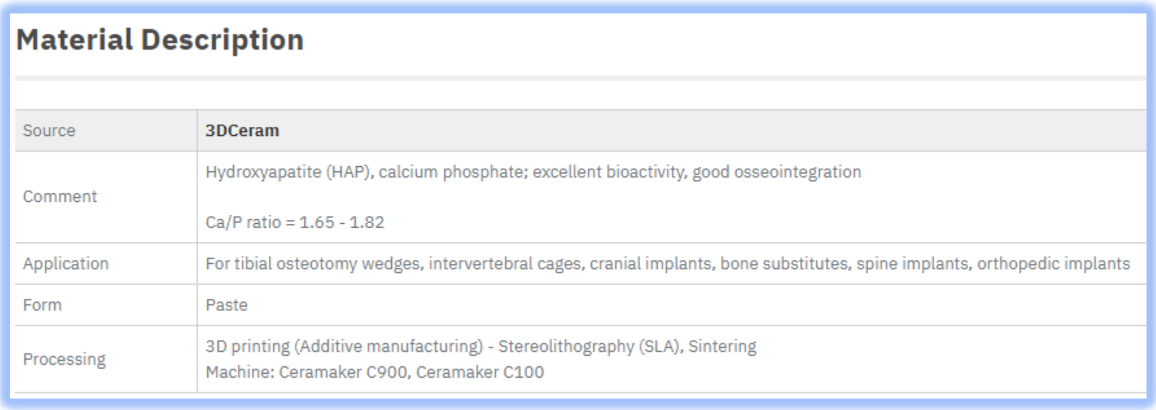

Material Description

Source	3DCeram
Comment	Hydroxyapatite (HAP), calcium phosphate; excellent bioactivity, good osseointegration Ca/P ratio = 1.65 - 1.82
Application	For tibial osteotomy wedges, intervertebral cages, cranial implants, bone substitutes, spine implants, orthopedic implants
Form	Paste
Processing	3D printing (Additive manufacturing) - Stereolithography (SLA), Sintering Machine: Ceramaker C900, Ceramaker C100

Fig.39. Material description of HAp

Hap is used in additive manufacturing in SLS and in SLA, using Ceramaker C900 or Ceramaker C100, the platform gives us inclusive information about the manufacturing systems that used this material. Hydroxyapatite is used as paste in the additive manufacturing process to obtain tibial osteotomy wedges, intervertebral cages, cranial implants, bone substitutes, spine implants or orthopaedic implants, as in the figure 39

This project has been funded with support from the Iceland Liechtenstein Norway Grants. This publication [communication] reflects the views only of the authors, and the Commission cannot be held responsible for any use which may be made of the information contained therein.

Concerning the composite materials, by example plywood, the database give us 3 results, such in the figures 40 and 41.

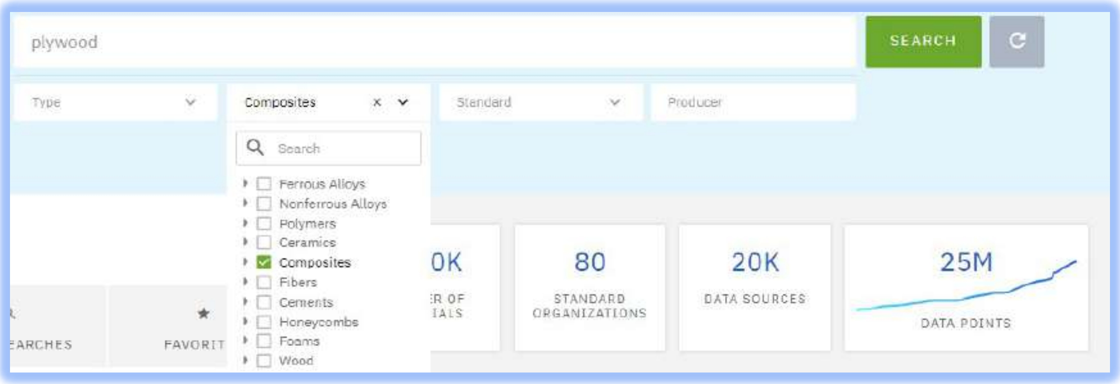

Fig.40. Quick search of plywood

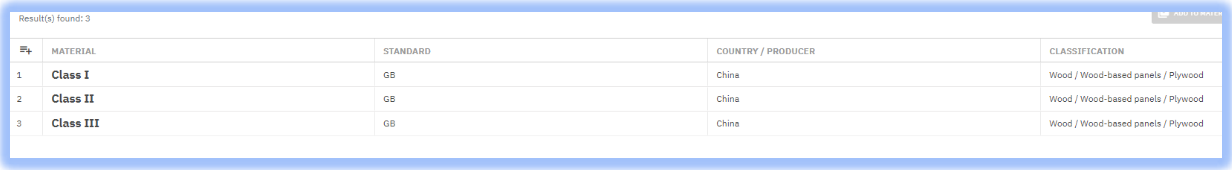

Result(s) found: 3

	MATERIAL	STANDARD	COUNTRY / PRODUCER	CLASSIFICATION
1	Class I	GB	China	Wood / Wood-based panels / Plywood
2	Class II	GB	China	Wood / Wood-based panels / Plywood
3	Class III	GB	China	Wood / Wood-based panels / Plywood

Fig.41. For composite plywood – 3 results

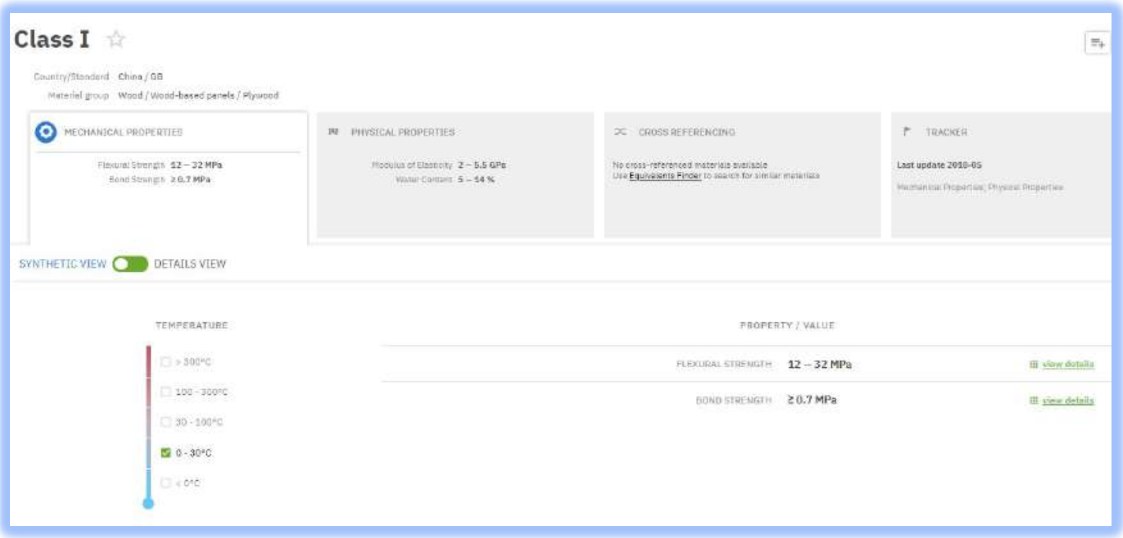

Fig.42. Mechanical properties of plywood class I

This project has been funded with support from the Iceland Liechtenstein Norway Grants. This publication [communication] reflects the views only of the authors, and the Commission cannot be held responsible for any use which may be made of the information contained therein.

In the figure 42 are presented the mechanical properties of plywood class I. In the figure 43 is presented the material description of plywood class I, that can be used in outdoor environment.

Material Description

Source	**GB/T 9846: 2015 / Plywood for general use**
Comment	Plywood which can pass boiling test and can be used in outdoor environment

Fig.43. Material description of plywood class I

5. Conclusions

In the last years, the materials developed very much, appeared different news materials with very interesting properties realized by different world companies, that can be used in Additive Manufacturing and in other manufacturing domain to realize medical parts or for industrial domain and grace to this database, all materials developed are introduced in this platform, giving us the possibility to choose, the chemical composition, the mechanical properties, or using the search algorithms, finding the unknown material, in function of the chemical or mechanical properties.

The implications of the present research would be interesting for the manufacture by Additive Manufacturing different medical parts, using different materials using the database Total Materia, or others to know the mechanical and chemical properties that are very important to establish the manufacturing parameters and manufacturing systems and tools.

References

1. Ratner Buddy D., Hoffman Allan S., Schoen Frederick J., Lemons Jack E.- Biomaterials Science, An introduction to materials in medicine –Academic Press, 2013;
2. Materia Total database - https://portal.totalmateria.com/en/search/advanced
3. https://link.springer.com/chapter/10.1007/978-3-662-46836-4_7

This project has been funded with support from the Iceland Liechtenstein Norway Grants. This publication [communication] reflects the views only of the authors, and the Commission cannot be held responsible for any use which may be made of the information contained therein.

EMERALD

The Education, Scholarships, Apprenticeships and Youth Entrepreneurship

EUROPEAN NETWORK FOR 3D PRINTING OF BIOMIMETIC MECHATRONIC SYSTEMS

E-toolkit –

Virtual Reality/Augmented Reality

Project Title	**European network for 3D printing of biomimetic mechatronic systems 21-COP-0019**
Output	**O2 - EMERALD e-toolkit manual for digital learningin producing biomimetic mechatronic systems**
Module	**Virtual Reality /Augmented Reality (VR/AR)**
Authors	**Martin ZELENAY, Branislav RABARA**

This project has been funded with support from the Iceland Liechtenstein Norway Grants. This publication [communication] reflects the views only of the authors, and the Commission cannot be held responsible for any use which may be made of the information contained therein.

CONTENT

This project has been funded with support from the Iceland Liechtenstein Norway Grants. This publication [communication] reflects the views only of the authors, and the Commission cannot be held responsible for any use which may be made of the information contained therein.

1 Introduction. Overview of whole process

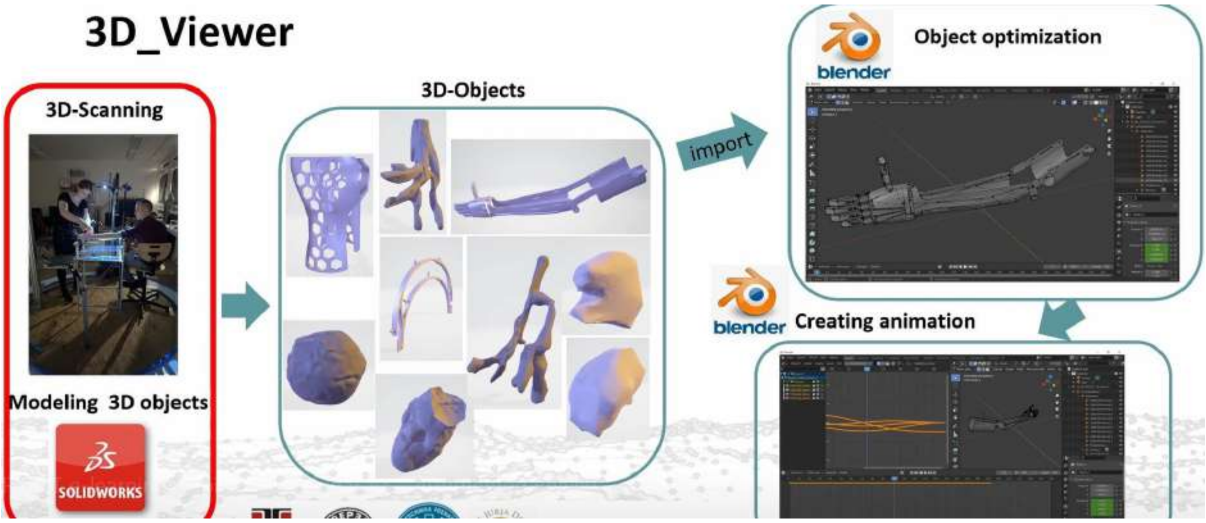

To create the 3D preview in Augmented reality we need 3D objects, we can get this through following steps:

- 3D scanning
- Or modeling of the 3D objects

Then there is a process which involves object optimization and creating animation.

Here we can see the scanning scanning of a hand in detail:

This project has been funded with support from the Iceland Liechtenstein Norway Grants. This publication [communication] reflects the views only of the authors, and the Commission cannot be held responsible for any use which may be made of the information contained therein.

2 Building Augmented Reality animations

2.1 Introduction to Blender software

We can also model an object in software called SolidWorks or similar.

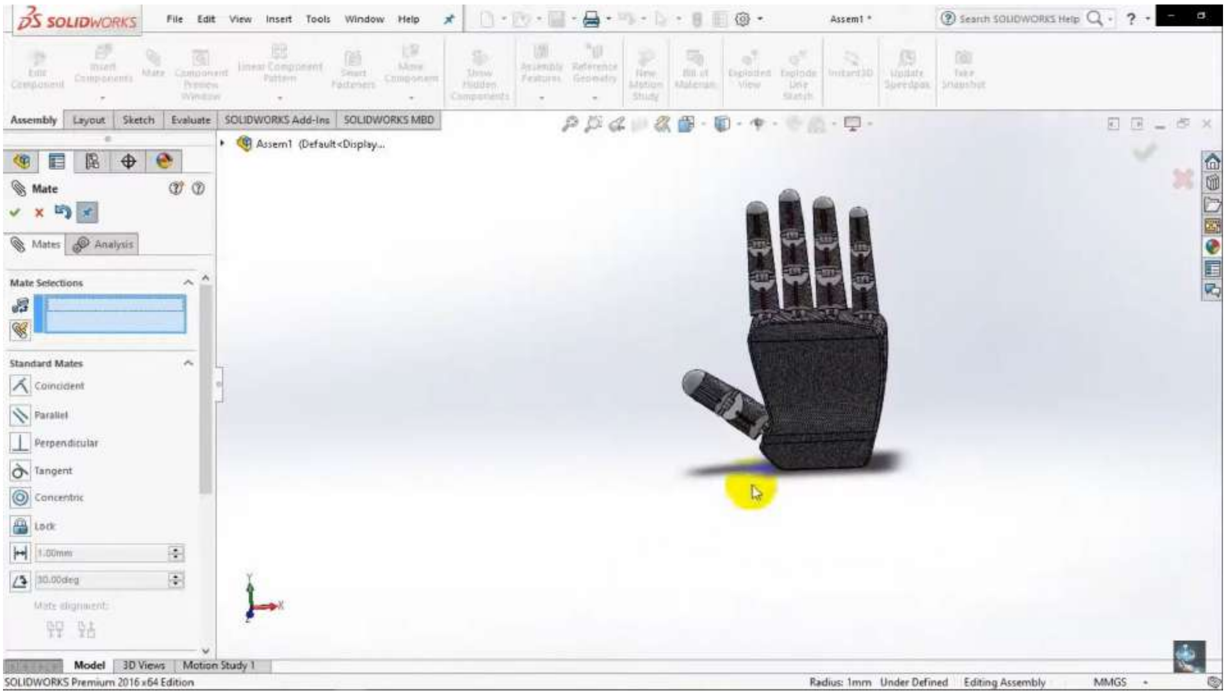

If we have the object in as a 3d object, we need to import them into program where we're going to optimize these – in our example we use Blender.

This project has been funded with support from the Iceland Liechtenstein Norway Grants. This publication [communication] reflects the views only of the authors, and the Commission cannot be held responsible for any use which may be made of the information contained therein.

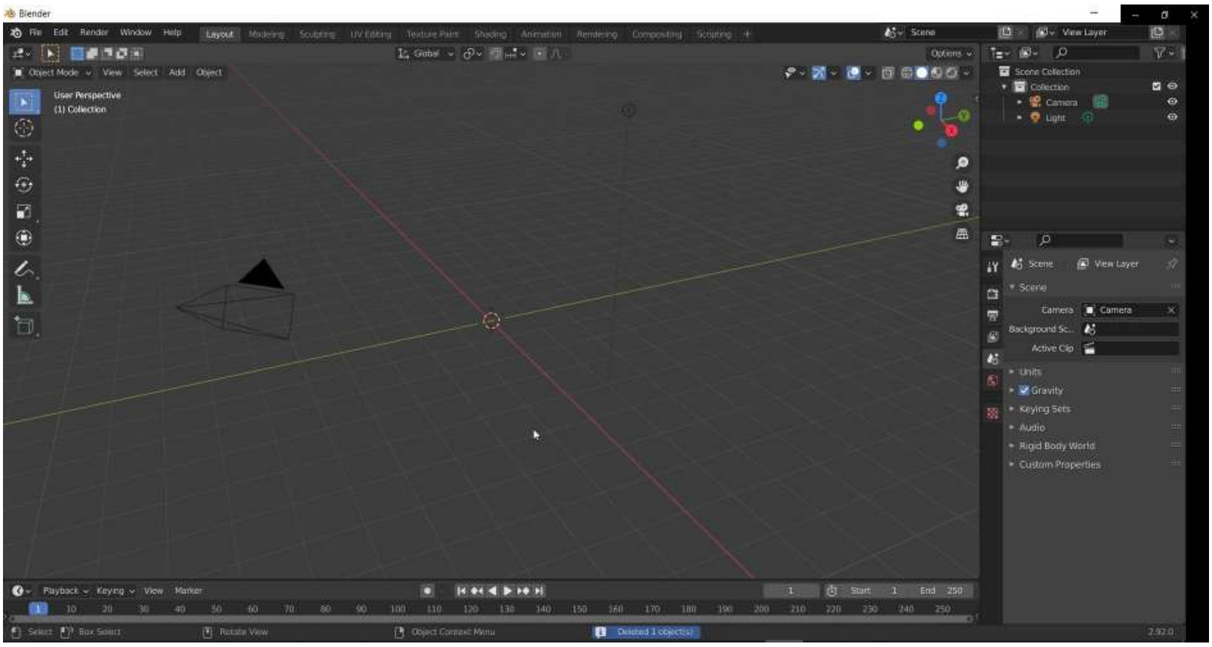

That means if we have a vertex files, we can create animation in Blender software. This is a simple process where we import the model first:

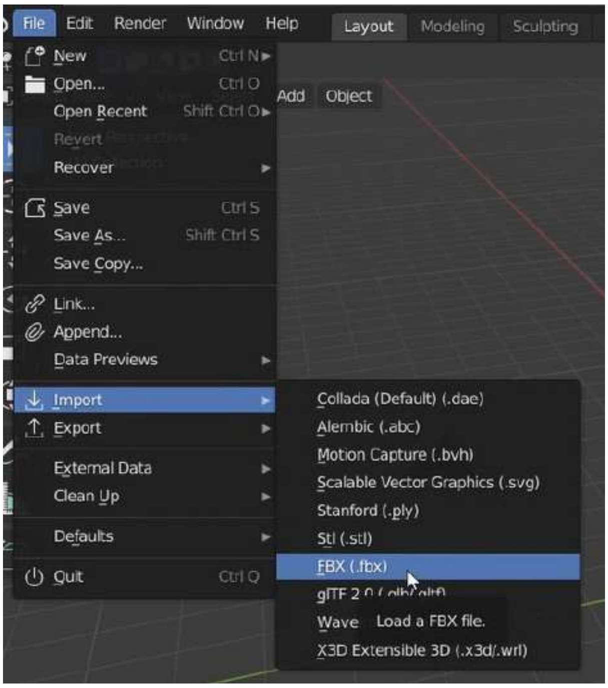

This project has been funded with support from the Iceland Liechtenstein Norway Grants. This publication [communication] reflects the views only of the authors, and the Commission cannot be held responsible for any use which may be made of the information contained therein.

We can change the materials or specifications of the object we will switch to view specifically color palette of this object in right bottom corner:

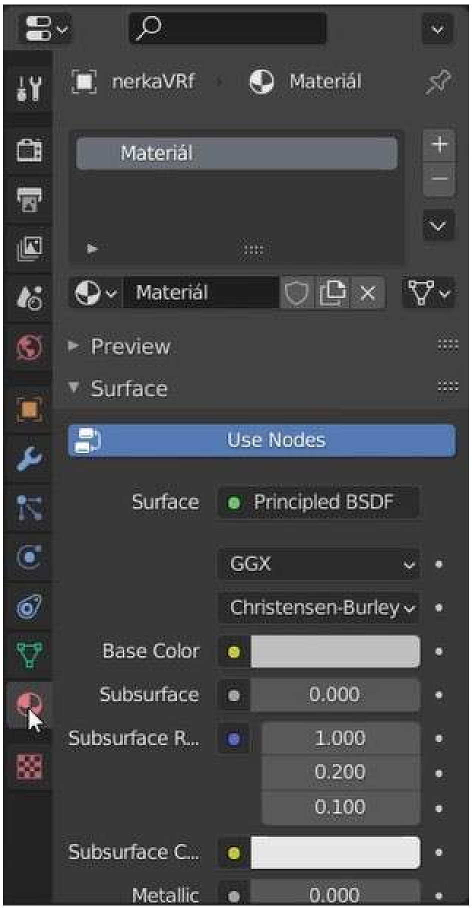

We have different axis in top right corner:

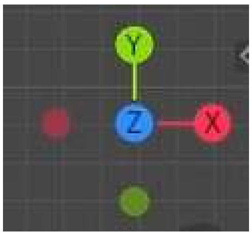

And from the bottom of the screen we can expand the timeline where we can create individual frame.

This project has been funded with support from the Iceland Liechtenstein Norway Grants. This publication [communication] reflects the views only of the authors, and the Commission cannot be held responsible for any use which may be made of the information contained therein.

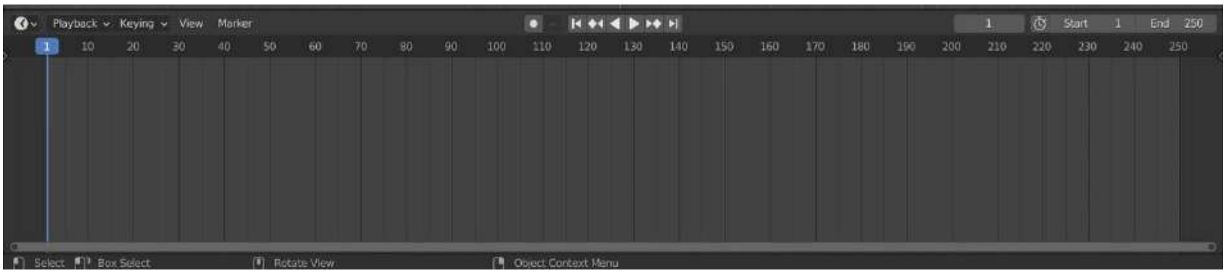

We will set the starting and ending of the timeline

On the first second of timeline, we will create a first frame of the rotation through axis y – by pressing the KEY button "I". Then selecting Rotation from the Edit Mode, or by pressing "R" we rotate the object through axis y.

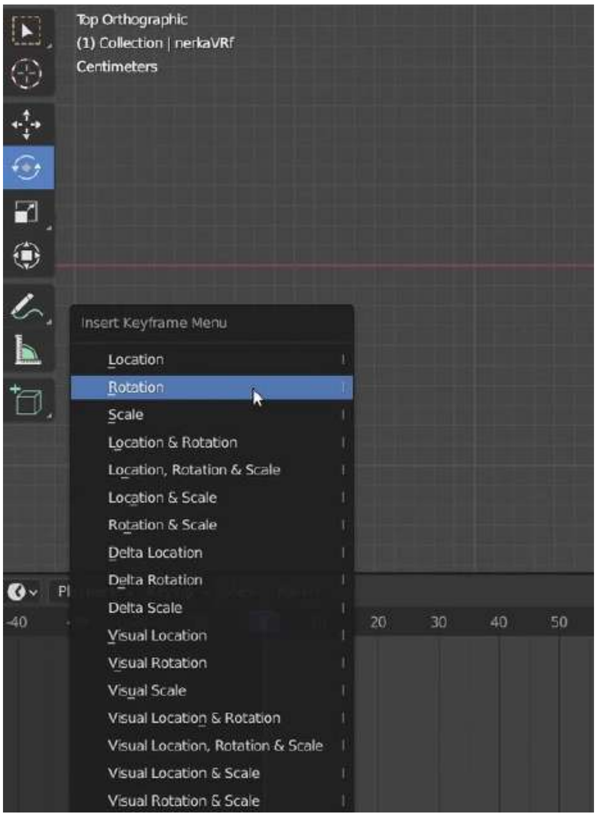

This project has been funded with support from the Iceland Liechtenstein Norway Grants. This publication [communication] reflects the views only of the authors, and the Commission cannot be held responsible for any use which may be made of the information contained therein.

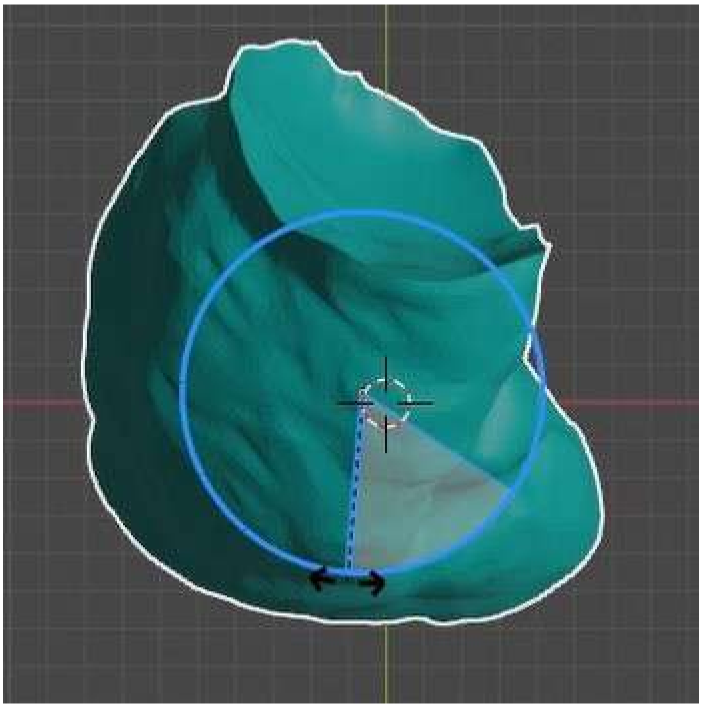

We will fix this position at 100. This means we will move to frame 100 with mouse and then rotate the object by pressing “R” and then pressing the KEY button “I” to fix it.

This project has been funded with support from the Iceland Liechtenstein Norway Grants. This publication [communication] reflects the views only of the authors, and the Commission cannot be held responsible for any use which may be made of the information contained therein.

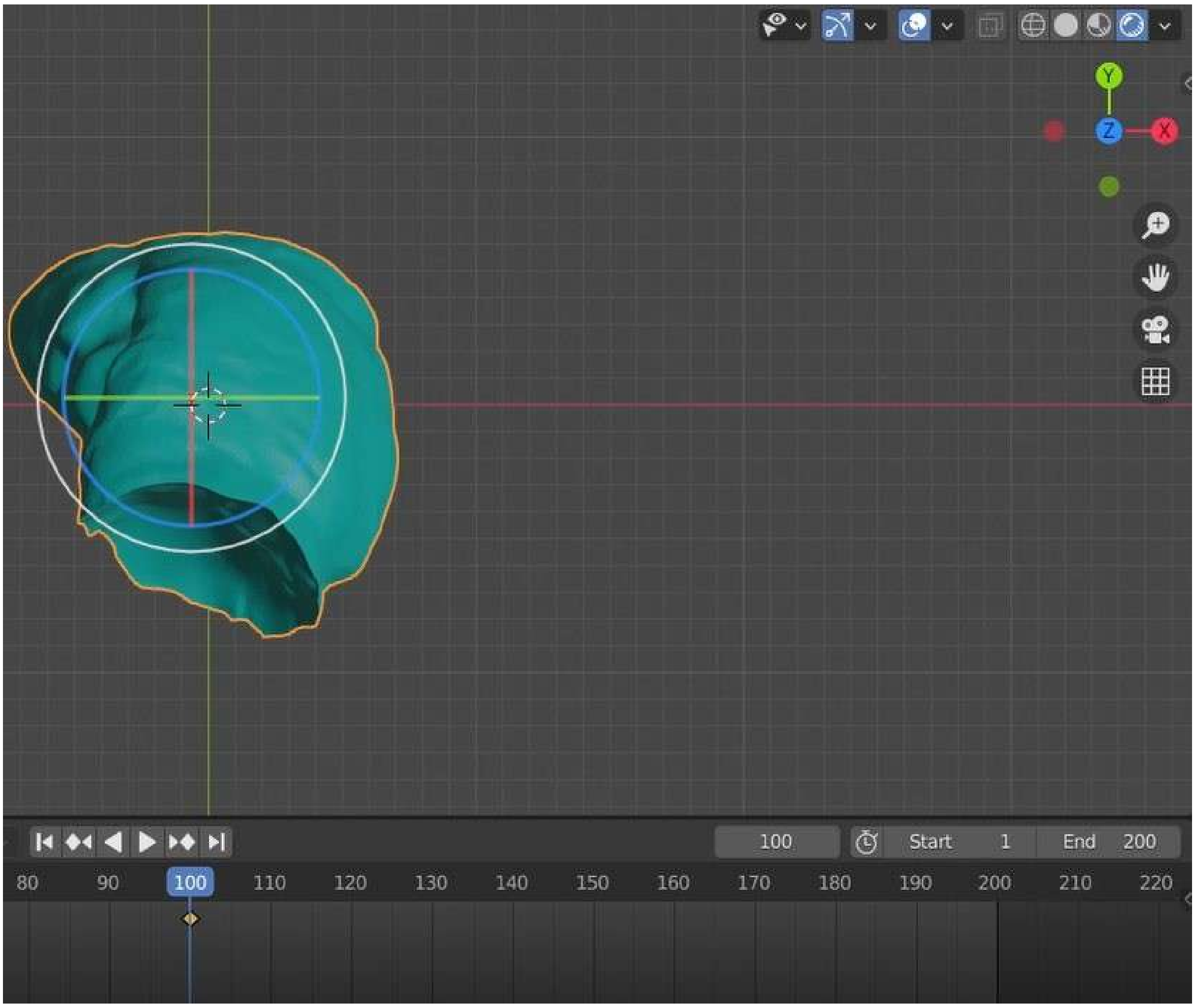

Then we will move to the frame 160 by mouse over Timeline and again rotating over axis y we rotate the object. And again, we will fix the position and by pressing “I” then moving to the last one at 200, rotating object again by “R”. We will fix the position.

If we are unsatisfied with specific frame, we can remove it With DELETE key and we can replace it, we need to rotate the object according to the axis Zed Z. And we can fix it again at this position on the timeline.

This project has been funded with support from the Iceland Liechtenstein Norway Grants. This publication [communication] reflects the views only of the authors, and the Commission cannot be held responsible for any use which may be made of the information contained therein.

Here is preview of another object where we created another animation:

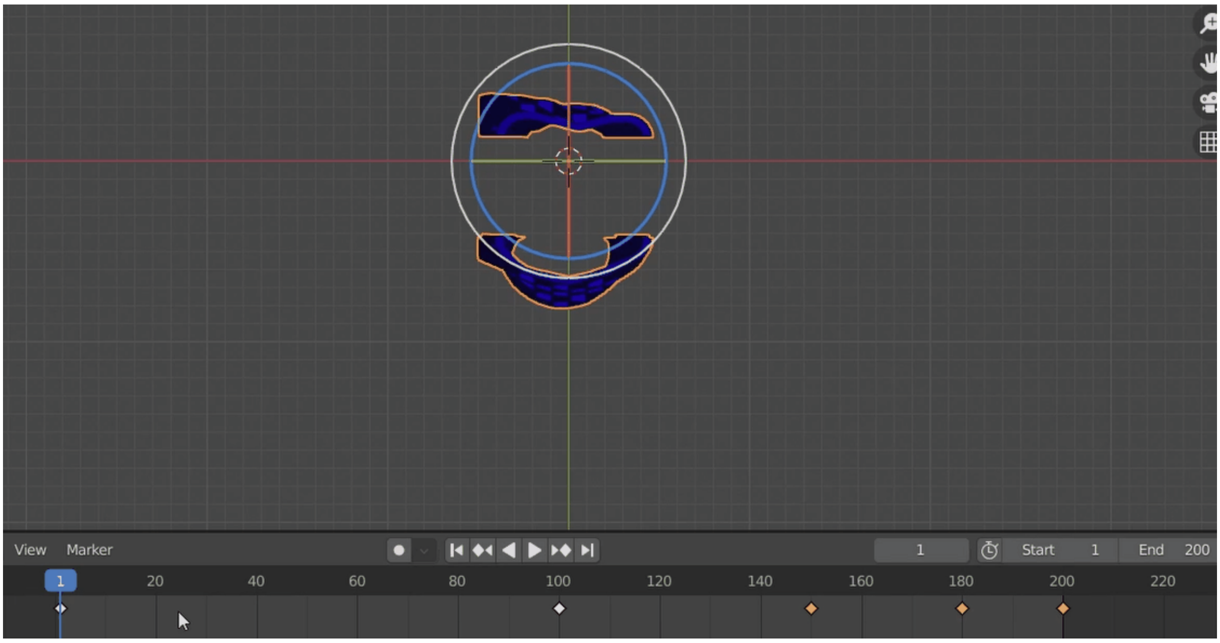

We can also create more complex animations.

Once we have the objects created, we need to save them and export them into Glb file for Android.

This project has been funded with support from the Iceland Liechtenstein Norway Grants. This publication [communication] reflects the views only of the authors, and the Commission cannot be held responsible for any use which may be made of the information contained therein.

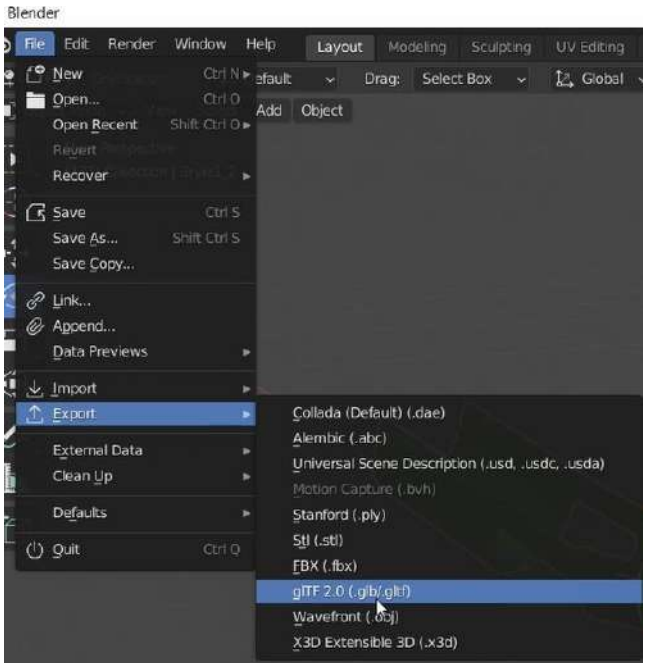

Or we can use the USDZ format, which is for IO OS, we can find the online core value converter for such.

This project has been funded with support from the Iceland Liechtenstein Norway Grants. This publication [communication] reflects the views only of the authors, and the Commission cannot be held responsible for any use which may be made of the information contained therein.

This project has been funded with support from the Iceland Liechtenstein Norway Grants. This publication [communication] reflects the views only of the authors, and the Commission cannot be held responsible for any use which may be made of the information contained therein.

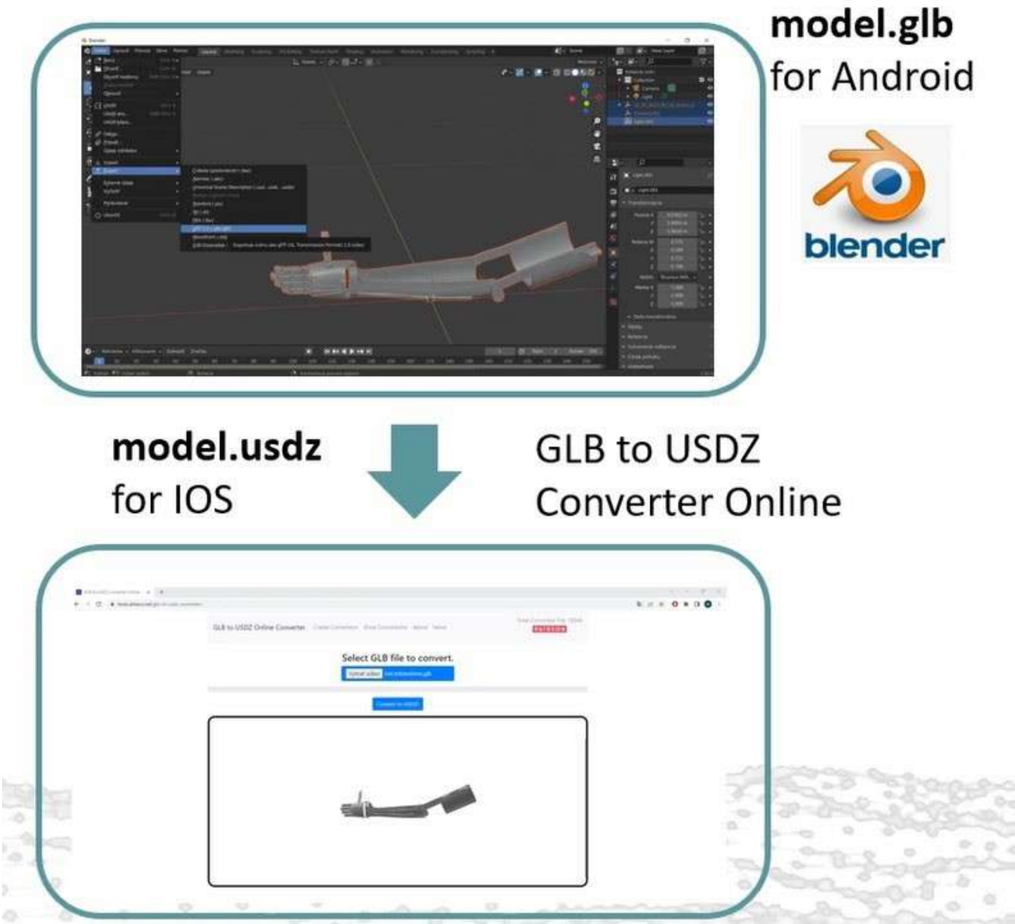

And here is the preview of online converter to create USDZ file.

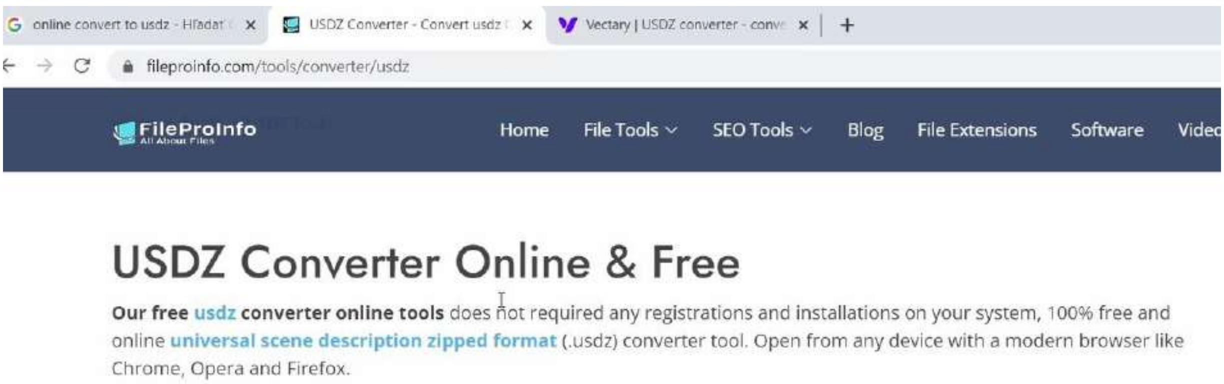

This project has been funded with support from the Iceland Liechtenstein Norway Grants. This publication [communication] reflects the views only of the authors, and the Commission cannot be held responsible for any use which may be made of the information contained therein.

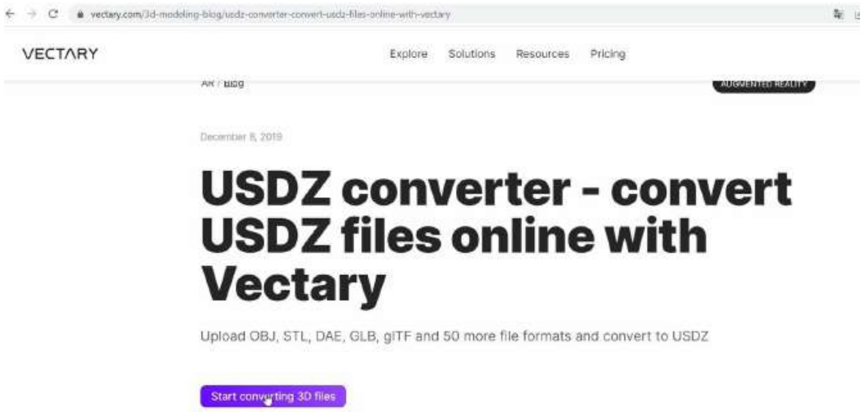

2.2. Creating website to display AR models

Once we have the individual models, we use the web interface WEB APP – 3D Viewer, which is used to create preview of the 3D models using the HTML code.

At www.modelviewer.dev we have the documentation and examples. This documentation is right iterated to the specific model viewer. And we can utilize the editor https://modelviewer.dev/editor/ where we can test our code, there are some examples from where we can get an inspiration.

This project has been funded with support from the Iceland Liechtenstein Norway Grants. This publication [communication] reflects the views only of the authors, and the Commission cannot be held responsible for any use which may be made of the information contained therein.

Once we have the code, we need to publish it. Either this could be own web server or it could be a code sandbox where we will publish our code. It's free it only requires registration at https://codesandbox.io/

There we can start a website. Here in our example we can see specific environment where we have index, which is a main site.

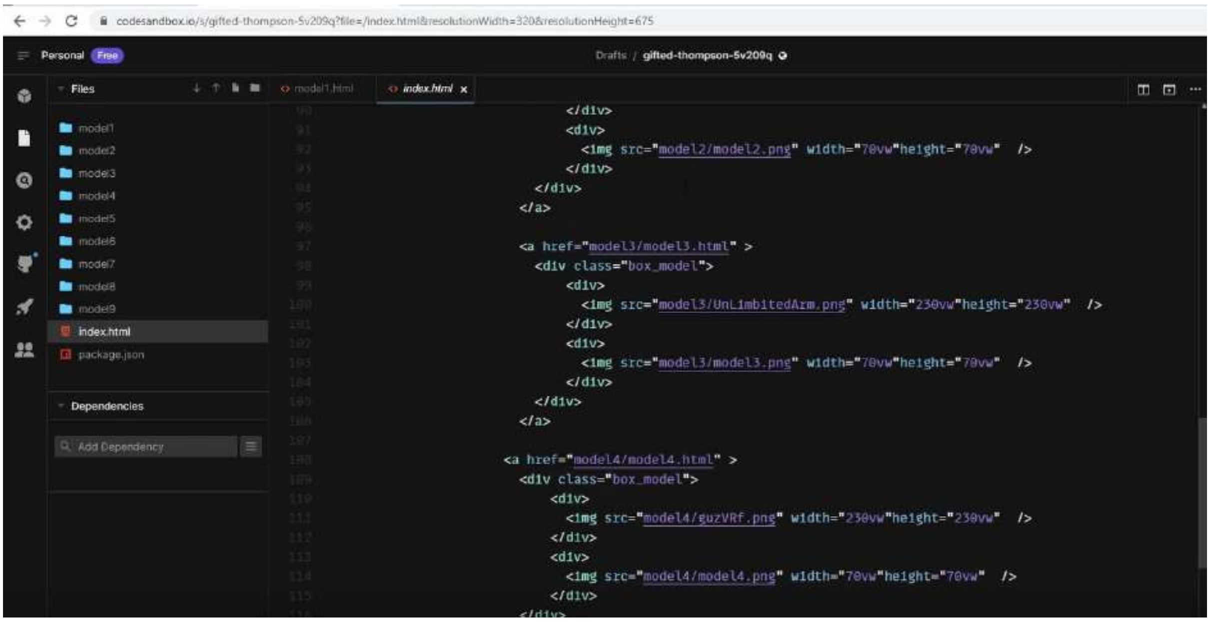

Through this we can redirect to other imported sub models. As you can see from the screenshot, it contains the models. For example, here we can click on the first object model1.html:

This project has been funded with support from the Iceland Liechtenstein Norway Grants. This publication [communication] reflects the views only of the authors, and the Commission cannot be held responsible for any use which may be made of the information contained therein.

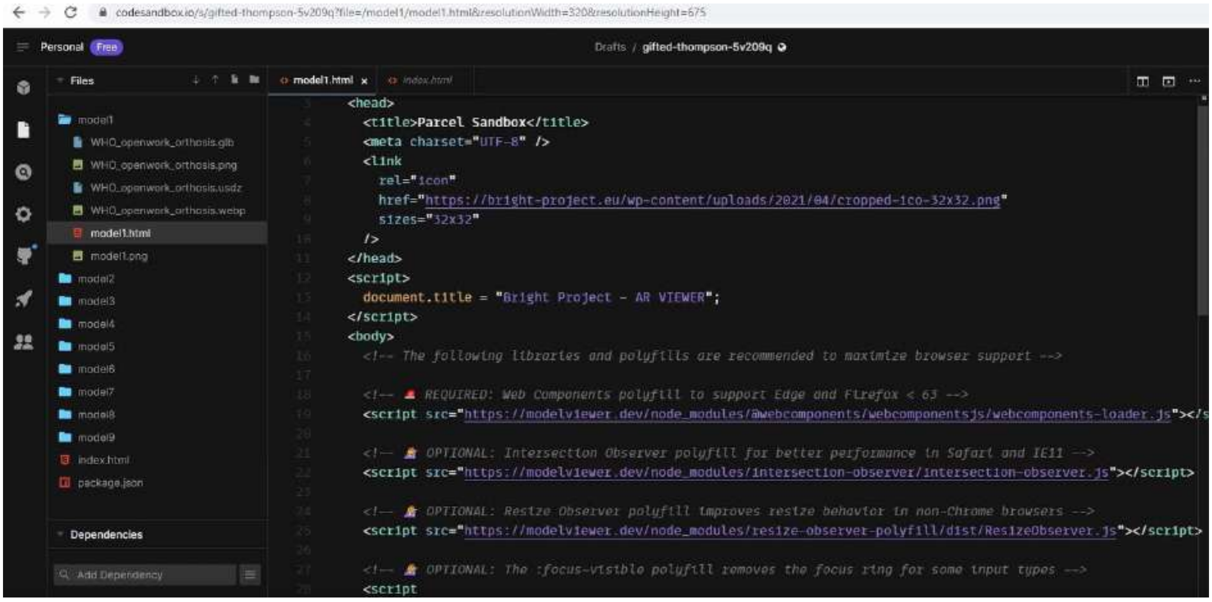

The sub site of the first object contains individual code as well.

The site will generate from 3Dmodel html code a model displayed in augmented reality, either Android or iOS. Which we can click, we can rotate it and interact with.

This project has been funded with support from the Iceland Liechtenstein Norway Grants. This publication [communication] reflects the views only of the authors, and the Commission cannot be held responsible for any use which may be made of the information contained therein.

Working together for a green, competitive and inclusive Europe

EMERALD

The Education, Scholarships, Apprenticeships and Youth Entrepreneurship

EUROPEAN NETWORK FOR 3D PRINTING OF BIOMIMETIC MECHATRONIC SYSTEMS

E-toolkit – 3D PRINTABLE ROBOTIC ARM

Project Title	**European network for 3D printing of biomimetic mechatronic systems 21-COP-0019**
Output	**O2 - EMERALD e-toolkit manual for digital learningin producing biomimetic mechatronic systems**
Module	**3D Printable Robotic Arm**
Authors	**Filippo SANFILIPPO, Martin Bjaadal ØKTER, Filip GÓRSKI**

This project has been funded with support from the Iceland Liechtenstein Norway Grants. This publication [communication] reflects the views only of the authors, and the Commission cannot be held responsible for any use which may be made of the information contained therein.

Content

This project has been funded with support from the Iceland Liechtenstein Norway Grants. This publication [communication] reflects the views only of the authors, and the Commission cannot be held responsible for any use which may be made of the information contained therein.

1. Introduction

This toolkit presents construction, programming, assembly and tests of a 3D printable robotic arm that can be used as a haptic device. The robotic arm was constructed as a project realized by University of Agder lecturers and students, as an educational example on how to construct and program simple robotic grippers. It has been used during the EMERALD project summer school in year 2022, by students of all universities involved in the project consortium.

This toolkit has been made openly available as a GitHub solution, available under the following link: https://github.com/Microttus/HapticSommerSchool/tree/main [1]. This document reflects the contents of the GitHub solution and also presents basic introduction to robotic grippers.

This project has been funded with support from the Iceland Liechtenstein Norway Grants. This publication [communication] reflects the views only of the authors, and the Commission cannot be held responsible for any use which may be made of the information contained therein.

2. 3D Printed programmable robotic grippers

2.1. Introduction to 3D printed robotics

Robotic arms have been an integral part of industrial automation, healthcare, and various other domains. The convergence of 3D printing technology with robotics has given rise to programmable robotic arms that offer enhanced versatility, cost-efficiency, and customization.

Various parts of robotic arms can be 3D printed, including joints, grippers, and even end-effectors. The ability to customize these parts to suit specific tasks is a notable advantage of 3D printing in robotics [2], with example of simple 3D printed parts shown in Figure 1.

Figure 1. Robotic arm parts 3D printed using low-cost FDM technology [2]

3D-printable robotics is characterized by its adaptability and customization. Robotic arms can be designed and printed to suit a range of applications, from educational platforms to industrial automation [3]. 3D-printed robotic arms have found a niche in education, enabling students and researchers to experiment with robotics and gain hands-on experience – which was also a point of this toolkit. The availability of DIY kits and open-source designs has democratized access to 3D-printable robotic arms, fostering innovation and experimentation in the robotics community [4].

3D-printed programmable robotic arms have made inroads into manufacturing, streamlining processes and increasing efficiency. They are used for tasks such as pick-and-place operations and quality control. In the medical field, these robotic arms can assist in surgeries, offering precision and minimally invasive procedures. Rehabilitation and physical therapy applications are also emerging [3].

This project has been funded with support from the Iceland Liechtenstein Norway Grants. This publication [communication] reflects the views only of the authors, and the Commission cannot be held responsible for any use which may be made of the information contained therein.

2.2. *Programming Robotic Arms using Arduino Platform*

A crucial component of any robotic arm is its manipulator. Robotic arms consist of joints and links that mimic the movements of a human arm. These are controlled by motors, and the coordination of these components enables precise movement and manipulation [5]. To achieve programmability, robotic arms require advanced control systems. These systems can be based on traditional methods like PID control or more advanced methods such as machine learning and computer vision [3].

Programming and controlling robotic arms is a critical aspect of robotics, and the Arduino platform has been widely used as a basic controller for various robotic arm applications. Several papers and resources discuss the integration of Arduino for this purpose.

In a paper titled "Arduino-Based Trainable Robotic Arm," the authors propose a trainable robotic arm implemented based on the Arduino platform. This approach leverages the "teach" function of Arduino for control [6]. Another publication titled "DIY Arduino Robot Arm with Smartphone Control" demonstrates the construction of a robotic arm that can be wirelessly controlled and programmed using an Arduino board. It includes custom-built Android applications for control (Figure 2) [7].

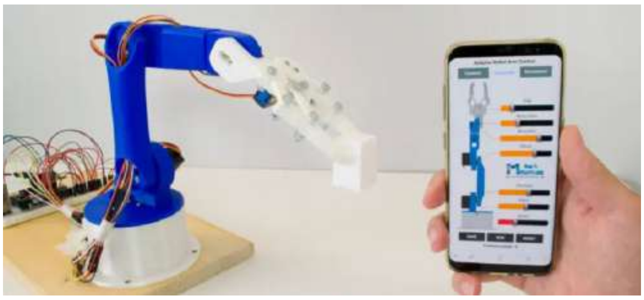

Figure 2. Use of Arduino in a “do-it-yourself” project for 3D printable robotic arm [7]

The "Development of an Arduino Controlled Robotic Arm" paper outlines the creation of a five-degree-of-freedom (5-DoF) robotic arm controlled by Arduino. This project is designed for pick and place applications and showcases the versatility of Arduino in controlling robotic arms [8]. The "DIY Arduino-Controlled Robotic Arm" demonstrates the creation of a robotic arm using Arduino for control. This resource showcases the use of Arduino as the central control unit for a functional robotic arm [9].

These papers and resources offer valuable insights into the use of Arduino for programming and controlling

This project has been funded with support from the Iceland Liechtenstein Norway Grants. This publication [communication] reflects the views only of the authors, and the Commission cannot be held responsible for any use which may be made of the information contained therein.

robotic arms, highlighting its versatility and applicability in various robotic arm projects. Researchers and enthusiasts can explore these references to gain a deeper understanding of Arduino-based robotic arm development.

2.3. Design and 3D printing of robotic arms

Current technology allows to use various 3D printing technologies in construction of low-cost robotic arms. As shown in previous chapters, many designs can be used as DIY projects, to create home-made or school-made robotics. Students and researchers interested in this topic may easily find many suitable projects, along with customization possibilities. Fused Filament Fabrication (FFF) is a versatile additive manufacturing method used to create 3D-printed robotic arm components, including grippers and whole arms. Several papers and research studies showcase the application of FFF for building functional robotic components.

A comprehensive review of robotic arm grippers is presented in the paper "Current Designs of Robotic Arm Grippers." This review discusses various designs of grippers, many of which can be created using Fused Filament Fabrication. It identifies benefits and drawbacks of different gripper designs, providing insights into the use of FFF for gripper fabrication [10].

In the paper titled "Design and 3D Printing of a Robotic Arm," the authors introduce the design concepts and the 3D printing procedure for a robotic arm created using 3D printing technology. While this paper primarily focuses on design concepts, it highlights the significance of 3D printing in the fabrication of robotic arms [11].

A paper titled "FDM Based Custom 3D Printer Development in Robotic" discusses the development of a custom 3D printer that can be utilized for robotic arm component fabrication. This research showcases the potential of 3D printers for creating robotic arm mechanical components with precision and low tolerances [12]. In "Current Designs of Robotic Arm Grippers," an underactuated adaptive 3D printed robotic gripper is presented. This gripper is designed for interactions with unpredictable environments and demonstrates the potential of 3D printing in creating adaptable robotic components, including grippers [13].

These papers and research studies underscore the use of Fused Filament Fabrication (FFF) as a viable method for creating robotic arm components such as grippers and whole arms. Researchers and robotics enthusiasts can explore these references to gain insights into the capabilities and applications of 3D printing in the realm of

This project has been funded with support from the Iceland Liechtenstein Norway Grants. This publication [communication] reflects the views only of the authors, and the Commission cannot be held responsible for any use which may be made of the information contained therein.

robotics.

2.4. *Use of robotic arms as haptic devices*

Haptic devices, which provide users with tactile feedback in virtual environments, have gained significant attention in various fields, including virtual reality, telemedicine, and robotics. Robotic arms, with their ability to simulate touch and force interactions, have emerged as valuable tools for creating immersive haptic experiences. In this chapter, the use of robotic arms as haptic devices is explored, highlighting key studies and developments in the field.

Robotic arms have been employed in teleoperation scenarios where human operators can remotely control robotic arms equipped with haptic feedback systems [14]. Virtual reality (VR) applications benefit greatly from the integration of robotic arms to enhance the sense of touch and presence [15]. Robotic arms as haptic devices play a vital role in medical training and simulation. Some researchers discuss the application of robotic arms in medical simulations for training medical professionals. Robotic arms can replicate complex medical procedures and provide trainees with realistic haptic feedback, improving their skills and reducing the risk associated with real patient interventions [16].

While the use of robotic arms as haptic devices offers numerous advantages, challenges remain, including cost, scalability, and the need for precise control algorithms. Future research should focus on developing more affordable and accessible robotic haptic systems, as well as enhancing their capabilities for a wider range of applications.

In conclusion, robotic arms as haptic devices have shown immense potential across various domains, from medicine to entertainment and accessibility. The integration of haptic feedback into robotic arms continues to evolve, offering new opportunities for realistic and immersive user experiences in virtual and physical environments.

This project has been funded with support from the Iceland Liechtenstein Norway Grants. This publication [communication] reflects the views only of the authors, and the Commission cannot be held responsible for any use which may be made of the information contained therein.

3. Biomimetic 3D printable robotic gripper

3.1. Introduction

The primary goal of the project presented in this toolkit was to design an easy-to-build and assemble haptic installation that can function as a haptic device. This is achieved through the utilization of a joint with integrated springs. By employing this innovative approach, it becomes feasible to achieve greater motor displacement for a relatively smaller amount of force when compared to a rigid robotic arm. This design allows for enhanced tactile feedback and improved user experience in haptic interactions.

Contents of this chapter are mostly taken from the GitHub solution, available under [1].

3.2. Construction

The robotic gripper was designed in 3D CAD with typical assumptions for simple, one-axis robotic arms. The basic construction is presented in Figure 3 and the 3D models for 3D printing are available in the GitHub repository at [1]. Also, a full disassembly instruction, containing animations of all steps with names of standardized parts was prepared. It is available online, under link [17]. Examples of operations presented in the online instruction are presented in Figure 4.

This project has been funded with support from the Iceland Liechtenstein Norway Grants. This publication [communication] reflects the views only of the authors, and the Commission cannot be held responsible for any use which may be made of the information contained therein.

Figure 3. The robotic gripper 3D design [17]

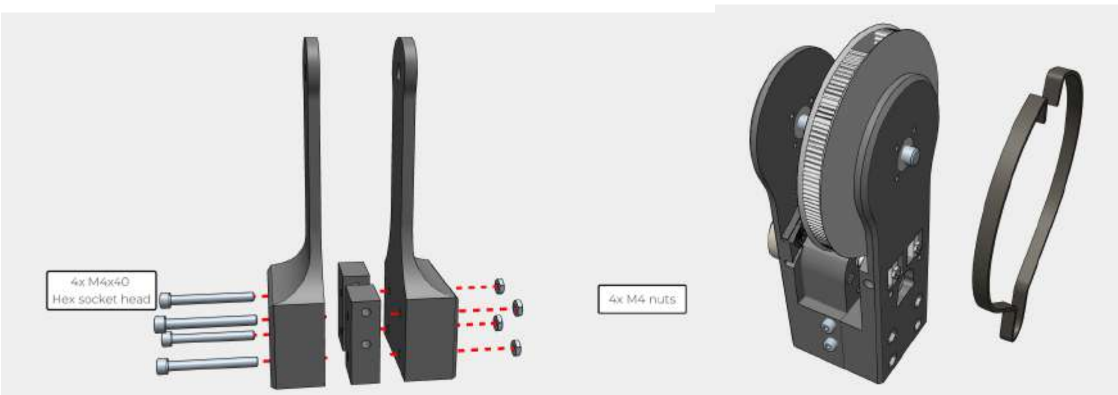

Figure 4. Disassembly instruction of the robotic arm, available at [17]

This project has been funded with support from the Iceland Liechtenstein Norway Grants. This publication [communication] reflects the views only of the authors, and the Commission cannot be held responsible for any use which may be made of the information contained therein.

3.3. Control

In Haptic devices there are two main ways for control. Impedance control aim to steer the position by reading the motor force. Admittance control aim to control the force of the device by adjusting the position. This two are integrated as methods and can be used directly, By the use of the low level libaries these control codes may also be created by the user. A descriptive block diagram of the two control loops is presented in Figure 5.

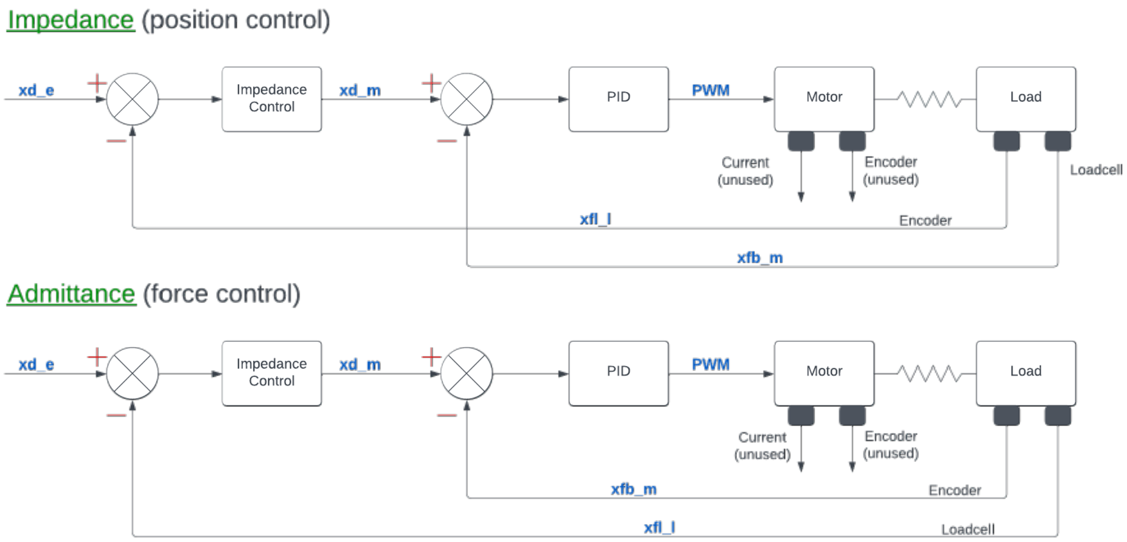

Figure 5. Control structure of the haptic arm [1]

3.4. Software

The software was built to be as modular as possible, aiming to ensure the easy operation of the robotic arm for users with varying programming backgrounds. The course is designed to cater to students with minimal to no prior experience in programming and control theory while also providing the opportunity for experienced personnel to conduct advanced control theory testing. For less experienced users, the steering library can be used, requiring adjustments only to control factor values. More experienced users have the option to build the control part themselves for implementing alternative steering methods. The basic libraries for data collection can be adapted and modified by experienced users to achieve optimal control, higher precision, and further

This project has been funded with support from the Iceland Liechtenstein Norway Grants. This publication [communication] reflects the views only of the authors, and the Commission cannot be held responsible for any use which may be made of the information contained therein.

system development.

The software comprises five classes. The AS5600 library, provided by Seed-Studio, facilitates the easy retrieval of data from the absolute magnetic encoder. Additionally, three low-level classes—PID, pwmMotor, and HapticSensor—are dedicated to data retrieval and the hard-coded control of the haptic arm. The final library, HapticArm, offers a variety of control methods based on control theory, utilizing the aforementioned classes for arm control.

3.4.1. AS5600

The AS5600 library is created and distributed by Seed-Studio, which is the producer of the encoder used in this project. The data are retrieved using I2C and memory access and the code are therefore manageable but too complicated to learn if you are not interested in the code side. The library gives the user an easy-to-use interface, retrieving the magnets position. This library needs to be put inside the programming folder or the main Arduino library folder for the program to work.

The *getRawAngle* is the only method used of this library. The command return the position of the magnet as a 12 bit signal (0-4095).

3.4.2. PID

The PID class are made for easy implementation of PID loops. It takes advantage of the object properties of classes for the user to easily be able to create multiple loops with different PID values based on the same class. The PID class have three public method in addition to the constructor. One which gives the possibility of a standard PID loop using Kp, Ki and Kd and one which provide the possibility of a PID controller with back calculation integration as an anti wind-up method. The last one is a complimentary filter which are used as a low pass filter on the sensor data. The PID method uses the same values and can be switch during operation if needed.

1. **PID(float Kp_in, float Ki_in, float Kd_in)**

The PID constructor is used to initialize the PID object. The constructor take Kp, Ki and Kd as input and a single PID object are intended to be used for a single PID loop. The values of the PID block cannot be changed during

This project has been funded with support from the Iceland Liechtenstein Norway Grants. This publication [communication] reflects the views only of the authors, and the Commission cannot be held responsible for any use which may be made of the information contained therein.

operation.

2. **calculate(float value, float target)**

The calculate method is used if a standard PID loop are intended to be used. This method do not have an anti wind-up integrated. The PID equation used are the standard European method, see equation 1.1. The method have the current value intended to be used and the target as input. The aim target may be changed during operation, which is a key feature for the use of control systems. The loop time is calculated for every loopback by the object for precision loop calculation. This makes the object independent of the clock frequency or the loop time. And the code may stagger without the PID failing, taking advantage of the variable loop time calculation.

$$u_d(k) = K_p e(k) + K_i(u_{i-1} + e(k) \cdot dt) + K_d \frac{e(k) - u_{d-1}}{dt} \tag{1.1}$$

ud is calculated value, *e(k)* is the error of the system, *ui* is calculated integral constant and *dt* the time step.

3. **backcalc(float value, float target, float backVal, float satutaionMin, float saturationMax)**

The backcalc method use the same equation as the calculation method, as well as iterate over the same loop time and uses the same Kp, Ki and Kd. These properties make it possible for the user to switch between these two methods. The value are the current value input for the calculation and the target value are the target for the calculation. In addition to these two, the backVal input is used for tuning the anti wind-up section. The saturtionMin and saturationMax inputs are used for the upper and lower limit for the anti wind-up.

The anti wind-up constant could be set to 1 which would work great. This method should be used as the final loop before sending the value to the motor. If this is the case, an upper limit of 255 and lower -255 is advised, corresponding to the upper and lower limit for PWM. In the backcalc method, the integral part of the PID calculation are switched with this equation 1.2.

$$u_d(k) = K_p e(k) + K_i(u_{i-1} + (e(k) + \frac{e_p(k) - u_{d-1}}{T}) \cdot dt) + K_d \frac{e(k) - u_{d-1}}{dt} \tag{1.2}$$

This project has been funded with support from the Iceland Liechtenstein Norway Grants. This publication [communication] reflects the views only of the authors, and the Commission cannot be held responsible for any use which may be made of the information contained therein.

e_p is the saturated u_d and T is the back calculation value.

4. compfilter(float in_val, float alpha)

The compfilter method is integrated as a way to use the equation for complimentary for values. The complimentary filter may be used as a low-pass filter or high-pass filter, depending on the inn-values. A low-pass filter can be essential for readable sensor-data. The in_val are the new data from the sensor used for calculation. A separate PID object should be initialized for every sensor in the system needing a filter. The earlier results are remembered by the object, and the same object cannot be used for different sensor-data. The alpha constant is the tuning value for the filter. This decides how much the new values are to be weighted. This value is set to 0.01 as standard and do not need to be given for this value, unless a different number is to be used.

The method return the final calculated value. The equation used is 1.3.

$$u_d = (1 - \alpha) \cdot u_{d-1} + \alpha \cdot e(k) \tag{1.3}$$

3.4.3. pwmMotor

The pwmMotor class are a collection of different method used for control of a PWM motor using a H-brigde style motor controller and collect data from a hall encoder. The class consist of five public methods in addition to two private ones and the constructor. The two private methods are used for the collection of data as interrupt from the hall encoder and are set to ”static void” as all methods interacting with interrupt variables do need to be of this data type. This is also the reason for the “static void” data type of the reset_hall_val method.

1. pwmMotor(int forwardPin_in, int backwardPin_in, int pwm_in, int hallPinOne_in, int hallPinTwo_in)

The constructor of the pwmMotor class have five inputs for correct setup of the connection between the microchip and the motor controller. The first two inputs are the microchip pins, which are to be connected to the directional control of the motor. These pins are used for digital signals. The third is the pin which the PWM signal are sent to. The last two are the pins which the hall sensor pins are connected. Mark: On Arduino Due the only two pins supporting interrupt are 0 and 1.

2. goToSpeed(int motorSpeed)

This project has been funded with support from the Iceland Liechtenstein Norway Grants. This publication [communication] reflects the views only of the authors, and the Commission cannot be held responsible for any use which may be made of the information contained therein.

This method is the main method used for control of the motor. The method receives the motor speed as an integer. Inside the method, the number will be limited to -255 to 255 to ensure the value do not exceed the capabilities of the microchip. The Arduino Due have an 8 bit DAC and these values are preset for this intent, but may be adjusted if a different chip set is to be used. If motorSpeed is negative the method will spin the motor backward and on the contrary if the value is positive the motor is spun forward. The method also check if the value is equal to the last value asked. The operation of changing direction may be more time conceiving than just adjust the PWM sequence. Checking if the value have changed and immediately break if the value are the same, saves computational time. A value of -1 for backward and one for forward, are additionally commutated and saved for the intent of being able to check the motor direction elsewhere in the code. This is used for the emergency brake.

3. stop()

The stop method immediately set both directional control pin to zero, and then adjust the PWM signal to zero as well. In this configuration, the motor will run free, which is the optimal configuration if the arm have hit something and need to be stopped immediately. This method is used by the emergency break due to endstops, but may also be implemented if the arm is used for obstacle avoidance or as a cobot.

4. check_rotation()

The check_rotation method return the angle of the arms based on the number of trigger events from the hall sensor interrupt routines. While reading the count, the interrupt routine have to be temporarily paused. This means that for every iteration of the method, steps may be missed.

5. reset_hall_val()

This method is used by the calibration method of the arm. At the end of the calibration sequence, the arm is situated at angle 0. Since the motor encoder is incremental, a fixed start position is necessary. The interrupt will start counting as soon as the motor object is initialized, and the count have to be zeroed at a known location. The calibration routine calls this method in the known zero position, which set both trigger event counts to zero.

6. return_motor_dir()

This project has been funded with support from the Iceland Liechtenstein Norway Grants. This publication [communication] reflects the views only of the authors, and the Commission cannot be held responsible for any use which may be made of the information contained therein.

The value saved by the goToSpeed method is internal, and the return_motor_dir method can be called to read the current value. This is used by the end stop emergency stop. The motor direction value is used for the trigger event detection as well.

3.4.4. HapticSensor

The Haptic Arm have five types of sensors which are integrated into the platform. The motor encoder is implemented in the pwmMotor library. The remaining four are the data collected through this library. The AS5600 library is used for the reading of the absolute position encoder. The library consist of five methods in addition to the constructor. Four are the methods for returning sensor data, and the last one is for configuration of the end positions of the arm for the position sensor.

1. **HapticSensor(int forcePin, int currentPin, int switchPinOne, int switch-PinTwo)**

The HapticSensor constructor takes four inputs, which are the pins which the sensors are connected to. ForcePin is the pin for the load cell, which has to be connected through an instrument amplifier and are read as an analogue signal. The currentPin is the pin connected to the current sensor, which is read as an analogue signal as well. switchPinOne and switchPinTwo are the pin which the signal side of the endstops. In the constructor, all the input pins are set as inputs, and the analogue read resolution set to 10 bit.

2. **readForce()**

The readForce method return the force exposed to the end of the arm. The signal read from the load cell is adjusted due to a graph found through testing with known weights at the connection point on the arm. The force is calculated from the weigh and adjusted for the current angle of the arm for neglecting the weight of the swing arm. The value is adjusted with a low pass filter via the PID library before returned as a float.

3. **readPos()**

The readPos method use the AS5600 library to retrieve the absolute position of the arm from the magnetic encoder. The belonging angle is calculated and returned as a float. The calculation use the values found by the calibration sequence for the value of the magnetic encoder at the endstops.

This project has been funded with support from the Iceland Liechtenstein Norway Grants. This publication [communication] reflects the views only of the authors, and the Commission cannot be held responsible for any use which may be made of the information contained therein.

4. readCurrent()

This method read the value provided by the current sensor, which is situated between the motor and the motor controller. The signal is converted from a bit value into volt and adjusted for the signal at zero current, roughly in the middle. The volt signal is then multiplied with the amp per volt value given for the sensor. A low-pass filter using a PID block are used to smooth out the signal. The current is returned as a float.

5. readSwitch()

The readSwitch method update both values in the list containing the state of the two endstop switches connected. And finally returning these as a pointer to the list. Therefore, the data type int* is used. The list need to be initiated as a class object and not initialized in the object, as the list in that case would be saved in the stack (which is temporary) and removed when the method returns.

6. calibrateEncoder(int newMinVal, int newMaxVal)

The values for the magnetic absolute encoder are saved as object parameters, such that the calibration sequence is not absolutely necessary if the values for a specific configuration are well known. These values are set in the constructor. After the calibration sequence, the found values are used to change these private values by the use of the calibrateEncoder method. The method return the current raw bit value of the magnetic encoder for the intent of using it during calibration. The argument are optional, but the values will be set to 0 if no value is provided.

3.4.5. HapticArm

The HapticArm library is a class combining the lower lever control classes of the Haptic Arm with the intent of controlling the arm using control theory. The library consist of four public and four private methods in addition to the constructor. The of the private method two are calculating the moved length, speed, and acceleration based on the current and part position using numerical mathematics and the same as angles. The last two are the emergency protocols witch read data to ensure the arm have a reasonable behaviour and engage the stop routines if not.

1. HapticArm(int motorSettings[ ], int sensorSettings[ ], int PIDset[ ][3])

The HapticArm constructor takes two list and one multidimensional list as input. The first list are the values used to set up the motor object, in total four values. The object for using the other classes are set up inside this class, which means that all necessary values have to be delivered by this object as a middle man. As a way to avoid having 15-20 input for the object, it is initialized with lists. The second list are the values for the sensor class, and need five objects. The constructor do not need to know the size of the list, but enough values have to be given for the constructor to succeed. The third list is a Nx3 matrix, and contains the values Kp, Ki and Kd for all PID objects which are used in the object. The objects are the defined in the constructor as well as other needed constant. One of this is the type of switch used. Original the endstop switches are set to normally closed (NC) corresponding to “1”. If the setup support NO, this would be better, but the Due does not support the needed pull-down resistor.

2. goToPos(float requiredPos)

This method is the basic inner loop of the motor control. It read the position of the arm and adjust the PWM signal sent to the motor, trying to achieve the given required position. This method use the Position PID object, which is the first three values given in the PID matrix. This PID should be the first to be tuned for optimal control of the arm, due to the fact that it is the inner loop for the goAdmittance method. For the PID calculation, back calculation is used for saturation of the signal.

3. calibrateArm()

The calibrateArm method are the main calibrate sequence which check the position of the magnet at the end stops and zero the motor encoder at 0 degrees. By reading both switches during the sequence, the switch located at zero degrees and 250 depresses is mapped, and take care of misplacement of these wires. The motor speed will be manual, set to the minimum safe speed which the arm will be able to rotate.

For visual confirmation of started sequence, the method will print “Calibration started” to the serial monitor. After successful calibration, the maximum and minimal magnetic value will be printed at the serial monitor. This value may be used to adjust the preset values in the code. The calibration sequence may be left out if the preset

This project has been funded with support from the Iceland Liechtenstein Norway Grants. This publication [communication] reflects the views only of the authors, and the Commission cannot be held responsible for any use which may be made of the information contained therein.

values are to be trusted and the motor encoder is not in active use.

4. **goImpedance(float massConstant, float damperConstant, float springConstant)**

This method enables the user to control the arm using Impedance control, which means reading the movement of the arm and adjusting the output torque of the motor. The private method movedAngle are used to find the radial movement of the arm and the current are read by using the sensor object. The movement values are then multiplied with the mass, spring, damper values, which are given by the user as inputs for the method. The equation used is 1.4.

$$\tau = M\ddot{\theta} + D\dot{\theta} + K\theta \tag{1.4}$$

The resulting torque is with the read current used to calculate a new speed and feed to the motor. The emergency test is embedded for safety.

5. **goAdmittance(float massConstant, float damperConstant, float spring- Constant, float initialPosition)**

This method enables the user to control the arm using Admittance control, which means reading the input force and controlling the position of the arm. The system will act as a spring damper system and centre around the given initial position value. The private method movedLenght is used to find the moved length since last iteration. The length is based on the given length of the arm and uses trigonometry. It is an estimate based on numerical iteration of a curve divided into triangles, and the frequency of the code are important for the validation of the method.

The current applied force are read by the use of the sensor object and the corresponding offset length are calculated using this equation 1.5.

$$x_{new} = \frac{F - D\dot{x} - M\ddot{x}}{K} \tag{1.5}$$

The calculated length is calculated as angle and applied to the initial angle value. Finally, the required angle is sent to the goToPosition method used for the inner loop. The emergency test is embedded in the goToPosition method.

6. **emergencyCheck()**

This project has been funded with support from the Iceland Liechtenstein Norway Grants. This publication [communication] reflects the views only of the authors, and the Commission cannot be held responsible for any use which may be made of the information contained therein.

The method check the current motor direction and if any of the end stop switches are activated. If one of the switches are activated and the motor direction is pushing the arm further into the switch, the emergency brake is activated. If the motor direction are away from the switch, it is assumed the motor are trying to fix the problem and the break are not activated.

3.5. Manufacturing and testing

The parts of the robot arm were 3D printed using the Fused Filament Fabrication technology, of PLA material. Using standard nuts and bolts, springs and other elements, mechanical part and actuators were assembled. Using Arduino, sensors and other electronic components, the electronic part was assembled. The result is presented in Figure 6. Total of 4 arms were manufactured and successfully launched.

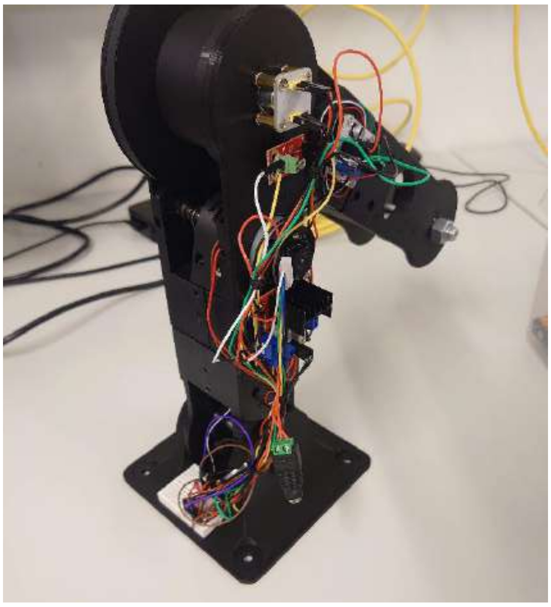

Figure 6. Assembled robotic arm made of 3D printed components [1]

Testing of the arm was also realized, checking correctness of movement and functioning as a haptic device. Some of its results can be found in a film, available under link [18] (Figure 7).

This project has been funded with support from the Iceland Liechtenstein Norway Grants. This publication [communication] reflects the views only of the authors, and the Commission cannot be held responsible for any use which may be made of the information contained therein.

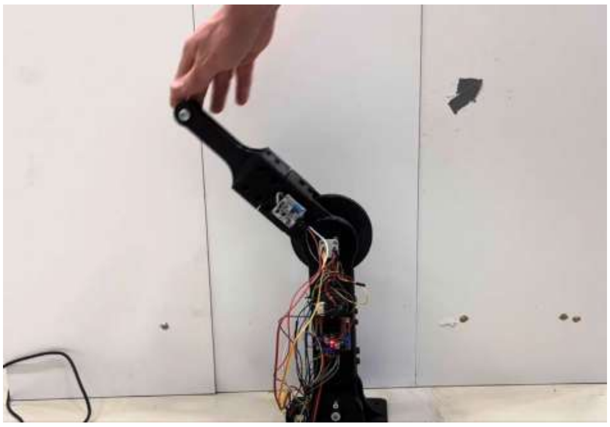

Figure 7. Haptic arm tests [18]

4. *Summary*

In this toolkit, a concept of a simple robotic arm usable as a haptic device was presented. The device was designed, 3D printed, programmed and tested using widely available technologies and low-cost components. The whole project was made freely available as an educational asset for the interested students and researchers worldwide through the GitHub platform. It was proven that it is possible to use available 3D printing and robotic technologies to manufacture simple, working robotic arms in short time.

This project has been funded with support from the Iceland Liechtenstein Norway Grants. This publication [communication] reflects the views only of the authors, and the Commission cannot be held responsible for any use which may be made of the information contained therein.

Literature

1. https://github.com/Microttus/HapticSommerSchool/tree/main, access: January 2023
2. https://www.instructables.com/3D-Printed-Robot-Arm/
3. Marín Garcés, J.; Veiga Almagro, C.; Lunghi, G.; Di Castro, M.; Buonocore, L.R.; Marín Prades, R.; Masi, A. MiniCERNBot Educational Platform: Antimatter Factory Mock-up Missions for Problem-Solving STEM Learning. Sensors 2021, 21, 1398. https://doi.org/10.3390/s21041398
4. https://all3dp.com/2/3d-printed-robot-arm-diy-robotic/
5. Anatoliotakis, N.; Paraskevopoulos, G.; Michalakis, G.; Michalellis, I.; Zacharaki, E.I.; Koustoumpardis, P.; Moustakas, K. Dynamic Human–Robot Collision Risk Based on Octree Representation. Machines 2023, 11, 793. https://doi.org/10.3390/machines11080793
6. Shweta, K & Pattar, Nikhil & Kuntoji, Rahul & V, Arpitha & B V, Chetan. (2017). Arduino Based Trainable Robotic Arm. 2. 337-339.
7. https://howtomechatronics.com/tutorials/arduino/diy-arduino-robot-arm-with-smartphone-control/
8. Shaibu, H. A. A., Ogakwu, P. A., Binfa, B., & Ibrahim, A. A. (2019). Development of an Arduino Controlled Robotic Arm. Journal of Good Governance and Sustainable Development in Africa, 5(2), 73-82.
9. Ali, Hussein & Hashim, Yasir & Alsakkal, Ghadah. (2022). Design and implementation of Arduino based robotic arm. International Journal of Electrical and Computer Engineering (IJECE). 12. 1411. 10.11591/ijece.v12i2.pp1411-1418.
10. Hernandez, Jaime & Sunny, Md. Samiul & Sanjuan, Javier & Rulik, Ivan & Islam, Ishrak & Ahamed, Sheikh & Ahmed, Helal & Rahman, Mohammad. (2023). Current Designs of Robotic Arm Grippers: A Comprehensive Systematic Review. Robotics. 12. 5. 10.3390/robotics12010005.
11. Kitsakis, Konstantinos & Petrou, Nick & Tanos, Ilias & Kechagias, John. (2016). Design and 3d Printing of a Robotic Arm.
12. Prianto, E., Herliansyah, M. K., Pramono, H. S., Husna, A. F., Adam, R., & Raditya, A. E. (2022, December). FDM Based Custom 3D Printer Development in Robotic Arm Mechanical Prototype Printing. In *Journal of Physics: Conference Series* (Vol. 2406, No. 1, p. 012005). IOP Publishing.
13. Hernandez, J.; Sunny, M.S.H.; Sanjuan, J.; Rulik, I.; Zarif, M.I.I.; Ahamed, S.I.; Ahmed, H.U.; Rahman, M.H. Current Designs of Robotic Arm Grippers: A Comprehensive Systematic Review. Robotics 2023, 12, 5. https://doi.org/10.3390/robotics12010005
14. Verner, L. N., Jeung, K. A., & Okamura, A. M. (2005). 15 effects of gripping and translational forces on teleoperation. Multi-point Interaction with Real and Virtual Objects, 231-241.
15. Van der Meijden, O. A., & Schijven, M. P. (2009). The value of haptic feedback in conventional and robot-assisted minimal invasive surgery and virtual reality training: a current review. Surgical endoscopy, 23, 1180-1190.
16. Ruthenbeck, G. S., & Reynolds, K. J. (2015). Virtual reality for medical training: the state-of-the-art. Journal of Simulation, 9, 16-26.
17. https://instructions.online/?id=3988-mechanical%20assembly
18. https://youtu.be/x0tvgowaUfE?si=nHkEfITcb-D-KBVI

This project has been funded with support from the Iceland Liechtenstein Norway Grants. This publication [communication] reflects the views only of the authors, and the Commission cannot be held responsible for any use which may be made of the information contained therein.

CONCLUSIONS

As one may notice while going through the EMERALD e-toolkit manual, it becomes clear that this guide is more than just a collection of methodologies and instructions. Developed by the EMERALD consortium partners, the e-toolkit manual is an essential tool that is continuing the theoretical aspects provided in the e-book to hands on real practical applications in the field of biomimetic mechatronic systems that are destined to support people with special needs (with amputated arms). Specifically designed for the conceiving, manufacturing and testing of biomimetic mechatronic systems realized by 3D printing technologies, the provided solutions are designed in the way to meet the real needs of people with amputated arms in the end.

The e-toolkit manual that has been produced as a collective effort of the EMERALD consortium partners is therefore an in-depth laboratory guide that transcends basic knowledge that has been provided in the e-book, offering step-by-step guiding for the conceiving, manufacturing and testing of biomimetic mechatronic systems - from the preliminary stages of Computer Aided Design and Computer Aided Engineering to the final stages of integrating the sensors, assembling, programming, and the applying of Virtual Reality / Augmented Reality methods for the conceived and produced biomimetic mechatronic systems. This comprehensive guide ensures that every crucial aspect of developing biomimetic mechatronic systems is addressed, providing a solid foundation for both students and professors that are involved in this field.

A primary objective of this e-toolkit manual is to inspire the practical implementation of theoretical concepts previously introduced in the e-book by involving and stimulating both professors and students to go deeper in the creating and implementing of the solutions they have been learning for real practical case studies, encouraging them in this way to take theory into practice. This approach not only deepens understanding, but also stimulates creativity and innovation, leading to the development and producing of biomimetic mechatronic solutions by 3D printing methods in a customized way to support real patients with amputated arms.

Moreover, the e-toolkit manual is intended to create one bridge between higher educational institutions, medical institutes and industrial partners, by extending beyond traditional teaching methods and by encouraging the exchange of new ideas and shared knowledge in the field of biomimetic mechatronic systems realized by different types of 3D printing technologies to support real patients with amputated arms in the end. By applying the solutions and methods presented in the e-toolkit manual, and by scaling and multiplying these applications among diverse institutions that are interested about this field, a significant contribution can be made to the lives of patients with special needs (with amputated arms) on a larger scale in the future.

The EMERALD e-toolkit manual serves as a strong example of collaborative learning and innovation by being not just a tool intended to be used for educational purposes, but also to be a stimulative resource for developing innovative real practical applications in order to bring real benefits in the field of biomimetic mechatronic systems that are aimed to be realized by using different types of 3D printing methods to support in a customized way patients with amputated arms in the end.

This project has been funded with support from the Iceland Liechtenstein Norway Grants. This publication [communication] reflects the views only of the authors, and the Commission cannot be held responsible for any use which may be made of the information contained therein.